Hydrologic Validation of Real-Time Weather Radar VPR Correction Methods

by

Erika Suzanne Klyszejko

A thesis
presented to the University of Waterloo
in fulfillment of the
thesis requirement for the degree of
Master of Applied Science
in
Civil Engineering

Waterloo, Ontario, Canada, 2006

Author's Declaration

I hereby declare that I am the sole author of this thesis. This is a true copy of the thesis, including any required final revisions, as accepted by my examiners.

I understand that my thesis may be made electronically available to the public.

Abstract

Weather radar has long been recognized as a potentially powerful tool for hydrological modelling. A single radar station is able to provide detailed precipitation information over entire watersheds. The operational use of radar in water resources applications, however, has been limited. Interpretation of raw radar data requires several rigorous analytical steps and a solid understanding of the technology. In general, hydrologists' lack of meteorological background and the persistence of systematic errors within the data, has led to a common mistrust of radar-estimated precipitation values.

As part of the Enhanced Nowcasting of Extreme Weather project, researchers at McGill University's J.S. Marshall Radar Observatory in Montreal have been working to improve real-time quantitative precipitation estimates (QPEs). The aim is to create real-time radar precipitation products for the water resource community that are reliable and properly validated.

The validation of QPEs is traditionally based on how well observed measurements agree with data from a precipitation gauge network. Comparisons between radar and precipitation gauge quantities, however, can be misleading. Data from a precipitation gauge network represents a series of single-point observations taken near ground surface. Radar, however, estimates the average rate of precipitation over a given area (i.e. a 1-km grid cell) based on the intensity of reflected microwaves at altitudes exceeding 1 km. Additionally, both measurement techniques are susceptible to a number of sources of error that further confound efforts to compare the two.

One of the greatest challenges facing radar meteorologists is the variation in the vertical profile of reflectivity (VPR). A radar unit creates a volumetric scan of the atmosphere by emitting microwave beams at several elevation angles. As a beam travels away from the radar, its distance from ground surface increases. Different precipitation types are sampled

at a number of heights (i.e. snow above the 0º C elevation and rain below it) that vary with range. The difficulty lies in estimating the intensity of precipitation at the Earth's surface, based on measurements taken aloft. Scientists at McGill University have incorporated VPR correction techniques into algorithms used to automatically convert raw radar data into quantitative hydrological products.

This thesis evaluates three real-time radar precipitation products from McGill University's J.S. Marshall Radar Observatory in the context of hydrological modelling. The C0 radar product consists of radar precipitation estimates that are filtered for erroneous data, such as ground clutter and anomalous precipitation. The C2 and C3 radar products use different VPR correction techniques to improve upon the C0 product. The WATFLOOD hydrological model is used to assess the ability of each radar product to estimate precipitation over several watersheds within the McGill radar domain. It is proposed that using a watershed as sample area can reduce the error associated with sampling differences between radar and precipitation gauges and allow for the evaluation of a precipitation product over space and time.

The WATFLOOD model is run continuously over a four-year period, using each radar product as precipitation input. Streamflow hydrographs are generated for 39 gauging stations within the radar domain, which includes parts of eastern Ontario, south-western Quebec and northern New York and Vermont, and compared to observed measurements. Streamflows are also modelled using distributed precipitation gauge data from 44 meteorological stations concentrated around the Montreal region.

Analysis of select streamflow events reveals that despite the non-ideal placement of precipitation gauges throughout the study area, distributed precipitation gauge data are able to reproduce hydrological events with greater accuracy and consistency than any of the provided radar products. Precipitation estimates within the McGill radar domain are found

to only be useful in areas within the Doppler range (120-km) where the radar beam is unobstructed by physiographic or man-made features.

Among radar products, the C2 VPR-corrected product performed best during the greatest number of the flood events throughout the study area.

Acknowledgements

I would like to thank my supervisors, Professors Nicholas Kouwen and Don Burn, for their aid and support in the writing of this thesis.

Aldo Bellon at the J.S. Marshall Radar Observatory aided immensely with the interpretation of radar images and provided great insight into the field of meteorology.

I would also like to thank Sandra Mancini at the South Nation conservation authority and Josi Sabourin at the Raisin Region conservation authority for their help through the timely provision of data.

Two University of Waterloo undergraduate co-operative education students assisted with data processing: Marian Saavedra and Angela Maclean.

This project was funded by the Canadian Foundation for Climate and Atmospheric Studies.

Table of Contents

List of Figures

List of Tables

1 Introduction

Since the introduction of weather radar over 50 years ago, considerable research has been aimed at improving the accuracy and reliability of radar-derived quantitative precipitation estimates and forecasts (QPEs and QPFs). With today's technology and understanding of atmospheric processes, meteorologists are able to generate radar products in real-time and derive short-term weather forecasts, also known as nowcasts. However, after half a century of research and precipitation measurements by radar, practical limitations continue to plague meteorologists and the use of quantitative radar data is limited (Bellon et al., 2002; Atlas et al., 1997).

Nevertheless, the use of real-time radar data for streamflow prediction is highly desirable because of radar's ability to capture the temporal and spatial variation of rainfall over a watershed much better than a precipitation gauge network. A look at a rainfall event passing through a rain gauge network clearly illustrates the problems. A rainfall event can be largely or entirely missed by a sparse rain gauge network. The underestimation of rainfall over a watershed leads to an under-prediction in peak and/or total discharge. Conversely, if the most severe area of the same storm is centered on a rain gauge, distribution of gauge data is likely to result in an overestimation of precipitation over a watershed and an over-prediction of streamflow.

Despite radar's obvious advantages over precipitation gauge networks, operational exploitation of radar data in hydrology has been somewhat limited (Einfalt and Semke, 1997). Often, a lack of knowledge in the field of meteorology or the misinterpretation of raw radar data, combined with traditional practices which emphasize conventional use of ground observations, results in limited confidence in radar-derived rainfall estimates. There is a clear need for readily available radar rainfall products where all systematic errors and

biases are removed from the data to leave only the unavoidable random error component (Zawadzki, 2001).

In October of 2000, the Enhanced Nowcasting of Extreme Weather project was initiated by the Canadian Weather Research Program of the Meteorological Service of Canada (CWRP-MSC). The project aims to address the highest priority of all regional MSC offices: the improvement of QPEs and QPFs (Zawadzki, 2001). A focus was placed on extracting quantitative meteorological information from the Canadian Radar Network that is reliable and properly validated. Scientists at McGill University's J.S. Marshall Radar Observatory near Montreal have developed algorithms that automatically convert raw radar data into quantitative hydrological products, thereby eliminating the potential for misinterpretation of raw data by the end-user. A systematic approach consisting of the following tasks is taken to convert raw radar data into a hydrological product (Bellon et al., 2002):

1. Elimination of non-precipitating echoes
2. Monitoring of radar calibration
3. Correction of attenuation by precipitation and wet radome (if not S-Band)
4. Correction for the vertical profile of reflectivity (VPR)
5. Determination of the structure of range dependent errors
6. Application of proper Z-R relationship

Bellon et al. (2005) found that the implementation of a basic VPR correction technique yielded a higher than expected improvement in rainfall accumulation estimates. Since December of 2002, emphasis has been placed on developing and implementing real-time VPR correction algorithms into the McGill radar system. Four hourly rainfall accumulation products from the J.S. Marshall Radar Observatory are archived in real-time by the University of Waterloo's Hydrology Lab. Each product is based on a different VPR

correction approach. Precipitation gauge data from an extensive mesonet surrounding the Montreal area were also collected.

As a sub-project to the Enhanced Nowcasting of Extreme Weather project, the goal of this thesis is to validate radar precipitation products using the WATFLOOD hydrological model. Modelled streamflow values are calculated using various precipitation inputs (radar or gauge) and compared to observed streamflow at 39 hydrometric stations in eastern Ontario, southern Quebec and northern Vermont and New York. Analysis is carried out over a period of approximately three years: from January 2003 up to, but not including, December 2005.

Traditionally, radar precipitation data are validated through direct comparison to ground observations (Fassnacht et al., 1999; Krajewski, 1997). However, the use of point data to validate radar measurements over an entire domain can be misleading due to the difference in the area sampled by each instrument. Problems associated with radar-rain gauge comparisons are further discussed in Section 4.2. The use of a distributed hydrological model allows for continuous sampling of precipitation over an entire watershed and eliminates the scale issues generally associated with direct radar-rain gauge comparisons.

In this thesis, WATFLOOD output from select flood events is used to determine whether VPR correction methods used by the J.S. Marshall Radar Observatory have improved QPEs by radar to the point where they are a reliable tool for operational hydrologists. The impact of watershed size and distance from the radar station on hydrological prediction skill is explored to determine the spatial limits of the McGill radar precipitation products.

2 Radar Meteorology

Weather radar has the capability of measuring precipitation over a large domain using a single observation station. Its ability to provide detailed information, in both space and time, about precipitation patterns is unsurpassed by other operationally used sensors (Krajewski, 1997). However, radar does not measure precipitation directly.

Most weather radar stations are monostatic, meaning the station transmits and receives microwaves using the same antenna. Microwaves are generated by the station's transmitter and focused by the antenna into a narrow beam. As the radar beam propagates through the atmosphere, some of its energy is absorbed, reflected or scattered by weather targets such as rain and snow. A portion of the reflected and scattered energy travels back along its original propagation path towards the station where it is detected by the station's receiver. The power of the returned signal and the time required for it to return to station is then used to determine the location and reflectivity of the target. A detailed description of this process is given by Juneja (2006).

Radar meteorologists attempt to extract useful information from backscattered microwave signals to generate various "products", such as rainfall accumulation maps and severe weather indicators. Radar products are most commonly used as input to short-term weather forecast models for the public and aviation sectors. Hydrological forecasting, however, is often considered as one of the most important applications of weather radar (Borga, 2002). Weather radar has the potential to improve our ability to observe extreme precipitation events and complex storm structures that are often poorly represented by rain gauge networks.

The term "nowcasting" is applied to very short-term weather forecasts. The U.S. National Weather Service (NWS) specifies a forecast time of zero to three hours, though up to six hours may be used by some (AMS, 2000). In this thesis, real-time QPEs by radar are used to

drive a hydrological model. The use of a real-time precipitation product implies that precipitation measurements were reported and corrections to the data were made instantaneously.

2.1 Wavelength Selection

Radar can emit microwaves at a variety of frequency bands and wavelengths. Selection of wavelength depends on the application for which the radar unit is to be used. Table 1 is a summary of the most common types of weather radar bands.

Table 1- Weather radar frequency bands (WMO, 2004)

Band	Frequency (MHz)	Wavelength (m)
S	1500-5200	0.1930-0.0577
C	3900-6200	0.0769-0.0484
X	5200-10900	0.0577-0.0275

Longer wavelengths are less likely to attenuate as they travel through the atmosphere and can therefore measure precipitation at greater ranges. S-band radars are capable of producing reliable measurements at ranges exceeding 200 km. However, longer wavelengths are also less likely to detect light rain or snow events. S-band units are significantly more costly as they require a large antenna (upwards of 8 m in diameter) and a large motor to power it.

C-band radars are often used for short-range observations, as attenuation becomes a problem at greater ranges. X-band radars are commonly used in urban settings where high-resolution data are required over a small area.

2.2 The Radar Equation and Reflectivity Factor

The radar equation is an expression of the power of a radar echo at the input of the receiving antenna of a radar as a function of the range and radar cross-section of a target (AMS, 2000). Many forms of the equation exist. The following equation is known as the "radar equation" and can be used for the detection of a distributed target, such as precipitation, by a monostatic, single-frequency radar system:

$$\overline{P}_r = P_t \frac{G^2 \theta \phi h |K|^2 \pi^3}{1024 \lambda^2 r^2 \ln 2} Z \qquad [1]$$

where, $\overline{P}_r$ is the average signal power of the returned (detected by receiver), [Watts]
P_t is the power transmitted, [Watts]
G is the gain of the radar antenna, [dimensionless]
θ and ϕ are the antenna beam widths in the horizontal and vertical planes, [º]
h is the pulse length of the transmitted signal, [mm]
$|K|^2$ is the dielectric factor for the hydrometeor, [dimensionless]
λ is the wavelength, [cm]
r is the distance to the target, [m]
Z is the radar reflectivity factor, [mm^6/m^3]

Equation 1 assumes that attenuation of the radar beam is negligible (appropriate for S-band radars), the wavelength greatly exceeds raindrop diameter and the cross-section of the radar beam is uniformly filled with rain at the given range (Marshall et al., 1947).

The radar reflectivity Z is a term used to express the sum of sixth powers of diameters of the drops, D, in unit volume, V. The value of Z obtained from a radar sample volume with many raindrops is expressed as:

$$Z = \int_0^\infty N(D) D^6 dD \qquad [2]$$

where, $N(D)\,dD$ is the number of drops per unit volume with diameters in the interval dD

The drop size distribution (DSD) is a simple function of the rain rate, and therefore allows us to determine the rate of rainfall using a simple exponential function or a two-parameter gamma distribution (Marshall et al., 1947; Marshall and Palmer, 1948; Vieux and Bedient, 2004). Equation 3 is known as the Marshall-Palmer (M-P) relation and is the most common relationship used to relate rainfall rates to observed radar data.

$$Z = aR^b \quad [3]$$

where, a and b are the calibration parameters
R is the rain rate, [mm/h]

The parameters a and b are determined through radar calibration with precipitation gauges. The reflectivity factor Z is most commonly expressed in terms of 10 times its base 10 logarithm.

$$dBZ = 10 \log Z \quad [4]$$

2.3 Dual-Polarization

Radar waves emitted from a transmitter generally oscillate parallel to the horizontal axis. The intensity of the radar waves returned is therefore related to the horizontal dimension of the weather target. However, by transmitting waves with different orientations, additional data can be obtained about the weather targets. For example, if horizontal and vertical waves are emitted the differential reflectivity of a hydrometeor can be calculated using the following equation:

$$\mathrm{dBZ_{DR}} \sim 10 \log \left(\frac{\mathrm{P_h}}{\mathrm{P_v}} \right) \quad [5]$$

where, P_h is the returned horizontally-polarized backscattered power received from the horizontally-polarized transmitted pulse, [Watts]
P_v is the returned vertically-polarized backscattererd power received from the vertically-polarized transmitted pulse, [Watts]

When the returned horizontally-polarized backscatter significantly exceeds the vertically-polarized backscatter, Z_{DR} is well above zero, indicating a hydrometeor of oblate orientation (i.e. rainfall). A Z_{DR} value close to zero indicates a spherically-shaped hydrometeor, as found with certain types of hailstones. Some graupel and hail hydrometeors with a conical shape can fall with their major axes oriented in the vertical. In such cases, Z_{DR} is be found to be negative (CIMMS, 2005).

2.4 Doppler Radar

In addition to reflectivity data obtained from conventional radar systems, Doppler radar systems can provide information concerning a weather target's speed and direction. A Doppler radar facility uses a very precise transmitting frequency and a receiver system that is highly sensitive to changes in frequency induced by a moving target (WMO, 2004). These changes in frequency between successive pulses are used to calculate the radial velocity. Radial velocity is the component of the wind going in the direction of the radar (either towards or away). Doppler information is valuable for weather forecasters especially in severe weather where rotation signatures (indicative of risk of tornado) and divergence signatures (indicative of strong downdrafts when observed near the surface) can be identified (MRO, 2006). Doppler radar is accurate up to a range of 120 km.

Another advantage of Doppler data is its usefulness in the removal of false echoes from the observed reflectivity measurements. For example, unlike hydrometeors, ground clutter and anomalous precipitation (later described in Sections 2.7.1 and 2.7.2, respectively) are stationary relative to the radar station and can be clearly identified by Doppler instruments (Einfalt and Semke, 1997). Signals returned from targets with a radial velocity of zero are identified as clutter and removed from the raw reflectivity data.

2.5 The PPI and CAPPI

The Plan Position Indicator (PPI) is a type of radar display created from a single elevation angle scan. The amalgamation of all PPIs measured by a radar system represents its volume scan.

The Constant Altitude Plan Position Indicator (CAPPI) is a horizontal cross-section of the radar volume scan created from PPIs. This image displays the intensity of echoes identified by the radar for given altitude. Figure 1 is an example of a CAPPI image from the J.S. Marshall Radar Observatory. The 1.5-km CAPPI image is the view most commonly displayed by television stations and Environment Canada for public viewing. However, the 1.5-km height is only true for a distance of approximately 90 km from the radar (Bellon et al., 2006). At further ranges, data from the lowest elevation scan exceed this height and are used in its place. The scale on the right allows the user to associate signal intensity with rainfall intensity. In general, a measured reflectivity is associated with a precipitation type and intensity, as shown in Table 2.

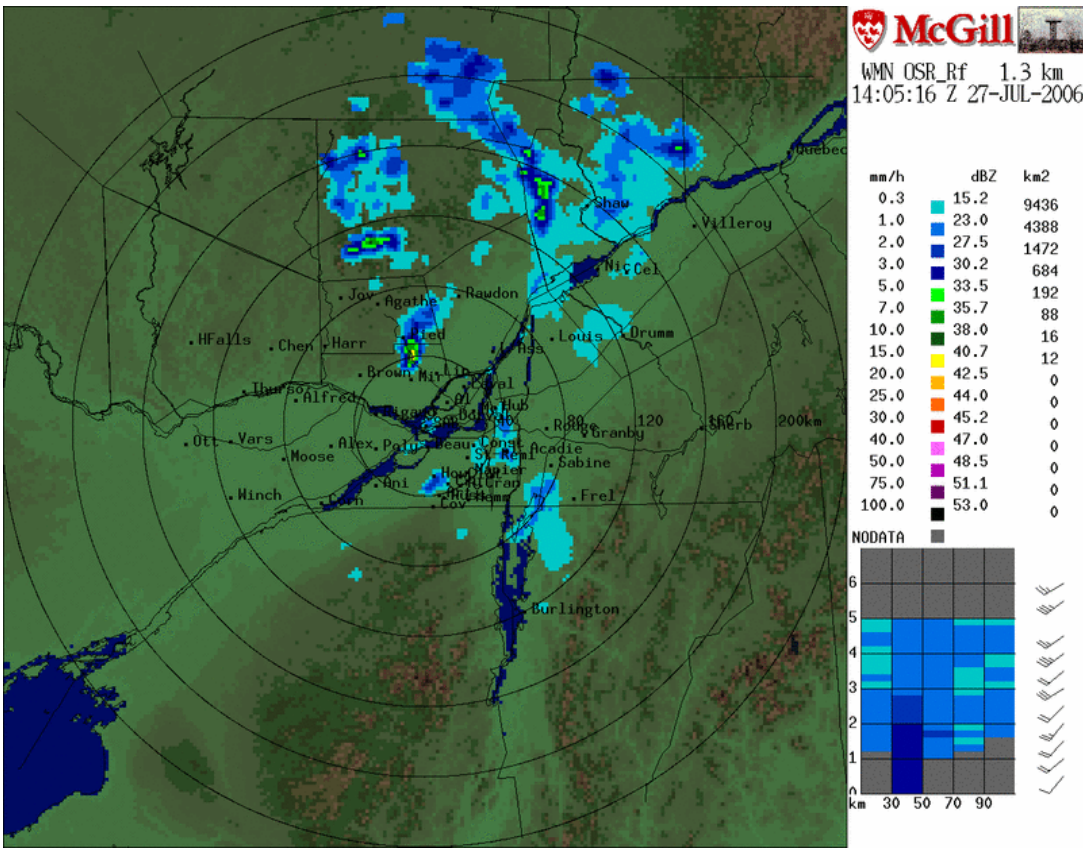

Figure 1- 1.3 km CAPPI from McGill radar station (MRO, 2006)

Table 2- Interpretation of the McGill radar reflectivity scale (MRO, 2006)

Precipitation Type	Precipitation Intensity	Reflectivity (dBZ)
Drizzle or clear air targets (bugs, etc.)		0
Very light rain or snow	A few raindrops or snowflakes	10
Light rain or snow	Typical of spring/fall: 1-2 mm/hr	25
Moderate precipitation	Strong for spring/fall: 5 mm/hr	35
Heavy rain	Summer showers: 20 mm/hr	45
Very heavy rain or hail	Peak of thunderstorms: 100 mm/hr	55

2.6 Vertical Profile of Reflectivity (VPR)

The vertical profile of reflectivity (VPR) is a vertical cross-section of the scanned radar volume. An azimuthally averaged VPR is often displayed with a CAPPI image, as shown in the lower right-hand corner of Figure 1. Five VPRs are shown for the 10 to 110 km interval, each over a 20-km range. The vertical resolution is 0.2 km. This information allows the user to determine the type of weather being sampled by the radar for a given range and CAPPI elevation (rain below melting layer, mixed precipitation within the melting layer or snow above the melting layer). The VPR is further discussed in Section 2.7.5.

2.7 Problems Associated with QPEs

Weather radar measures precipitation indirectly using reflectivity measurements from varying elevations and precipitation types. It is therefore a great challenge to use these data to determine the amount of precipitation that occurs at ground surface. The following section describes some of the most common obstacles faced by radar meteorologists when producing QPEs. Table 3 is a summary of the errors associated with radar precipitation accumulations as noted by Fabry (2004).

Table 3- Error associated with hourly radar accumulations over a 100 km^2 area at 120 km, with 5-min accumulations over 1 km^2 at 30 km in curly brackets (Fabry, 2004)

Nature of error	Magnitude estimate	Magnitude after correction	Comments	Knowledge of magnitude estimate	Knowledge of error after correction
1a. Variability in transmit power	? (small until failure?)	Small if correction is regularly updated?	Estimated by power measurement	Good to poor (system specific)	If it exists, knowledge is not well disseminated
1b. Poorly known characteristics of components (antenna, filters)	~ 15%	Small?	Corrected by solar calibration and external methods (clutter strength, gauges…)	Poor per se, but extremely slow time evolution helps	Not a major issue?
1c. Receiver miscalibration, non-linearity	15-20% (time varying bias)	Small if correction is often updated	Corrected by solar calibration, clutter strength methods, gauge adjustments	Approximate (Joe & Smith, 2001)	Not a major issue?
2a. Wet radome attenuation	Can be large (>50% at C-band)	?	Extremely difficult correction by clutter strength because of azimuthal dependence	Poor	Poor
2b. Beam blockage	Site specific biases	Small in flat terrain if well done	Good site survey needed; problematic in mountains	Very good to poor (site specific)	Good to poor; OK in flat terrain
2c. Path attenuation (gas)	20% bias {5% bias}	Small if well done	Well understood but generally not properly corrected for (~25% of error is left on average)	Very good	Correction dependent
2d. Path attenuation (precipitation)	Possibly huge bias	Possibly huge	Extremely difficult correction (many variations)	Fair (S-band) to very poor (X); site specific	Good to very poor; major error source
2e. Ground target contamination	Variable, site specific	Tolerably small if well done	Corrected by Doppler and/or texture methods	Good	Fair to poor
2f. Echo fluctuations	<1% noise {5% noise}	<1% {2%}	Reduced by taking storm advection into account	Very good	Good
3a. Converting Z aloft to R aloft	30% noise {50%}	5% ? {10%?}	Correction requires gauge/DSD info.	Fair, site and event specific	Poor
3b. Vertical profile correction	0-140% {0-50%} bias	25% {10%?}	Strong dependence on 0°C level; many elevations required	Good to fair	Fair to poor; major error source
3c. Precipitation drift	<5% noise in rain {5-50%}	<2% {5-20%}	Largest for snow and tiny basins; event specific	Fair to poor	Poor
3d. Simplistic calculation of accumulation	1-4% noise {25-100%}, event specific	<1 % {5-25%}	Reduced by taking storm advection and evolution into account	Fair	Fair

2.7.1 Ground clutter

Ground clutter is the result of the interception of radar waves by a permanent object such as tall building, tree or hill. These false echoes appear consistently in the reflectivity data collected by the radar. Although removal of ground clutter is often easily achieved, reflectivity data for areas shadowed by the object are lost.

2.7.2 Anomalous Precipitation (AP)

Radar waves travel along a curved path due to the refraction caused by atmospheric gases. The radius of curvature of the path is approximately four-thirds the mean radius of the Earth. Sharp vertical moisture gradients can cause additional refractive bending and lead to false measurements of precipitation known as AP. The term "ducting" is often used when the radar beam is bent downwards and is intercepted by the ground surface. A strong signal is returned to the radar and may be misinterpreted as intense precipitation. Ducting is common during strong temperature inversions when cool moist air exists at low-levels and warmer and drier air exists above. This generally occurs during the early morning hours following a clear night as air aloft warms with the rising sun and air near the surface remains cool. An example of a radar image contaminated by AP is shown in Figure 2.

Similarly, trapping occurs when the radar beam is sharply bent upwards, often overshooting precipitation or taking measurements at higher elevations than intended. The meteorological conditions for the occurrence of AP can be determined mathematically (WMO, 2004).

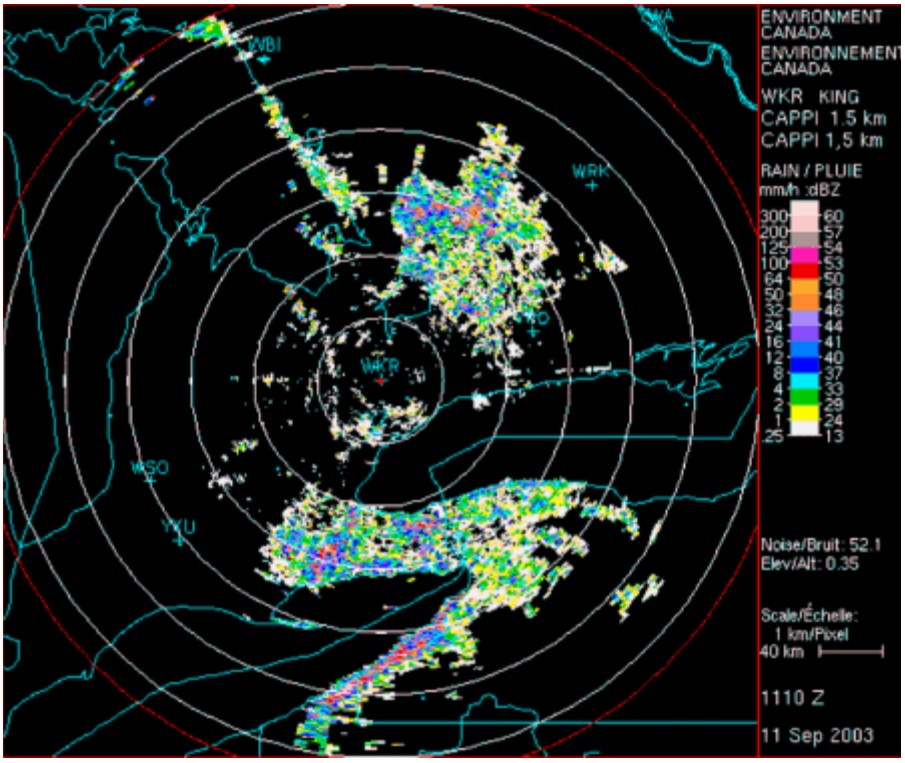

Figure 2- CAPPI with AP contamination (EC, 2003)

2.7.3 Virga

Virga is precipitation detected by the radar that does not reach ground surface. When dry conditions exist near the surface, it is possible for precipitation to evaporate before reaching the ground. Since radar measurements are taken at elevations exceeding 1-km, reflectivity measurements taken aloft will overestimate precipitation under such conditions, sometimes detecting precipitation in areas where none has occurred.

2.7.4 Bright Band

Since air temperature varies with altitude, precipitation in the atmosphere can exist in several forms. Precipitation exists as snow (or ice) above the 0ºC elevation, and as rain below it. However, a few hundred meters below the freezing level, a layer of water forms around snowflakes as they begin to melt. Since water is far more reflective than snow, the

hydrometeors in this region appear as large raindrops and produce large reflectivity values. This melting layer, also known as the bright band, may be of the order of 200 m in thickness (Fabry et al., 1992). Contamination of radar data by bright-band precipitation may lead to an overestimate (up to a factor of 5 or 6) of precipitation (Collier, 1989). Figure 3 is an image taken from a vertically-pointed radar. The region of intense reflectivity found between the elevations of 2 to 3 km above ground surface clearly indicates the location of the bright band on November 1st, 2004.

The height of the bright band varies seasonally: it is highest in the summer, often non-existent during the winter. However, the bright-band shape, strength and thickness can vary from storm to storm and even within storms (Fabry et al., 1992). Short term variations in the melting layer, as demonstrated by the discontinuity of the bright band in Figure 3, can be caused by changes in the vertical velocity, such as sudden updrafts. During periods of deep convection, the vertical profile of reflectivity tends to be somewhat uniform and there is never a clear reflectivity signature associated with the melting layer (Fabry et al., 1992; Fabry and Zawadzki, 1994; Berne et al., 2005).

Identification of the bright band region is crucial when processing radar data so as not to mistake intense reflectivities from the melting layer as regions of intense precipitation. Collier (1989) stated that significant improvement of radar data affected by the bright band can only be achieved using methods based on the vertical profile of reflectivity (VPR).

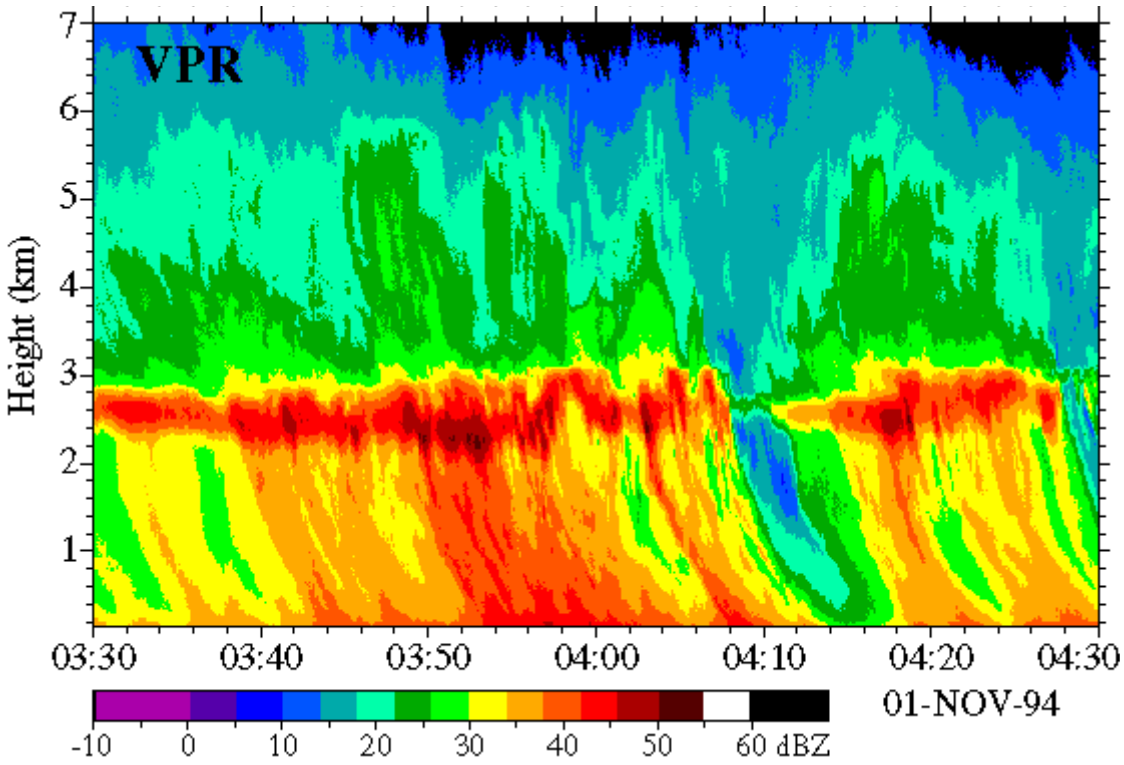

Figure 3- Reflectivity from a vertically-pointed radar (MRO, 2006)

2.7.5 Range or VPR Effects

A radar beam widens as it travels away from the station, resulting in an increase in sample volume with an increase in distance. For example, a beam width of 1º widens to approximately 1.6 km at a 100-km range. At a distance of 200 to 300 km, the beam may have spread to 3 to 5 km in extent (Potter and Colman, 2003). At the same time, the centre of the radar beam increases in height with increased distance (depending on its elevation angle). Thus, the measured reflectivity is a weighted average within the beam volume with the radar beam centered at a certain height above the ground (Bellon et al., 2005). At great distances, the radar takes large samples of the atmosphere at heights well above the earth that may not be representative of conditions at ground surface. Additionally, within a large sample volume, several types of precipitation may exist, especially if the sample is contaminated by the bright band.

Because range variability implies height variability, range effects are most often attributed to the vertical profile of reflectivity (VPR), especially in cases where attenuation of the radar beam is negligible (S-band radar). Therefore "range" and "VPR" effects can be used interchangeably (Bellon et al., 2005). VPR effects are more pronounced in cold months as winter storms tend to be shallower in vertical extent with larger vertical reflectivity gradients (Seo and Johnson, 1997).

2.7.6 Attenuation

Microwaves weaken as they pass through the atmosphere. A portion of the energy is scattered when the waves encounter precipitation particles, and a small amount is absorbed by the atmosphere and converted to heat. Since attenuation of the radar beam is proportional to the inverse square of the wavelength (Potter and Colman, 2003), shorter wavelength radiation suffers more from attenuation than longer wavelength radiation. Table 4 shows the relative power loss due to attenuation experienced by varying wavelengths for different rainfall rates.

Table 4- Distance (km) over which precipitation must extend to give an attenuation of 10dB (WMO, 2004)

Band	Wavelength (m)	Rate of rainfall (mm/hr)				
		1.0	5.0	10.0	50.0	100.0
S	0.1	33000	6600	3300	600	300
C	0.057	4500	690	310	47	21
X	0.032	1350	164	66	8	3.2

2.7.7 Estimation of the Z-R Relationship

Improper estimation of the Z-R relationship may be the greatest source of error in the generation of QPEs. Firstly, rain gauge data are often used to estimate the *a* and *b* parameters of Equation 3. Values of *a* and *b* are selected to minimize the error observed between radar-estimated and gauge-measured precipitation values. However, the sampling differences between the radar and rain gauge data may be too great to allow direct comparison between measurement methods. Section 4.1 further discusses this problem. Secondly, uncertainties in the derivation of the local Z-R relationship are sometimes attributed to improper radar calibration and contamination of radar data by false echoes, bright-band and range effects. Lastly, the high variability in the distribution of raindrop size and precipitation type over time and space can severely hinder the efforts to find an optimal Z-R relationship that can be applied over the entire radar domain at all times.

Lee and Zawadzki (2005) demonstrated that the variability of drop-size distribution (DSD) determines the theoretical limit of the precision of precipitation measurement by radar. Using 5 years of reliable disdrometer data, it was shown that the DSD of precipitation for the Montreal area can vary significantly on a day to day basis, between storms on the same day or within a storm itself. The DSD's variability leads on average to a random absolute

error of 41% in instantaneous rain-rate estimation. It has been suggested that the application of different Z-R relationships for different types of precipitation (i.e. classified by synoptic information, polarimetric data etc.) to different types of precipitation may drastically improve operational estimation of rainfall by radar (Lee and Zawadzki, 2005; Seed et al., 1997). Atlas et al. (1997) stated that it is an exercise in futility to apply any single Z-R relationship to a point in the space-time domain.

Hirayama et al. (1997) attempted to eliminate radar-rain gauge scale differences by using run-off analysis to select the optimal Z-R relationship over a basin. Although results seemed promising, scale issues remained in the selection of basin size that should be used for analysis.

2.7.8 Scanning Frequency

Radars scan the atmosphere at regular intervals. The cycle time refers to the time required for the radar to perform scans for all specified elevation angles. Weather radar systems typically complete a volume scan within four to fifteen minutes. In convective situations where the average life expectancy of a thunderstorm is likely to be of the order of 20 to 30 minutes, a 15-minute scanning cycle will impose severe constraints on the accuracy of the radar data (Seed et al., 1997). However, from a financial point of view, one must weigh the gain in accuracy of a given sampling strategy with the costs of its hardware implementation and the necessary logistics required to take advantage of the higher resolution data (Fabry et al., 1994).

2.7.9 Wind drift

Precipitation sampled by a radar scan may travel a significant distance before arriving at ground surface. The effects of wind drift may be insignificant for low resolution data sets, where grid sizes exceed the possible drift distance of hydrometeors, but becomes increasingly important with high resolution data (i.e. less than 1 km). Fabry et al. (1994)

demonstrated the importance of considering the effects of wind drift when producing rainfall accumulation estimates. Fabry et al. (1994) stressed that maps of instantaneous rainfall should not simply be summed; the evolution and movement of a storm between sampling intervals must be considered. In the hydrological modelling of small basins, the effects of wind drift can result in gross under or overestimations of runoff. For example, if radar data indicate that a storm exists above a small basin, wind drift may cause the precipitation to entirely overshoot the basin. Conversely, precipitation from a storm outside a basin may, in reality, fall within basin boundaries. Even with a sampling time as short as 5 min, the error in hourly accumulations for 250 m grid size data set can approach 40% when accumulation are improperly computed (Fabry et al., 1994).

3 The McGill Radar

The J.S. Marshall Radar Observatory (Figure 4) is owned and operated by McGill University. It is located on the university's McDonald campus in Ste-Anne de Bellevue, approximately 30-km west of downtown Montreal, Quebec. The station is part of the Canadian Radar Network and is used by Environment Canada's Montreal Region Meteorological Office for real-time weather monitoring.

Figure 4- J.S. Marshall Radar Observatory (Infoscan, 2006)

The radar station is equipped with a dual-polarization, Doppler, S-band scanning system. With its 9 m antenna sitting on top of a tower, the S-band radar is the largest weather radar in Canada and one of the most sophisticated weather radars in the world (MRO, 2006). The radar measures the intensity, velocity, and shape of weather targets within a 250-km radius of the station.

The radar scans the atmosphere using a regular scanning strategy. Data are collected at 24 elevations angles (from 0.5° to 34.4°) every 5 minutes. This fast cycle time makes this radar particularly well suited for studying rapidly evolving severe weather events (MRO, 2006). Due to the radar's location in the shallow valley of the St. Lawrence River, reflectivity data are heavily contaminated by ground clutter and anomalous propagation (Bellon et al., 2006).

3.1 McGill Radar Products

Precipitation information from radar data is usually obtained from low-level CAPPI maps. However, many of the problems described in Section 2.7 render data for certain altitudes useless and can result in data gaps in areas affected by bright-band or beam blocking. Zawadzki (2001) suggested that in order to obtain the best estimate of surface rainfall rate, it may be necessary to depart from the constant altitude (CAPPI) or constant angle elevation (PPI) maps. Instead, the reflectivity over each pixel should be at an optimal height selected on the basis of ground echo, shadow and VPR consideration.

The McGill Radar data Analysis, Processing and Interactive Display (RAPID) System uses reflectivity, velocity and polarization data to generate various radar products. As part of the Enhanced Nowcasting of Extreme Weather project, four 1-hour rainfall accumulation products are tested; C0, C1, C2 and C3. Each product uses a different vertical profile of reflectivity (VPR) correction method to estimate rainfall within a 240-km x 240-km area. Products available at both 1- and 2-km resolutions are created in real-time. Sections 3.1.1 to 3.1.4 are summarized descriptions of each product as given by Bellon et al. (2006). Figure 6 (following Section 3.1.4) compares the generated 1-hour rainfall accumulation maps for each product for June 15th, 2002 at 22:00 GMT.

3.1.1 C0- VPR Uncorrected

The C0 product has no VPR correction applied. The data within the 5-minute CAPPI accumulations (usually at a height of ~1.3 km) are filtered to remove ground clutter and AP then integrated over a 1-h interval to produce an hourly rainfall accumulation map. Since the average speed of precipitation for the Montreal area is approximately 50 km/h (Bellon et al., 2005) accumulations based on the 5-minute data are performed using the method suggested by Fabry et al. (1994) to account for the effects of wind drift.

3.1.2 C1- Correction of 1-h Accumulations

The C1 product applies a VPR correction to the 1-h accumulation map generated as described for the C0 product, using CAPPIs centered at 2 km. Five VPRs, each 20-km in range, between the distances of 10 and 110 km from the radar are derived from the 24 elevation angles. A range-height correction factor in units dbZ is calculated for each of the computed VPRs as described by Bellon et al. (2005). Each correction factor is converted into a rainfall rate factor and interpolated in range at every kilometre. The rainfall rate factor calculated for each pixel is applied to the 1-h accumulations to produce the final C1 product.

3.1.3 C2- Optimum Surface Precipitation (OSP)

The C2 method aims to make use of information that is lost by applying a VPR correction subsequent to the accumulation process. The VPR can change rapidly over space and time, notably in periods less than 1-hr (Fabry and Zawadzki, 1995; Fabry et al., 1992). Therefore, the C2 method uses VPR correction factors that are derived over a shorter period (typically 30 to 45 minutes). Correction factors are applied to each 5-minute volume scan prior to accumulation.

In convective situations, the vertical profile of reflectivity of showers observed using a vertically pointed radar are shown to have constant reflectivity up to 1 km from echo top. Even in deep convective systems associated with thunderstorms and squall lines, strong reflectivities extend several kilometres up and there is never a clearly defined bright band (Fabry and Zawadzki, 1995). Therefore, convective pixels are identified and excluded in the derivation of the space-time averaged VPR. They are not corrected for the VPR.

Furthermore, Lee and Zawadzki (2005) suggested that most of the error associated with the calculation of rainfall rate from radar reflectivity is caused by the systemic change of DSD variability between physically homogeneous processes. Therefore the McGill radar uses different Z-R relationships for stratiform ($Z=200R^{1.5}$) and convective pixels ($Z=300R^{1.4}$).

3.1.4 C3- Climatological Correction

A climatological correction implies that corrections to the VPR are performed based on VPRs that are generated using data collected over large areas for an extended period of time. The C1 and C2 products suffer when an insufficient amount of precipitation is detected with a 90-km range to derive a VPR. Climatological VPRs, however, are independent of the real-time observed VPR and can be applied at any time.

Bellon et al. (2005) used a data set of 287 hours of extensive stratiform precipitation in the Montreal area in order to compute climatological profiles, shown in Figure 5a-c. Each profile represents the most likely reflectivity for a given height relative to the bright band, based on the reflectivity measured aloft. The C3 product relies on the Rapid Update Cycle (RUC; NOAA, 2006) model to produce information concerning the height of the 0ºC isotherm. Climatological corrections factors for 1-hour accumulation maps are calculated using the most appropriate curve for a given range, height (relative to bright band) and observed mean reflectivity.

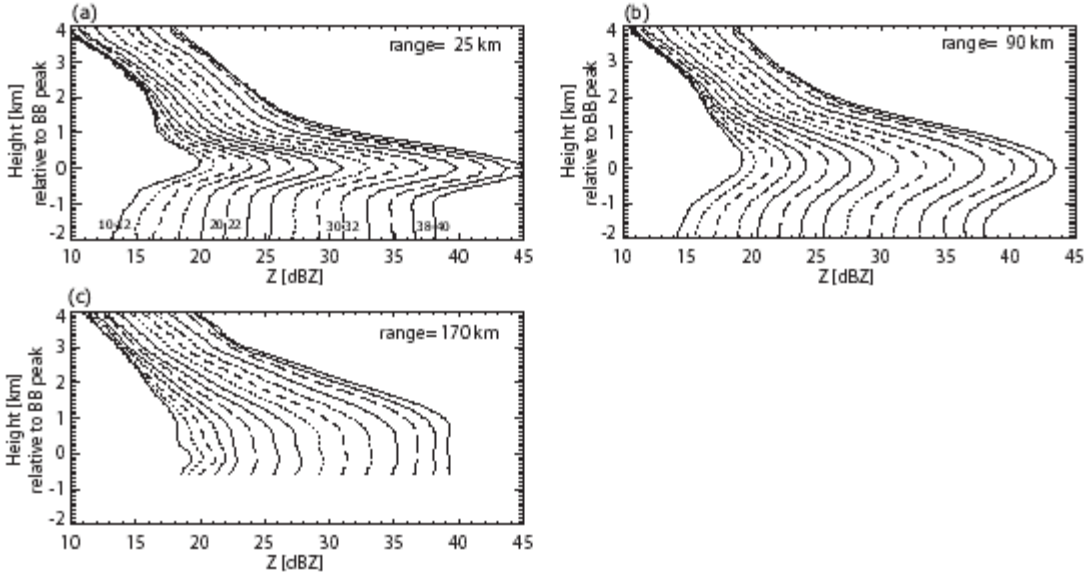

Figure 5- Climatological VPRs derived for various ranges (Bellon et al., 2006)

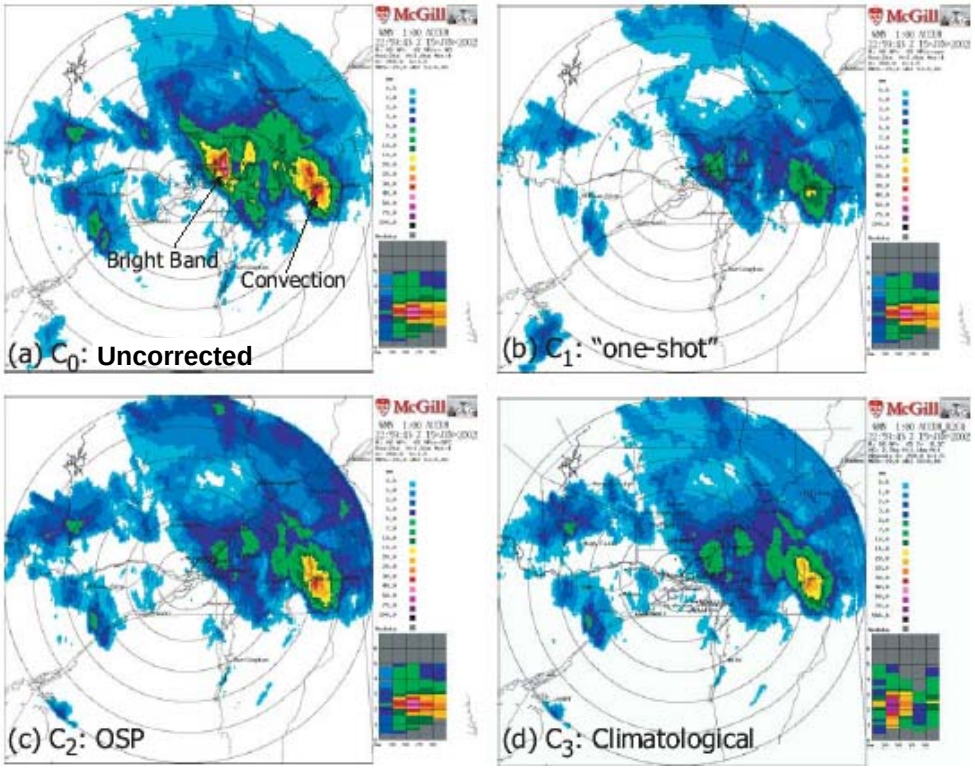

Figure 6- Comparison of each radar product for June 15th, 2002 at 22:00 (Bellon et al., 2006)

4 Precipitation Gauges

Precipitation gauges are typically used for calibration *and* validation of radar precipitation measurements. It is therefore imperative to address the shortcomings of this technology. A precipitation gauge measurement represents a point location. Given that rainfall can vary substantially over small distances, the assumption that a single gauge value accurately defines precipitation over any given area may not be true. Records have shown differences of 20 percent or more in the catch of rain gauges less than 6-m apart (Viessman and Lewis, 1995). For hydrologic purposes, spatial precipitation patterns over a watershed are determined using various distribution techniques such as the isohyetal and Thiessen methods. The major limitation of such methods, however, is that the estimation of rainfall for any given area never results in values greater than the largest amount observed or less than the smallest (Kouwen and Garland, 1989). The ability of a precipitation gauge network to accurately represent storms is highly dependent on gauge density. It has been shown that an increase in gauge density can significantly improve the spatial definition of rainfall and consequently lead to improved hydrologic simulation (St-Hilaire et al., 2003).

Precipitation gauges used in this study are of two types: tipping bucket and weighing type gauges. Although rain gauge observations are considered to be as close as possible to the true rainfall estimate with the present technology (Krajewski, 1997), precipitation gauges can also suffer from measurement inaccuracies. For example, wind effects generally reduce the amount of water collected by gauges. Improper site selection can result in wind and precipitation patterns that may not represent precipitation falling on the surrounding area (WMO, 2004; Krajewski, 1997; Viessman and Lewis, 1995).

Tipping bucket rain gauges are limited to measuring liquid precipitation only (i.e. rain). The World Meteorological Organization's Guide to Hydrological Practices (6th edition) lists the following disadvantages of the tipping bucket rain gauge, but suggests that for many

hydrological purposes, in particular for heavy rain-fall areas and flood-warning systems, 0.5 to 1.0 millimetre buckets are satisfactory:

- The bucket takes a small but finite time to tip, and during the first half of its motion, the rain is being fed into the compartment already containing the calculated amount of rainfall. This is applicable only in heavy rainfall.

- With the usual design of the bucket, the exposed water surface is relatively large. Thus, significant evaporation losses can occur in hot regions. This will be most appreciable in light rain.

- Because of the discontinuous nature of the record, the instrument is not satisfactory for use in light drizzle or very light rain. The time of beginning and ending of rainfall cannot be determined accurately.

Weighing gauges can operate year-round if anti-freeze is used during cold temperatures to prevent the stored water from freezing and to melt frozen precipitation. As well, evaporation losses can be minimized by adding enough oil to the storage unit to form a continuous layer on top of the collected rainwater. Since precipitation is measured through changes in weight of accumulated precipitation in its storage chamber, strong winds can cause the gauge to vibrate and result in noisy data.

4.1 Correction of Radar Data Using Precipitation Gauge Measurements

Precipitation gauge data are commonly used to adjust radar measurements prior to use in a hydrological model. Rain gauges provide an independent source of measurements that are useful for correcting systematic errors in the radar accumulations, yet should not be considered as ground truth (Vieux and Bedient, 2004). Typically, radar rainfall estimates are compared to rain gauge data at a certain accumulation time-step (hourly, daily, storm total etc.) to estimate a mean field bias (MFB) coefficient, which is subsequently applied

uniformly across the domain (Borga, 2002; Vieux and Bedient 2004). The MFB coefficient is determined using the following equation:

$$MFB = \frac{\sum_{i=1}^{N_S} G_i}{\sum_{i=1}^{N_S} R_i} \quad [6]$$

where G_i and R_i are the corresponding rain gauge and radar cell daily rainfall values for each precipitation gauge station i, and N_s is the number of stations for a given day. Other methods, such as Brandes method, are widely accepted as methods of correcting radar data. It has been shown that adjustment of radar data using precipitation gauges can significantly improve hydrologic model results (Borga 2002; Velasco-Forero, 2005). In convective rainfall calibration has on average a smaller effect, although it may have a large effect in individual cases (Collier, 1986).

4.2 Radar-Gauge Comparisons

The accuracy of radar-estimated precipitation data is most often evaluated based on direct comparisons with precipitation gauge data. Separate data sets should be used for correction and validation of radar data. Scatter plots, such as those shown in Figure 7, are typically used to show the correlation between radar and rain gauge accumulations for each rain gauge location. Perfect agreement between data sets would result in a plot in which all data points fall along the 1:1 line, indicating a perfect correlation. In reality, a high degree of scatter is observed and scatter plots can be misleading or difficult to interpret.

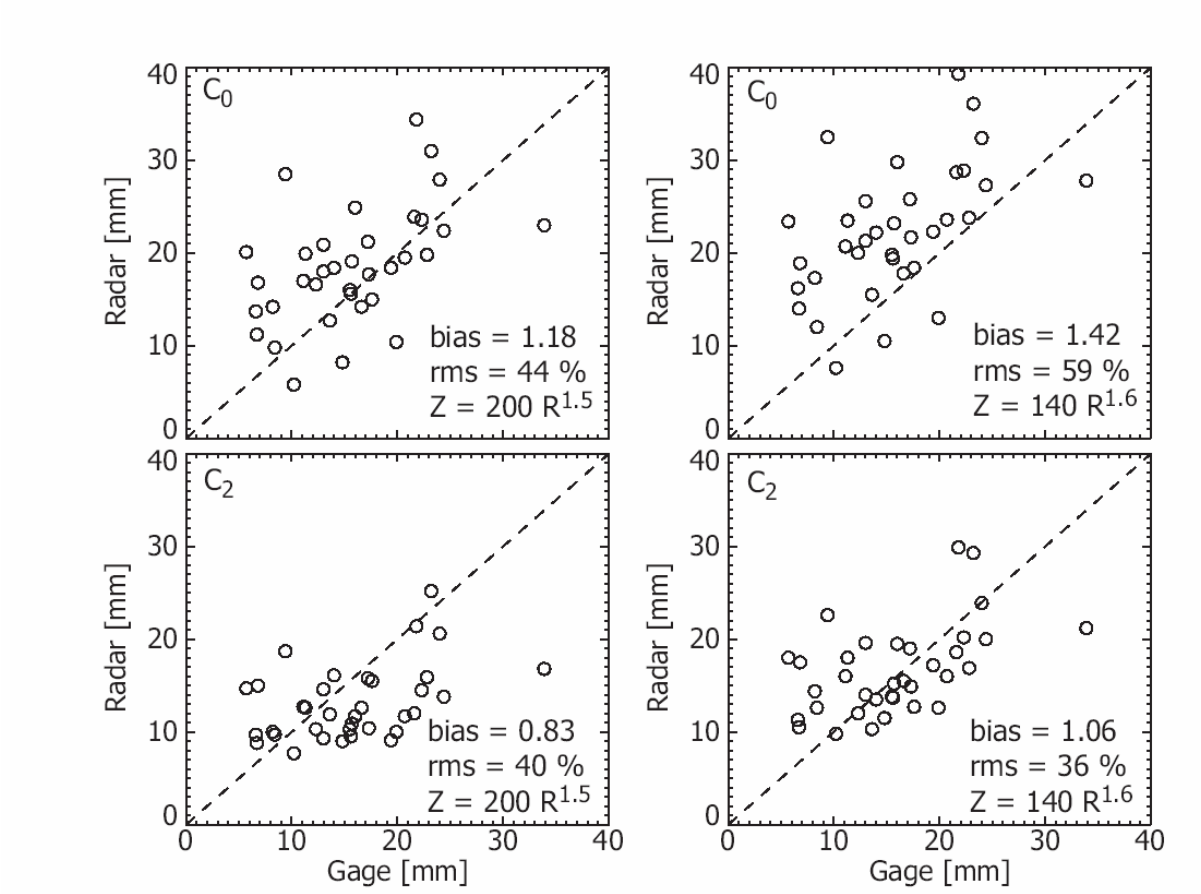

Figure 7- Example of radar-rain gauge scatter plots, 24-hr accumulations (Bellon et al., 2006)

As described in Section 4, rain gauge measurements are rarely without error. An intense rainfall event with high wind velocities may be lead to significant undercatchment in precipitation gauges. It is difficult to determine using scatter plots alone which instrument miscalculated rainfall.

The most important consideration when comparing radar and precipitation gauge measurements is their difference in sampling techniques. A precipitation gauge measures the volume of precipitation that falls at ground surface within a given period of time, for a single point location. Weather radar, however, measures the instantaneous reflectivity from

a volume of atmosphere over a defined area (i.e. a 1 km grid cell). The Z-R relationship (Equation 3) is used to estimate a rainfall rate which is integrated over cycle time to calculate rainfall accumulation. Since rainfall can vary drastically over short distances, rainfall amounts calculated using either technology may not agree, yet each may be accurate in their own right. Therefore it is likely that direct comparison between radar and precipitation gauge accumulations provides little information on radar's ability to properly represent precipitation quantitatively or qualitatively over a given area.

Krajewski and Smith (2002) stated that to eliminate the effects of random factors on bias identification, radar rainfall and rain gauge rainfall accumulations should be integrated over a certain time scale. If the time scale is too short (i.e. 15 min), the spatial variability of rainfall will mask the bias. However if the time scale is too long, seasonal effect may be mixed.

4.3 Montreal Mesonet

In this study, precipitation estimates from the J.S. Marshall Radar Observatory are compared with measurements from several surrounding precipitation gauges. The Montreal Mesonet is a co-operative network of meteorological stations managed by the University of Laval, McGill University and Environment Canada. It was created to support meteorological and hydrological research and is used as a data source by Environment Canada and Hydro-Quebec. Forty-two stations are located within approximately a 100-km radius of the city of Montreal in Quebec. Thirty-seven stations are equipped with tipping bucket rain gauges, and twelve are equipped with weighing gauges. Figure 8 shows the location of each mesonet station. All stations are located in Canada.

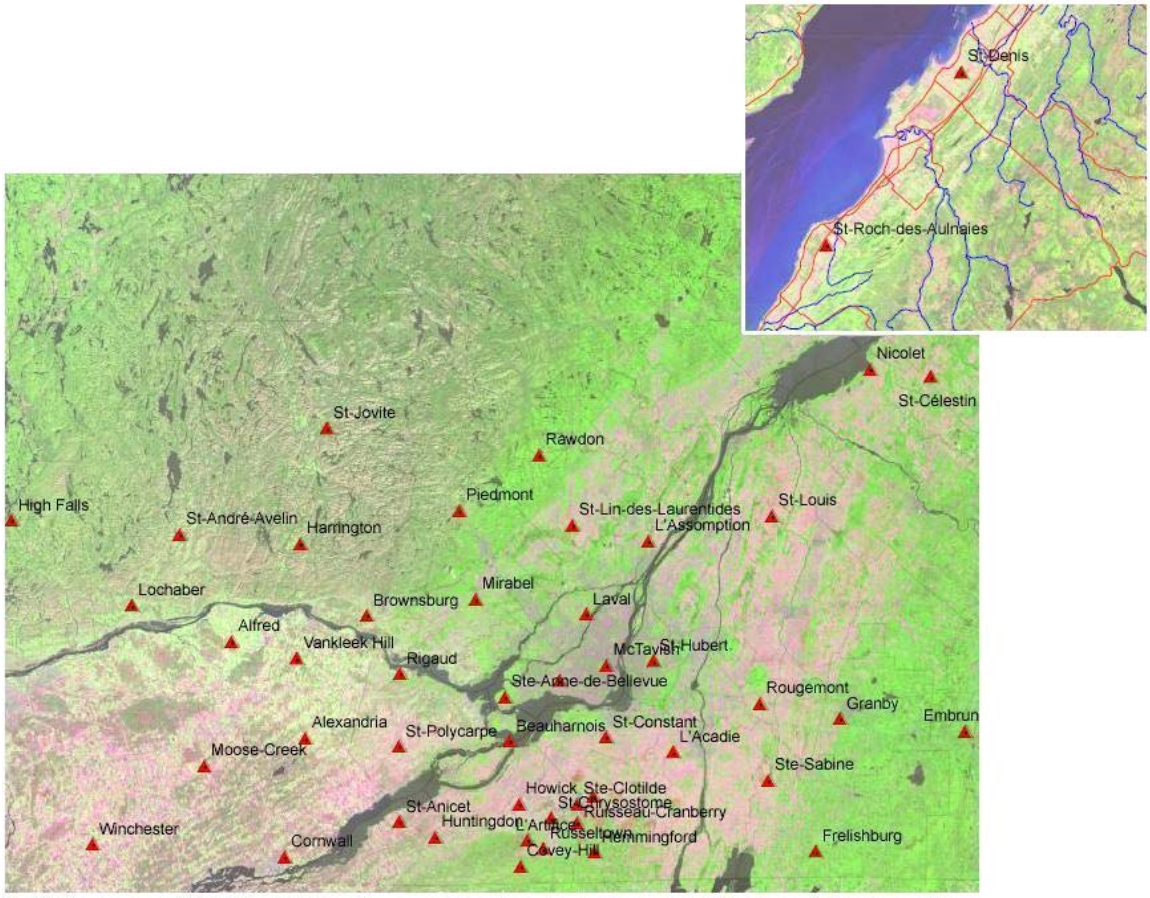

Figure 8- Meteorological stations of the Montreal Mesonet (Mésonet Montréal, 2006)

5 Radar Hydrology

With the availability of digital radar data, hydrologists immediately recognized the potential for radar to provide very detailed precipitation information over entire basins. However, to date, operational hydrologists have found radar measurements to be of marginal use due to the numerous corrections required by data sets. Even with corrections applied, the mean errors in real-time radar estimates of rainfall over a river basin typically range between 20 and 30% (Collier, 1989; Joss and Lee, 1995). Since watershed response to rainfall is non-linear and largely dependent on antecedent conditions, errors in rainfall estimations from a particular storm can have varying effects on flow predictions. In continuous hydrological modelling, errors can accumulate over time. For example, several periods of light rain or snow that go unreported can have a substantial cumulative effect on the watershed's response to a larger event following this light rain (Kouwen et al., 2004). For hydrological modelling purposes, it is not sufficient for a radar system to perform well "on average". The algorithms used to convert raw radar data to precipitation estimates must be robust enough to handle various meteorological conditions and synoptic events observed throughout the radar domain.

In this thesis, real-time precipitation products are evaluated using the WATFLOOD hydrological model. Each precipitation input is evaluated based upon the quality of model output it produces. Using a watershed as sample area can reduce the error associated with sampling differences between radar and precipitation gauges and allow for the evaluation of a precipitation product over space and time. As with any measurement, uncertainty in precipitation estimates results from two types of error: random and systematic. Hydrologic prediction error depends heavily on systematic error (Vieux and Bedient, 2004). This is especially true in the modelling large basins, as random errors in precipitation tend to cancel each other out over large areas.

However, a hydrological model may introduce its own errors in converting rainfall to streamflow and the uncertainty associated with model parameters. A hydrological model must properly compute a basin's delayed response to precipitation due to storage and the return of water to the atmosphere (Kouwen, 2006; Joss and Lee, 1995). Nevertheless, a hydrologic model is seen as a useful tool for evaluating radar precipitation products and allows the user to identify the systematic errors present within the data.

Today, many hydrological models, such as WATFLOOD, have advanced to the point where precipitation errors exceed modelling errors (Kouwen et al., 2003). Hydrologists have improved rainfall-runoff models to have real-time capabilities and fully use spatially detailed information. In fact, the full efficiency of distributed hydrologic modelling cannot be achieved without distributed input data that is accurate. Rainfall input errors are known to be a major limitation in any hydrologic forecasting scheme (Vieux and Bedient, 2004).

5.1 Overview of Weather Radar in Hydrology

From 1977 to 1985, the United Kingdom's North West Radar Project (NWRP) established the first unmanned radar station in the country, producing precipitation radar data in real-time (Collinge, 1987). One of the major objectives of the project was to incorporate real-time weather radar data into an operational flood forecasting system (Cluckie and Owens, 1987). The completion of the project was marked by the Weather Radar and Flood Forecasting symposium at the University of Lancaster in September 1985. At the symposium, Collier (1987) suggested that calibrated radar estimates of rainfall are better than estimates made using telemetry gauges alone, most notably for frontal precipitation events. Collier recognized the limitations of the technology, such as range, bright band contamination and the possibility of inappropriate calibration. The importance of quality control to avoid gross errors in flow predictions was stressed.

Walsh and Lewis (1987) suggested ways in which hydrological data collection and manipulation in real-time should be integrated with meteorological information as part of

an efficient communication network to benefit water resources. Similarly, Ryder and Collier (1987) noted how the very effective partnership between the United Kingdom's Meteorological Office and some sections of water industry played a crucial role in the development of the UK Weather Radar Network. The potential for the use of quantitative precipitation estimated from a network of weather radars, particularly for use in flood forecasting, was clearly established (Douglas and Dobson, 1987; Cluckie and Owens, 1987; Moore, 1987).

However years later, at the 1997 Weather Radar Technology for Water Resources Management conference in Sao Paolo, Brazil, Einfalt and Semke (1997) noted that little progress had been made to produce reliable quantitative radar data. They pointed out that although significant advancement had been achieved in the individual fields of hydrological modelling and radar meteorology, a lack of standards governing the usage of radar products for hydrological purposes inhibited the operational use of radar data, especially amongst those that are unfamiliar with the technology. Einfalt and Semke (1997) also stated that interdisciplinary approaches are required not only for research and standard-setting but also for informing potential users about achievable benefits.

At the Sixth International Symposium on Hydrological Applications of Weather Radar in 2004, Fabry (2004) expressed the opinion that the lack of progress in producing QPEs with useful accuracy is largely due to the fact that the radar community as a whole has not done a proper job of quantifying the radar errors. Kouwen et al. (2004) stated that after more than 30 years of research, the word 'promising' is still used too often when radar data are applied for hydrological purposes. The sources of error associated with rainfall estimates have been well characterized and little original work is left to be done in the field of radar meteorology, except for the painstaking detailed validation and description of the errors (Fabry, 2004).

5.2 Review of Hydrologic Modelling Studies Using Radar QPEs

Researchers at McGill University's J.S. Marshall Radar Observatory have developed algorithms that create radar precipitation products in real-time (Section 3.1). These products represent best estimates of precipitation reaching the ground and are developed for use in hydrological models. The goal is to generate a product that eliminates the need for hydrologists to perform rigorous data correction and quality control schemes. Particular focus was placed on the correction of range effects.

Several studies have demonstrated that range effects can significantly impact hydrologic model results (Innes, 2001; Borga, 2002; Neary et al., 2004; Berne et al., 2005; Ding et al., 2005). It has been shown that at far ranges, radar tends to under-predict precipitation amounts as information is lost due to beam height and increase in sampling volume.

Borga (2002) identified the VPR effects on hydrological model simulations in the Brue catchment (135.2 km^2) in South-West England. Using a continuous, lumped rainfall-runoff model, Borga demonstrated that VPR effects, particularly within higher radar scans, preclude the use of uncorrected estimates for runoff modelling. It was shown by Vignal et al. (1999) that streamflow simulations improved when a VPR correction method was applied to the radar data and adjustment of the MFB was performed across the radar domain. Streamflow predictions driven by adjusted radar data may attain simulation efficiencies close to those obtained from the gauge-based reference rainfall (Borga, 2002).

Ding et al. (2005) tested the Range Correction Algorithm (RCA) and Convective Storm Separation Algorithm (CSSA) developed by the US National Weather Service (NWS) Office of Hydrologic Development (OHD) to determine if the algorithms were able to mitigate range-dependent biases in precipitation estimates. The NWS Hydrology Laboratory Research Modelling System (HL-RMS) was applied to five basins within the WSR-88D (Weather Surveillance Radar- 1988 Doppler) KCCX radar domain near State College, Pennsylvania. Model results were not compared to observed streamflows. Instead, output

from radar products (with and without the algorithms applied) was compared to model output based on a precipitation data field created from multiple radars and a dense rain gauge network. This precipitation product, referred to as OPERATION, is assumed to be an optimal estimate of the spatial distribution of precipitation over the basins. The HL-RMS model was run for a single storm event in January of 2003 using five different precipitation products: the OPERATION product, radar precipitation data with and without RCA/CSSA correction and MFB-corrected radar precipitation data with and without RCA/CSSA correction. Results showed that the RCA/CSSA noticeably corrected the precipitation overestimation from bright band effect and mitigated underestimation from beam overshooting (Ding et al., 2005). However, correction of the MFB (which approximately doubled the raw radar precipitation estimates) was required to achieve results similar to those obtained using OPERATION precipitation.

Neary et al. (2004) used the NEXRAD Stage III operational radar-derived precipitation product to drive the HEC-HMS model for the Dale Hollow watershed in Tennessee. The Stage III product involves correction of the MFB, as well as the integration of data from other radar stations with overlapping coverage. Precipitation gauge data were also used and the model was calibrated for each precipitation product to account for the bias between the products. It was found that Stage III radar precipitation products suffer from a systematic underestimation of precipitation. Poor detection of precipitation by the radar was noted during periods of very light rainfall. It was concluded that, for the studied basin, the use of radar precipitation estimates as input to a hydrologic model failed to improve upon model results obtained using rain gauge data alone.

Bellon et al. (2006) noted that biases are not known in real-time. Methods such as the KED (kriging with external drift) method (Velasco-Forero et al., 2005) have been proposed to blend radar and rain gauge data in real-time. However, if validation using gauges is to take place subsequent to adjustment, measurements from some gauges must be withheld in the

calibration process. This evaluation design potentially reduces the accuracy of the precipitation estimates and relies on a dense network of gauges (Gourley and Vieux, 2005).

It should be noted that the hydrological models used by Borga (2002), Ding et al. (2005) and Neary et al. (2004) are lumped models. The WATFLOOD model used in this study is a distributed model. Lumped models fail to take advantage of the spatial information offered by radar. Furthermore, Moore (1987) warns again using gauge-calibrated radar rainfall estimates in operational hydrology. Moore stated that the lesser variability of radar-derived rainfall compared to the greater variability of gauge-derived rainfall estimates results in the tendency to under-predict large flood events and over-predict small events.

At the Weather Radar Information and Distributed Hydrological Modelling symposium held in Sapporo, Japan in 2003, Georgakakos and Carpenter (2003) proposed a method for assessing the utility of distributed model forecasts. The question was directed at whether the added complexity of a distributed model was truly beneficial given the uncertainty in rainfall estimation by radar. Ensemble flow simulations for the Blue River basin near Blue Oklahoma were used to account for the uncertainty due to erroneous model parameter values and noisy radar rainfall input. Georgakakos and Carpenter showed that the ensemble flow simulations from distributed and lumped models were significantly different with a high degree of confidence. In general, the distributed model has a better performance than the lumped model, particularly for medium flow events.

Reed et al. (2006) noted that for flash flood applications, the key question is whether a distributed model can use radar data to produce useful simulations at ungauged interior locations. A goal of the NWS's River Forecast Centers (RFCs) is to increase lead-time accuracy for water warnings and forecasts. Three small basins (105 km^2 or less) in eastern Oklahoma and north-western Arkansas were modelled using short-term nowcast data from the NWS WSR-88D radar network in conjunction with the Hydrology Laboratory Reasearch Modeling System (HL-RMS). Reed et al. found that streamflow forecasts compared well

with observed streamflow data, although no comparison was made with model results from local precipitation gauge networks.

Although the majority of studies discussed in this section deal with radar's ability to accurately estimate rainfall, the importance of winter precipitation measurements within the McGill Radar domain must also be addressed. In the McGill radar domain, late-winter melting of the accumulated snow-pack often results in the highest peak streamflows observed at a hydrometric station with a given year. Since the WATFLOOD model is applied on a continuous basis, the model must accurately track the accumulation of winter precipitation. Snowfall precipitation rates can be over or underestimated by 100% or more due to the presence of mixed precipitation and signal variation due to different snow particles (Fassnacht et al., 1999). However, precipitation gauge measurements of snowfall are known to suffer from undercatchment, largely due to the effects of wind drift. stated Although no satisfactory method has been developed for making accurate snowfall measurements, Fassnacht et al. (1999) demonstrated that weather radar can provide better estimates of winter precipitation than gridded precipitation gauge data, in terms of runoff generation.

6 Study Areas

The study initially incorporated 102 streamflow stations within the McGill radar domain. For various technical reasons such as hydraulic controls and unreliable stage-discharge curves, the number of flow stations used in the final analysis was reduced to 39. For computational purposes, the study area was broken down into four different regions: eastern Ontario, Quebec- north of the St. Lawrence River, Quebec- south of the St. Lawrence River and the Lake Champlain Basin. Figure 9 is a topographic map showing basin outlines for all watersheds within the study area. The red letter 'R' indicates the location of the McGill radar station and the orange and red circles show the approximate Doppler (120 km) and conventional radar (240 km) extents, respectively. Distortion of the radar's coverage area is due to the map projection.

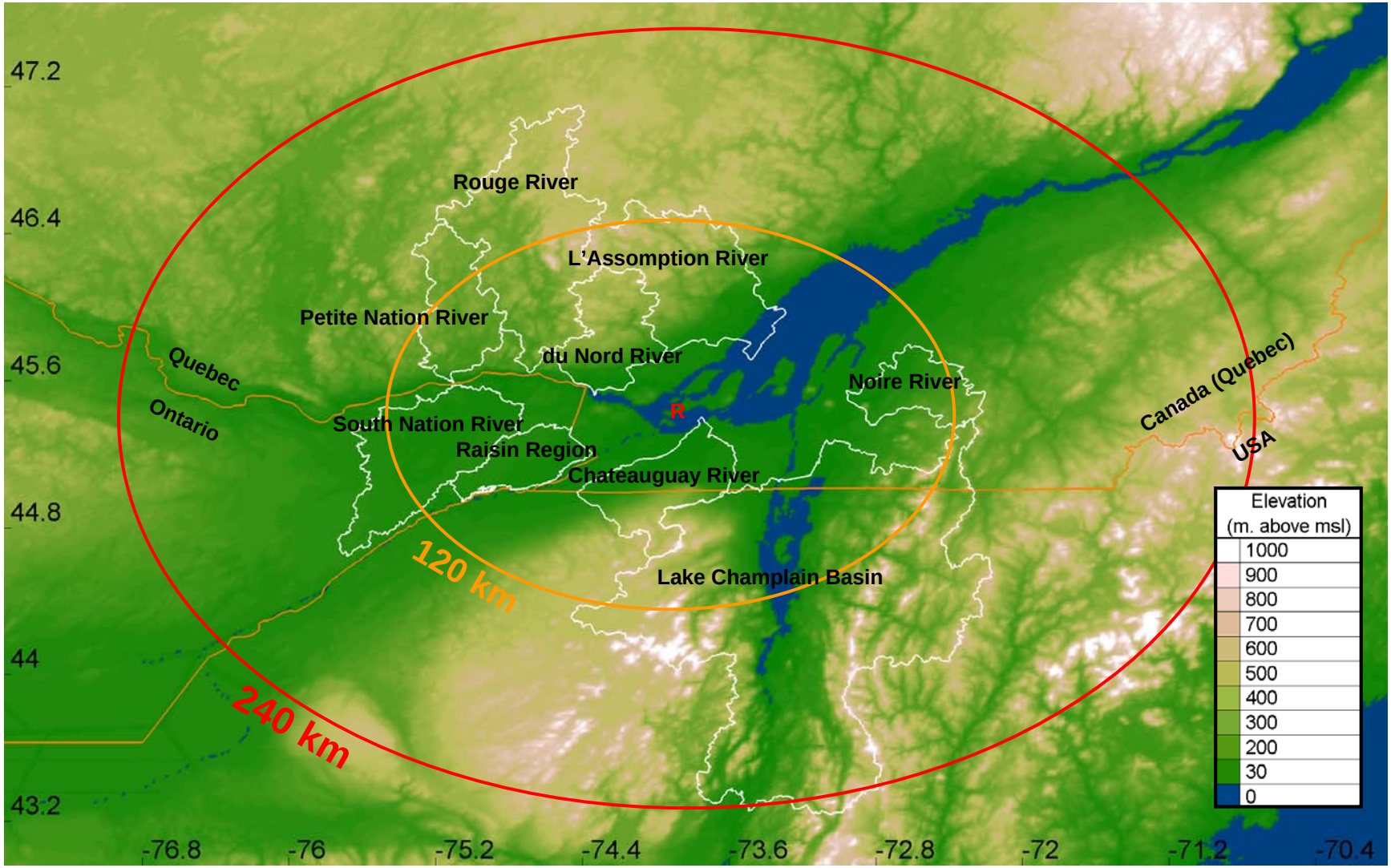

Figure 9- Topographic map of study area with basin outlines

6.1 Eastern Ontario

The eastern Ontario study region consists of the South Nation River basin and the Ontario portion of the Raisin Region. Figure 10 shows the location of hydrometric and precipitation stations in the area. Table 5 lists the Water Survey of Canada (WSC) station identification number, station name, drainage area and location of each hydrometric station. Water levels in the area are unaffected by control structures and all channels are characterize by a natural flow regime.

Table 5- Eastern Ontario hydrometric station details

WSC ID	Station Name	Drainage Area (km^2)	Latitude (Dec. Deg.)	Longitude (Dec. Deg.)
02LB008	Bearbrook near Bourget	440	45.4269 N	75.1533 W
02LB006	Castor River at Russell	433	45.2619 N	75.3444 W
02LB005	South Nation River near Plantagenet	3810	45.5175 N	74.9789 W
02LB007	South Nation River at Spencerville	246	44.8422 N	75.5439 W
02MC026	Beaudette River near Glen Nevis	124	45.2742 N	74.4936 W
02MC028	Delisle River near Alexandria	85.4	45.3269 N	74.6442 W
02MC030	South Raisin River near Cornwall	25.8	45.0514 N	74.7736 W
02MC001	Raisin River near Williamstown	404	45.3175 N	74.6014 W

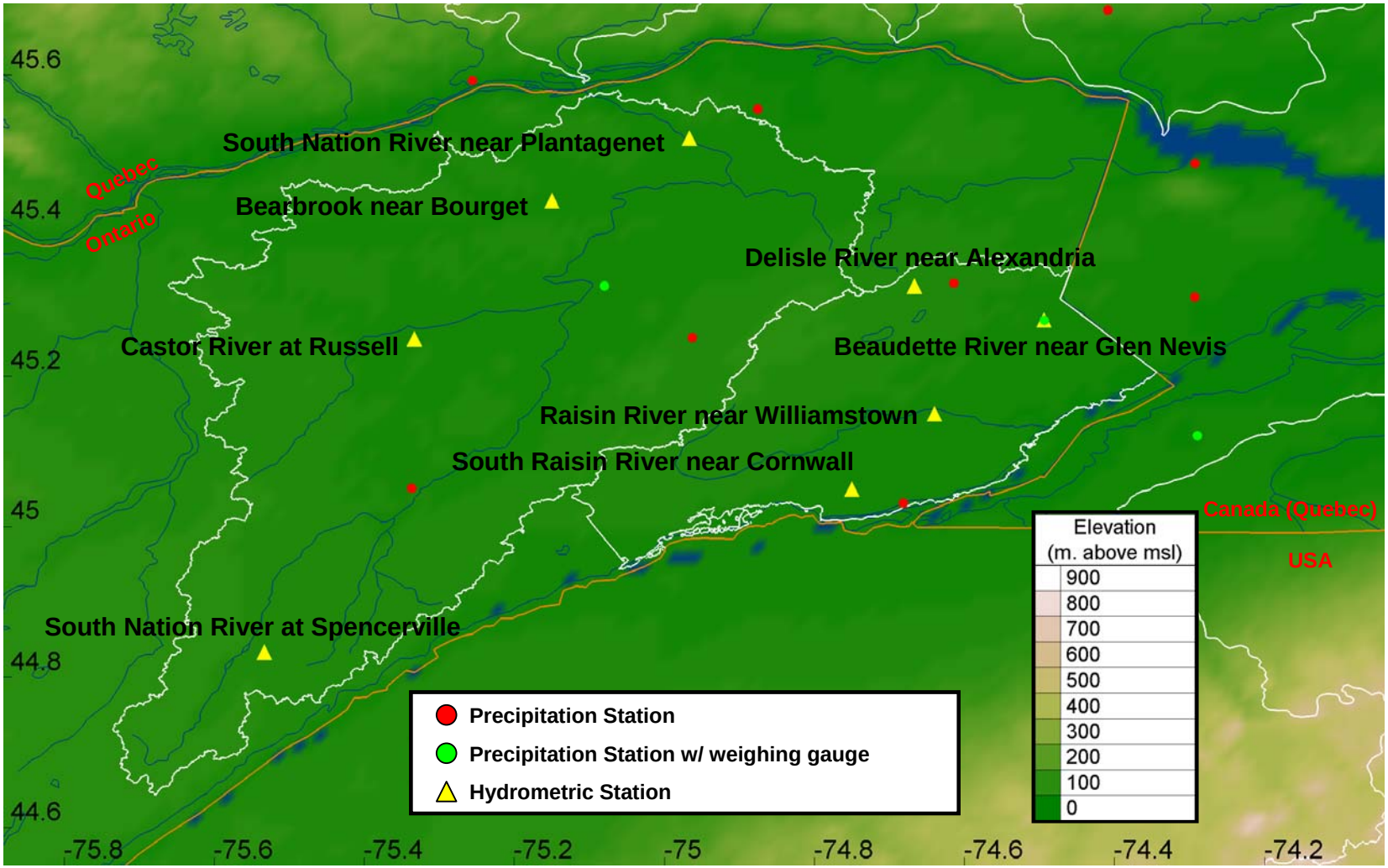

Figure 10- Eastern Ontario study region

6.1.1 South Nation River Basin

The South Nation River is located east of Ottawa, Ontario. The river drains an area of approximately 3,810 km^2 and flows in a north-easterly direction. Its headwaters originate near Brockville, Ontario and its confluence with the Ottawa River is located near the village of Plantagenet, Ontario. The average mean discharge of the South Nation River at Plantagenet is 42.1 m^3/s (Haughton, 2002).

The South Nation River is fed by several tributaries, such as the Bearbrook, Castor, Scotch and Payne Rivers. South Nation Conservation (SNC) monitors water levels within the watershed. Observations from four hydrometric stations were used for this project. Two stations are located on the South Nation River, and one each on the Bearbrook and the Castor Rivers tributaries.

Over its 175-km long course, the South Nation River drops only 85 metres. This flat landscape contributes to poor drainage and encourages the existence of several wetlands (Haughton, 2002). Agricultural land and forests dominate the area, accounting for approximately 50% and 45% of the basin's land cover, respectively. Table 6 provides a breakdown of land cover for each gauged subbasin within the South Nation and Raisin Region watersheds. A description of each land class is provided in Section 7.1.2.

Table 6- Eastern Ontario: percent land cover of area drained by each hydrometric station

Station Name	Impervious	Coniferous Forest	Deciduous Forest	Crops	Woodlands	Mixed	Wetlands	Water
Bearbrook near Bourget	0	1	28	38	1	30	3	0
Castor River at Russell	0	1	15	51	1	28	4	0
South Nation River near Plantagenet	0	1	21	50	2	23	4	0
South Nation River at Spencerville	0	1	16	13	0	51	19	0
Beaudette River near Glen Nevis	0	2	44	11	0	39	3	0
Delisle River near Alexandria	0	0	67	7	0	26	0	0
South Raisin River near Cornwall	2	1	2	63	3	29	0	0
Raisin River near Williamstown	0	0	51	4	0	42	3	0

The main branch of the South Nation River is a wide sand-bottom, meandering channel with high degree of bank erosion. Most tributaries originate in one of several wetlands within the basin and consist of cobble or heavily vegetated channels.

6.1.2 Raisin Region

The Raisin Region Conservation Authority (RRCA) has jurisdiction over an area of 1,680 km^2. This area includes the Beaudette, Delisle and Raisin River basins in addition to a number of secondary streams that drain into the St. Lawrence River. The Beaudette and Delisle Rivers flow in an easterly direction and through the province of Quebec prior to discharging into the St. Lawrence River. Hydrometric stations used in this region are located in Ontario only.

As in the nearby South Nation watershed, the area is characterized by a low relief landscape comprised mostly of agricultural and forested areas. Table 6 provides a breakdown of the land cover for areas drained by each hydrometric gauging station.

Channel characteristics of the Raisin Region rivers are similar to those described for the South Nation River basin.

6.1.3 Radar and Gauge Network Coverage

Due to its low relief and proximity to the McGill radar station, reflectivity measurements obtained over the South Nation River and Raisin River basins are unaffected by beam blocking. Doppler coverage extends throughout most of the region (Figure 9).

The precipitation gauge network for the region can be characterized as sparse. Network coverage is especially poor for the Castor and Bearbrook tributaries and the headwaters of the South Nation River above Spencerville.

6.2 Quebec- North of the St. Lawrence River

Five basins make up the region: the Petite Nation, Rouge, du Nord and L'Assomption. Two streamflow stations are located in each the L'Assomption and the du Nord basins, and one in each of the remainders. Figure 11 shows basin outlines and hydrometric and precipitation stations in the area. Table 7 lists Water Survey of Canada (WSC) station identification numbers, station names, drainage areas and locations for each hydrometric station. Table 8 provides a breakdown of land cover for each subbasin within the region.

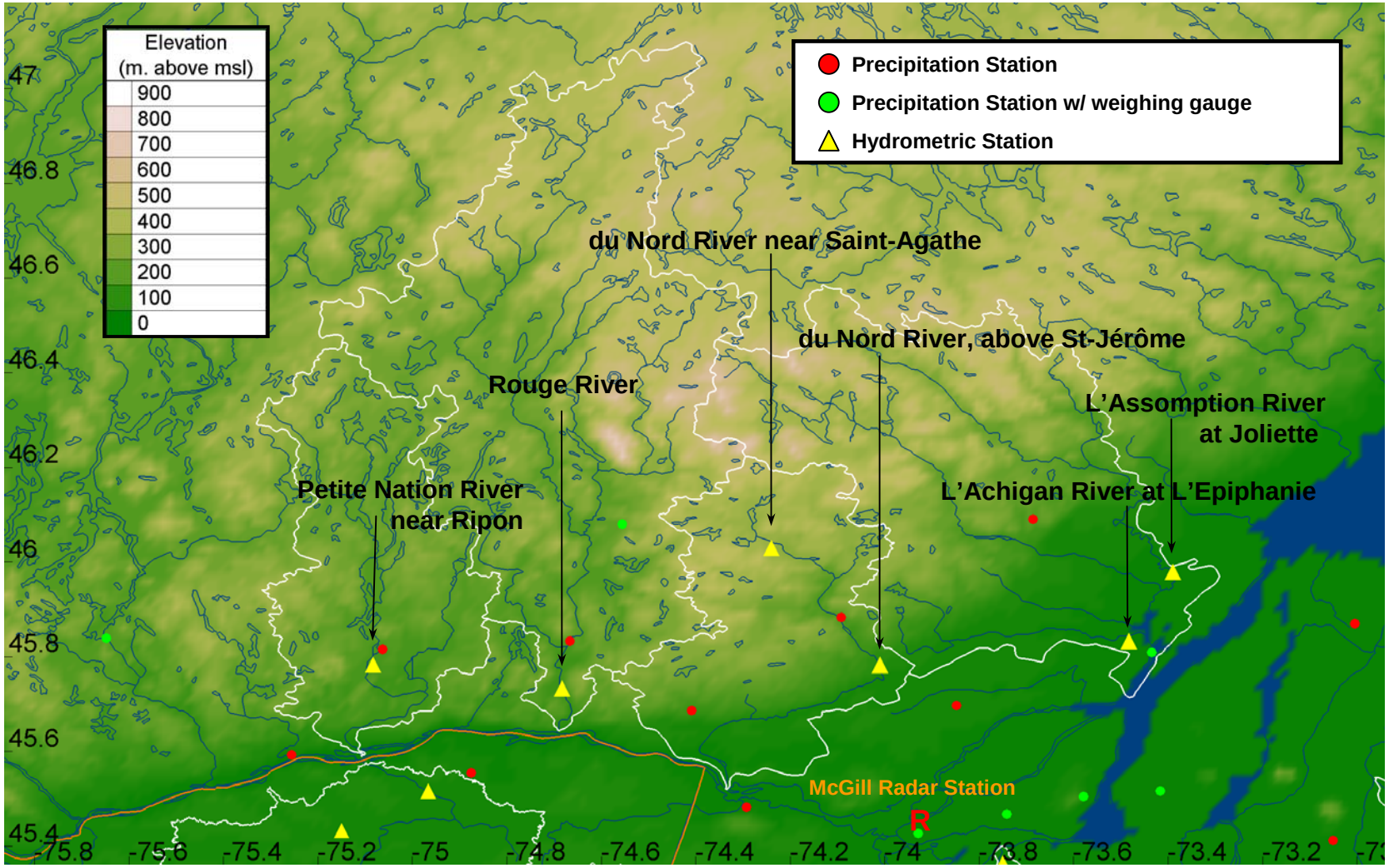

Figure 11- Quebec, north of the St. Lawrence River, study region

Table 7- Quebec, north of the St. Lawrence River, hydrometric station details

WSC ID	Station Name	Drainage Area (km^2)	Latitude (Dec. Deg.)	Longitude (Dec. Deg.)
02LC008	Rivière du Nord at Saint-Jérôme	1170	45.7931 N	74.0128 W
02LC021	Rivière du Nord near Saint-Agathe	311	46.0458 N	74.2528 W
02LC029	Rivière Rouge	5460	45.7364 N	74.6897 W
02LD005	Rivière de la Petite Nation near Ripon	1330	45.7917 N	75.0914 W
02OB008	Rivière de l'Assomption at Joliette	1340	46.0103 N	73.4275 W
02OB037	Rivière de l'Achigan at L'Epiphanie	647	45.8464 N	73.4931 W

Table 8- Quebec, north of the St. Lawrence River: percent land cover of area drained by each hydrometric station

Station Name	Impervious	Coniferous Forest	Deciduous Forest	Crops	Woodlands	Mixed	Wetlands	Water
Rivière du Nord at Saint-Jérôme	0	0	76	2	0	17	5	0
Rivière du Nord near Saint-Agathe	0	0	72	1	0	17	8	2
Rivière Rouge	0	0	67	1	0	25	5	2
Rivière de la Petite Nation near Ripon	0	0	63	1	0	23	7	6
Rivière de l'Assomption at Joliette	0	0	71	6	1	17	5	0
Rivière de l'Achigan at L'Epiphanie	0	0	67	13	1	16	1	1

A large number of control structures are found along the channels in the region. Figure 12 shows the location of all structures within the region, as inventoried by the Centre

d'Expertise Hydrique du Québec (CEHQ). Most control structures consist of small weirs created for erosion control purposes and are not expected to significantly influence flow regime.

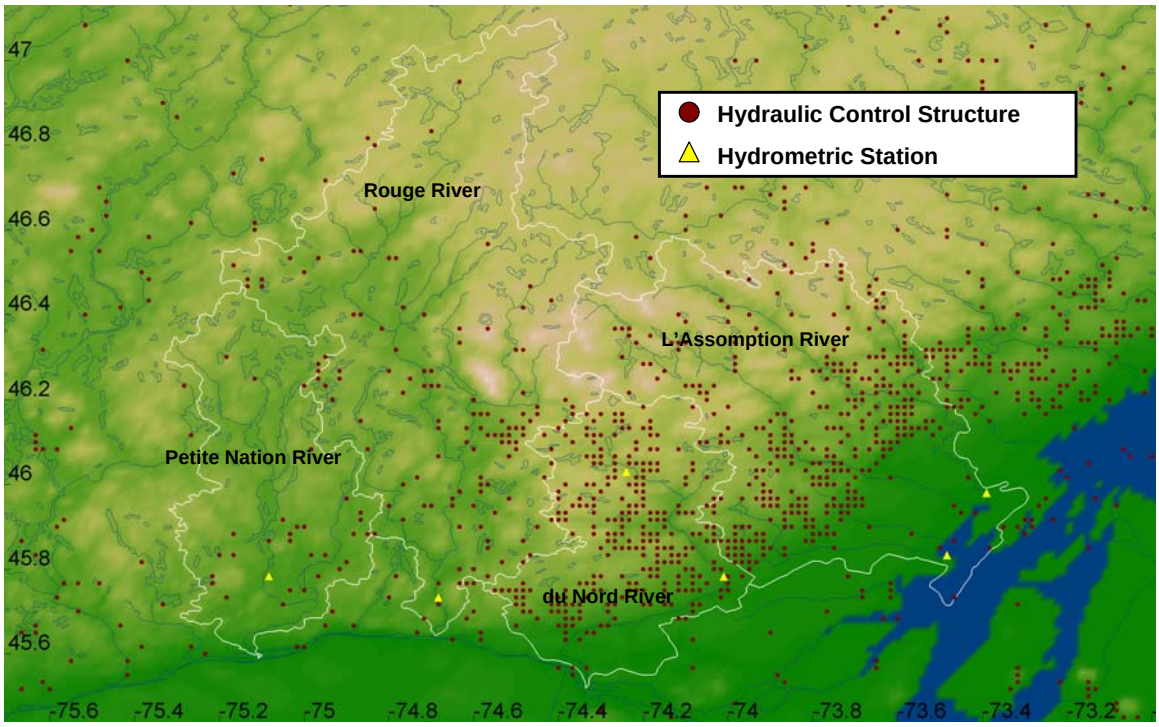

Figure 12- Hydraulic control structure in Quebec, north of the St. Lawrence River

6.2.1 Petite Nation River Basin

The Petite Nation River is located in western Quebec and drains an area of approximately 2,717 km^2. The river flows south towards the Ottawa River. Numerous lakes located along the main channel act to significantly dampen flows.

6.2.2 Rouge River Basin

The Rouge River flows south from the Mont-Tremblant provincial park to the Ottawa River. It has a drainage area of 5,543 km^2. A number of rapids exist along steep sections of the channels.

6.2.3 du Nord River Basin

The du Nord River has a drainage area of approximately 2,213 km^2. The river flows south from the Mont-Tremblant provincial park to the Ottawa River. Data from two hydrometric stations are used in this study, each located upstream of the city of St-Jérôme and any major hydraulic structure. The basin is heavily forested with many lakes and perched wetlands.

6.2.4 L'Assomption River Basin

The L'Assomption River basin extends from the Mont-Tremblant provincial park to the St. Lawrence River. It has a drainage area of approximately 4,220 km^2, the majority of which is heavily forested with many lakes and perched wetlands. Agricultural fields expand over most of the low-lying areas to the south of the basin. The L'Assomption River drops approximately 250 m in elevation over its 200 km course, traversing the Laurentian plateau, the Laurentian foothills and St. Lawrence lowlands (CARA, 2006). The L'Achigan River is a major tributary to the L'Assomption River.

6.2.5 Radar and Gauge Network Coverage

Due to the presence of the Laurentian Mountains, beam blocking is a major problem in the region. Range effects are also likely to affect the Rouge and Petite Nation River basins, which extend well beyond the Doppler range. The L'Achigan subbasin is the only watershed with unobstructed radar coverage due to its close proximity to the station and large areas of low relief.

Precipitation gauges within the region are concentrated to the south and gauge coverage in the northern reaches of each watershed is poor (Figure 10).

6.3 Quebec- South of the St. Lawrence River

The study region is comprised of two watersheds: the Chateauguay and Noire River basins. Figure 13 shows basin outlines and hydrometric and precipitation stations in the region.

Table 9 lists WSC station identification number, station name, drainage area and location of each hydrometric station. Table 10 provides a breakdown of land cover for the areas drained by each station.

Table 9- Quebec, south of the St. Lawrence River, hydrometric station details

WSC ID	Station Name	Drainage Area (km^2)	Latitude (Dec. Deg.)	Longitude (Dec. Deg.)
02OA054	Chateauguay River	2490	45.36667 W	73.75 N
02OA057	English River	643	45.16667 W	73.84 N
02OG019	Noire River	1490	45.48333 W	72.9 N

Table 10- Quebec, south of the St. Lawrence River: percent land cover of area drained by each hydrometric station

Station Name	Impervious	Coniferous Forest	Deciduous Forest	Crops	Woodlands	Mixed	Wetlands	Water
Chateauguay River	0	1	36	19	6	39	0	0
English River	0	0	39	21	2	38	0	0
Noire River	0	0	22	33	2	43	0	0

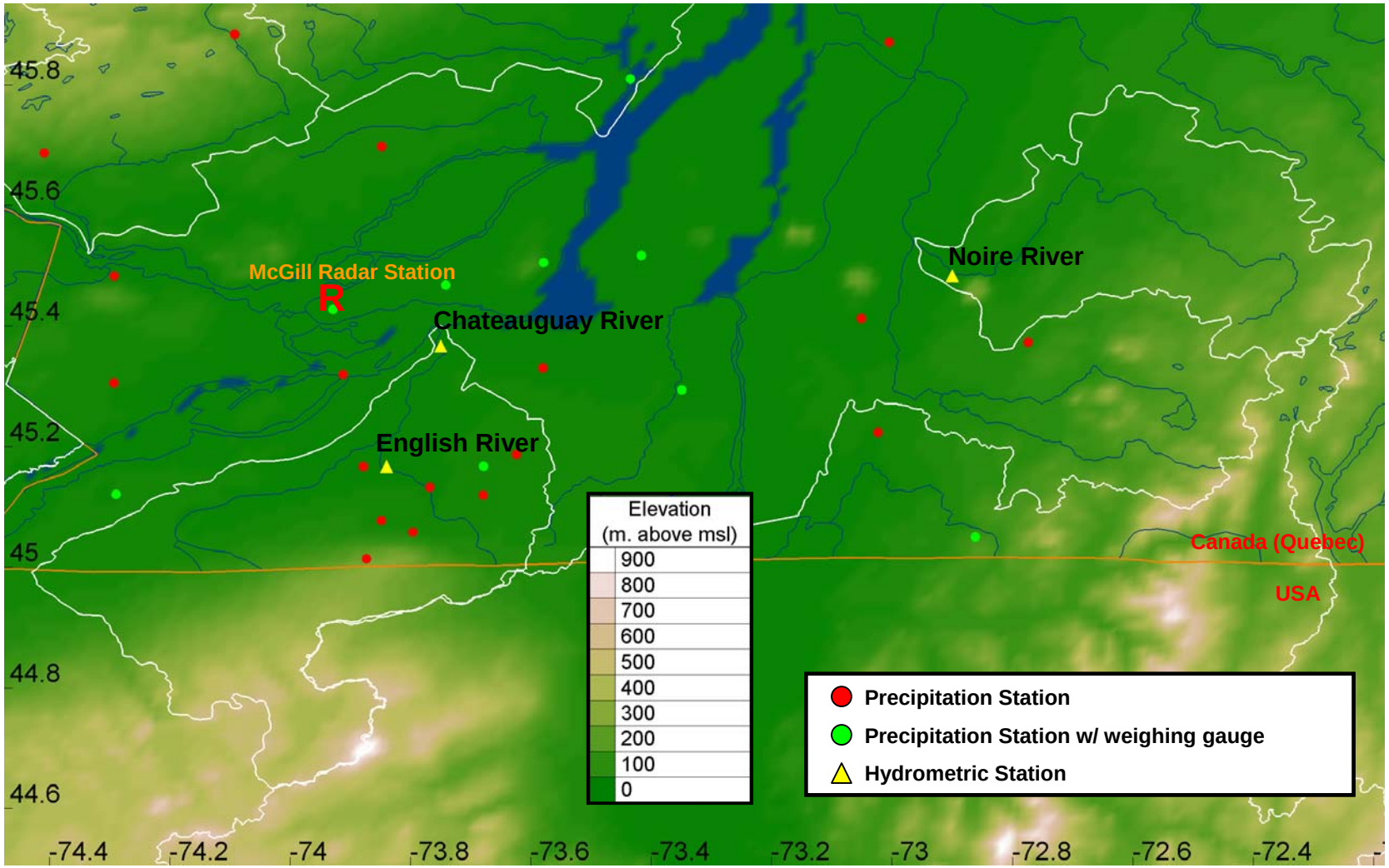

Figure 13- Quebec, south of the St. Lawrence River, study region

6.3.1 Chateauguay River Basin

The Chateauguay River originates in New York State's Adirondack Mountains. The river flows north towards the St. Lawrence River, through the St. Lawrence lowlands in Quebec. The basin drains an area of 2,543 km^2 of which 1,085 km^2 are in the United States. The spring flood usually occurs in March and April (average flow of 94.3 m^3/s). The low water level reaches its minimum in July (average flow of 8 m^3/s) (SCABRIC, 2006).

Six major tributaries flow into the Chateauguay River: the English, Trout, Outards, Sturgeon, Hinchinbrook and Bean Rivers. Two streamflow stations located within the basin were used in this study: one located on the English River upstream of its confluence with the Chateauguay River, and the other on the Chateauguay River, upstream of its confluence with the St. Lawrence River.

The mountainous region of the watershed to the south is characterized by heavily forested areas, with steep bedrock or cobble channels. As the river encounters the agricultural areas of the St. Lawrence lowlands the channel becomes a wide meandering sand-bottom river.

Although several dams exist along the Chateauguay River, any fluctuation of the water level cannot be attributed to the dams' management because there are no controls to alter it that rapidly and reservoir storage capacity is very small (SCABRIC, 2006).

6.3.2 Noire River Basin

The Noire River is a major tributary to the Yamaska River, draining approximately 1,571 km^2. The river's headwaters are located in the foothills of the Appalachian Mountains and flow west into the St. Lawrence lowlands. The river has an average flow of 27.4 m^3/s. Due to a lack of lakes and hydraulic controls, the low-lying regions of the basin are susceptible to periods of severe drought and flooding (COGEBY, 2006).

Land cover and channel characteristic of the Noire River basin are similar to those described for the Chateauguay River basin in the previous section. Observations from one streamflow station, located upstream of the river's confluence with the Yamaska River, were used in the study.

6.3.3 Radar and Gauge Network Coverage

The Chateauguay and English River basins are located directly south of the McGill Radar station and entirely within Doppler range. However, a tall building, located nearby and to the south of the radar station, forces the use of data from higher elevation scans to obtain precipitation information for regions of the Chateauguay River basin. As well, a small degree of beam blocking occurs in the headwaters of the Chateauguay River due to the presence of the Adirondack Mountains.

The McGill radar has an unobstructed view of the Noire River basin. Doppler coverage exists for approximately the lower 75-80 percent the watershed (Figure 9).

Precipitation gauges are numerous in the Chateauguay region, however none are located in the American portion of the watershed. No gauges are located within or to the east of the Noire River basin (Figure 10).

6.4 Lake Champlain Basin

Lake Champlain is located along the Vermont-New York border and extends partially into Quebec, where it flows north to its outlet at the Richelieu River. The Lake Champlain basin consists of several rivers and streams that empty into Lake Champlain. The lake covers an approximate area of 1,127 km^2 and drains an area of approximately 21,326 km^2. Fifty-six percent of the Basin is in Vermont, 37% is in New York, and 7% is in the Province of Quebec (LCBP, 2004). Figure 14 shows subbasins and hydrometric stations within the watershed. Table 11 lists USGS station identification number, station name, drainage area and location

of each hydrometric station. Table 12 provides a breakdown of land cover for the area drained by each station.

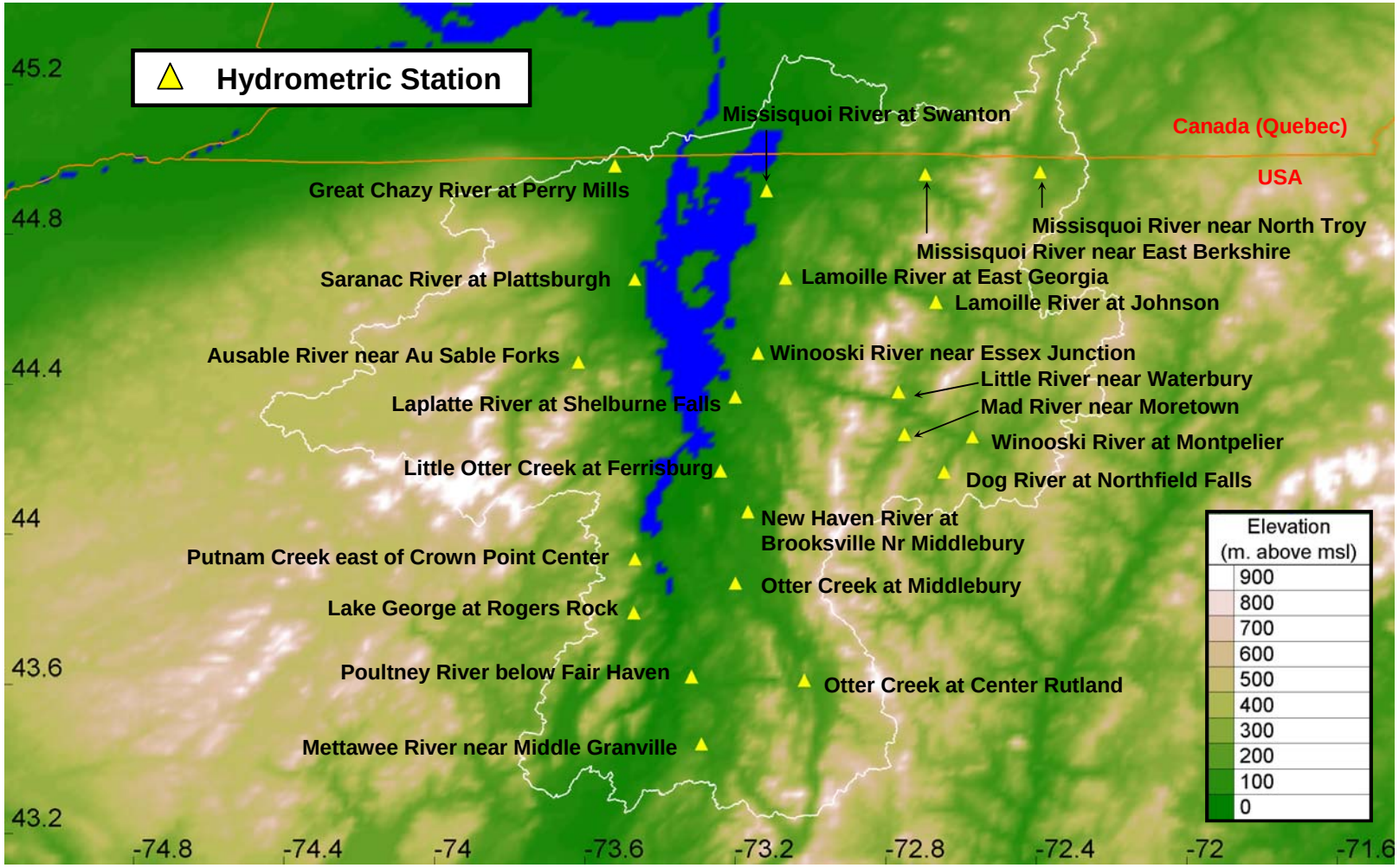

Figure 14- Lake Champlain study region

Table 11- Lake Champlain basin hydrometric station details

USGS ID	Station Name	Drainage Area (km^2)	Latitude (Dec. Deg.)	Longitude (Dec. Deg.)
04271500	Great Chazy River at Perry Mills NY	629	45.000 N	73.501 W
04273500	Saranac River at Plattsburgh NY	1575	44.682 N	73.472 W
04275500	Ausable River near Au Sable Forks NY	1155	44.451 N	73.643 W
04276842	Putnam Creek east of Crown Point Center, NY	134	43.943 N	73.464 W
04278000	Lake George at Rogers Rock NY	603	43.808 N	73.458 W
04280000	Poultney River below Fair Haven, VT	484	43.620 N	73.317 N
04280450	Mettawee River near Middle Granville, NY	433	43.440 N	73.290 N
0428200	Otter Creek at Center Rutland, VT	795	43.610 N	73.017 N
04282500	Otter Creek at Middlebury, VT	1627	43.870 N	73.200 N
04282525	New Haven River at Brooksville Nr Middlebury, VT	298	44.062 N	73.171 W
04282650	Little Otter Creek at Ferrisburg, VT	148	44.170 N	73.240 W
04282795	Laplatte River at Shelburne Falls, VT.	116	44.370 N	73.217 W
04286000	Winooski River at Montpelier, VT	1028	44.256 N	72.593 W
04287000	Dog River at Northfield Falls, VT	197	44.183 N	72.641 W
04288000	Mad River near Moretown, VT	360	44.277 N	72.743 W
04289000	Little River near Waterbury, VT	287	44.370 N	72.770 W
04290500	Winooski River near Essex Junction, VT	2704	44.479 N	73.139 W
04292000	Lamoille River at Johnson, VT	803	44.623 N	72.677 W
04292500	Lamoille River at East Georgia, VT	1777	44.679 N	73.073 W
04293000	Missisquoi River near North Troy, VT	339	44.973 N	72.386 W
04293500	Missisquoi River near East Berkshire, VT	1241	44.960 N	72.697 W
04294000	Missisquoi River at Swanton, VT	2201	44.917 N	73.129 W

Table 12- Lake Champlain basin: percent land cover of area drained by each hydrometric station

Station Name	Impervious	Coniferous Forest	Deciduous Forest	Crops	Woodlands	Mixed	Wetlands	Water
Great Chazy River at Perry Mills NY	0	1	36	4	0	59	0	0
Saranac River at Plattsburgh NY	0	9	28	2	0	60	0	0
Ausable River near Au Sable Forks NY	0	3	19	0	0	77	0	0
Putnam Creek east of Crown Point	0	3	13	0	0	84	0	0
Lake George at Rogers Rock NY	0	13	27	0	0	60	0	0
Poultney River below Fair Haven, VT	0	2	22	6	0	69	0	0
Mettawee River near Middle Granville,	0	2	43	6	0	49	0	0
Otter Creek at Center Rutland, VT	1	0	39	5	1	55	0	0
Otter Creek at Middlebury, VT	0	1	27	17	1	54	0	0
New Haven River at Brooksville Nr	0	0	34	14	0	52	0	0
Little Otter Creek at Ferrisburg, VT	0	0	5	58	0	37	0	0
Laplatte River at Shelburne Falls, VT.	0	1	11	46	0	43	0	0
Winooski River at Montpelier, VT	0	1	36	4	0	58	0	0
Dog River at Northfield Falls, VT	0	0	26	1	0	74	0	0
Mad River near Moretown, VT	0	0	24	0	0	76	0	0
Little River near Waterbury, VT	0	1	43	2	0	54	0	0
Winooski River near Essex Junction, VT	0	0	27	8	1	64	0	0
Lamoille River at Johnson, VT	0	1	37	2	0	60	0	0
Lamoille River at East Georgia, VT	0	0	51	2	0	47	0	0
Missisquoi River near North Troy, VT	0	0	55	1	0	44	0	0
Missisquoi River near East Berkshire,	0	0	46	9	0	45	0	0
Missisquoi River at Swanton, VT	0	1	33	15	0	51	0	0

6.4.1 Radar and Gauge Network Coverage

No precipitation stations used in the study are located within or near the Champlain River basin. The Champlain Lake Basin extends past the southern reaches of the McGill radar's coverage. Beam blocking is likely to occur due to the presence of the Adirondack Mountains.

7 The WATFLOOD Hydrological Model

WATFLOOD is a hydrological modelling system consisting of a series of computer programs used for processing data required by the hydrological modelling component of the system, SPL. The model was developed by Dr. Nicholas Kouwen (Kouwen, 2006), beginning in 1972, with the intention of making optimal use of remotely sensed data, such as radar precipitation estimates and gridded land cover data. The model is used to forecast river flows, predict reservoir inflows and study watershed response to changes in climatic and environmental conditions.

WATFLOOD breaks down a watershed into a number of grid cells, generally greater than 1 km^2. The gridded model format enables direct incorporation of gridded data from sources such as weather radar, numerical weather models, digital elevation models (DEMs), and remotely sense land cover and soil parameters. Streamflow, however, is calculated on a subwatershed basis and water is routed from grid to grid (Kouwen et al, 2005).

Areas with similar hydrologic response, often defined by land cover, are combined into several grouped-response units (GRUs) that represent a fraction of each grid cell. The hydrologic response of the grid cell is calculated as the sum of the response from each GRU. Each GRU is associated with a unique set of model parameters that are transferable between watersheds, thereby reducing the amount of calibration needed to perform reliable model runs. For example, a coniferous forest should produce a similar hydrologic response regardless of its geographical location.

A detailed description of the WATFLOOD model is given by Kouwen et al. (2005) and is available on the WATFLOOD website at www.watflood.ca.

7.1 Model Setup

The WATFLOOD model was configured for thirty-nine subbasins within the McGill radar domain. For computational purposes four regions, described in Section 6, were used. A WATFLOOD MAP file was created for each region. The MAP file contains gridded information for all watershed properties including channel elevation, river class, contour density, channel density, and land cover information. The model was setup using a 1.5' by 1.5' grid cell (approximately 2.0 km by 2.8 km). The study area was defined as the area covered by the radar products and ranged from approximately 43.2529 N to 47.5094 N in latitude, and 76.9312 W to 70.7070 W in longitude. The radar station is located at the centre of the grid.

EnSim Hydrologic, developed at the National Research Council's Canadian Hydraulic Center (NRC-CHC), is a pre- and post-processing tool and graphical display for hydrological models. The program has GIS capabilities that allow the user to import various formats of distributed data. EnSim Hydrologic was used to generate the MAP files, display input files and view model output.

7.1.1 Watershed Delineation

EnSim Hydrologic was used to automatically derive channel elevation, drainage direction, basin boundaries and other MAP file properties from a digital elevation model (DEM). A 1-m DEM, obtained from the National Topographic Survey of Canada (NTS) 1:250 000 scale digital elevation model database, was used for all Canadian regions of the study area. The 30 arc-second DEM (GTOPO30) was used to delineate watersheds located in the United States and can be downloaded from http://edcdaac.usgs.gov/gtopo30/gtopo30.html.

The error difference between EnSim-calculated subbasin drainage areas and those published by the Water Survey of Canada (WSC) and the United States Geological Survey (USGS) are shown in Appendix A.

7.1.2 Land Cover Classification

The Global Land Cover Facility (GLCF) classification for Canada and the United States was used to define land classes for the McGill radar domain. Land cover types were further grouped into the following land cover classes: coniferous forest, deciduous forest, crops, woodland, mixed forest, water and impervious (Figure 15). Table 13 lists the land cover types grouped to create each land class.

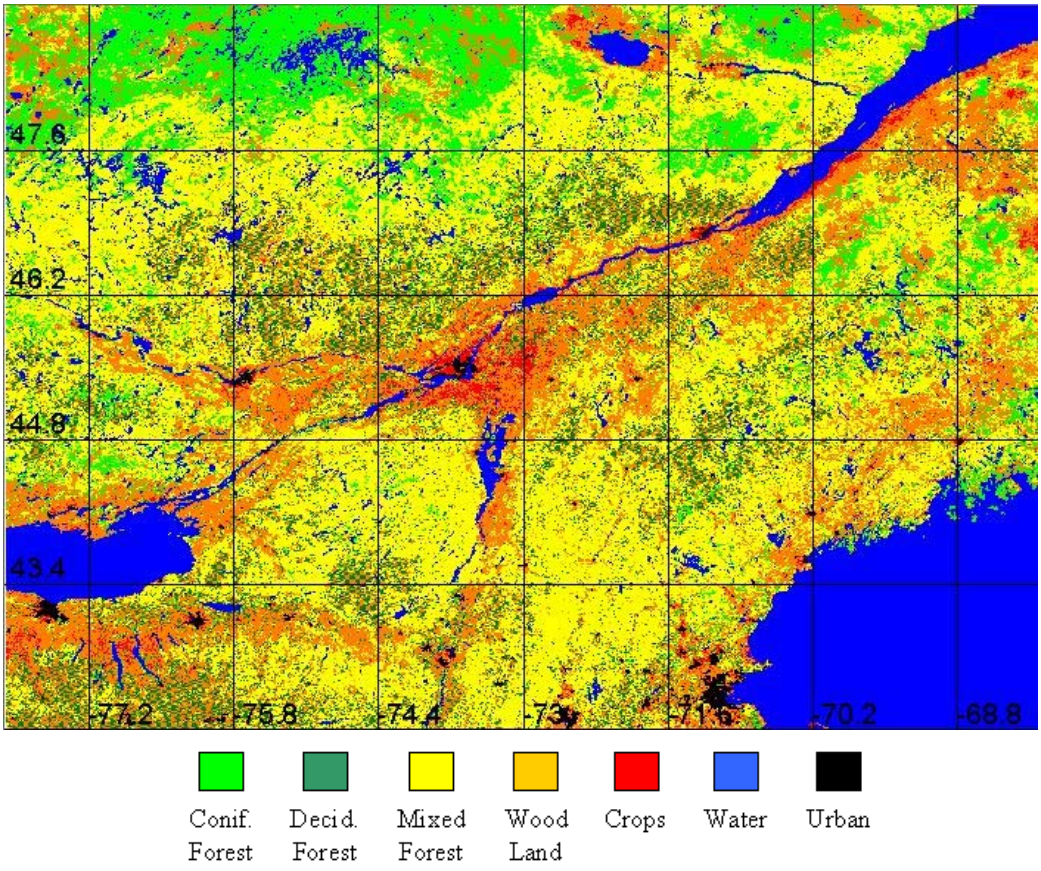

Figure 15- Land Cover classes from Global Land Cover Facility (Kouwen et al., 2003)

Table 13- List of land covers to amalgamate for WATFLOOD (Kouwen et al., 2003)

GLCF #	Land Cover Name	WATFLOOD Amalgamated Land Cover Name
0	Water	Water
1	Evergreen Needleleaf Forest	Coniferous Forest
2	Evergreen Broadleaf Forest	
3	Deciduous Needleleaf Forest	Deciduous Forest
4	Deciduous Broadleaf Forest	
5	Mixed Forest	Mixed Forest
6	Woodland	Woodland
7	Wooded Grassland	
8	Closed Shrubland	
9	Open Shrubland	
10	Grassland	Low Crops
11	Cropland	
12	Bare Ground	(Does not exist in region)
13	Urban and Built-Up	Urban

The resolution of the land cover database is 30 arc-seconds. The data can be downloaded from http://gaia.umiacs.umd.edu:8811/landcover/index.html. Data from the 1996 Canadian Land Inventory (CLI) were used to identify wetlands in regions where wetland hydrology has a significant impact on streamflows. A wetland class was introduced into the Eastern Ontario and Quebec, north of the St. Lawrence River regions.

7.1.3 Temperature Inputs

Temperature data from 25 airports in Canada and the United States were used in this study. Hourly temperature values were distributed to grid cells across the study area using WATFLOOD's TMP program, which uses a distance weighting technique (Kouwen, 2006).

Table 14 lists the city, airport code and location of each station used in the study.

Temperature data for all Canadian stations are downloaded from the following Meteorological Service of Canada (MSC) websites, where "CODE" is replaced by the three-letter airport designation listed in Table 14: http://weatheroffice.ec.gc.ca/scripts/citygen.pl?client=ECCDN_e&city=CODE.

Temperature data for all America stations are downloaded from the following National Weather Service (NWS) websites, where "CODE" is replaced by the four-letter airport designation listed inTable 14: http://weather.noaa.gov/weather/current/CODE.html. Each website contains a 24-hour summary and data was downloaded daily. All data are stored in monthly data files containing hourly data.

Table 14- Airport temperature stations (Kouwen et al., 2003)

City	Station Code	Latitude (decimal degrees)	Longitude (decimal degrees)
Montreal, Quebec	YUL	45.4667 N	73.7500 W
Quebec City, Quebec	YQB	46.8000 N	71.3833 W
Maniwaki, Quebec	WMJ	46.2600 N	76.000 W
Sherbrooke, Quebec	YSC	45.4333 N	71.6833 W
Trois Rivières, Quebec	WTY	46.3500 N	72.6833 W
Shawinigan, Quebec	XSH	46.5667 N	72.7333 W
Petawawa, Ontario	YWA	45.9500 N	77.3167 W
Varennes, Quebec	WHM	45.7167 N	73.3833 W
St. Hubert, Quebec	YHU	45.5167 N	73.4167 W
Nicolet, Quebec	WNQ	46.2333 N	72.6500 W
La Tuque, Quebec	WDQ	47.4167 N	72.7833 W
Kingston, Ontario	YGK	44.2167 N	76.6000 W
Ottawa, Ontario	YOW	45.3167 N	75.6667 W
Syracuse, New York	KSYR	43.1167 N	76.1000 W
Glens Falls, New York	KGFL	43.3333 N	73.6167 W
Ogdensburg, New York	KOGS	44.6833 N	75.4000 W
Plattsburgh, New York	KPLB	44.6833 N	73.5167 W
Saranac L, New York	KSLK	44.3833 N	74.2000 W
Utica, New York	KUCA	43.1500 N	75.3833 W
Burlington, Vermont	KBTV	44.4667 N	73.1500 W
Rutland, Vermont	KRUT	43.5333 N	72.9500 W
Montpelier, Vermont	KMPV	44.2000 N	72.5833 W
Berlin, New Hampshire	KBML	44.5833 N	71.1833 W
Lebanon, New Hampshire	KLEB	43.6333 N	72.3000 W
Concord, New Hampshire	KCON	43.2000 N	71.5000 W

Temperature data from additional sources were used to fill in data gaps from the above stations. From January 1st to 22nd 2002, the average daily temperatures for six cities in or near the McGill Radar region were used. The data were downloaded from http://www.engr.udayton.edu/weather. The cities are listed in Table 15. During the month of November 2004, temperature values from the South Nation Conservation Authority's temperature gauge, located in Casselman, Ontario, were used across the entire radar domain.

Table 15- Additional temperature station locations (Kouwen et al., 2003)

City	Latitude	Longitude
Montréal, Quebec	45.1680 N	73.7500 W
Québec, Quebec	46.8000 N	71.3833 W
Ottawa, Ontario	45.3167 N	75.6667 W
Syracuse, New York	43.1167 N	76.1000 W
Burlington, Vermont	44.1680 N	73.1500 W
Concord, New Hampshire	43.2000 N	71.5000 W

7.1.4 Precipitation Inputs

Four different precipitation data sets were used in this study: McGill University's C0, C2 and C3 radar products and distributed precipitation gauge data. It should be noted that the C1 radar product was abandoned during the study period and was therefore not analyzed in this thesis.

7.1.4.1 Radar-derived Input

The C0, C2 and C3 precipitation products were obtained from the J.S. Marshall Radar Observatory and archived in real-time. Each product consists of hourly precipitation

accumulations with a 2-km spatial resolution. Interpolation from the UTM grid to the 1.5-minute by 1.5-minute WATFLOOD MAP file grid was performed using the *translate_new_rapid_files.f* program written by Allyson Bingeman. Precipitation within each MAP file grid cell is calculated as an area-weighted average of all radar pixels that fall within (fully or partially) the grid cell.

In April of 2005, it is was recommended by Bellon (2005) at the J.S. Marshall Radar Observatory to multiply all precipitation values by 1.4 for the period of December 2004 to March 2005, due to an error in radar calibration. It was decided, however, that for the purpose of this thesis, radar values should not be adjusted as such a correction does not reflect a real-time situation. Similarly, experiments performed by Juneja (2006) used an adjustment factor of 2.0 during winter months (December to February) for all radar precipitation estimates. Although such arbitrary adjustments are typically made by hydrologists when using radar-derived precipitation, prior knowledge of precipitation underestimation by radar is not known in a real-time scenario. No adjustment of radar-derived precipitation values were made to radar data in this study.

7.1.4.2 Precipitation Gauge-derived Input

Hourly precipitation values from the Montreal Mesonet were downloaded through the University of Laval's Montreal-Mesonet ftp site: ftp://ftp.gaap.ulaval.ca/. Quality control codes were available for each data entry. Only data labeled as "Good" were used as input to the WATFLOOD model. Fifteen-minute precipitation data for two gauges in Ontario were obtained from the South Nation and Raisin Region conservation authorities. The location and type of precipitation gauge used are listed in Table A.5 in Appendix A. Certain mesonet stations are equipped with both tipping-bucket and weighing gauges. In the case where two precipitation values exist for the same location and time interval (i.e. rainfall events only),

the average of the two recorded values is calculated as precipitation for the grid containing the two gauges.

From April 1st, 2003 to August 31st, 2003 the McGill radar station was not in operation as system upgrades and maintenance were performed. During this period, precipitation gauge data were used to fill in precipitation gaps for all radar products for all regions.

Precipitation gauge data were compiled into monthly files containing hourly values for each gauge. Point-data were distributed across the WATFLOOD grid using WATFLOOD's RAGMET program which uses the Reciprocal Distance Weighting Technique to determine precipitation within each grid cell. The area surrounding the midpoint of each grid element is divided into four quadrants. The rain gauge closest to each quadrant is used to calculate rainfall for that particular quadrant. Thus the rainfall in any grid cell is computed as a weighted average of a maximum of four rain gauges. The weights are assumed to be an inverse function of the distance between the grid element midpoint and the rain gauge (Kouwen, 2006).

As with many precipitation distribution methods, rainfall for any given grid cell never results in a value greater than the largest or less than the smallest amount observed. This method also assigns rainfall to each grid element regardless of the areal extent of the actual rain event (Kouwen, 2006).

7.1.5 Streamflow Data

Fifteen-minute streamflow data were obtained for the entire study period. Data for stations in Quebec were downloaded from the Centre d'Expertise Hydrique du Québec (CEHQ) website: http://www.cehq.gouv.qc.ca/suivihydro/default.asp. Similar data for the South Nation River basin and Raisin Region were provided by the South Nation and Raisin Region conservation authorities, respectively. Hourly data for all American stations were

downloaded from the USGS website (http://waterdata.usgs.gov/nwis/uv?format=rdb&period=8&site_no=CODE, where "CODE" represents the USGS hydrometric stations number, Table 11, Section 6.4). Streamflow data for each region are stored in monthly files containing hourly data.

7.1.6 Classification of Rivers

During the summer and fall of 2005, fieldwork was conducted to improve the routing component of the hydrological model. An extensive field survey of the South Nation, Raisin Region, du Nord, L'Assomption, Chateauguay and Noire River basins was carried out. Channel profile and streambed material data were collected at many locations along rivers and tributaries. The location of wetlands within each basin was also noted and ground truthing was performed to improve land cover data accuracy. Mens (2005) used the field data gathered to create a river classification system based on channel slope. Channels within an individual WATFLOOD grid cell can be classified into one of the following four classes: sand bottom, cobble, vegetated and headwater streams. The classification of rivers simplifies model calibration by allowing the user to attach a physical meaning to river class parameters. For example, it is expected that the Manning's n value for a channel within the cobble river class would be significantly higher than a channel within the sand river class.

7.1.7 Lakes and Control Structures

Lake operating rules were added for some of the larger lakes in Quebec, north of the St. Lawrence River, where major lakes along the channels dampen flows.

7.2 Model Calibration

A parameter file (.PAR) contains most of the model parameters used by WATFLOOD. Most parameters are associated with either a river class or land class (GRU). Model calibration was performed manually starting from a pre-existing "universal" parameter set for the

Grand River basin in southern Ontario, as an initial estimate of each parameter. This Grand River parameter file, given in Appendix A (GR10K.PAR) is available for download from the WATFLOOD website.

Calibration of model parameters was performed using rain gauge data only and was based on a series of streamflow events from September to December 2003. Initially, GRU parameters were adjusted for the Quebec, south of the St. Lawrence River region. Since no "Wetlands" class exists for this region, parameters for the other seven land classes were transferred to the PAR files for all other regions. Further calibration was performed separately for the Eastern Ontario and Quebec, north of the St. Lawrence River regions. Calibration was not performed for the Champlain River basin as no rain gauge data were available for the area. The same parameter set used for the Quebec, south of the St. Lawrence River region was applied to the Champlain River Basin region.

Final model parameters for each region are contained in their respective PAR files listed in Appendix A. Streamflow hydrographs for the calibration period for each hydrometric station used in the study are in Appendix B.

8 Results

The WATFLOOD model was executed as a continuous simulation for all four regions for the period from December 1st 2002 to November 30th 2005. The first year of simulation was used as a spin-up period to allow the model to properly initialize. Evaluation of each precipitation input was based on model performance from January 1st 2003 to November 30th 2005, excluding the calibration period (September to December 2003) and any period with missing radar data. Since calibration was not performed for each individual precipitation input (i.e. separate calibration for rain gauges and each radar product), results are expected to show bias towards precipitation gauge-driven model results. However, similar simulation results were obtained for the calibration period using precipitation gauge data and the C2 and C3 radar products. Therefore, it is unlikely that the final parameter sets would have differed significantly had the model been calibrated using radar data for the chosen calibration period.

In order to identify local problems within each radar product, the annual cumulative precipitation for the entire radar domain was calculated. The McGill radar station was not in operation during the summer of 2003 for maintenance reasons. Therefore, the estimated precipitation accumulation over each grid was calculated for 2004 (January 1st to December 31st) and 2005 (January 1st to November 30th) for all radar products and distributed gauge data (Figures B.7 to B.14, Appendix B). The approximate extents of the Doppler and conventional radar units are indicated by dashed white ovals.

Environment Canada's mean observed precipitation accumulation (calculated from 1961 to 1990) for the McGill radar domain region is approximately 800 to 1000 mm per year (Figures B.1 to B.4, Appendix B). Figures B.5 and B.6, derived from Environment Canada's Climate Trends and Variations Bulletin reports for 2004 and 2005, respectively, show annual total

precipitation departure from normal for all regions of Canada. The McGill radar region shows near normal precipitation values for 2004 and 2005. Eastern Ontario and Quebec, south of the St. Lawrence River saw slightly higher precipitation totals in 2005. Therefore, it is expected that calculated precipitation accumulations for 2004 and 2005 for all regions within the 240 km radius of the radar station fall within or near an expected range of 1600 to 2000 mm.

Regions within the McGill radar that suffer from a consistent under or overestimation of precipitation by radar are immediately obvious in Figures B.7 to B.14, Appendix B. Extensive shadows, created by the beam blocking effects of the Laurentian Mountains, extend northwest of the radar and cover much of the Rouge and Petite Nation watersheds, as well as the headwater area of the du Nord River basin. Similar shadows appear to a lesser extent within the northern region of the L'Assomption basin. VPR corrections applied to the C3 radar product show some improvement to shadowed areas, yet these regions still suffer from significant under-prediction of precipitation. The presence of shadows in this region explains how a sparse gauge network, concentrated around the Montreal area, can estimate precipitation within most basins better than all three radar products (later shown in this Section). Since there are no mesonet stations located within the shadowed areas, such extensive areas of underestimation can go unnoticed when using radar-rain gauge scatter plots to evaluate radar performance. As well, persistent under or overestimation of precipitation in a given area may not be apparent from single-event observations; the high degree of scatter expected within a radar-rain gauge scatter plot can mask such a problem.

Another shadow, caused by a building adjacent to the McGill radar station, affects a large area to the south of the radar station. As a result, precipitation estimates over the headwaters of the Chateauguay River basin, as well as several subbasins within the Lake Champlain region, are impacted. Radar-derived hydrological predictions for all basins affected by beam blocking are likely to, on average, underestimate streamflow volume.

Another problem area is evident outside of the modelling regions, west of the Chateauguay watershed. It is likely that uncorrected clutter remains in this area and causes a persistent overestimation of precipitation. Consequently, a shadow is created behind it. The C2 and C3 radar products show little improvement in this area over the C0 product. Other "hot spots" are noticeable in 2005 in areas southeast of the radar station.

Figures B.7 to B.14 show that the use of radar precipitation estimates for hydrological modelling remain useful only in areas where the radar signal is unobstructed. Attempts to correct precipitation measurements for shadowed areas using VPR correction techniques are unsuccessful within the McGill radar domain.

Annual precipitation accumulations derived from precipitation gauge measurements offer values that are more realistic. Precipitation totals for 2004 and 2005 generally fall within the expected ranges as described by Environment Canada. It is likely that distributed gauge data produces an underestimation of precipitation during winter months due to the limited network coverage and undercatchment by gauges.

8.1 Streamflow Hydrographs

The WATFLOOD model outputs volumetric streamflow for specified grid cells within a watershed. Hydrographs are used as a means of visually comparing calculated and observed streamflow measurements for grid cells containing hydrometric stations. A qualitative evaluation of the model's performance is made based on how well model output reflects observed streamflows in the timing and magnitude of flood event peaks, and the slope of the rising limbs and recession curves.

Appendix C contains streamflow hydrographs for the evaluation period for all hydrometric stations within each study region. The spin-up period from January to December 2002 is not shown. A solid black line with grey fill represents observed streamflow at each station.

Model results from the C0, C2 and C3 radar products are indicated by red, blue and green solid lines, respectively. WATFLOOD output produced using precipitation gauge data are shown as a dashed black line. Since precipitation gauge data were not available for the Lake Champlain basin, only model results from radar products are shown.

8.2 Statistical analysis of flood events

In order to determine which real-time precipitation product (radar or gauge) optimally predicted major hydrological events within the McGill radar domain, statistical analysis was performed on select flood events within each region. The following statistical criteria were calculated based on hourly streamflow output from the WATFLOOD model: the Nash-Sutcliffe coefficient, correlation coefficient, root mean squared error, deviation of runoff volumes, absolute percent bias, bias and mean absolute error. Sections 8.2.1 to 8.2.7 are derived from Juneja (2006) and provide a description of each criterion.

8.2.1 Nash-Sutcliffe Coefficient (N_r)

The Nash-Sutcliffe coefficient (N_r) is a measure of statistical association, which indicates the percentage of the observed variance that is explained by the predicted data. The Nash-Sutcliffe coefficient, also known as the efficiency criterion, is perhaps the most common measurement mentioned in hydrological literature for evaluating the performance of a model. It evaluates how well the calculated and observed hydrographs compare in both volume and shape. N_r is determined using Equation 7:

$$N_r = 1 - \frac{\sum_{i=1}^{N} (S_i - O_i)^2}{\sum_{i=1}^{N} (O_i - O_i^*)^2} \qquad [7]$$

S_i and O_i are the simulated and observed discharge for each time step, respectively. O_i^* is the average measured discharge. N is the total number of values within the period of analysis. The second term in Equation 7 represents the ratio between the mean square error (*MSE*) and the variance of the observed data. Thus, a value of N_r equal to zero indicates that the model output is not better than that obtained using the simple averaged observed streamflow for the entire period of analysis. The closer N_r is to one, the better the fit between the modelled and observed data series. The Nash-Sutcliffe statistic puts more emphasis on extreme events than on average flows. Additionally, the timing of the predicted series greatly influences the value of the coefficient

8.2.2 Correlation Coefficient (R)

The *R* statistic describes the degree of colinearity between the observed and modelled time series. A value of one, as calculated using Equation 8, would indicate perfect correlation between observed and modelled values.

$$R = \frac{\frac{1}{N} * \sum_{i=1}^{N} (O_i - O_i^*) * (S_i - S_i^*)}{\sqrt{\left(\frac{N * \sum_{i=1}^{N} O_i^2 - \left(\sum_{i=1}^{N} O_i \right)^2}{N * (N-1)} \right)} * \sqrt{\left(\frac{N * \sum_{i=1}^{N} S_i^2 - \left(\sum_{i=1}^{N} S_i \right)^2}{N * (N-1)} \right)}} \quad [8]$$

As with the Nash-Sutcliffe statistic, the correlation coefficient is more sensitive to outliers than to values near the observed mean. The WATFLOOD's STATS program calculates the squared correlation (R^2). This value range from zero, indicating no correlation between observed and measured discharge, to one, indicating perfect correlation.

8.2.3 Root Mean Square Error (RMSE)

The RMSE, measured in units of streamflow (m^3/s), is an estimate of the total error (random and systematic) between observed and modelled values and is calculated using the following equation:

$$RMSE = \left[\frac{1}{N} \sum_{i=1}^{N} (S_i - O_i)^2 \right]^{1/2} \quad [9]$$

The RMSE can be normalized by the average streamflow observed at a given station to allow comparison between model performance for different subbasins.

8.2.4 Deviation of Runoff Volume (D_v)

The deviation of runoff volumes D_v, also known as the percentage bias, measures the total systematic error in the total streamflow volume. Its value is calculated using Equation 10:

$$D_v(\%) = \frac{\sum_{i=1}^{N} (S_i - O_i)}{\sum_{i=1}^{N} O_i} * 100 \quad [10]$$

For a perfect model, D_v is equal to zero. The smaller the D_v value, the better the performance of the model.

8.2.5 Absolute Percent Bias (APB)

The absolute percent bias is a measure of the timing difference between the streamflow observations and the model simulations. The APB is usually used in conjunction with the D_v criterion. Given an observed and simulated series where the D_v value is small and the APB is large, one could conclude that both series share similar volumes but that their timing is

not as close. Thus, a good agreement in timing and volume requires D_v and APB to be small. APB is always greater than D_v, and its value is determined using Equation 11:

$$APB(\%) = \frac{\sum_{i=1}^{N} \left| S_i - O_i \right|}{\sum_{i=1}^{N} O_i} * 100 \quad [11]$$

8.2.6 Bias (b)

The bias is measured in units of streamflow (m^3/s). This criterion is used to quantify the systematic error between observed and modelled streamflow values.

$$b = \frac{\sum_{i=1}^{N} (S_i - O_i)}{N} \quad [12]$$

8.2.7 Mean Absolute Error (MAE)

The MAE, measured in units of streamflow (m^3/s), is a measure of the model's accuracy in replicating the observed time series.

$$MAE = \frac{\sum_{i=1}^{N} \left| S_i - O_i \right|}{N} \quad [13]$$

8.3 Discussion of Results

Figures D.1 to D.54 in Appendix D consist of streamflow hydrographs for select flood events throughout the study period. Following each set of hydrographs is a table that details statistical criteria calculated for the event. Table cells are highlighted to indicate which precipitation input produced the best statistical result for each streamflow gauge. The cell containing the best statistical criterion is highlighted in yellow if it is produced using

precipitation gauge data, or in green is if it is produced using a radar product. If the best overall statistic was calculated using precipitation gauge-derived results, the best result among radar products is highlighted in blue. A similar analytical approach was taken by Juneja (2006). In this thesis, several more hydrological events are analyzed over a longer simulation period to examine radar product performance throughout the study period. Additionally, significant improvements were made to model results through the correction of drainage areas and the introduction of additional channel morphology data collected during field investigations. Particular improvement to streamflow prediction was made for both Quebec regions and the Lake Champlain basin.

8.3.1 Eastern Ontario

Figures C.4 to C.9 are the resultant streamflow hydrographs for the Eastern Ontario region. WATFLOOD-calculated values are able to successfully reproduce events at most hydrometric stations within the region. One notable exception is the Delisle River subbasin. According to the available land cover data, no wetlands exist upstream of the Delisle River hydrometric station (Table 6, Section 6.1.1). However, the dampened flows of the observed hydrograph are similar to those of the Beaudette River, where wetland hydrology has a significant impact on streamflow. It is likely that land cover for areas upstream of the Delisle River streamflow gauge is not properly characterized. There are many wooded swamps in the area that are likely classified as coniferous forests. Therefore, peak streamflow values calculated by the WATFLOOD model often exceed observed values.

The timing of the spring 2003 melt within the South Nation River basin was far too early. Temperature stations in the area were not in operation for this period and it is possible that distributed temperature data from other stations did not reflect local conditions. The early melt also affected the streamflow event in early April. Following the spring melt, hydrological response of a basin is very sensitive to minor changes in precipitation. As

upper and lower zone storage capacities are exhausted and the ground is saturated, any additional precipitation over a watershed is converted to runoff.

The model underestimates spring melt volumes from most subbasins in the region for all precipitation inputs. Since the magnitude of the spring melt event is dependent on snow pack accumulation over winter months, the lack of streamflow volume indicates either an under-prediction of precipitation by both radar and gauges or a problem with the model's accounting of frozen precipitation. Table 16 to Table 18 compare cumulative winter precipitation and total observed runoff from each basin. Runoff and precipitation volumes are normalized by basin area to facilitate comparison. It should be noted that the C3 radar product was only extended beyond the Doppler range in 2004. Therefore, cumulative precipitation values for the South Nation watershed during the winter of 2002/2003 suffer from a lack of data.

Table 16- December 1st 2002 to March 31st 2003: Precipitation comparison with observed runoff

	Cumulative Precipitation (mm)				Observed Runoff (mm)
Subbasin	**Precip. Gauge**	**C0 radar**	**C2 radar**	**C3 radar**	
Bearbrook	66	74	69	59	115
Castor River	63	78	73	27	141
SNR near Plantagenet	71	99	89	90	79
SNR at Spencerville	62	107	86	0	116
Beaudette River	101	114	105	121	127
Delisle River	91	116	106	120	131
S. Raisin River	93	136	121	129	n/a
Raisin River	87	137	121	131	113

Table 17- January 1st 2004 to March 31st 2004: Precipitation comparison with observed runoff

	Cumulative Precipitation (mm)				Observed Runoff (mm)
Subbasin	Precip. Gauge	C0 radar	C2 radar	C3 radar	
Bearbrook	74	88	84	82	287
Castor River	70	84	77	84	192
SNR near Plantagenet	66	87	80	82	96
SNR at Spencerville	70	74	71	80	131
Beaudette River	55	84	75	75	176
Delisle River	61	85	77	77	184
S. Raisin River	62	91	83	93	n/a
Raisin River	64	89	81	84	153

Table 18- December 1st 2004 to March 31st 2005: Precipitation comparison with observed runoff

	Cumulative Precipitation (mm)				Observed Runoff (mm)
Subbasin	Precip. Gauge	C0 radar	C2 radar	C3 radar	
Bearbrook	118	100	83	98	182
Castor River	122	103	84	104	409
SNR near Plantagenet	111	112	92	109	97
SNR at Spencerville	125	85	76	100	155
Beaudette River	112	116	91	107	183
Delisle River	112	122	98	112	20
S. Raisin River	114	130	104	121	n/a
Raisin River	112	126	102	116	165

Although the 2005 spring melt continued into the month of April, cumulative precipitation values were only calculated up to and including the month of March so as not to overestimate precipitation. Total runoff values calculated for the South Raisin River hydrometric station are not reported in the above tables, as the streamflow gauge at the station consistently reports a minimum flow of 1 m^3/s. This station is included in the analysis because useful data are reported for the larger flows.

Observed total runoff values for the winter and spring melt often exceed cumulative precipitation amounts for the same period. Therefore, it is most likely that winter precipitation in Eastern Ontario is underestimated by both radar and gauges.

Underestimation of snow pack accumulation by radar may be attributed to periods of light snowfall that go unnoticed by the radar. The long wavelength of an S-band radar unit, such as the McGill radar station, is less likely to detect light rain or snow events. Therefore, errors in snowfall detection accumulate over the winter months and significantly impact the spring melt. Additionally, winter precipitation often results from low-level storms that may be overshot by the radar beam. Seo and Johnson (1997) noted that range effects are more pronounced during cold months. It is likely that the existing McGill VPR correction methods do not offer a significant level of correction for snowfall.

Underestimation of snow pack accumulation by precipitation gauges may be attributed to undercatchment by gauges. It should also be noted that once precipitation begins to fall as snow, the density of the precipitation gauge network is drastically reduced, as only those stations equipped with weighing gauges are in operation.

Since the focus of the Enhanced Nowcasting project is on the accurate prediction of extreme weather events, only large non-melt flood events were selected for further analysis. The following eight events were used to visually and statistically determine which precipitation input is able to best reproduce hydrological events using the WATFLOOD model:

1. April 14th to May 1st 2003
2. September 26th to December 31st 2003 (calibration period)
3. April 13th to April 30th 2004
4. September 9th to September 16th 2004
5. November 1st to November 13th 2004
6. November 24th to December 6th 2004
7. April 21st to May 7th 2005
8. June 15th to June 24th 2005

Hydrographs for the above events are represented by Figures D.1 to D.8. Tables D.1 to D.8 show the statistical criteria calculated for each event. Tables D.9 and D.10 summarize the results for all events. The letter "X" denotes the precipitation product that performed best for a given event and subbasin. The calibration period was not considered in determining the best overall precipitation input (Table D.9). Since the model was calibrated using precipitation gauge data, model results are particularly biased precipitation gauges during this event.

Table D.9 indicates that precipitation gauge data produced the best overall model results for the Eastern Ontario region. The C0 and C3 radar products performed best for the greatest number of events for the Castor River and Bearbrook subbasins, respectively. This result is likely due to the lack of precipitation gauge coverage in the western portion of the South Nation River basin. The C2 product outperformed all other precipitation inputs for the Beaudetter River subbasin.

Among radar products, the C2 product performed best for all Raisin Region subbasins. The Bearbrook was best modelled using the C3 radar product, whereas the Castor River and South Nation River (at Spencerville) subbasins were best modelled by the C0 radar product.

The South Nation River (at Plantagenet) performed best for an equal number of events using the C2 and C3 radar products.

8.3.2 Quebec- North of the St. Lawrence River

Figures C.10 to C.15 are the resultant streamflow hydrographs for Quebec, north of the St. Lawrence River. The following six events were isolated to visually and statistically determine which precipitation input is able to best reproduce hydrological events using the WATFLOOD model:

1. September 26th to December 31st 2003 (calibration period)
2. April 13th to April 30th 2004
3. September 9th to September 16th 2004
4. November 1st to November 13th 2004
5. November 24th to December 6th 2004
6. April 21st to May 7th 2005

Hydrographs for the above events are represented by Figures D.9 to D.14. Tables D.11 to D.16 show the statistical criteria calculated for each event. Tables D.17 and D.18 indicate the precipitation product that performed best for a given event and subbasin.

Despite the low gauge density and lack of network coverage for most of the region, model results derived from precipitation gauge data outperformed all radar products in the region. This is largely because distributed gauge data resulted in larger flows during most events, whereas beam blocking affected radar measurements in the Rouge, Petite Nation and du Nord River basins. The L'Assomption River basin was the sole exception, where the C0 radar product performed best for the greatest number selected events.

The Rouge and Petite Nation River basins were poorly modelled regardless of inputs. A large number of lakes and control structures that exist within the region are not defined within the model due to a lack of data. However, despite the poor correlation between modelled and observed flows for all model runs, it is immediately obvious that the gauge precipitation data can best estimate streamflow volumes, particularly during widespread rain events. Winter and spring streamflow simulations suffer from similar problems as described for the Eastern Ontario region. All radar products consistently underestimated streamflow volumes in both the Rouge and Petite Nation River basins. As shown in annual accumulation for radar products (Figures B.7 to B12), beam blocking due to the region's topography is the most likely factor affecting radar precipitation estimates in these basins. WATFLOOD results indicate that the VPR correction algorithms applied to the C2 and C3 radar products do little to improve precipitation estimates within these two basins. In fact, among radar products, the uncorrected C0 product produced the best results for the region.

8.3.3 Quebec- South of the St. Lawrence River

Figures C.16 to C.18 are the resultant streamflow hydrographs for Quebec, south of the St. Lawrence River. The following thirteen events were isolated to visually and statistically determine which precipitation input is able to best reproduce hydrological events using the WATFLOOD model:

1. April 14th to May 1st 2003
2. September 26th to December 31st 2003 (calibration period)
3. April 13th to April 30th 2004
4. May 23rd to June 10th 2004
5. July 5th to July 30th 2004
6. July 30th to Aug 8th 2004

7. August 12th to August 18th 2004
8. September 9th to September 16th 2004
9. November 5th to November 13th 2004
10. November 20th to December 19th 2004
11. April 23rd to May 7th 2005
12. June 15th to June 24th 2005
13. August 16th to September 24th 2005

Hydrographs for the above events are represented by Figures D.15 to D.27. Tables D.19 to D.31 show the statistical criteria calculated for each event. Tables D.32 and D.33 indicate the precipitation product that performed best for a given event and subbasin.

For the Quebec, south of the St. Lawrence River region, precipitation gauge data produced better streamflow simulation results than radar products. Even within the Noire River basin, where no mesonet stations exist, distributed precipitation data from gauges outside the basin were still able to accurately predict many flood events. Since several mesonet stations within the region are equipped with weighing gauges, spring melt events are better simulated than in other regions. The timing of the 2005-modelled spring melt began later than observed values indicate.

Among radar products, the C2 product performed best within the Noire and English River basins during the selected events. The C0 radar product performed better than the VPR-corrected products for the Chateauguay watershed. This may be explained by a small degree of beam blocking that occurs in the headwaters of the Chateauguay River basin. The general overestimation of the C0 product tends to falsely correct for the underestimation due to beam blocking. This is similar to the results for areas north of the St. Lawrence River,

where beam blocking is a problem, and parts of the South Nation River basin where range effects persist despite VPR correction.

8.3.4 Lake Champlain Basin

Figures C.19 to C.36 are the resultant streamflow hydrographs for the Lake Champlain basin region. The following nine events were selected to visually and statistically determine which precipitation input is able to best reproduce hydrological events using the WATFLOOD model:

1. April 14th to May 5th 2003
2. March 23rd to April 30th 2004
3. May 31st to June 10th 2004
4. July 1st to August 8th 2004
5. September 8th to September 17th 2004
6. November 20th to December 11th 2004
7. March 29th to May 5th 2005
8. June 9th to June 23rd 2005
9. October 7th to November 30th 2005

Hydrographs for the above events are represented by Figures D.28 to D.54. Tables D.35 to D.42 show the statistical criteria calculated for each event for each radar product. Tables D.43 and D.44 indicate the precipitation product that performed best for a given event and subbasin.

Statistical results from certain hydrometric stations are not considered in the evaluation of radar product performance. For example, flows at the Otter Creek at Middlebury station

(1573 km^2) are dampened by upstream wetlands that are not accounted for within the model setup due to a lack of data. Similarly, the Sarnac River at Plattsburgh exhibits signs of a possible upstream control structure. The Little River at Waterbury gauge malfunctioned throughout the study period. The Lake George at Rogers Rock gauge was not in operation until the summer of 2005.

Although the model was not calibrated for this region, certain events were simulated well for several subbasins. Streamflow volumes at stations west of the Lake are generally underestimated. Although the C3 radar product outperformed the other radar products for most events, model results for the region can be described as erratic, with no one radar product consistently producing accurate streamflow simulations. Additional data (such as wetland areas) should be introduced into the model setup. Calibration is necessary to further improve model results and properly assess the performance of each radar product. Presently, the Lake Champlain basin region provides little insight into the skill of each radar product.

8.4 Overall Assessment of Radar Products

Results from the visual and statistical analysis of selected flood events do not clearly indicate which of the three radar products are best suited to hydrological modelling of the radar domain. Radar product performance appears to vary between regions and even between subbasins within the same region.

Based on hydrographs in Appendix C, it is evident that the VPR-corrected radar products (C2 and C3) offer some improvement over the C0 product. Benefits are most noticeable in areas closest to the radar station and within Doppler range (Raisin region, L'Achigan River basin and Quebec, south of the St. Lawrence River). The uncorrected C0 product tends to produce hydrographs with exaggerated peaks for these areas. Basins at further ranges from the radar, such as the South Nation River at Spencerville and much of the Quebec, north of

the St. Lawrence River region, appear to benefit from the over-prediction of precipitation by the C0 product. Generally, at longer range, beam filling and possibly some attenuation become a problem. It is unclear whether the success of VPR correction techniques within the Doppler range can be attributed to the added information provided by the Doppler radar unit or the beam elevation up to a distance of 120-km from the station.

Based on radar/precipitation gauge comparisons of several storm events in the Montreal area, Bellon et al. (2006) found that the VPR correction method used by the C2 radar product yielded the largest error reduction. It was noted that although the C3 product performed with some skill during fall events, it yielded negligible improvement over the entire spring period. Hydrological simulations show similar results for basins within Doppler range of the radar. During the summer and fall months, model output from the C3 product performs equally as well or in some cases better than runs performed using the C2 product. Bellon et al. (2006) concluded that the climatological algorithm used to generate the C3 radar product cannot be applied to all types of precipitation and is therefore not suitable for real-time precipitation estimation.

Estimation of springtime flows using radar-derived precipitation estimates for the McGill radar domain is generally unsuccessful. Snowfall accumulation over the winter months is underestimated for most regions. The added complexity of mixed precipitation events renders it impossible to apply a suitable Z-R relationship over the entire radar domain during such events. The nowcasting of events involving mixed precipitation remains a major problem for radar meteorologists (Bellon, 2005).

8.5 Effects of Basin Size and Distance from Radar

Carpenter et al. (2004) note that as the drainage area of a basin decreases, the uncertainty in flow simulation from a distributed model increases in a well-defined manner. However this statement is only true if all systematic errors are removed from model input. This is clearly

not the case when using radar-derived precipitation estimates to drive a hydrological model. In fact, some smaller watersheds, such as those in the Raisin Region, were often modelled with greater success than many basins with drainage areas exceeding 1 000 km^2. Radar introduces a number of errors that depend on range, location and type of synoptic event. A large watershed is more likely to include areas that suffer from the effects of beam blocking or range effects.

Figure 16 and Figure 17 attempt to relate basin size and distance from radar (calculated from basin centroid to radar station, Tables A.1 to A.3, Appendix A) to model performance. Drainage area and distance are plotted against the Nash-Sutcliffe coefficient for the calibration period (September 23rd to December 31st 2003). Results for precipitation gauges and the C2 radar product are shown for each hydrometric station in Canada.

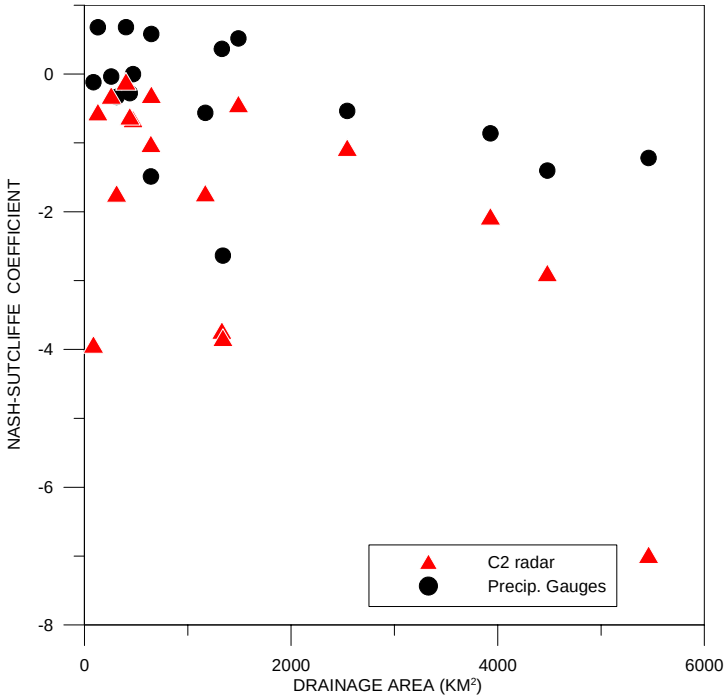

Figure 16- Drainage area vs. Nash-Sutcliffe coefficient, calibration period

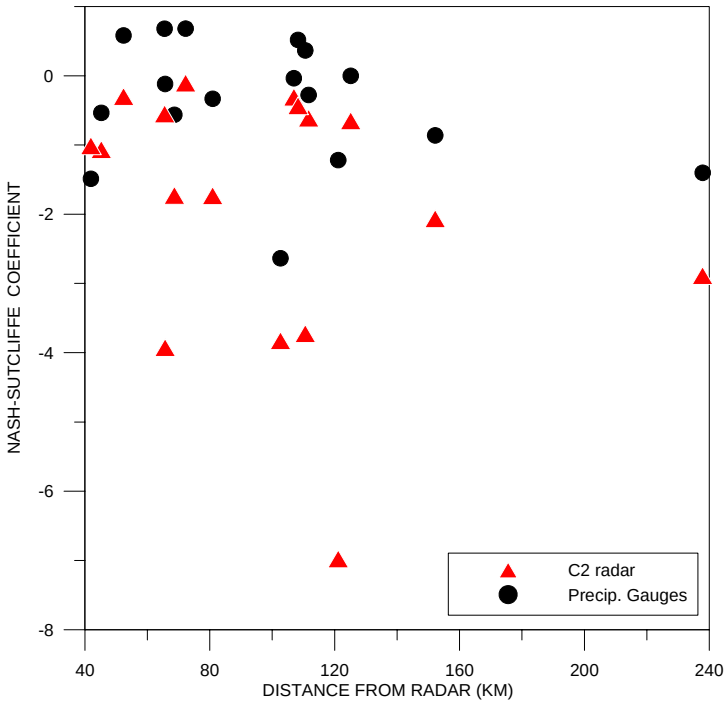

Figure 17- Distance to radar vs. Nash-Sutcliffe coefficient, calibration period

Contrary to the findings of Carpenter et al., model performance decreased with increased basin size due a lack of gauge coverage throughout much of the study area. Similarly, Figure 17 implies that the efficiency of gauge-based model results also decreased with distance from the radar, since basins with centroids furthest from the radar station tend to suffer from poor network coverage.

Similar weak correlations can be seen using radar data. Watersheds at further distances from the radar station suffer most from range effects, while larger watersheds are more likely to include areas impacted by beam blocking in this region. Similar results were obtained when comparing basin size and distance to other statistical criteria.

8.6 Event Analysis

Although the Enhanced Nowcasting Project places emphasis on the prediction of extreme weather events, it is vital to continuous hydrological modelling that basin conditions be properly estimated at all times. Antecedent conditions must be accurately calculated prior to a flood event in order to successfully predict the true impact of precipitation. Therefore, radar-processing algorithms must consistently provide accurate rainfall estimates in order to produce a radar product that is suitable for use in flood forecasting systems. The following events were selected to demonstrate the strengths and weaknesses of the McGill radar precipitation products as input to the WATFLOOD hydrological model.

8.6.1 May 23rd to June 10th 2004, Quebec, South of the St. Lawrence River

Three storms passed through the Quebec, south of the St. Lawrence River region between May 21st and June 1st, 2004. Basin response to these precipitation events (Figure D.18) was very well simulated by the WATFLOOD model using distributed precipitation gauge data, specifically for the Chateauguay and English Rivers. Flows in the Noire River were overestimated due to poor mesonet coverage. Figure 18 shows the location of mesonet gauges surrounding the Noire River basin and the 24-hour cumulative precipitation calculated from the C2 radar product for May 24th, 2004. Radar data reveal that during the event, precipitation gauge locations received greater amounts of rainfall than most areas within the basin. Therefore the distribution of observed precipitation gauge data resulted in an overestimation of precipitation over the Noire River basin, as shown in Figure D.18.

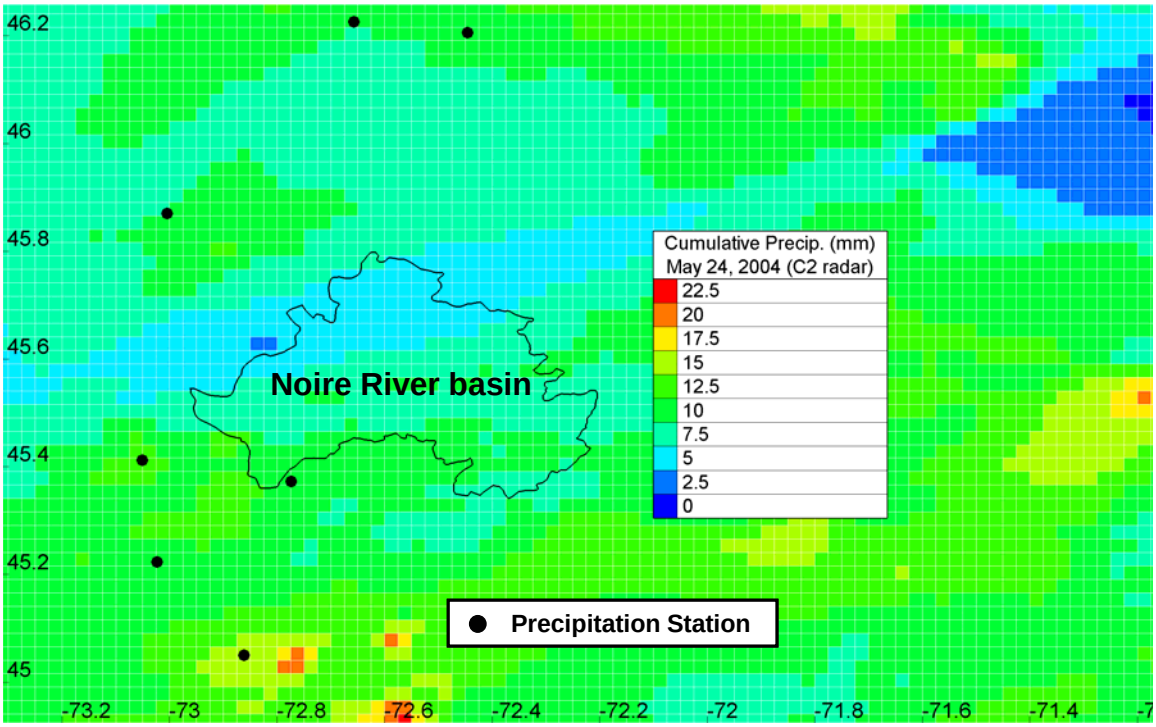

Figure 18- C2 radar cumulative precipitation for the Noire River basin, May 24th 2004

Figure D.18 shows two distinct streamflow peaks in hydrographs for the Chateauguay and English Rivers between May 23rd and June 10th 2004. Flows generated by radar products resulted in an underestimation of peak streamflow during both flood events. Figure 19 consists of scatter plots for storm events on May 21st and 24th and June 1st. Daily rainfall accumulations from gauge and C2 radar observations are plotted for each gauge location in and around the Chateauguay watershed. Scatter plots indicate that the C2 radar product underestimates precipitation accumulations during the first two storms. The June 1st storm event, however, shows relatively good correlation between the C2 radar product and precipitation gauges.

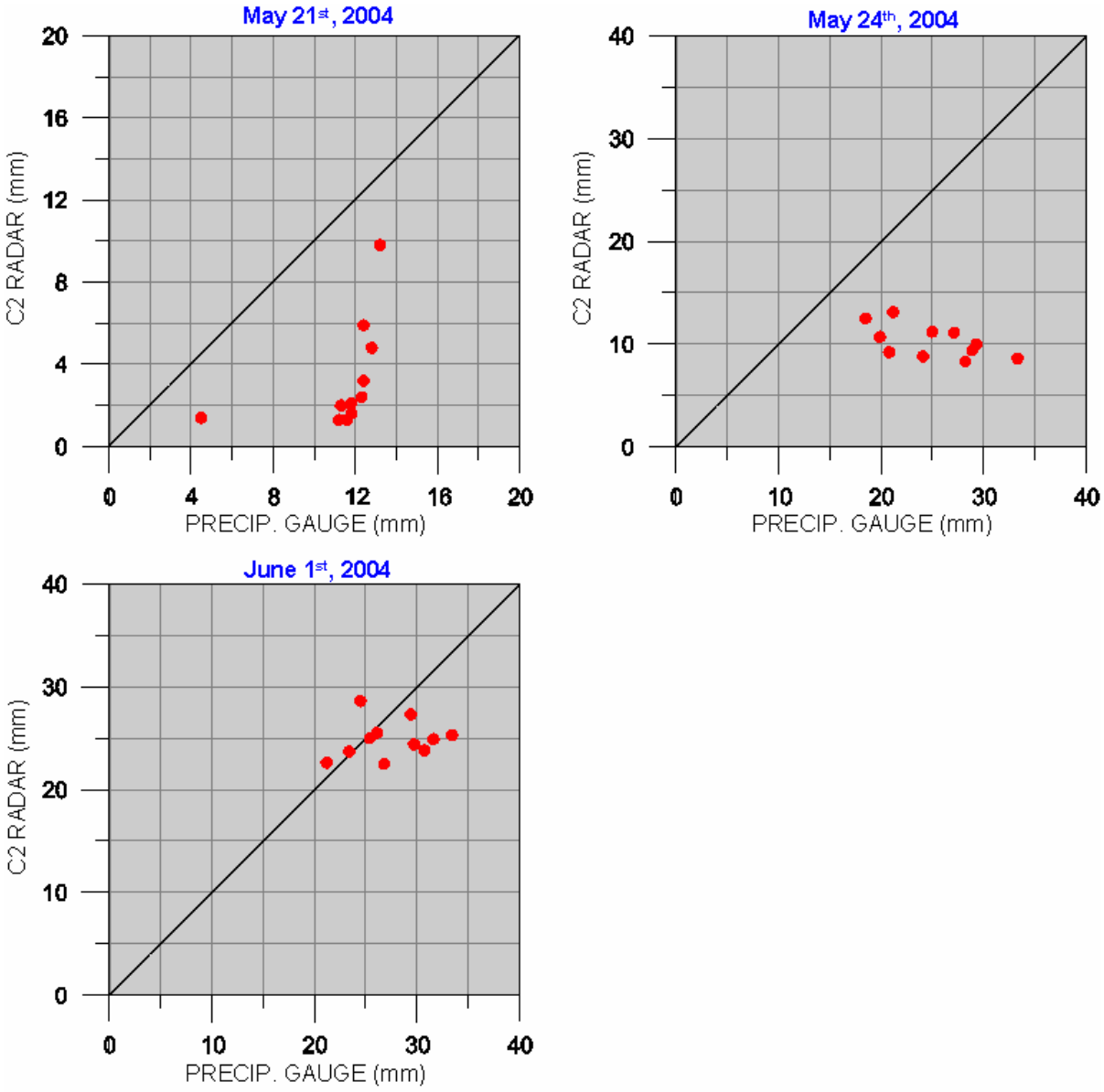

Figure 19- Scatter plots for May/June 2004 storms for the Chateauguay River basin

This event is a very good example of how errors in precipitation estimation can amplify over time within a hydrological prediction system. Although rainfall estimates by radar for the June 1st event may have been accurate, the underestimation of precipitation during previous storms resulted in reduced soil moisture values for the Chateauguay River and

English River basins. As a result, streamflow estimates derived from the radar products failed to attain observed values. Table 19 shows the difference in cumulative basin-averaged precipitation and calculated runoff for the second flood event between June 1st and June 10th, 2004 for each subbasin. Although differences in precipitation values measured over each basin by gauges and radar are small, much greater differences are seen between calculated runoff values.

Table 19- Comparison of precipitation and runoff generated by gauge and C2 radar, June 1st to June 10th 2004

	Cumulative Precipitation (mm)			Calculated Runoff (mm)			Observed Runoff (mm)
Subbasin	**Gauge**	**C2 radar**	**Difference**	**Gauge**	**C2 radar**	**Difference**	
Chateauguay	33	32	**1**	11	4	**7**	14
English	37	36	**1**	15	2	**13**	15
Noire	44	41	**3**	25	9	**16**	15

If the June 1st to June 10th 2004 event is re-run for each radar product using initial watershed conditions calculated from distributed gauge data, a notable improvement in streamflow hydrograph is observed within the Chateauguay watershed. Figure 20 illustrates the change in predicted streamflow derived from radar products for each basin due to a change in initial watershed conditions. The plots on the left are based on continuous modeling using each precipitation input (similar to Figure D.18). Those on the right, use gauge to initialize model parameters prior to the flood event. The increase in calculated discharge from the Noire River basin results in an over-prediction of streamflow volume for the event. This can be attributed to the over-prediction by distributed gauges of basin-averaged precipitation during the May 24th storm, as illustrated by Figure 18.

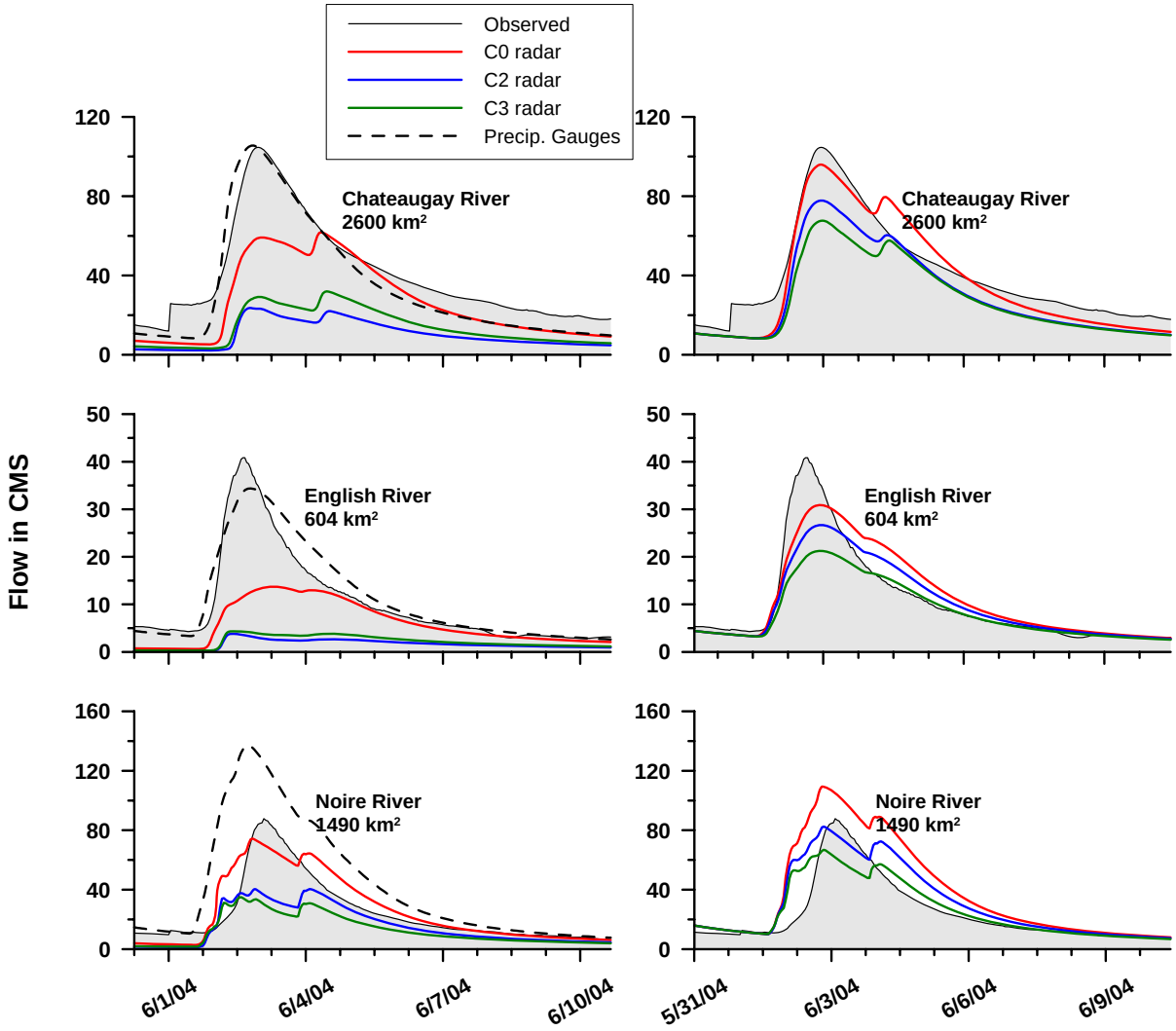

Figure 20- Change in forecasted streamflow using radar data with change in antecedent conditions

8.6.2 April 2004, Quebec, North of the St. Lawrence River

WATFLOOD results derived from precipitation gauge measurements produced the best statistical results for the April 13th to April 30th 2004 event in the Quebec, north of the St. Lawrence River region (Figure D.10, Table D.12 in Appendix D). However, upon observation of streamflow hydrographs for the event, it is apparent that modelled results

from precipitation gauges were only able to capture the initial peak at the L'Achigan River hydrometric station and failed to predict streamflow patterns at other stations. Statistical results were largely influenced by the magnitude of predicted streamflows for the event yet still reflect what is shown by streamflow hydrographs. Calculated $\%D_v$ values indicate that total streamflow volumes for the event were best estimated by rain gauges. The best correlation values (R^2), however, were obtained using the C2 radar product as model results best reflected observed streamflow patterns. This higher value of R^2 shows that the spatial and temporal variation of rainfall captured by the radar is superior to that of gauge-based rainfall, even though precipitation quantities are not. The L'Achigan River subbasin is an exception for the region as it does not suffer from beam blocking or range effects and has fair mesonet coverage.

Similar results were obtained in the region for the June 2005 event (Figure D.14), where radar products failed to produce a significant amount of runoff. These events demonstrate that the existing precipitation gauge network fails to capture the variation of precipitation within the region. Distributed gauge data is only useful during widespread precipitation events.

8.6.3 June 2005, Eastern Ontario and Quebec, South of the St. Lawrence River

In June of 2005, two successive intense periods of precipitation resulted in major flooding throughout regions of eastern Ontario and southern Quebec. In south-western Quebec, 80 to 95% of monthly precipitation was observed over four rather active days, during which two low-pressure systems crossed the region (CRIACC, 2006). Basin response for the South Nation River watershed and Quebec, south of the St. Lawrence River region is shown in Figure 21 and Figure 22, respectively. A scatter plot representing the four-day (June 14th to 17th 2005) storm accumulation observed over each precipitation station accompanies each set of hydrographs. Each scatter plot data point is labelled with its corresponding precipitation

station number. Cumulative rainfall maps for the four-day event are shown in Figure 23 and Figure 24. During the event, there was a suspected gauge malfunction at the South Nation River at Plantagenet hydrometric station.

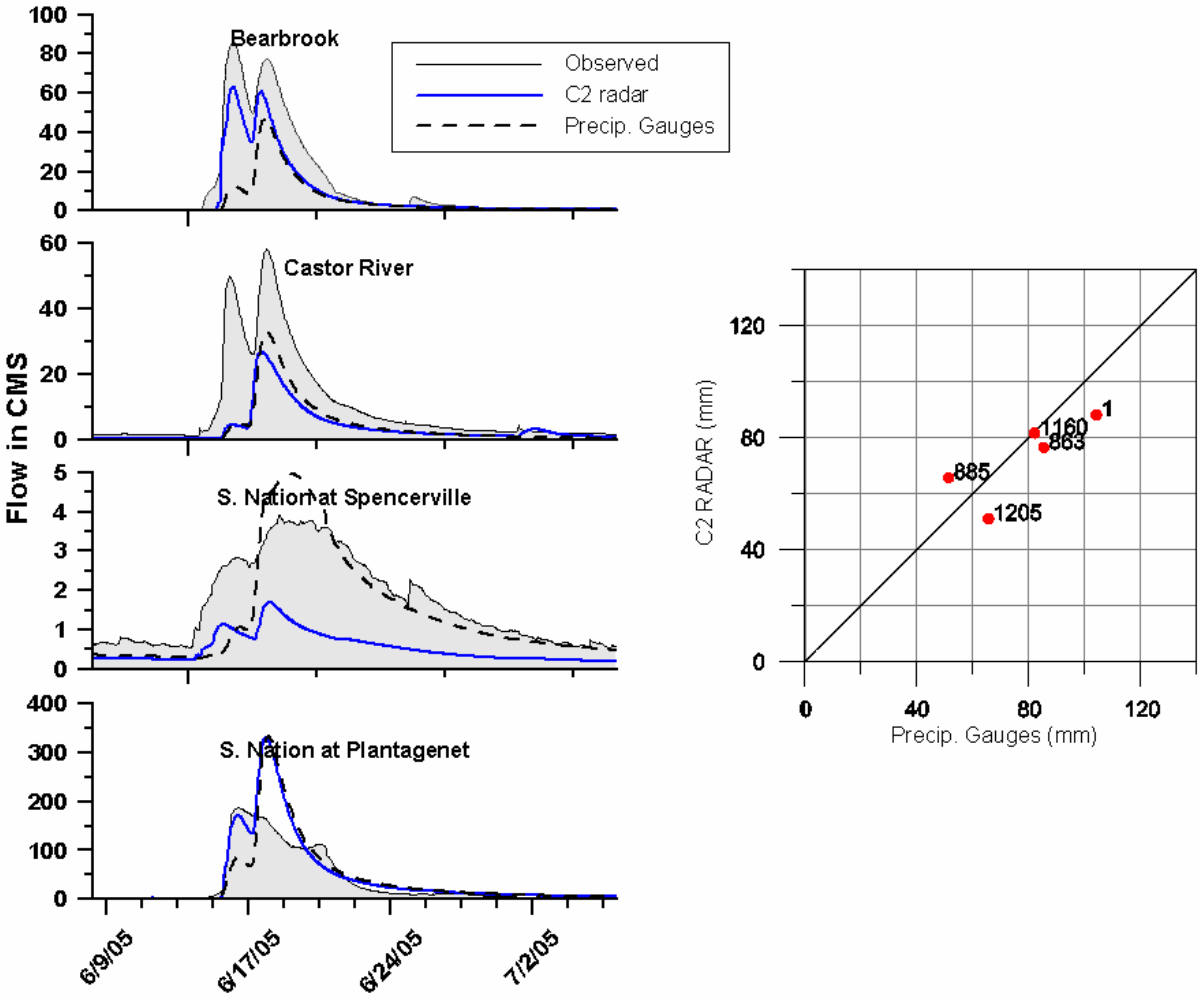

Figure 21- June 2005 flood event– South Nation River

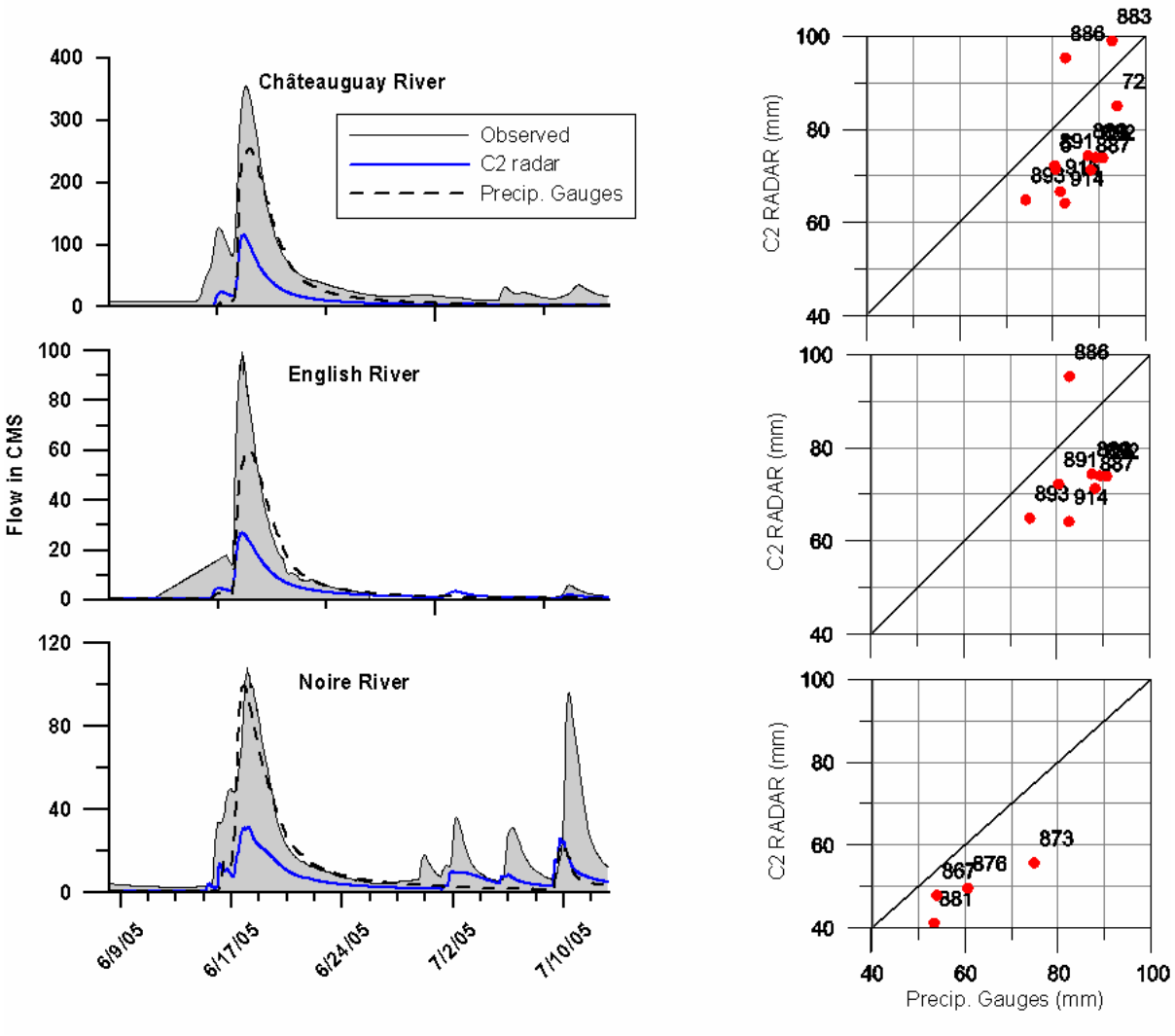

Figure 22- June 2005 flood event– Quebec, south of the St. Lawrence River

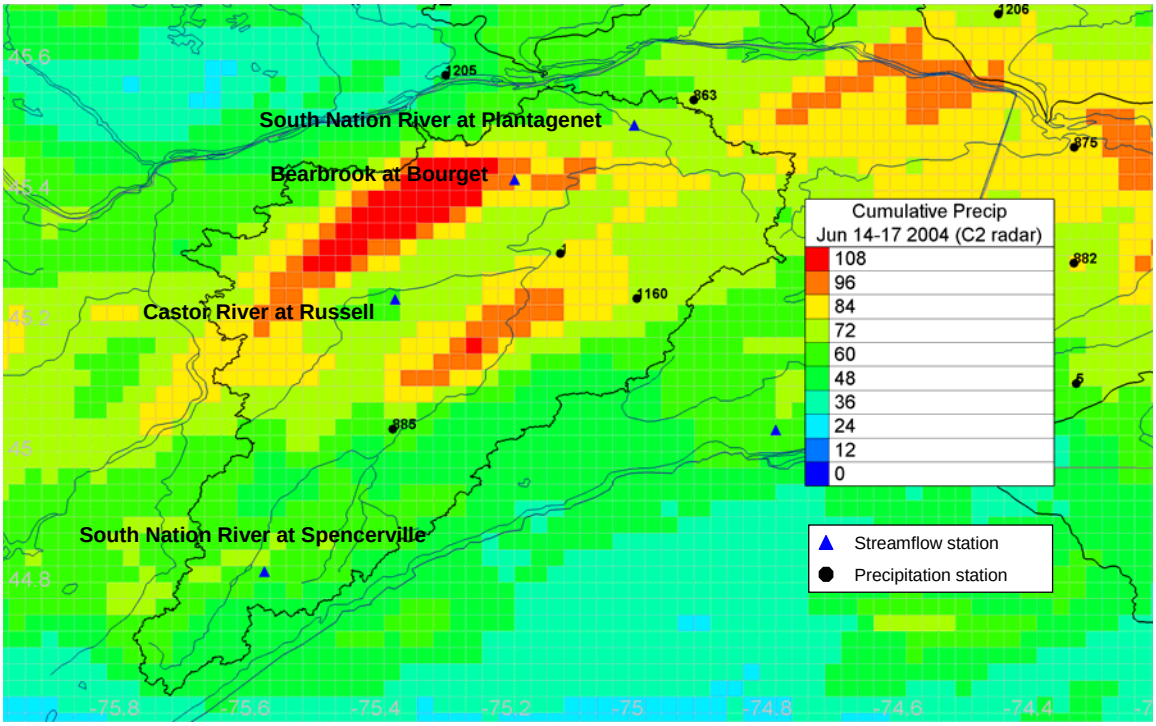

Figure 23- Cumulative precipitation for the South Nation River basin

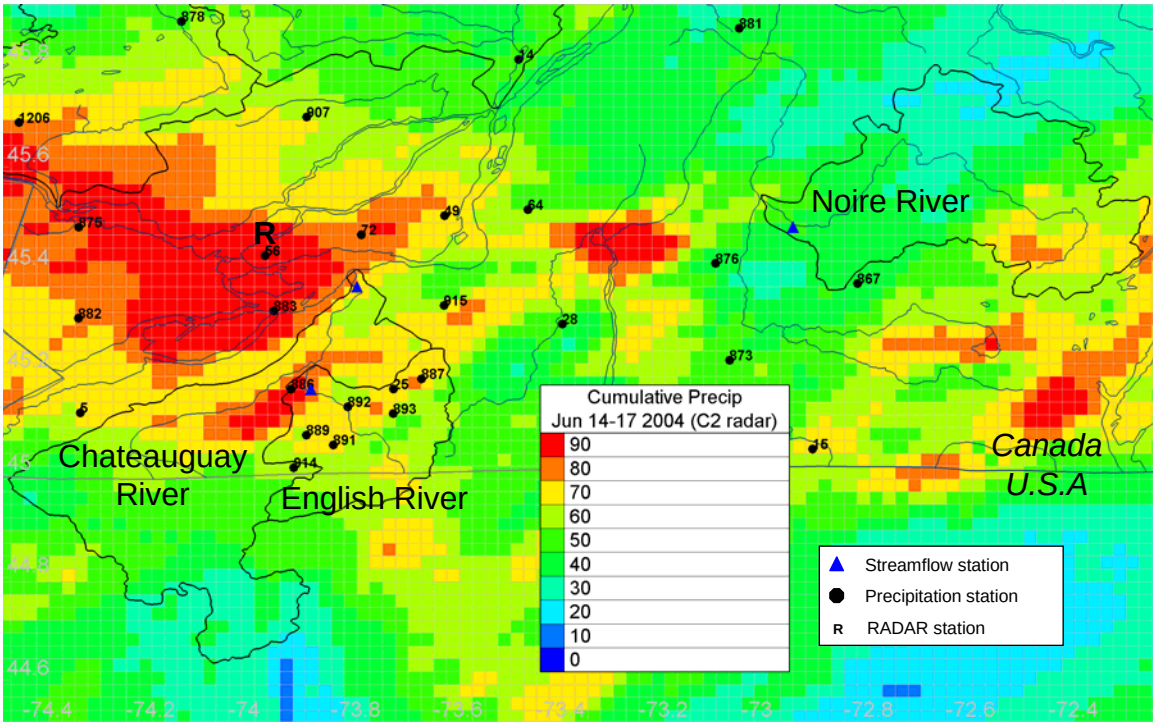

Figure 24- Cumulative precipitation for Quebec, south of the St. Lawrence River region

The scatter plot for the South Nation River basin shows relatively good correlation between radar and rain gauges. However, upon observation of the cumulative precipitation map for the watershed (Figure 21), areas that received the most intense precipitation were entirely missed by the precipitation gauge network. The underestimation of modelled streamflow by gauge data was therefore expected. Distribution of observed rain gauge values could not produce sufficient precipitation over each subbasin to generate observed runoff. The underestimation of modelled streamflow by radar, however is somewhat perplexing. Although the C2 radar product was able to capture the spatial variability of precipitation, little improvement was seen in model results. In fact, the South Nation River at Spencerville subbasin was far better modelled using rain gauge data, although recorded flows at this stations were very low. This event suggests that precipitation estimates by radar may be accurate for some areas of a storm and not others, possibility due to the error associated

with DSD. It can be surmised that during this event, precipitation at greater intensities was underestimated and that the Z-R relationship applied to reflectivity measurements did not accurately describe precipitation in all areas.

In the Quebec, south of the St. Lawrence River region, a negative bias is seen in scatter plots. A significant underestimation of streamflow by radar is evident for all basins. Again, the most intense area of the storm within the Chateauguay River basin was missed by the mesonet; although so were the least intense areas. Table 20 shows that basin-averaged precipitation amounts observed by rain gauges during the event were significantly higher than radar-estimated values. Furthermore, this table underlines the non-linearity of hydrological systems. Smaller differences in precipitation can translate into much larger differences in runoff.

Table 20- Effect of basin-averaged precipitation on runoff, June 13th to 26th 2005

Subbasin	Data source	Precipitation (mm)	% difference	Computed runoff (mm)	% difference
Chateauguay	Gauge	89	24	27	59
	C2 radar	68		11	
English	Gauge	91	19	26	58
	C2 radar	74		11	
Noire	Gauge	74	18	19	58
	C2 radar	61		8	

9 Conclusions and Recommendations

The WATFLOOD hydrological model was used to assess the ability of radar-derived quantitative precipitation estimates to accurately predict precipitation in space and time. Emphasis was placed on severe weather events that resulted in increased streamflow in rivers within the study area. Three radar precipitation products were obtained in real-time from McGill University's J.S. Marshall Radar Observatory near Montreal, Quebec. The C0 radar product consists of radar precipitation estimates that are filtered for erroneous data caused by ground clutter and anomalous precipitation. In addition to the filters applied to the C0 product, the C2 and C3 radar products are corrected for the effects of the vertical profile of reflectivity using different techniques. VPR correction methods were expected to greatly improve radar performance and result in a precipitation product that can be readily used by the water resource community.

Thirty-nine subbasins within the McGill radar domain were used as sample areas. The WATFLOOD model was calibrated using precipitation gauge data from a mesonet surrounding the Montreal area. The model was run continuously over a four-year period using each of the three radar products and precipitation gauge data. Streamflow hydrographs were used to visually compare observed and WATFLOOD-calculated streamflow values for each subbasin and precipitation input. Statistical analysis of select flood events was additionally performed to determine which product is best able to accurately and consistently estimate precipitation over the modelled area.

It was found that the use of radar precipitation estimates for hydrological modelling remains useful only in areas where the radar has an unobstructed view of the basin. Beam blocking by physiographic and man-made features force reflectivity measurements to be taken at greater heights within the atmosphere, where conditions are not representative of

conditions at ground surface. Attempts to correct precipitation measurements for shadowed areas using VPR correction techniques were unsuccessful within the McGill radar domain. Areas that experience consistent overestimation of precipitation were also identified.

Despite the non-ideal distribution of mesonet stations throughout the radar domain, WATFLOOD model results using precipitation gauge data outperformed radar products during most flood events. Precipitation gauges perform best during widespread rainfall events and are unable to capture localized storms.

The VPR correction technique applied to the C2 radar product resulted in the best hydrological results among radar products. The climatological algorithm used to generate the C3 radar product did offer improvement over the uncorrected C0 product, most notably during the summer and fall events. However, Bellon et al. (2006) determined that the C3 product cannot be applied to all types of precipitation and is therefore not suitable for real-time precipitation estimation. The C0 product, which tends to over-predict precipitation, was found to perform best in areas affected by beam blocking or range effects. Its tendency to overestimate precipitation resulted in increased storm volumes thus, to a certain extent, offsetting the beam blocking and range effects. However the C0 should not be considered as a reliable source of precipitation for any region within the McGill radar domain due to its known weaknesses (bright-band contamination and VPR effects).

All precipitation products, including precipitation gauge data, under-predict snowfall accumulation over the winter months. The Chateauguay River basin, which is entirely within Doppler range and has the highest density of mesonet stations equipped with weighing gauges, was the only basin in which modelled springtime streamflow volumes from either precipitation source reasonably approximated observed values.

Radar-derived model results were best for watersheds within the Doppler range. However, this experiment does not indicate whether the success of VPR correction techniques within

the Doppler range can be attributed to the added information provided by the Doppler radar unit or the beam elevation up to a distance of 120-km from the station. The ability of radar data to successfully measure precipitation over a basin within the McGill radar domain is not dependent on basin size. Neither is there a detectable range dependency within the Doppler range. The lack of obstruction of the radar beam, and therefore the ability of the radar to collect data from the lowest elevation scan possible, is the key factor.

It is recommended that the current mesonet be expanded to represent precipitation throughout the radar domain. Shadowed areas would greatly benefit from additional precipitation data. Even if an adjustment of radar data using existing gauge values was performed for the McGill radar products, precipitation for shadowed regions are not likely to improve, as no gauges exist within them. In order to improve rainfall estimates, a gauge network needs to be designed to deal with these artefacts.

Existing algorithms within the McGill RAPID system allow for the use of different Z-R relationships for convective and stratiform precipitation. However, temporal and spatial variability of drop size distribution may require further flexibility in the application of the Z-R relationship. Researchers at McGill University are currently investigating the use of a Z-R relationship that is allowed to vary in space and time. Using rain gauge and disdrometer data, Z-R relationships are calculated in real-time for a given event. However, the hydrological usefulness of this approach may again be limited to a small portion of the radar domain if the issue of shadowed areas is not addressed. Information from an overlapping network may provide additional data.

Although weather radar is a potentially powerful tool for hydrologists, its usefulness in flood forecasting is limited. Currently, problems such as mixed precipitation events, or persistent slight under- or over-predictions of precipitation cannot be corrected for in a real-

time setting. Hydrologists have no choice but to rely on gauge network data to drive flood forecasting models, despite its known disadvantages.

9.1 Future work

It is recommended that continued investigation into radar product performance be carried out with a focus on areas of the McGill radar domain that are unaffected by beam blocking. A better understanding of each product's strengths and weaknesses may be achieved by categorizing modelled streamflow events based on the types of precipitation events that produces them (seasonal or synoptic).

Calibration may be performed for individual precipitation inputs in order to compare model results from radar and precipitation gauges without bias. A longer calibration period, extending over an entire water year will further improve estimation of model parameters. Additional model output, such as upper zone storage or evaporation, should be compared to observed data sets to further verify calibration parameters.

Previous studies have involved radar precipitation data that is calibrated with information from a precipitation gauge network. These studies have produced mixed results and blending of radar and gauge data may not necessarily result in a superior precipitation product. It may however, be useful to evaluate the success of radar calibration with gauges based on synoptic events. Real-time decisions methods may be necessary to determine whether radar precipitation measurements will benefit from gauge calibration.

10 References

Atlas, David, D. Rosenfield and A.R. Jameson. 1997. Evolution of radar rainfall measurements: steps and mis-steps. In: B. Braga and O. Massambani, editors. Weather radar technology for water resource management. Online at http://www.unesco.org.uy/phi/libros/radar/tapa.html (accessed 16 May 2006).

American Meteorological Society. 2000. Glossary of Meteorology. http://amsglossary.allenpress.com/glossary (accessed July 19, 2006).

Bellon, Aldo, G.W. Lee, A. Kilambi, I. Zawadzki. 2006. Real-time comparison of VPR-corrected daily rainfall estimates with a gauge mesonet. Journal of Applied Meteorology. In press.

Bellon, Aldo. Radar calibration, 2 March 2005, personal e-mail (2 March 2005).

Bellon, Aldo, G.W. Lee and I. Zawadzki. 2005. Error statistics of VPR corrections in stratiform precipitation. Journal of Applied Meteorology, 44: 998-1015.

Bellon, Aldo, G.W. Lee and I. Zawadzki. 2002. Optimal surface precipitation map. Proceedings, the CWRP-CFCAS Extreme Weather Workshop, Rimouski, Quebec.

Berne, A., M. ten Heggeler, R. Uijlenhoet, L. Delobbe, P.H. Dierickx, M. de Wit. 2005. A preliminary investigation of radar rainfall estimation in the Ardennes region and a first hydrological application for the Ourthe catchment. Natural Hazards and Earth System Sciences, 5:267-274.

Borga, Marco. 2002. Accuracy of radar rainfall estimates for streamflow simulation. Journal of Hydrology, 267:26-39.

Carpenter, Theresa M. and K.P. Georgakakos. 2004. Impacts of parametric and radar rainfall uncertainty on the ensemble streamflow simulation of a distributed hydrological model. Journal of Applied Hydrology, 298:202-221.

Centre de Resources en Impacts et Adaptation au Climat et à ses Changements (CRIACC). 2006. Climate monitoring. http://www.criacc.qc.ca/climat/index_e.html (accessed 8 October 2006).

Cluckie, I.D. and M.D. Owens. 1987. Real-time rainfall-runoff models and use of weather radar information. In: V.K. Collinge and C. Kirby, editors. Weather radar and flood forecasting. United Kingdom: John Wiley & Sons. pp. 171-190.

Collier, C.G. 1989. Application of weather radar systems; a guide to uses of radar data in meteorology and hydrology. West Sussex, UK: Ellis Horwood Limited.

Collier, C.G. 1986. Accuracy of rainfall estimates by radar, part I: calibration by telemetering raingauges. Journal of Hydrology, 83:207-223.

Collinge, V.K. 1987. The development of weather radar in the United Kingdom. In: V.K. Collinge and C. Kirby, editors. Weather radar and flood forecasting. United Kingdom: John Wiley & Sons. pp. 3-18.

Conseil de la gestion du bassin versant de la Yamaska (COGEBY). 2006. Le bassin versant. http://www.cogeby.qc.ca/bassin.htm (accessed 21 June 2006).

Corporation de l'Aménagement de la Rivière l'Assomption (CARA). 2006. Territoire d'intervention. http://www.cara.qc.ca/territoire/territoire.html (accessed 21 June 2006).

Ding, Feng, D. Kitzmiller, D. Riley, K. Shrestha, F. Moreda, D.-J. Seo. 2005. Evaluation of the range correction algorithm and convective stratiform algorithm for improving hydrological modelling. Proceedings, the American Meteorological Society 20th Conference on Hydrology, Atlanta, Georgia.

Douglas, J.R. and C. Dobson. 1987. Real-time flood forecasting in diverse drainage basins. In: V.K. Collinge and C. Kirby, editors. Weather radar and flood forecasting. United Kingdom: John Wiley & Sons. pp. 153-170.

Einfalt, Thomas and M. Semke. 1997. Reliable quantitative radar data- how long do hydrologists still have to wait? In: B. Braga and O. Massambani, editors. Weather radar technology for water resource management. Online at http://www.unesco.org.uy/phi/libros/radar/tapa.html (accessed 16 May 2006).

Fabry, F. 2006. J.S. Marshall Radar Observatory (MRO). http://www.radar.mcgill.ca/ (accessed 24 October 2004).

Fabry, F. 2004. Obstacles to the greater use of weather radar information. Proceedings, the 6th International Symposium on Hydrological Applications of Weather Radar, Melbourne, Australia.

Fabry, F. and I. Zawadzki. 1995. Long-term radar observation of the melting layer of precipitation and their interpretation. Journal of Atmospheric Sciences, 52(7):838-850.

Fabry, F., A. Bellon, M.R. Duncan, G.L. Austin. 1994. High resolution rainfall measurements by radar for very small basins: the sampling problem re-examined. Journal of Hydrology, 161:415-428.

Fabry, F., G.L. Austin and D. Tees. 1992. The accuracy of rainfall estimates by radar as a function of range. Quarterly Journal of the Royal Meteorological Society, 118:435-453.

Fassnacht, S.R., E.D. Soulis, and N. Kouwen. 1999. Algorithm application to improve weather snowfall estimates for winter modelling. Hydrological Processes, 13:3017-3039.

Georgakakos, K. P. and T.M. Carpenter. 2003. A methodology for assessing the utility of distributed model forecast applications in an operational environment. In: E. Nakakita, Y. Tachikawa, B.E. Vieux, K.P. Georgakakos, editors. Weather Radar Information and Distributed Hydrological Modelling. (Proceedings, the XXIII General Assembly of the International Union of Geodesy and Geophysics, Sapporo, Japan). pp. 85-92.

Gourley, Jonathan and B.E. Vieux. 2005. A method for evaluating the accuracy of quantitative precipitation estimates from a hydrologic modeling perspective. Journal of Hydrometeorology, 6(2):115-133.

Haughton, Jennifer. 2002. State of the Nation: a state of the environment report for the South Nation River watershed. Submitted to the South Nation River Conservation Authority, Berwick, Ontario. 71 p.

Hirayama, Daisuke, M. Fujita, H. Nakagawa. 1997. The identification of optimum Z-R relation based on runoff analysis. In: B. Braga and O. Massambani, editors. Weather radar technology for water resource management. Online at http://www.unesco.org.uy/phi/libros/radar/tapa.html (accessed 16 May 2006).

Infoscan. 2006. Forum Infoscan- Photo Album Thumbnails. http://www.infoscan.urgence.qc.ca/photos/photo-thumbnails.asp?albumid=45 (accessed December 17, 2006).

Innes, J. 2001. An assessment of weather radar for the operation of hydrologic models (MASc thesis). Waterloo, Ontario: University of Waterloo. 150 p.

Joss, J. and G.W. Lee. 1995. The application of radar-gauge comparisons to operational precipitation profile corrections. Journal of Applied Meteorology 34:2612-2630.

Juneja, R.K. 2006. Hydrologic validation of radar precipitation estimates (MASc thesis). Waterloo, Ontario: University of Waterloo. 246 p.

Kouwen, N. 2006. WATFLOOD/WATROUTE Hydrological model & flow forecasting system (user manual). Waterloo, Ontario: Department of Civil Engineering, University of Waterloo. 191 p.

Kouwen, N., A. Bingeman and a. Pietroniro. 2003. Enhanced nowcasting of extreme weather, sub-project B ii) Hydrological validation: Year 2 progress report. Submitted to J.S. Marshall Radar Observatory, Ste-Anne de Bellevue, Quebec. 101 p.

Kouwen, N., A. Bingeman, A. Bellon, I. Zawadzki. 2004. Operational issues: real-time correction and hydrological validation of radar data. Proceedings, the 6th International Symposium on Hydrological Applications of Weather Radar, Melbourne, Australia.

Kouwen, N, M. Danard, A. Bingeman, W. Luo, F.R. Seglenieks, E.D. Soulis. 2005. Case study: watershed modeling with distributed weather model data. Journal of Hydraulic Engineering, 10(1):23-37.

Kouwen, N, and G. Garland. 1989. Resolution consideration in using radar rainfall data for flood forecasting. Canadian Journal of Civil Engineering, 16:279-289.

Krajewski, W. F. 1997. Rainfall estimation using weather radar and ground stations. In: B. Braga and O. Massambani, editors. Weather radar technology for water resource management. Online at http://www.unesco.org.uy/phi/libros/radar/tapa.html (accessed 16 May 2006).

Krajewski, W. F and J.A. Smith. 2002. Radar hydrology: rainfall estimation. Advances in Water Resources, 25(8):1387-1394.

Lake Champlain Basin Program (LCBP). 2006. Lake Champlain basin program. http://www.lcbp.org/ (accessed 5 September 2006).

Lee, G.-W. and I. Zawadzki. 2005. Variability of drop size distributions: time-scale dependence of the variability and its effects on rain estimation. Journal of Applied Meteorology, 44:241-254.

Marshall, J.S., R.C Langille and W.McK. Palmer. 1947. Measurement of rainfall by radar. Journal of Meteorology, 4:186-192.

Marshall, J.S. and W.McK. Palmer. 1948. The distribution of raindrop with size. Journal of Meteorology, 5(4):165-166.

Mens, Marjolein. 2005. Making a river classification for the hydrological model WATFLOOD. Submitted to N. Kouwen, Department of Civil Engineering, University of Waterloo, Waterloo, Ontario. 47 p.

Mésonet Montréal. 2006. Mésonet Montréal. http://www.mesonet-montreal.ca/ (accessed 26 January 2006).

Meteorological Services of Canada (MSC). 2006. Weather radar fact sheet http://www.msc.ec.gc.ca/cd/factsheets/weather_radar/index_e.cfm (accessed 25 October 2005).

Moore, ID. 1987. Towards more effective use of radar data for flood forecasting. In: V.K. Collinge and C. Kirby, editors. Weather radar and flood forecasting. United Kingdom: John Wiley & Sons. pp. 223-228.

Neary, V.S., E. Habib and M. Fleming. 2004. Hydrologic modelling with NEXRAD precipitation in middle Tennessee. Journal of Hydrologic Engineering, 9(5):339-49.

Potter, Thomas and B.R. Colman. 2003. Handbook of weather, climate and water: dynamics, climate, physical meteorology, weather systems, and measurements. Hoboken, New Jersey: John Wiley and Sons Inc.

Reed, Sean, R. Fulton, Z. Zhang, S. Guan. 2006. Use of 4 km, 1 hr, precipitation forecasts to drive a distributed hydrologic model for flash flood prediction. Proceedings, the American Meteorological Society 20th Conference on Hydrology, Atlanta, Georgia.

Ryder, P. and C.G. Collier. 1987. Future development of the UK weather radar network. In: V.K. Collinge and C. Kirby, editors. Weather radar and flood forecasting. United Kingdom: John Wiley & Sons. pp. 271-285.

Seed, A.W., J. Nicol, G.L. Austin, C.D. Stow, S.G. Bradley. 1997. A physical basis for parameter selection for Z-R relationships. In: B. Braga and O. Massambani, editors. Weather radar technology for water resource management. Online at http://www.unesco.org.uy/phi/libros/radar/tapa.html (accessed 16 May 2006).

Seo, Dong-Jun, and E.R. Johnson. 1997. The WSR-88D precipitation processing subsystem: an overview and a performance evaluation. In: B. Braga and O. Massambani, editors. Weather radar technology for water resource management. Online at http://www.unesco.org.uy/phi/libros/radar/tapa.html (accessed 16 May 2006).

Société de conservation et d'aménagement du basin de la rivière Châteauguay (SCABRIC). 2006. The valley of the Chateauguay River. http://www.rivierechateauguay.qc.ca/ (accessed 21 June 2006).

Scharfenberg, Kevin. 2005. Polaritmetric radar case studies. http://cimms.ou.edu/~kscharf/pol/zdr.html. (accessed June 12, 2006).

St-Hilaire, André, T.B.M.J. Ouarda, M. Lachance, B. Bobée, J. Gaudet, C. Gignac. 2003. Assessment of the impact of meteorological network density on the estimation of basin precipitation and runoff: a case study. Hydrological Processes, 17:3561-3580.

Velasco-Forero, Carlos, D. Sempere-Torres, R. Sánchez-Diezma, E. Cassiraga, J. Gómez-Hernández. 2005. Automatic estimation of rainfall fields for hydrological applications: blending radar and rain gauge data in real time. Proceedings, the American Meteorological Society 32nd Conference on Radar Meteorology, Albuquerque, New Mexico.

Vignal, B., H. Andrieu and J.D. Creutin. 1999. Identification of vertical profiles of reflectivity from volume scan radar data. Journal of Applied Meteorology, 38(8):1214-1228.

Viessman, W. and G.L. Lewis. 1995. Introduction to Hydrology, fourth edition. USA: Addison-Wesley Educational Publishers.

Vieux, B.E. and P.B. Bedient, 2004. Hydrologic prediction accuracy assessment using radar rainfall. Proceedings, the World Water Congress: Critical Transitions in Water and Environmental Resources Management, Salt Lake City, UT. CD-ROM.

Walsh, P.D., and A.M. Lewis. 1987. The role of radar and automated data capture in information systems for water management. In: V.K. Collinge and C. Kirby, editors. Weather radar and flood forecasting. United Kingdom: John Wiley & Sons. pp. 211-222.

World Meteorological Organization (WMO). 2004. Guide to Hydrological Practices, 6th edition. In press.

Zawadzki, I. 2001. Proposal for research project: Enhanced nowcasting of extreme weather (draft). Submitted to the Canadian Foundation for Climate and Atmospheric Sciences, Ottawa, Ontario.

Appendix A

WATFLOOD Input Data

Table A.1- Error in EnSim-calculated drainage area for Eastern Ontario subasins

WSC ID	Station Name	Dist. From Radar (km)	WSC Drainage Area (km^2)	EnSim Drainage Area (km^2)	Percent Difference
02LB008	Bearbrook near Bourget	112	440	470	6.82
02LB006	Castor River at Russell	125	433	439	1.39
02LB005	South Nation River near Plantagenet	107	3810	3929	312
02LB007	South Nation River at Spencerville	152	246	259	5.28
02MC026	Beaudette River near Glen Nevis	66	124	130	4.84
02MC028	Delisle River near Alexandria	66	85.4	87	1.87
02MC030	South Rasin River near Cornwall	78	25.8	27	4.65
02MC001	Raisin River near Williamstown	72	404	402	-0.50

Table A.2- Error in EnSim-calculated drainage area for Quebec, north of the St. Lawrence River subasins

WSC ID	Station Name	Dist. From Radar (km)	WSC Drainage Area (km^2)	EnSim Drainage Area (km^2)	Percent Difference
02LC008	Rivière du Nord at Saint-Jérôme	69	1170	1122	-4.10
02LC021	Rivière du Nord near Saint-Agathe	81	311	311	0.00
02LC029	Rivière Rouge	121	5460	5361	-1.81
02LD005	Rivière de la Petite Nation near Ripon	111	1330	1361	2.33
02OB008	Rivière de l'Assomption at Joliette	103	1340	1341	0.07
02OB037	Rivière de l'Achigan at L'Epiphanie	52	647	630	-2.63

Table A.3- Error in EnSim-calculated drainage area for Quebec, south of the St. Lawrence River subasins

WSC ID	Station Name	Dist. From Radar (km)	WSC Drainage Area (km^2)	EnSim Drainage Area (km^2)	Percent Difference
02OA054	Chateauguay River	45	2490	2600	4.42
02OA057	English River	42	643	640	-0.47
02OG019	Noire River	108	1490	1494	0.27

Table A.4- Error in EnSim-calculated drainage area for Lake Champlain subasin

USGS ID	Station Name	USGS Drainage Area (km^2)	EnSim Drainage Area (km^2)	Percent Difference
04271500	Great Chazy River at Perry Mills NY	629	620	-1.43
04273500	Saranac River at Plattsburgh NY	1575	1717	9.02
04275500	Ausable River near Au Sable Forks NY	1155	1098	-4.94
04276842	Putnam Creek east of Crown Point Center, NY	134	136	1.49
04278000	Lake George at Rogers Rock NY	603	606	0.50
04280000	Poultney River below Fair Haven, VT	484	472	-2.48
04280450	Mettawee River near Middle Granville, NY	433	420	-3.00
0428200	Otter Creek at Center Rutland, VT	795	789	-0.75
04282500	Otter Creek at Middlebury, VT	1627	1573	-3.32
04282525	New Haven River at Brooksville Nr Middlebury, VT	298	299	0.34
04282650	Little Otter Creek at Ferrisburg, VT	148	141	-4.73
04282795	Laplatte River at Shelburne Falls, VT.	116	114	-1.72
04286000	Winooski River at Montpelier, VT	1028	1001	-2.63
04287000	Dog River at Northfield Falls, VT	197	198	0.51
04288000	Mad River near Moretown, VT	360	350	-2.78
04289000	Little River near Waterbury, VT	287	293	2.09
04290500	Winooski River near Essex Junction, VT	2704	2640	-2.37
04292000	Lamoille River at Johnson, VT	803	770	-4.11
04292500	Lamoille River at East Georgia, VT	1777	1758	-1.07
04293000	Missisquoi River near North Troy, VT	339	326	-3.83
04293500	Missisquoi River near East Berkshire, VT	1241	1152	-7.17
04294000	Missisquoi River at Swanton, VT	2201	2249	2.18

Table A.5- Precipitation gauge location and type

Station No.	Location	Longitude (decimal degrees)	Latitude (decimal degrees)	Station Owner	Tipping Bucket Gauge	Weigh Gauge
5	St-Anicet	-74.2895	45.1208	EC	X	X
14	L'Assomption	-73.4347	45.8094	EC	X	X
15	Frelighsburg	-72.8617	45.0503	EC	X	X
25	Ste-Clotilde	-73.6789	45.1672	Laval	X	X
28	L'Acadie	-73.3494	45.2939	EC	X	X
30	St-Jovite	-74.5558	46.0802	EC		X
35	Nicolet	-72.6572	46.2258	EC		X
49	McTavish	-73.5792	45.5050	EC		X
56	Ste-Anne-de-Bellevue	-73.9292	45.4272	Laval	X	X
64	St-Hubert	-73.4167	45.5167	EC		X
72	Montreal/Dorval Int'l	-73.7417	45.4678	EC	X	X
685	High Falls	-75.6482	45.8394	EC		X
860	Harrington	-74.6667	45.8333	McGill	X	
861	Saint-Andre-Avelin	-75.0632	45.8158	McGill	X	
863	Alfred	-74.8756	45.5550	McGill	X	
867	Granby	-72.7739	45.3728	McGill	X	
873	Sainte-Sabine	-73.0233	45.2233	McGill	X	
874	Rawdon	-73.6861	46.0906	McGill	X	
875	Rigaud	-74.2926	45.4826	McGill	X	
876	Rougemont	-73.0508	45.4122	McGill	X	
878	Piedmont	-74.0922	45.8833	McGill	X	
881	Saint-Louis	-73.0047	45.8702	McGill	X	
882	Saint-Polycarpe	-74.2931	45.3053	McGill	X	
883	Beauharnois	-73.9122	45.3194	McGill	X	
885	Winchester	-75.3367	45.0511	McGill	X	
886	Howick	-73.8785	45.1669	Laval	X	
887	Saint-Michel-de-Napierville	-73.6242	45.1869	Laval	X	
889	L'Artifice	-73.8487	45.0774	Laval	X	

Station No.	Location	Longitude (decimal degrees)	Latitude (decimal degrees)	Station Owner	Tipping Bucket Gauge	Weigh Gauge
891	Russeltown	-73.7962	45.0582	Laval	X	
892	Saint-Chrysostome	-73.7680	45.1325	Laval	X	
893	Ruisseau Cranberry	-73.6794	45.1194	Laval	X	
894	Saint-Denis-de-Kamouraska	-69.8833	47.5119	Laval	X	
896	Saint-Celestin	-72.4458	46.2058	Laval	X	
907	Saint-Lin-des-Laurentide	-73.8481	45.6972	McGill	X	
912	Cornwall	-74.6814	45.0314	McGill	X	
914	Covey-Hill	-73.8734	45.0139	Laval	X	
915	Saint-Constant	-73.5802	45.3301	Laval	X	
1160	Moose Creek	-74.9628	45.2511	McGill	X	
1161	Saint-Roch-des-Aulnais	-70.1722	47.2786	Laval	X	
1170	Alexandria	-74.6142	45.3236	McGill	X	
1205	Thurso	-75.2558	45.5931	McGill	X	
1206	Brownsburg	-74.4089	45.6867	McGill	X	
-	Casselman	-75.0800	45.3200	SNC		X
-	Beaudette	-74.4936	45.2742	RRC		X

EC= Environement Canada

McGill= McGill University

Laval= University of Laval

SNC= South Nation Conservation

RRC= Raisin Region Conservation

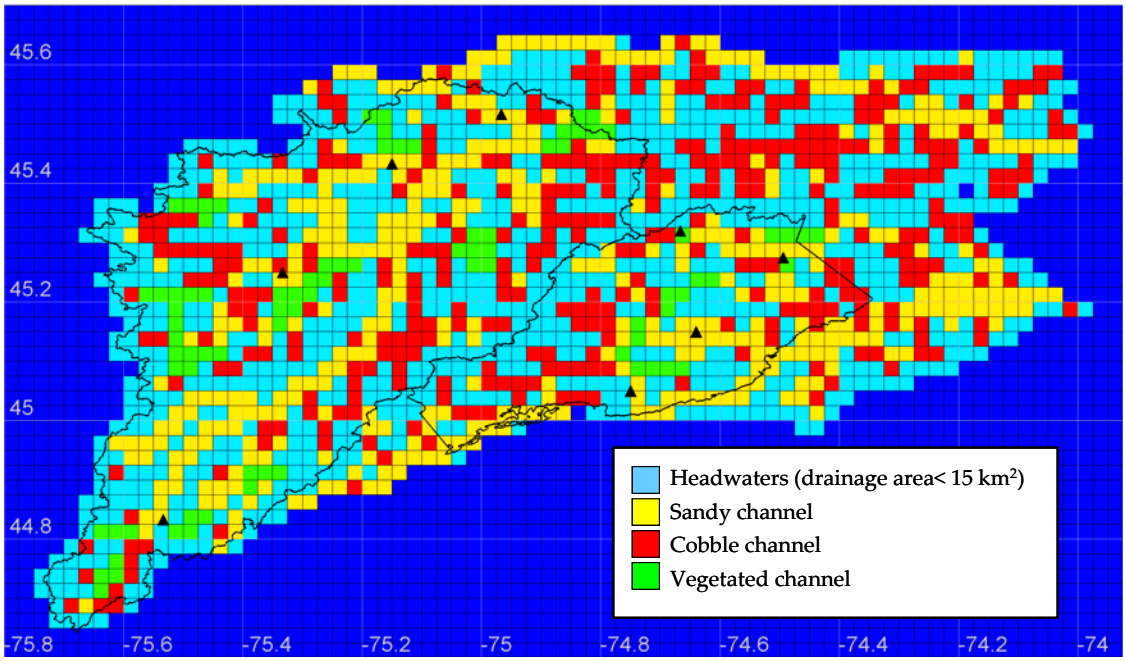

Figure A.1- River classification for Eastern Ontario

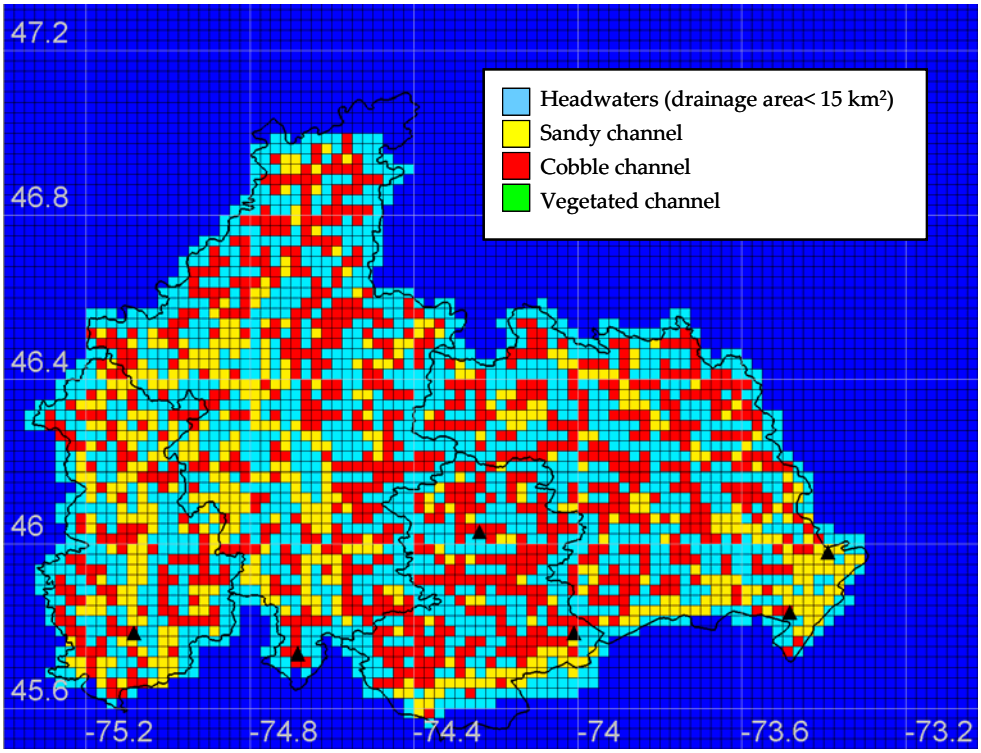

Figure A.2- River classification for Quebec, north of the St. Lawrence River

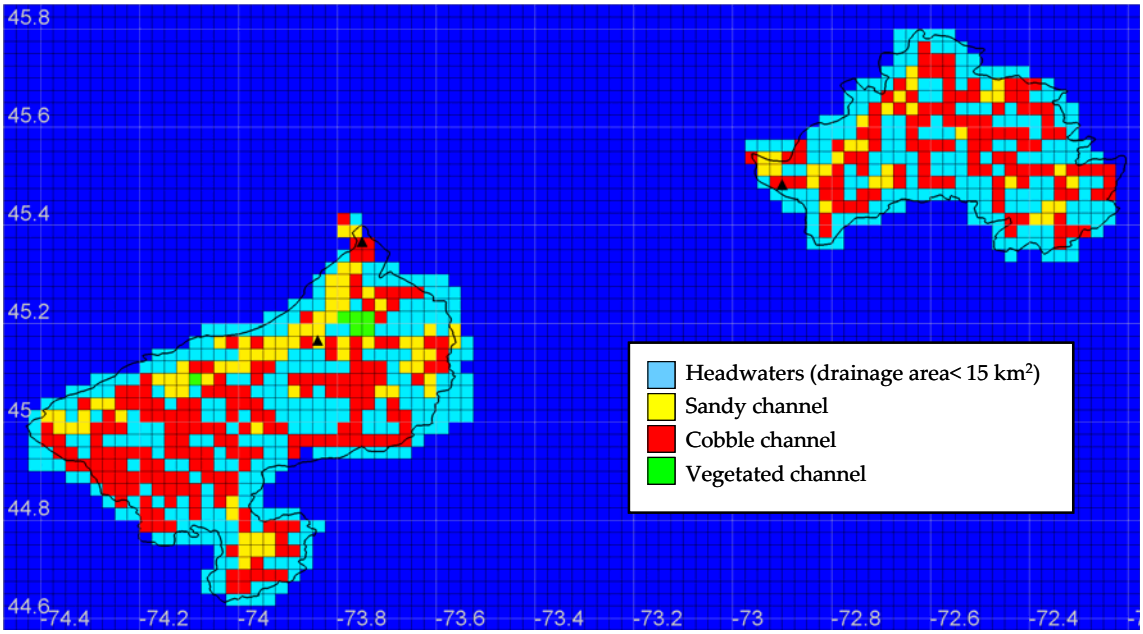

Figure A.3- River classification for Quebec, south of the St. Lawrence River

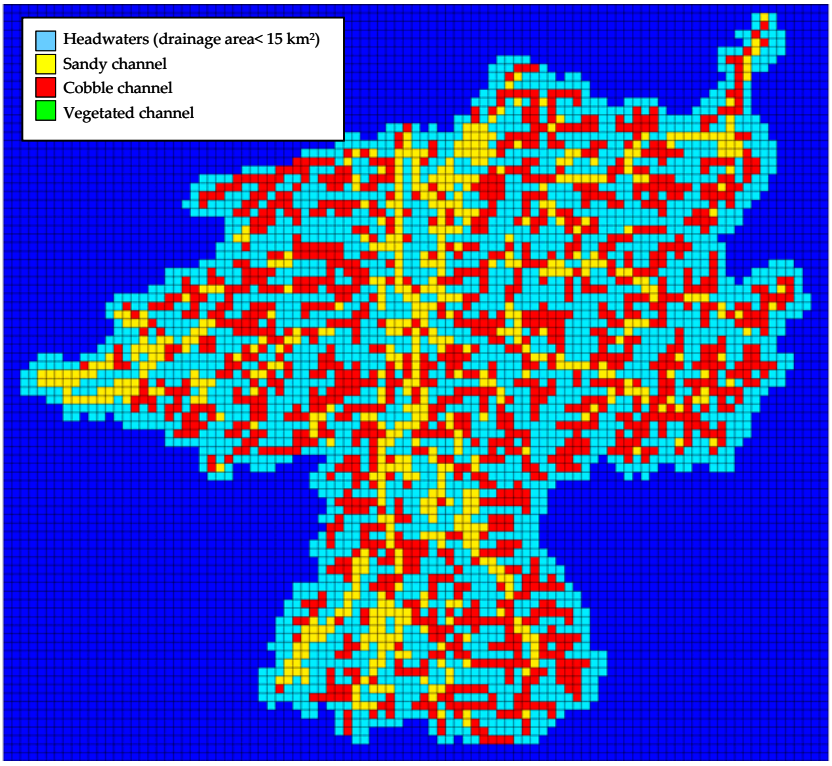

Figure A.4- River classification for the Lake Champlain Basin

Grand River WATFLOOD parameter file (GR10K.PAR)-

```
# runtime    11:07:40
# rundate  2004-04-29
ver       9.200     parameter file version number
iopt          02     debug level
itype          0
numa           0     PS optimization 0=no 1=yes
nper           0     opt delta 0-absolute
kc             5     no of times delta halved
maxn           2     max no of trials
ddsfl          0     DDS optimization 0=no  1=yes
itrce        100
iiout          4
typeo          4     no of land classes optimized(part 2)
nbsn           5     no of river classes optimized (part 2)
a1      -999.999
a2      -999.999
a3      -999.999
a4      -999.999
a5         0.985     API coefficient
a6       900.000     Minimum routing time step in seconds
a7         0.500     weighting factor - old vs. new sca value
a8         0.100     min temperature time offset
a9         0.333     max heat deficit to swe ratio
a10        1.000     uz discharge function exponent
a11        0.010
a12        0.000     min precip rate for smearing
      rivtype1  rivtype2  rivtype3  rivtype4  rivtype5
lzf   0.100E-05 0.100E-05 0.100E-05 0.100E-05 0.100E-05
pwr   0.300E+01 0.300E+01 0.300E+01 0.300E+01 0.300E+01
R1n   0.400E-01 0.400E-01 0.400E-01 0.400E-01 0.400E-01
R2n   0.107E-01 0.186E-01 0.132E-01 0.100E-01 0.157E-01
mndr  0.100E+01 0.100E+01 0.100E+01 0.100E+01 0.100E+01
aa2   0.110E+00 0.110E+00 0.110E+00 0.110E+00 0.110E+00
aa3   0.430E-01 0.430E-01 0.430E-01 0.430E-01 0.430E-01
aa4   0.100E+01 0.100E+01 0.100E+01 0.100E+01 0.100E+01
theta 0.100E+01 0.100E+01 0.100E+01 0.100E+01 0.100E+01
widep 0.200E+02 0.200E+02 0.200E+02 0.200E+02 0.200E+02
kcond 0.100E+00 0.100E+00 0.100E+00 0.100E+02 0.100E+00
      bare_soil forest    crops     wetland   water
ds    0.100E+01 0.100E+02 0.200E+01 0.100E+10 0.000E+00 0.100E+01
dsfs  0.100E+01 0.100E+02 0.200E+01 0.100E+10 0.000E+00 0.100E+01
Re    0.400E+00 0.800E+00 0.600E+00 0.100E+00 0.100E+00 0.100E+00
AK    0.300E+01 0.120E+02 0.300E+01 0.400E+03-0.100E+00 0.100E-10
AKfs  0.300E-01 0.120E+01 0.300E+00 0.400E+03-0.100E+00 0.100E-10
retn  0.400E+02 0.700E+02 0.400E+02 0.400E+00 0.100E+00 0.100E+00
ak2   0.200E-02 0.320E-02 0.200E-02 0.200E-10 0.100E-02 0.100E-10
ak2fs 0.800E-02 0.120E-01 0.800E-02 0.750E-10 0.100E-02 0.100E-10
R3    0.197E+00 0.848E-01 0.197E+00 0.898E-01 0.400E-01 0.400E-01
R3fs  0.100E+00 0.100E+00 0.200E+00 0.100E+00 0.400E-01 0.400E-01
r4    0.100E+01 0.100E+02 0.100E+02 0.100E+02 0.100E+02 0.100E+02
ch    0.100E+01 0.900E+00 0.700E+00 0.700E+00 0.600E+00 0.600E+00
MF    0.110E+00 0.100E+00 0.110E+00 0.110E+00 0.150E+00 0.150E+00
BASE -0.250E+01-0.150E+01-0.200E+01-0.200E+00-0.250E+01 0.000E+00
NMF   0.100E+00 0.100E+00 0.100E+00 0.100E+00 0.100E+00 0.100E+00
UADJ  0.000E+00 0.000E+00 0.000E+00 0.000E+00 0.000E+00 0.000E+00
TIPM  0.100E+00 0.100E+00 0.100E+00 0.100E+00 0.100E+00 0.100E+00
RHO   0.333E+00 0.333E+00 0.333E+00 0.333E+00 0.333E+00 0.333E+00
WHCL  0.350E-01 0.350E-01 0.350E-01 0.350E-01 0.350E-01 0.350E-01
fmadj     0.000     0.000     0.000     0.000     0.000     0.000
flgev      2.00     1 = pan; 2 = Hargreaves; 3 = Priestley-Taylor
albed      0.11
aw-a       0.18      0.11      0.11      0.11      0.11
fpet       1.00      3.00      2.00      2.00      0.00
ftal       1.00      0.70      0.90      1.00      1.00
flint       1.        1.        1.        1.        1.
fcap       0.15      0.15      0.15      0.15      0.15
ffcap      0.10      0.10      0.10      0.10      0.10
spore      0.30      0.30      0.30      0.30      0.30
sublm       00.       00.       00.       00.       00.
tempa       50.
temp3       50.
```

```
tton         0.
lat.        50.
mxmn  10.2 12.3 12.1 12.3 14.3 14.2 13.8 14.0 13.1 10.6  8.2  9.3
humid 59.5 60.5 62.5 55.5 50.0 54.5 59.0 58.5 63.5 58.0 64.5 62.5
pres  95.1 95.1 95.1 95.1 95.1 95.1 95.1 95.1 95.1 95.1 95.1 95.1
ti2    jan  feb  mar  apr  may  jun  jul  aug  sep  oct  nov  dec
h1    0.04 0.04 0.04 0.04 0.53 0.53 0.53 0.53 0.53 0.28 0.04 0.04
h2    1.13 1.13 1.13 1.13 1.53 1.83 1.83 1.83 1.83 1.13 1.13 1.13
h3    0.58 0.58 0.58 0.58 0.78 0.93 0.93 0.93 0.93 0.58 0.58 0.58
h4    0.58 0.58 0.58 0.58 0.78 0.93 0.93 0.93 0.93 0.58 0.58 0.58
h5    0.04 0.04 0.04 0.04 0.04 0.04 0.04 0.04 0.04 0.04 0.04 0.04
```

Quebec, south of the St. Lawrence River/Lake Champlain Basin WATFLOOD parameter file (NOIRE.PAR/MG_USN.PAR)-

```
# runtime    14:40:30
# rundate  2006-03-15
ver       9.300     parameter file version number
iopt          0     debug level
itype         0
numa          0     optimization 0=no 1=yes
nper          1     opt delta 1-absolute
kc            5     no of times delta halved
maxn         50     max no of trials
iw            0
ix            1
iiout         4
typeo         5     no of land classes optimized(part 2)
nbsn          4     no of river classes optimized (part 2)
a1        0.250
aa2    -999.999
aa3    -999.999
aa4    -999.999
a5        0.985     API coefficient
a6      900.000     Minimum routing time step in seconds
a7        0.500     weighting factor - old vs. new sca value
a8        0.100     min temperature time offset
a9        0.333
a10       1.000
a11       0.010
a12       0.000     min precip rate for smearing
          Rest       Veg      Sand    Cobble
lzf   0.200E-04 0.500E-04 0.500E-04 0.500E-04
pwr   0.350E+01 0.250E+01 0.385E+01 0.292E+01
R1n   0.200E-01 0.500E-01 0.750E-02 0.750E-02
R2n   0.797E-02 0.400E-01 0.399E-02 0.897E-02
mndr  0.100E+01 0.150E+01 0.100E+01 0.100E+01
aa2   0.270E+00 0.270E+00 0.620E+00 0.710E+00
aa3   0.570E+00 0.570E+00-0.200E+00-0.690E+00
aa4  -0.100E+01-0.100E+01-0.100E+01-0.100E+01
theta 0.131E+00 0.200E+00 0.137E+00 0.100E+00
widep 0.100E+02 0.200E+02 0.300E+02 0.200E+02
kcond 0.200E-01 0.200E+01 0.163E-01 0.174E+01
     conif     decid     crops     woodland  mixed     water     impervious
ds    0.100E+02 0.100E+02 0.200E+01 0.100E+02 0.100E+02 0.000E+00 0.000E+00
dsfs  0.100E+02 0.200E+02 0.300E+01 0.200E+02 0.200E+02 0.000E+00 0.000E+00
Re    0.150E+00 0.150E+00 0.242E+01 0.150E+00 0.147E+00 0.100E+01 0.100E+01
AK    0.160E+02 0.160E+02 0.590E+01 0.160E+02 0.160E+02 0.000E+00 0.100E-10
AKfs  0.160E+01 0.148E+01 0.590E+01 0.393E+01 0.443E+01 0.000E+00 0.100E-10
retn  0.400E+02 0.400E+02 0.250E+02 0.400E+02 0.400E+02 0.000E+00 0.000E+00
ak2   0.200E-01 0.199E-01 0.503E-01 0.199E-01 0.199E-01 0.000E+00 0.000E+00
ak2fs 0.100E-01 0.994E-02 0.252E-01 0.994E-02 0.994E-02 0.000E+00 0.000E+00
R3    0.848E+01 0.848E+01 0.197E+02 0.848E+01 0.848E+01 0.000E+00 0.100E+01
R3fs  0.100E+02 0.100E+02 0.200E+02 0.100E+02 0.100E+02 0.000E+00 0.100E+01
r4    0.100E+02 0.100E+02 0.100E+02 0.100E+02 0.100E+02 0.000E+00 0.000E+00
ch    0.900E+00 0.900E+00 0.800E+00 0.700E+00 0.700E+00 0.600E+01 0.500E+01
MF    0.100E+00 0.100E+00 0.110E+00 0.100E+00 0.100E+00 0.150E+00 0.150E+00
BASE  0.100E+01 0.100E+01-0.100E+01 0.100E+01 0.100E+01 0.000E+00 0.000E+00
NMF   0.100E+00 0.100E+00 0.100E+00 0.100E+00 0.100E+00 0.100E+00 0.100E+00
UADJ  0.000E+00 0.000E+00 0.000E+00 0.000E+00 0.000E+00 0.000E+00 0.000E+00
TIPM  0.100E+00 0.100E+00 0.100E+00 0.100E+00 0.100E+00 0.100E+00 0.100E+00
RHO   0.333E+00 0.333E+00 0.333E+00 0.333E+00 0.333E+00 0.333E+00 0.333E+00
```

```
WHCL  0.350E-01 0.350E-01 0.350E-01 0.350E-01 0.350E-01 0.350E-01 0.350E-01
fmadj     0.000
fmlow     0.000
fmhgh     0.000
gladj     0.000
rlaps     0.000
elvrf     0.000
flgev      2.00 1 = pan; 2 = Hargreaves; 3 = Priestley-Taylor
albed      0.11
aw-a       0.11      0.11      0.18      0.11      0.11      0.11
fpet       1.50      1.50      1.00      1.50      1.50      1.50
ftal       0.70      0.70      0.70      0.70      0.70      0.70
flint        1.        1.        1.        1.        1.        1.
fcap       0.15      0.15      0.15      0.15      0.15      0.15
ffcap      0.10      0.10      0.10      0.10      0.10      0.10
spore      0.30      0.30      0.30      0.30      0.30      0.30
tempa         0.        0.        0.        0.        0.        0.
tempa        50.
temp3        50.
tton          0.
lat.         50.
mxmn  10.2 12.3 12.1 12.3 14.3 14.2 13.8 14.0 13.1 10.6  8.2  9.3
humid 59.5 60.5 62.5 55.5 50.0 54.5 59.0 58.5 63.5 58.0 64.5 62.5
pres  95.1 95.1 95.1 95.1 95.1 95.1 95.1 95.1 95.1 95.1 95.1 95.1
ti2    jan  feb  mar  apr  may  jun  jul  aug  sep  oct  nov  dec
h1    1.83 1.83 1.83 1.83 1.83 1.83 1.83 1.83 1.83 1.83 1.83 1.83
h2    1.13 1.13 1.13 1.13 1.53 1.83 1.83 1.83 1.83 1.13 1.13 1.13
h3    0.04 0.04 0.04 0.04 0.53 0.53 0.53 0.53 0.53 0.28 0.04 0.04
h4    0.50 0.50 0.50 0.50 2.00 2.50 2.50 2.50 2.50 0.50 0.50 0.50
h5    1.13 1.13 1.13 1.13 1.53 1.83 1.83 1.83 1.83 1.13 1.13 1.13
h6    0.11 0.11 0.11 0.11 0.11 0.11 0.11 0.11 0.11 0.11 0.11 0.11
```

Eastern Ontario WATFLOOD parameter file (MG_ONT.PAR)-

```
# runtime    13:58:32
# rundate  2005-11-16
ver       9.300     parameter file version number
iopt          0     debug level
itype         0
numa          0     optimization 0=no 1=yes
nper          0     opt delta 1-absolute
kc            5     no of times delta halved
maxn       5000     max no of trials
iw            0
ix            1
iiout         4
typeo         6     no of land classes optimized(part 2)
nbsn          4     no of river classes optimized (part 2)
a1        0.250
aa2    -999.999
aa3    -999.999
aa4    -999.999
a5        0.985     API coefficient
a6      900.000     Minimum routing time step in seconds
a7        0.500     weighting factor - old vs. new sca value
a8        0.100     min temperature time offset
a9        0.333
a10       1.000
a11       0.010
a12       0.000     min precip rate for smearing
      Rest        Vegetation      Sand    Cobble
lzf   0.200E-04 0.500E-04 0.500E-04 0.500E-04
pwr   0.350E+01 0.250E+01 0.385E+01 0.292E+01
R1n   0.200E-01 0.500E-01 0.750E-02 0.750E-02
R2n   0.797E-02 0.400E-01 0.399E-02 0.897E-02
mndr  0.100E+01 0.150E+01 0.100E+01 0.100E+01
aa2   0.270E+00 0.270E+00 0.620E+00 0.710E+00
aa3   0.570E+00 0.570E+00-0.200E+00-0.690E+00
aa4  -0.100E+01-0.100E+01-0.100E+01-0.100E+01
theta 0.150E+00 0.200E+00 0.330E+00 0.150E+00
widep 0.100E+02 0.200E+02 0.300E+02 0.200E+02
kcond 0.100E+00 0.200E+01 0.200E-01 0.100E+00
```

```
      conif     decid     crops     woodland  mixed    wetland
ds    0.100E+02 0.100E+02 0.200E+01 0.100E+02 0.100E+02 0.200E+02 0.000E+00
dsfs  0.100E+02 0.200E+02 0.300E+01 0.200E+02 0.200E+02 0.200E+02 0.000E+00
Re    0.150E+00 0.150E+00 0.242E+01 0.150E+00 0.147E+00 0.412E+02 0.100E+01
AK    0.160E+02 0.160E+02 0.590E+01 0.160E+02 0.160E+02 0.160E+02 0.000E+00
AKfs  0.160E+01 0.148E+01 0.590E+01 0.393E+01 0.443E+01 0.160E+02 0.000E+00
retn  0.400E+02 0.400E+02 0.250E+02 0.400E+02 0.400E+02 0.900E+02 0.100E+00
ak2   0.200E-01 0.199E-01 0.503E-01 0.199E-01 0.199E-01 0.200E-01 0.000E+00
ak2fs 0.100E-01 0.994E-02 0.252E-01 0.994E-02 0.994E-02 0.200E-01 0.000E+00
R3    0.848E+01 0.848E+01 0.197E+02 0.848E+01 0.848E+01 0.848E+01 0.000E+00
R3fs  0.100E+02 0.100E+02 0.200E+02 0.100E+02 0.100E+02 0.100E+02 0.000E+00
r4    0.100E+02 0.100E+02 0.100E+02 0.100E+02 0.100E+02 0.100E+02 0.000E+00
ch    0.900E+00 0.900E+00 0.800E+00 0.700E+00 0.700E+00 0.600E+00 6.000E+00
MF    0.100E+00 0.100E+00 0.110E+00 0.100E+00 0.100E+00 0.100E+00 0.150E+00 0.150E+00
BASE  0.100E+01 0.100E+01-0.100E+01 0.100E+01 0.100E+01-0.200E+01 0.000E+00 0.000E+00
NMF   0.100E+00 0.100E+00 0.100E+00 0.100E+00 0.100E+00 0.100E+00 0.100E+00 0.100E+00
UADJ  0.000E+00 0.000E+00 0.000E+00 0.000E+00 0.000E+00 0.000E+00 0.000E+00 0.000E+00
TIPM  0.100E+00 0.100E+00 0.100E+00 0.100E+00 0.100E+00 0.100E+00 0.100E+00 0.100E+00
RHO   0.333E+00 0.333E+00 0.333E+00 0.333E+00 0.333E+00 0.333E+00 0.333E+00 0.333E+00
WHCL  0.350E-01 0.350E-01 0.350E-01 0.350E-01 0.350E-01 0.350E-01 0.350E-01 0.350E-01
fmadj     0.000
fmlow     0.000
fmhgh     0.000
gladj     0.000
rlaps     0.000
elvrf     0.000
flgev      2.00 1 = pan; 2 = Hargreaves; 3 = Priestley-Taylor
albed      0.11
aw-a       0.11      0.11      0.18      0.11      0.11      0.11      0.11
fpet       2.00      2.00      1.50      2.00      2.00      2.00      0.70
ftal       0.70      0.70      0.70      0.70      0.70      0.70      0.50
flint        1.        1.        1.        1.        1.        1.        1.
fcap       0.15      0.15      0.15      0.15      0.15      0.15      0.15
ffcap      0.10      0.10      0.10      0.10      0.10      0.10      0.10
spore      0.30      0.30      0.30      0.30      0.30      0.30      0.30
sublm         0.        0.        0.        0.        0.        0.        0.
tempa        50.
temp3        50.
tton          0.
lat.         50.
mxmn  10.2 12.3 12.1 12.3 14.3 14.2 13.8 14.0 13.1 10.6  8.2  9.3
humid 59.5 60.5 62.5 55.5 50.0 54.5 59.0 58.5 63.5 58.0 64.5 62.5
pres  95.1 95.1 95.1 95.1 95.1 95.1 95.1 95.1 95.1 95.1 95.1 95.1
ti2    jan  feb  mar  apr  may  jun  jul  aug  sep  oct  nov  dec
h1    1.83 1.83 1.83 1.83 1.83 1.83 1.83 1.83 1.83 1.83 1.83 1.83
h2    1.13 1.13 1.13 1.13 1.53 1.83 1.83 1.83 1.83 1.13 1.13 1.13
h3    0.04 0.04 0.04 0.04 0.53 0.53 0.53 0.53 0.53 0.28 0.04 0.04
h4    0.50 0.50 0.50 0.50 2.00 2.50 2.50 2.50 2.50 0.50 0.50 0.50
h5    1.13 1.13 1.13 1.13 1.53 1.83 1.83 1.83 1.83 1.13 1.13 1.13
h6    1.19 1.19 1.19 1.19 1.39 1.39 1.39 1.59 1.59 1.19 1.19 1.19
h6    0.00 0.00 0.00 0.00 0.00 0.00 0.00 0.00 0.00 0.00 0.00 0.00
```

Quebec, north of the St. Lawrence River WATFLOOD parameter file (MG_QUE.PAR)-

```
# runtime    22:09:08
# rundate  2006-03-16
ver       9.300     parameter file version number
iopt          0          debug level
itype         0
numa          0     optimization 0=no 1=yes
nper          1     opt delta 1-absolute
kc            5     no of times delta halved
maxn         50     max no of trials
ddsfl         0     DDS optimization 0=no  1=yes
ix            1
iiout         4
typeo         6     no of land classes optimized(part 2)
nbsn          4     no of river classes optimized (part 2)
a1        0.250
aa2    -999.999
aa3    -999.999
aa4    -999.999
a5        0.985     API coefficient
```

```
a6      900.000     Minimum routing time step in seconds
a7        0.500     weighting factor - old vs. new sca value
a8        0.100     min temperature time offset
a9        0.333
a10       1.000
a11       0.010
a12       0.000     min precip rate for smearing
      Rest     VegetationSand      Cobble
lzf   0.100E-05 0.500E-04 0.400E-04 0.100E-05
pwr   0.300E+01 0.300E+01 0.350E+01 0.300E+01
R1n   0.400E-01 0.500E-01 0.750E-02 0.600E-01
R2n   0.400E-01 0.400E-01 0.550E-02 0.400E-01
mndr  0.100E+01 0.150E+01 0.100E+01 0.100E+01
aa2   0.270E+00 0.270E+00 0.620E+00 0.710E+00
aa3   0.570E+00 0.570E+00-0.200E+00-0.690E+00
aa4  -0.100E+01-0.100E+01-0.100E+01-0.100E+01
theta 0.330E+00 0.200E+00 0.330E+00 0.330E+00
widep 0.100E+02 0.200E+02 0.350E+02 0.200E+02
kcond 0.200E+01 0.200E+00 0.200E+00 0.200E+01
      conif     decid     crops     woodland  mixed    wetland
ds    0.100E+02 0.100E+02 0.200E+01 0.100E+02 0.100E+02 0.200E+02 0.000E+00
dsfs  0.100E+02 0.100E+02 0.200E+01 0.100E+02 0.100E+02 0.200E+02 0.000E+00
Re    0.800E+00 0.800E+00 0.500E+00 0.800E+00 0.800E+00 0.412E+02 0.100E+01
AK    0.120E+02 0.120E+02 0.300E+01 0.120E+02 0.120E+02 0.160E+02 0.000E+00
AKfs  0.120E+01 0.120E+01 0.200E+01 0.120E+01 0.120E+01 0.160E+02 0.000E+00
retn  0.700E+02 0.700E+02 0.500E+02 0.700E+02 0.700E+02 0.900E+02 0.100E+00
ak2   0.500E-01 0.240E-01 0.660E-01 0.500E-01 0.500E-01 0.200E-01 0.000E+00
ak2   0.500E-01 0.240E-01 0.660E-01 0.500E-01 0.500E-01 0.200E-01 0.000E+00
R3    0.848E+01 0.848E+01 0.197E+02 0.848E+01 0.848E+01 0.848E+01 0.000E+00
R3fs  0.100E+02 0.100E+02 0.200E+02 0.100E+02 0.100E+02 0.100E+02 0.000E+00
r4    0.100E+02 0.100E+02 0.100E+02 0.100E+02 0.100E+02 0.100E+02 0.000E+00
ch    0.900E+00 0.900E+00 0.800E+00 0.700E+00 0.700E+00 0.600E+00 0.600E+01
MF    0.100E+00 0.100E+00 0.110E+00 0.100E+00 0.100E+00 0.100E+00 0.150E+00 0.150E+00
BASE  0.100E+01 0.100E+01-0.100E+01 0.100E+01 0.100E+01-0.200E+01 0.000E+00 0.000E+00
NMF   0.100E+00 0.100E+00 0.100E+00 0.100E+00 0.100E+00 0.100E+00 0.100E+00 0.100E+00
UADJ  0.000E+00 0.000E+00 0.000E+00 0.000E+00 0.000E+00 0.000E+00 0.000E+00 0.000E+00
TIPM  0.100E+00 0.100E+00 0.100E+00 0.100E+00 0.100E+00 0.100E+00 0.100E+00 0.100E+00
RHO   0.333E+00 0.333E+00 0.333E+00 0.333E+00 0.333E+00 0.333E+00 0.333E+00 0.333E+00
WHCL  0.350E-01 0.350E-01 0.350E-01 0.350E-01 0.350E-01 0.350E-01 0.350E-01 0.350E-01
fmadj     0.000
fmlow     0.000
fmhgh     0.000
gladj     0.000
rlaps     0.000
elvrf     0.000
flgev      2.00 1 = pan; 2 = Hargreaves; 3 = Priestley-Taylor
albed     0.11
aw-a      0.11      0.11      0.18      0.11      0.11      0.11      0.11
fpet      2.00      2.00      1.50      2.00      2.00      2.00      0.70
ftal      0.70      0.70      0.70      0.70      0.70      0.70      0.50
flint        1.        1.        1.        1.        1.        1.        1.
fcap      0.15      0.15      0.15      0.15      0.15      0.15      0.15
ffcap     0.10      0.10      0.10      0.10      0.10      0.10      0.10
spore     0.30      0.30      0.30      0.30      0.30      0.30      0.30
sublm        0.        0.        0.        0.        0.        0.        0.
tempa       50.
temp3       50.
tton         0.
lat.        50.
mxmn  10.2 12.3 12.1 12.3 14.3 14.2 13.8 14.0 13.1 10.6  8.2  9.3
humid 59.5 60.5 62.5 55.5 50.0 54.5 59.0 58.5 63.5 58.0 64.5 62.5
pres  95.1 95.1 95.1 95.1 95.1 95.1 95.1 95.1 95.1 95.1 95.1 95.1
ti2    jan  feb  mar  apr  may  jun  jul  aug  sep  oct  nov  dec
h1    1.83 1.83 1.83 1.83 1.83 1.83 1.83 1.83 1.83 1.83 1.83 1.83
h2    1.13 1.13 1.13 1.13 1.53 1.83 1.83 1.83 1.83 1.13 1.13 1.13
h3    0.04 0.04 0.04 0.04 0.53 0.53 0.53 0.53 0.53 0.28 0.04 0.04
h4    0.50 0.50 0.50 0.50 2.00 2.50 2.50 2.50 2.50 0.50 0.50 0.50
h5    1.13 1.13 1.13 1.13 1.53 1.83 1.83 1.83 1.83 1.13 1.13 1.13
h6    1.19 1.19 1.19 1.19 1.39 1.39 1.39 1.59 1.59 1.19 1.19 1.19
h6    0.01 0.01 0.01 0.01 0.01 0.01 0.01 0.01 0.01 0.01 0.01 0.01
```

Appendix B

Annual Precipitation Accumulations

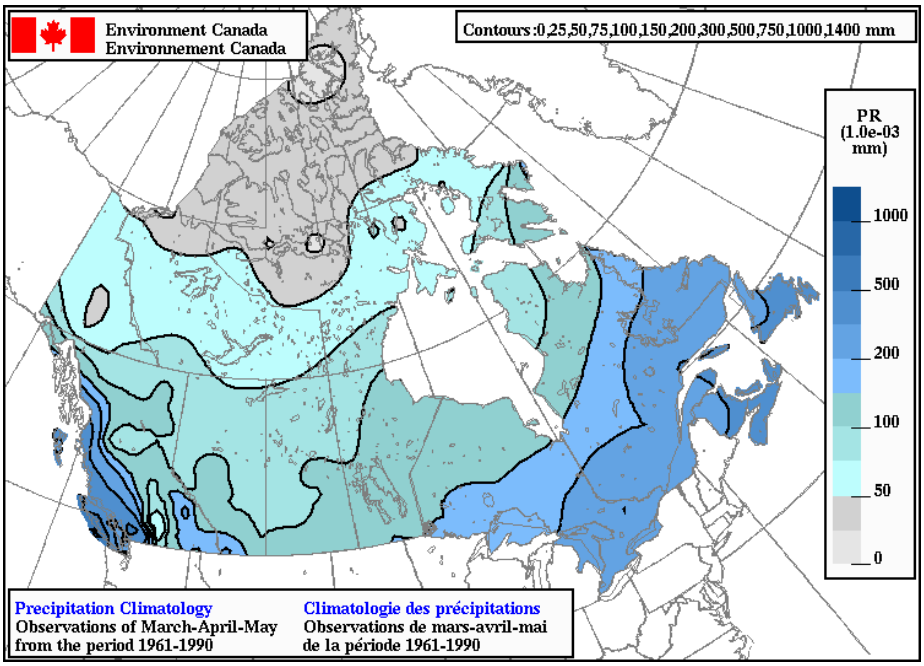

Figure B.1- Average precipitation accumulation for Canada, Spring (EC, 2002)

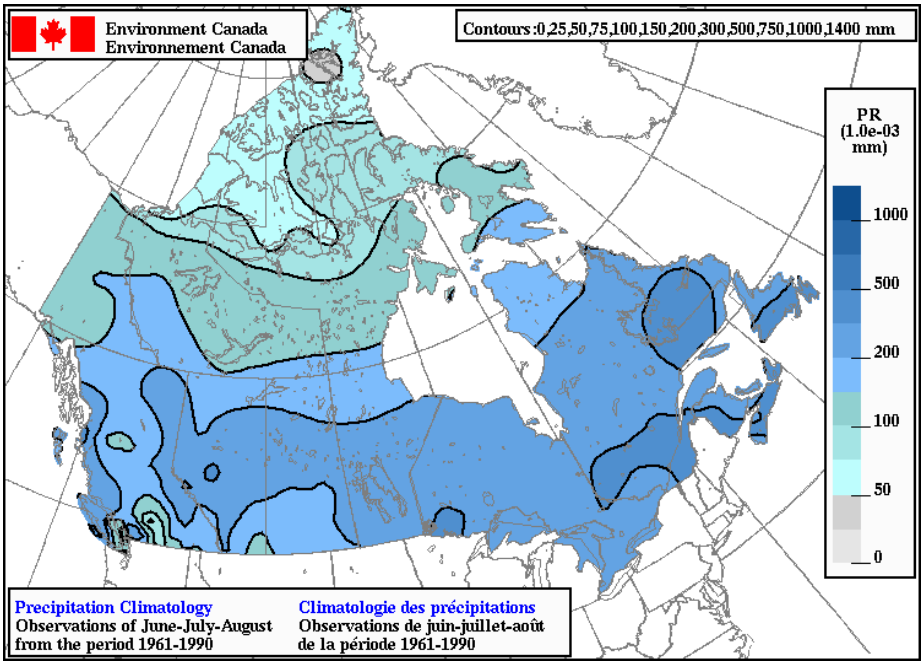

Figure B.2- Average precipitation accumulation for Canada, Summer (EC, 2002)

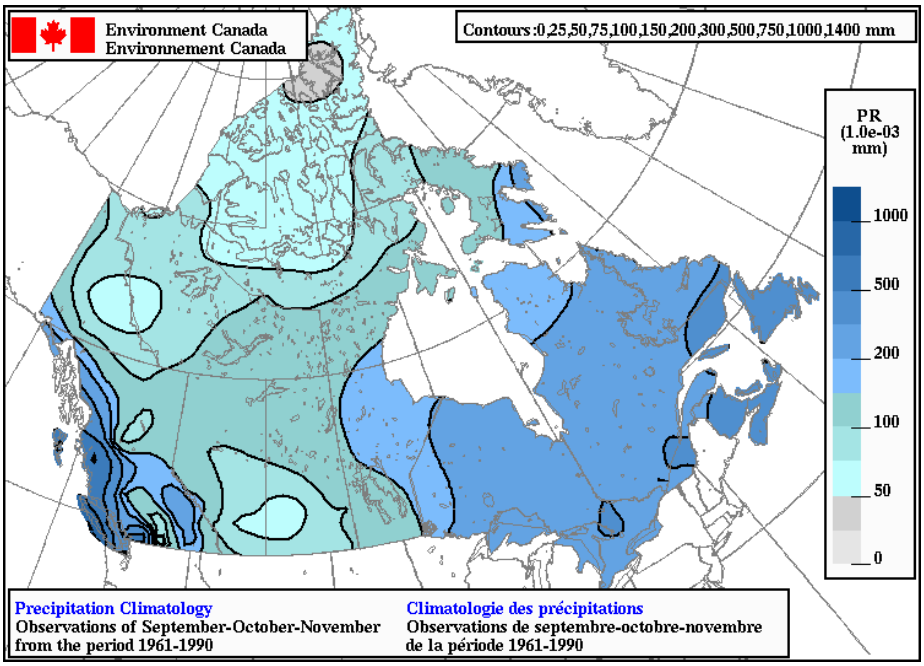

Figure B.3- Average precipitation accumulation for Canada, Fall (EC, 2002)

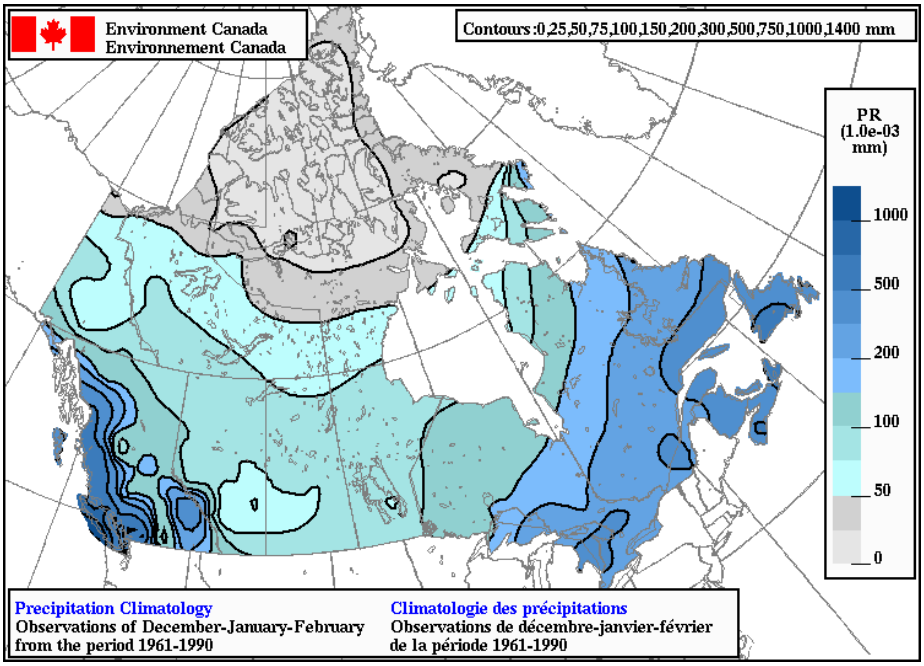

Figure B.4- Average precipitation accumulation for Canada, Winter (EC, 2002)

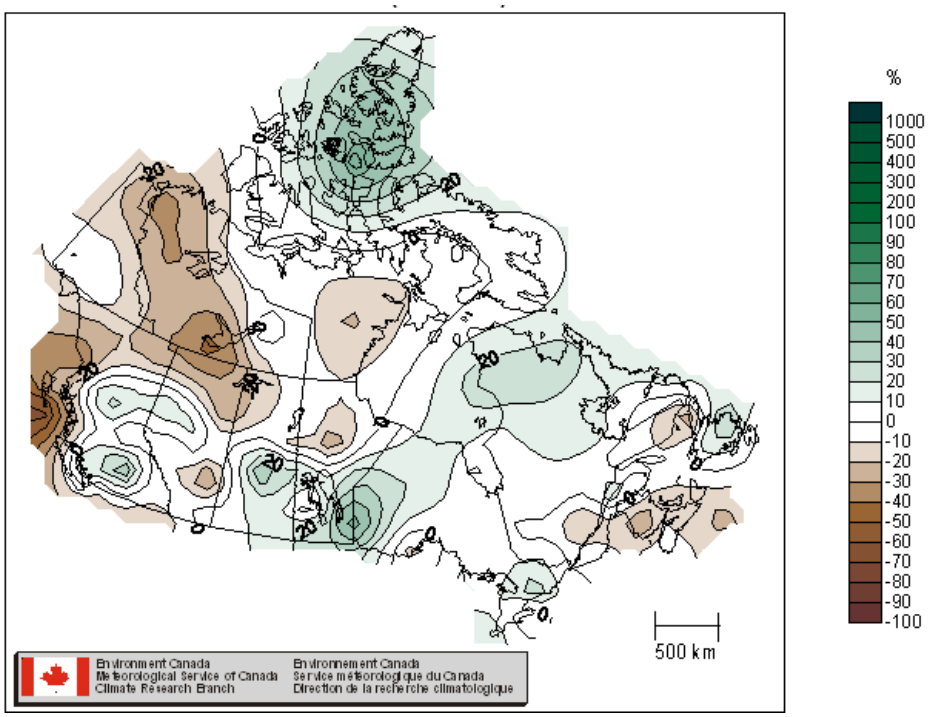

Figure B.5- Precipitation departures from normal: January to December 2004 (EC, 2002)

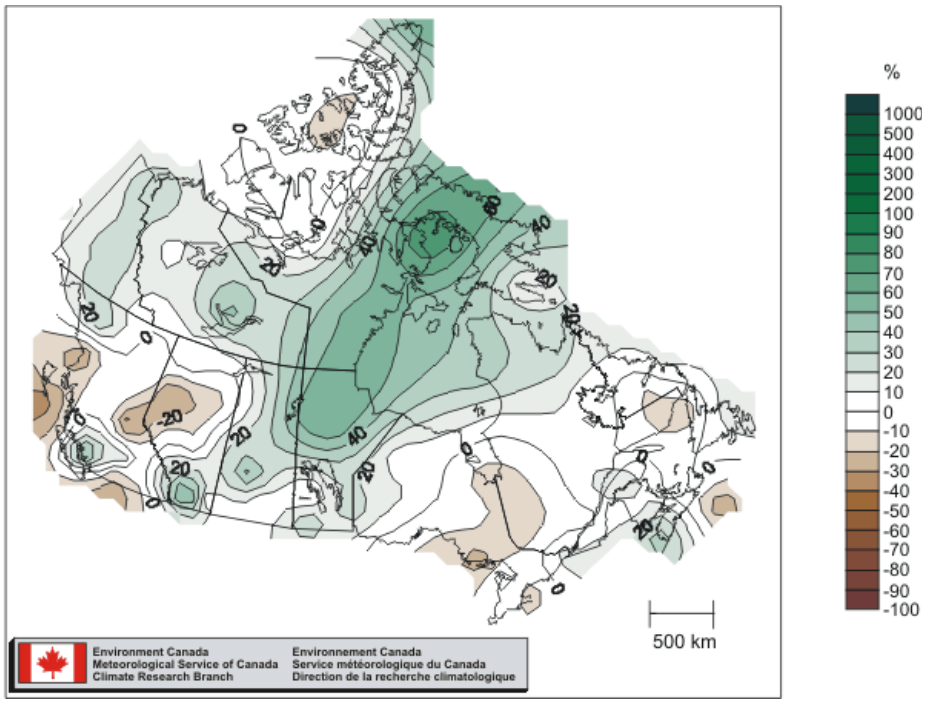

Figure B.6- Precipitation departures from normal: January to December 2005 (EC, 2002)

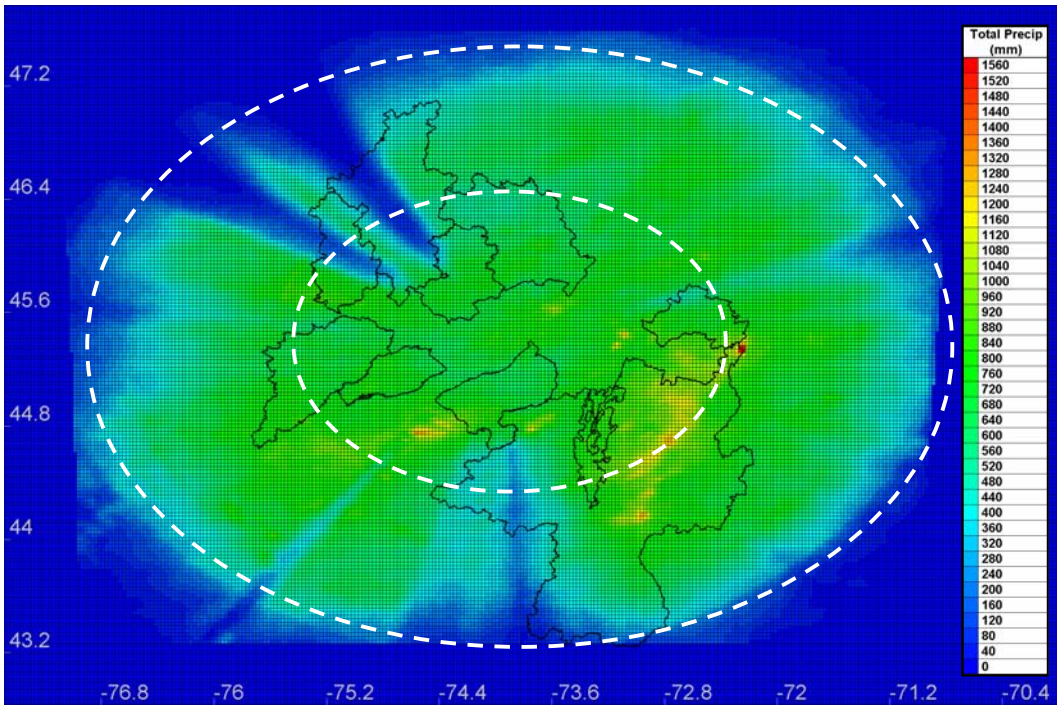

Figure B.7- Cumulative precipitation for C0 radar product: January to December 2004

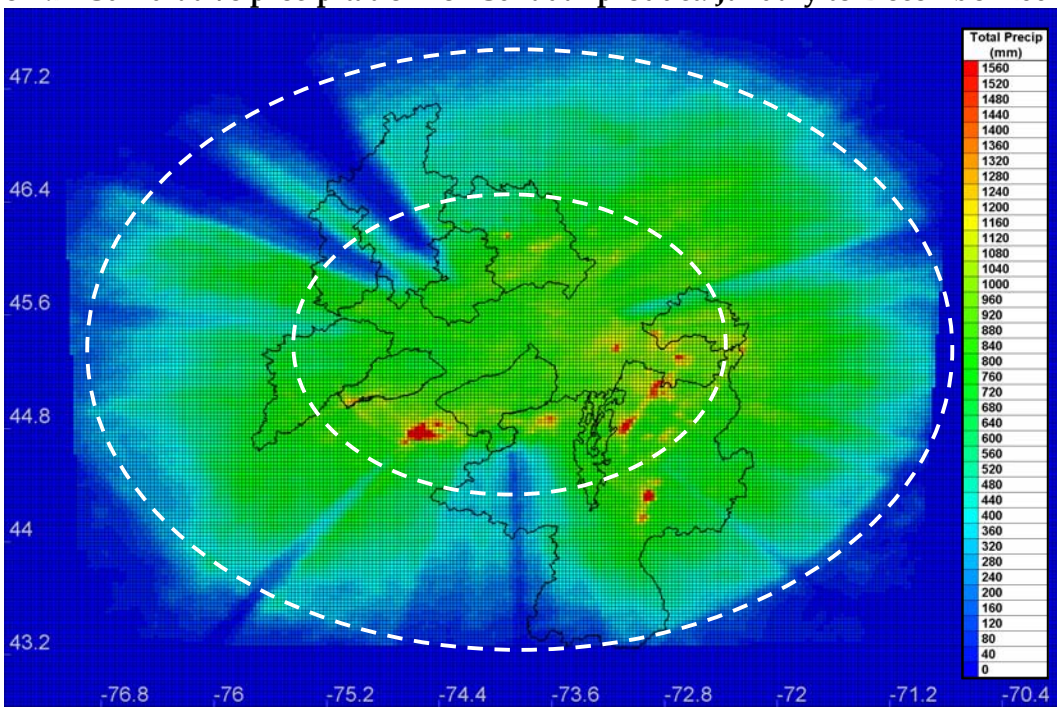

Figure B.8- Cumulative precipitation for C0 radar product: January to November 2005

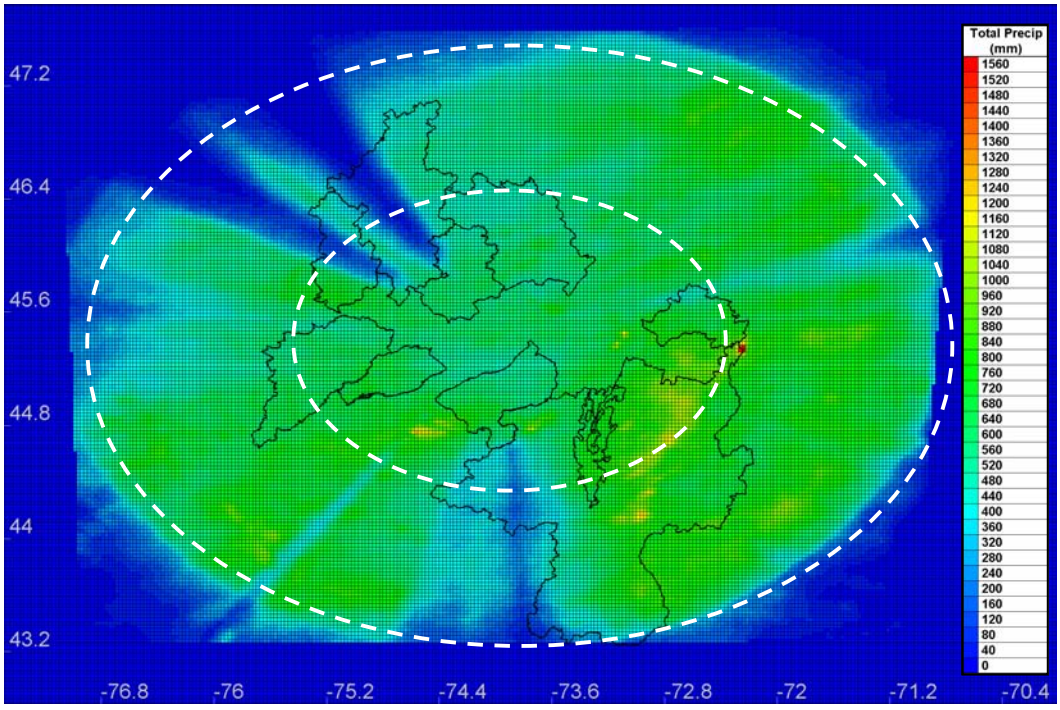

Figure B.9- Cumulative precipitation for C2 radar product: January to December 2004

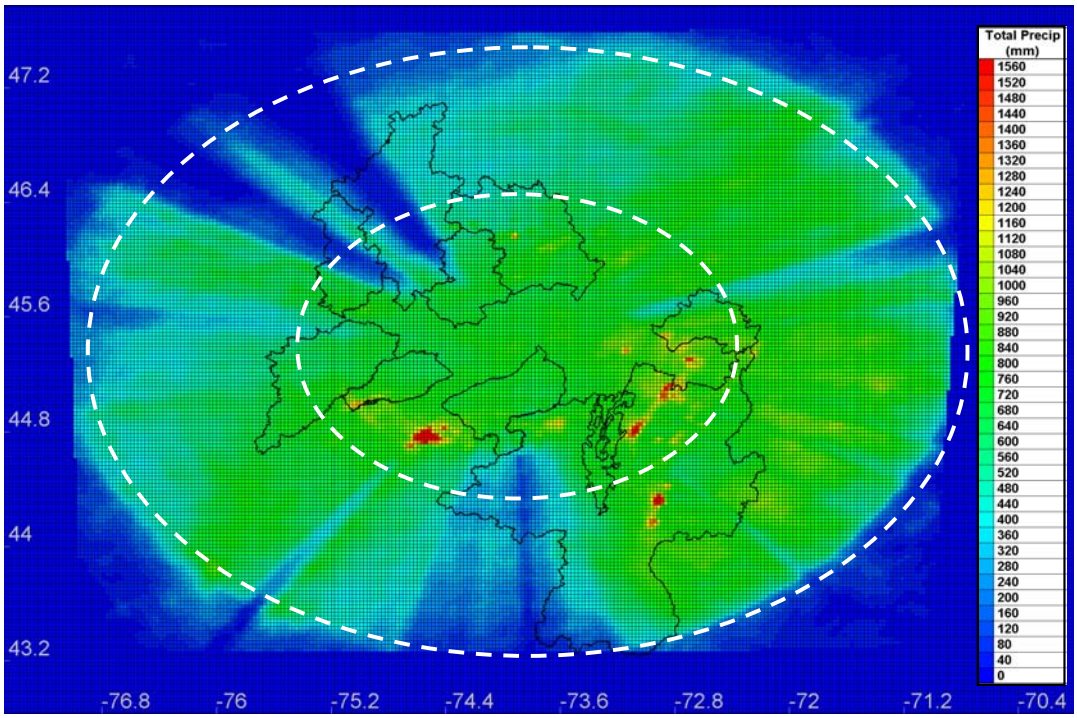

Figure B.10- Cumulative precipitation for C2 radar product: January to November 2005

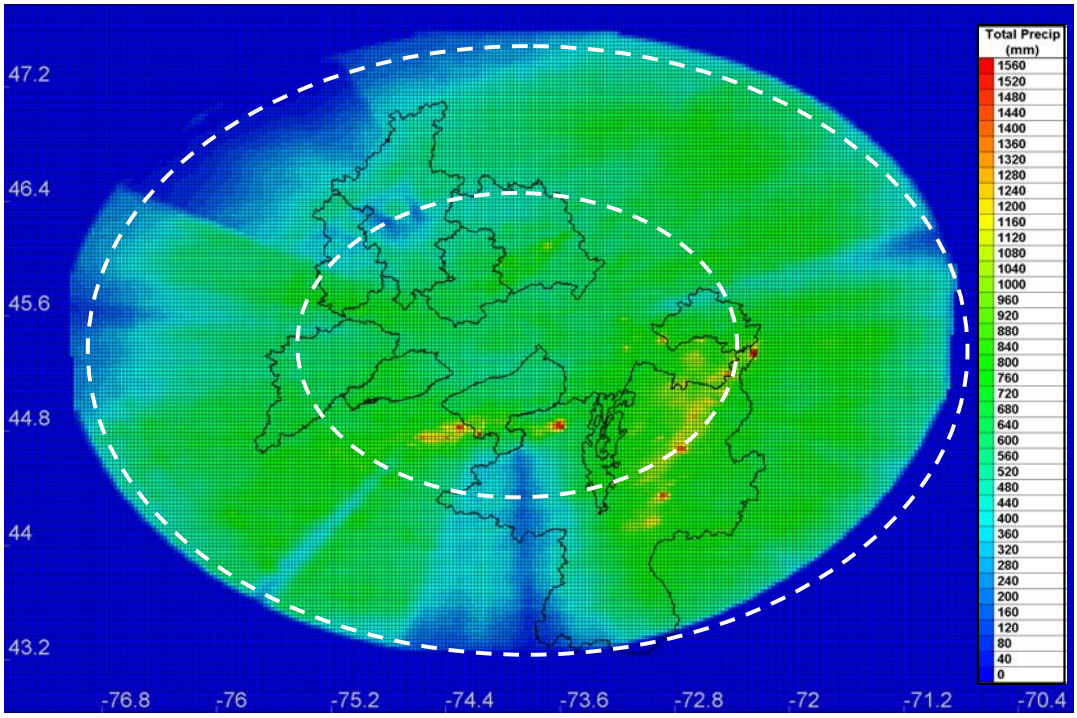

Figure B.11- Cumulative precipitation for C3 radar product: January to December 2004

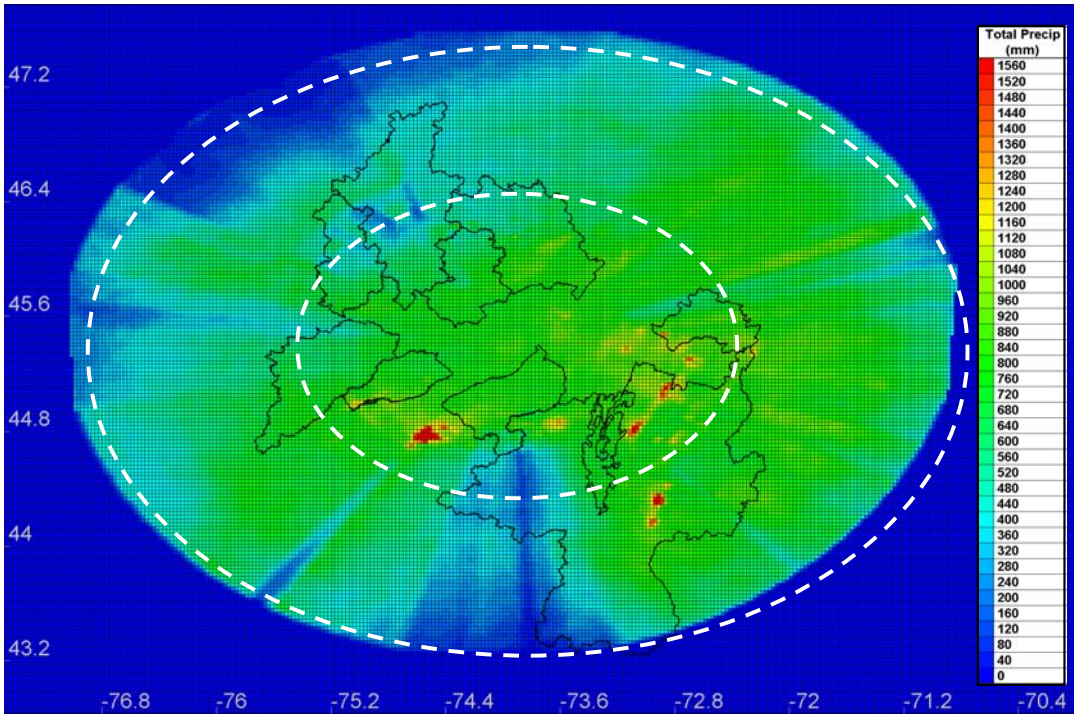

Figure B.12- Cumulative precipitation for C3 radar product: January to November 2005

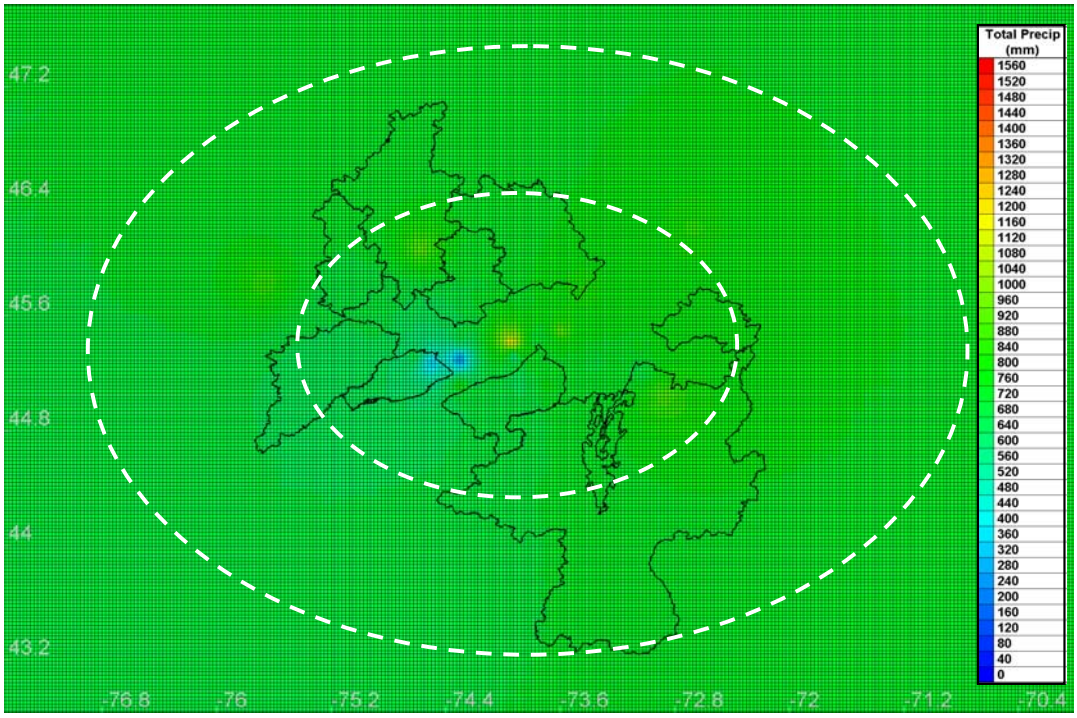

Figure B.13- Cumulative precipitation for precipitation gauges: January to December 2004

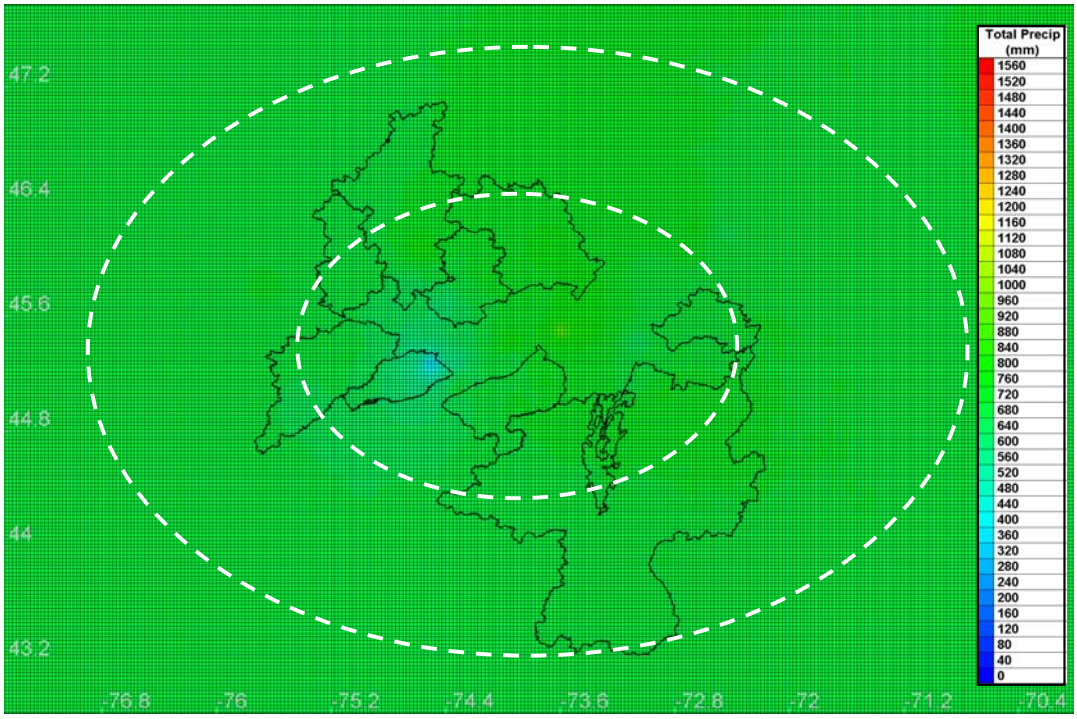

Figure B.14- Cumulative precipitation for precipitation gauges: January to November 2004

Appendix C

Streamflow Hydrographs

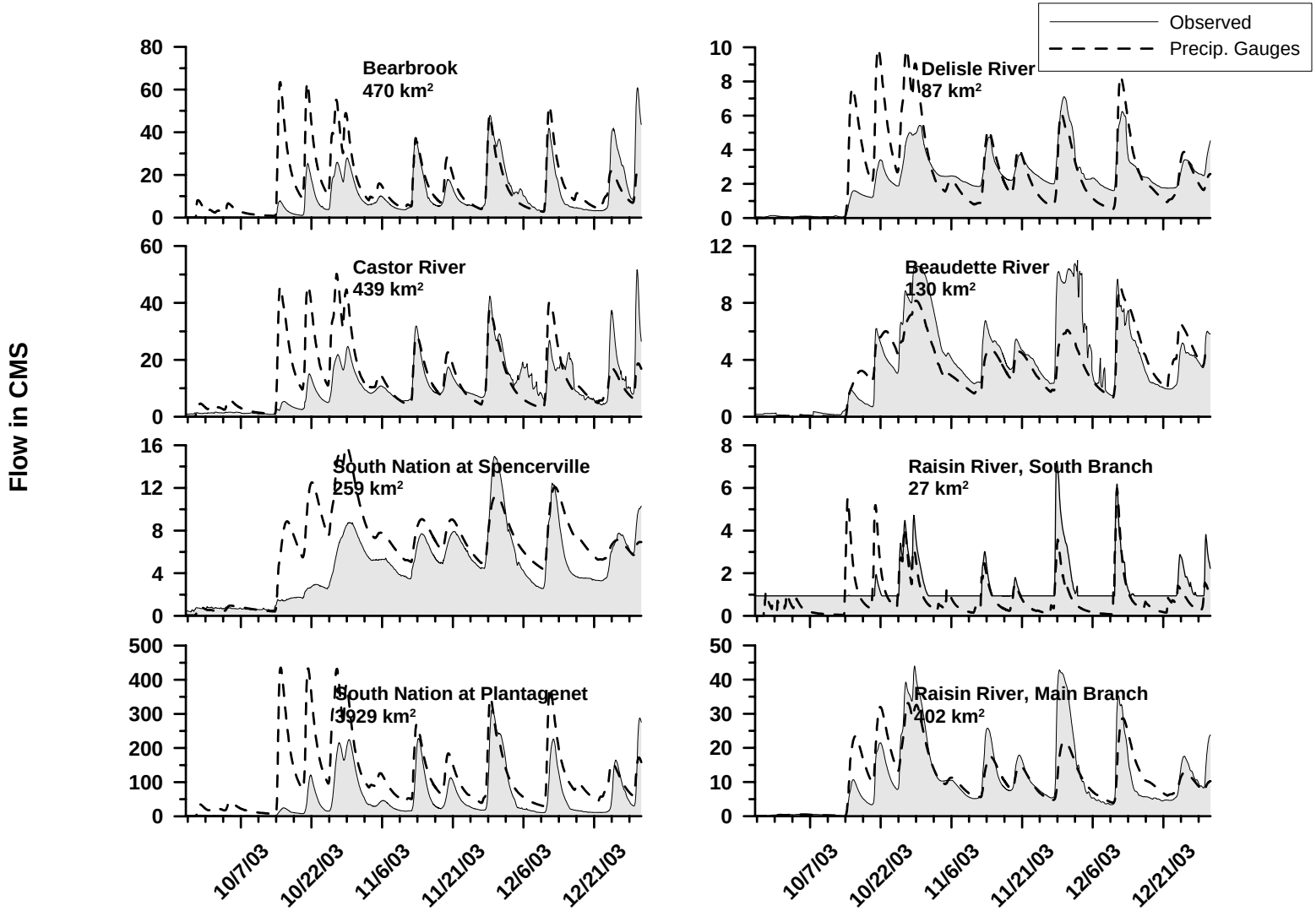

Figure C.1- Eastern Ontario calibration period: September 26th to December 31st 2003

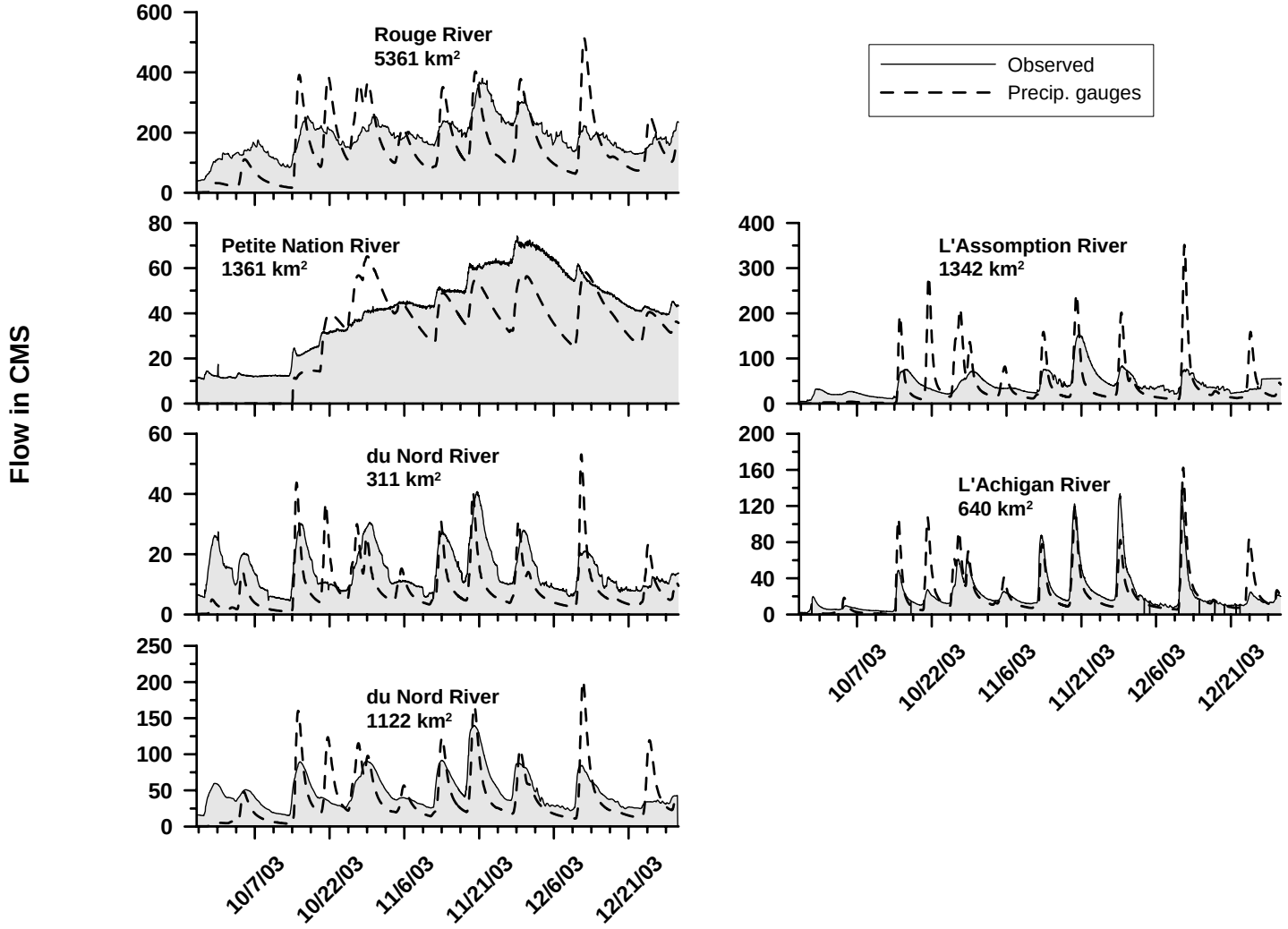

Figure C.2- Quebec, north of the St. Lawrence River calibration period: September 26th to December 31st 2003

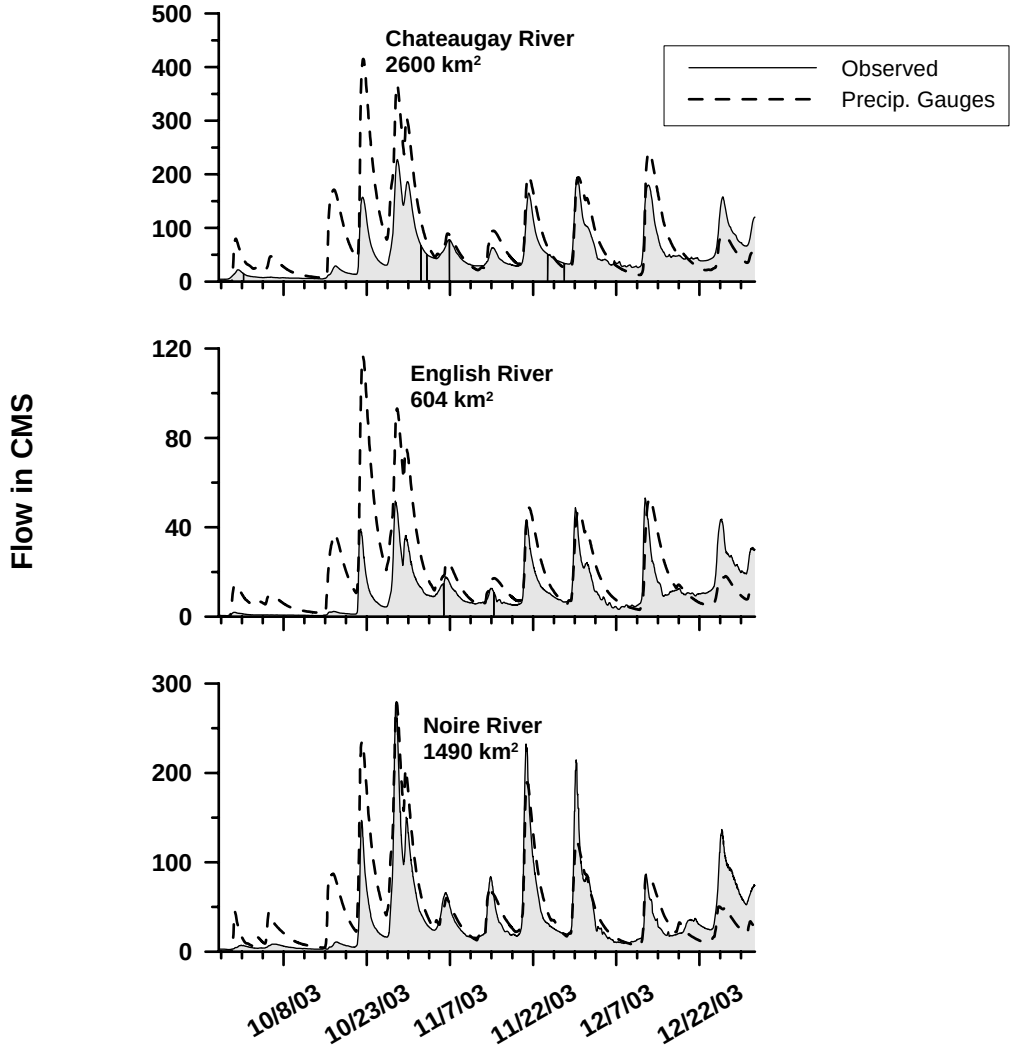

Figure C.3- Quebec, south of the St. Lawrence River calibration period: September 26th to December 31st 2003

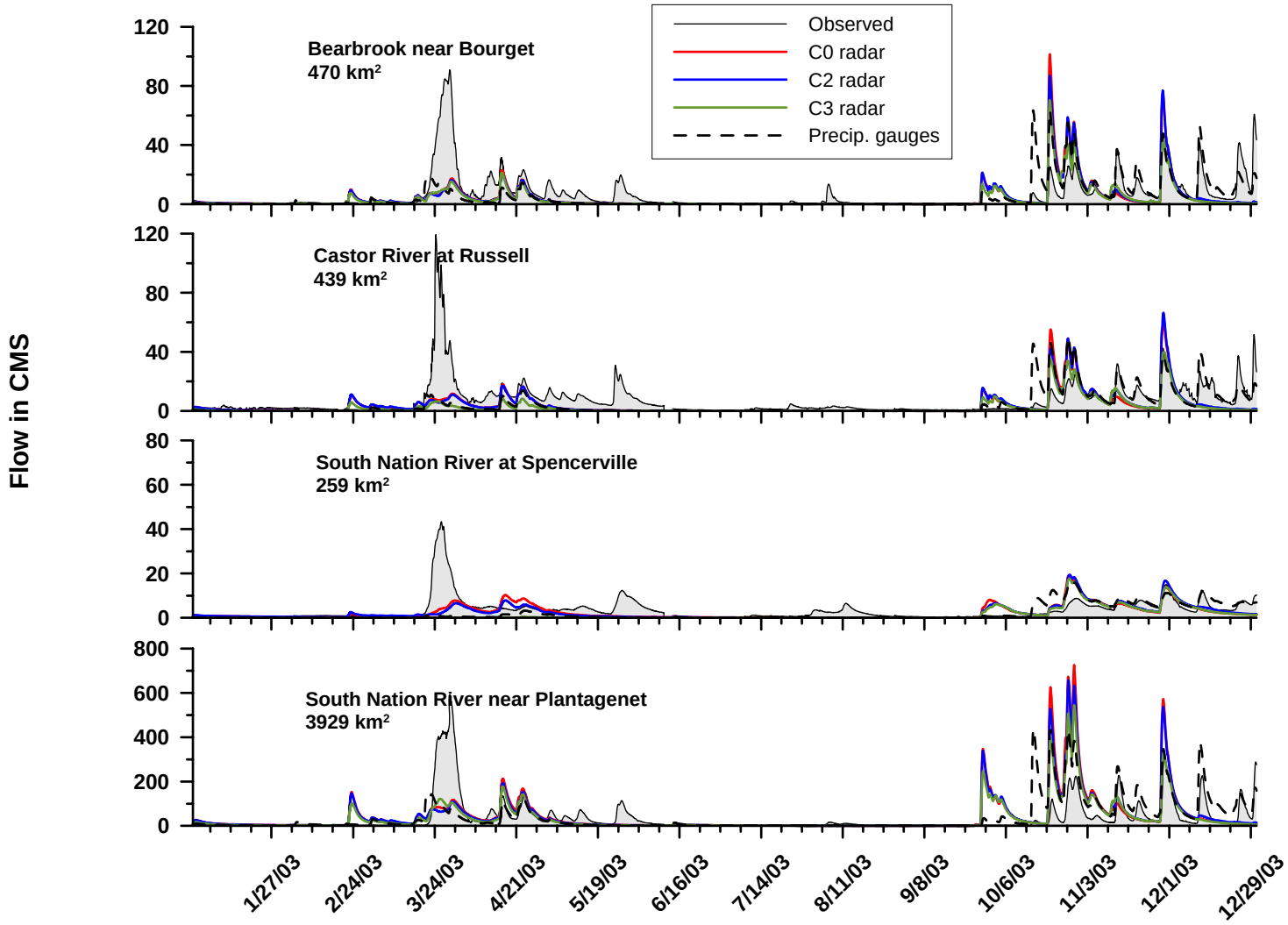

Figure C.4- Eastern Ontario streamflows: January to December 2003

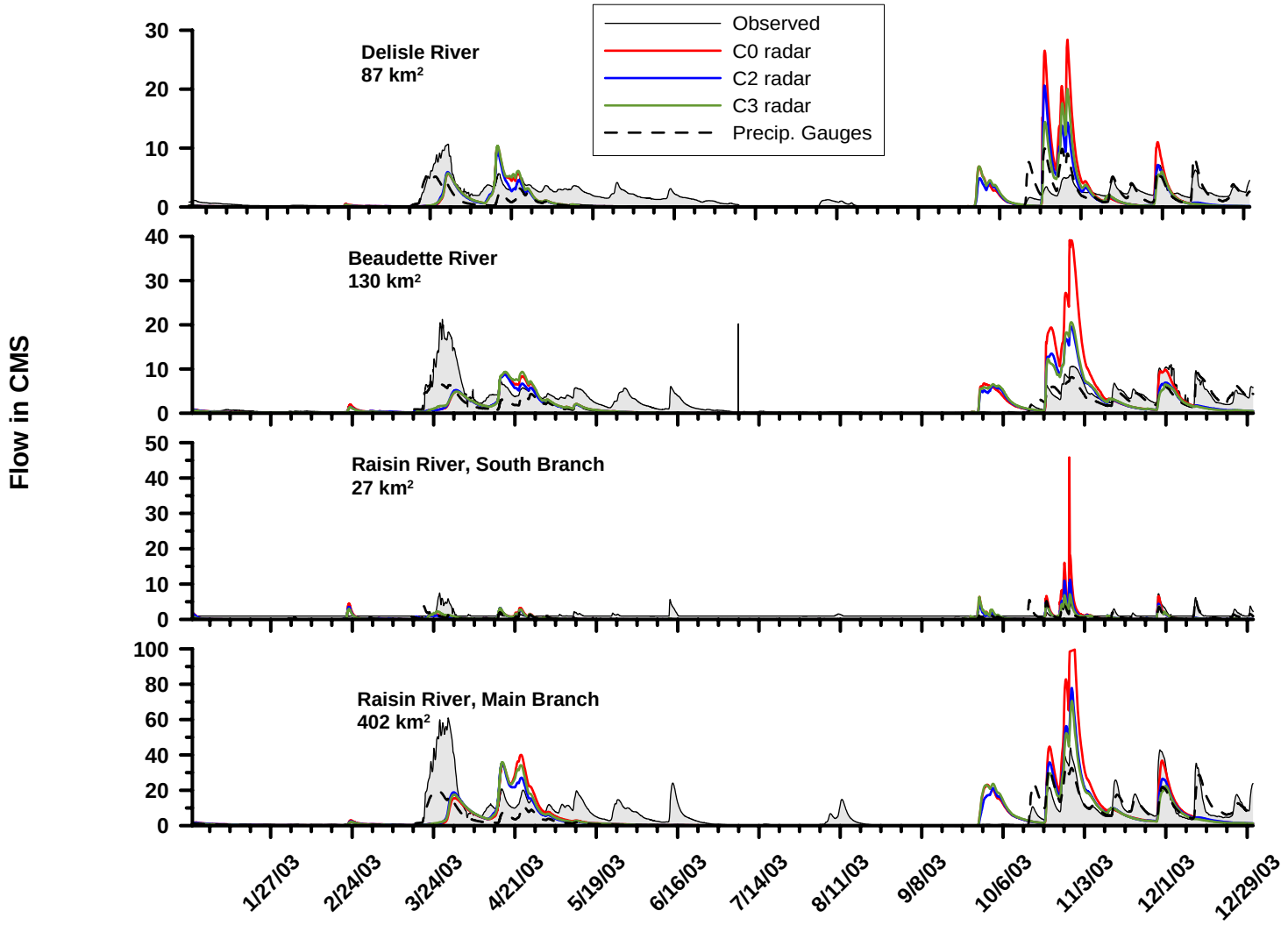

Figure C.5- Eastern Ontario streamflows: January to December 2003 (continued)

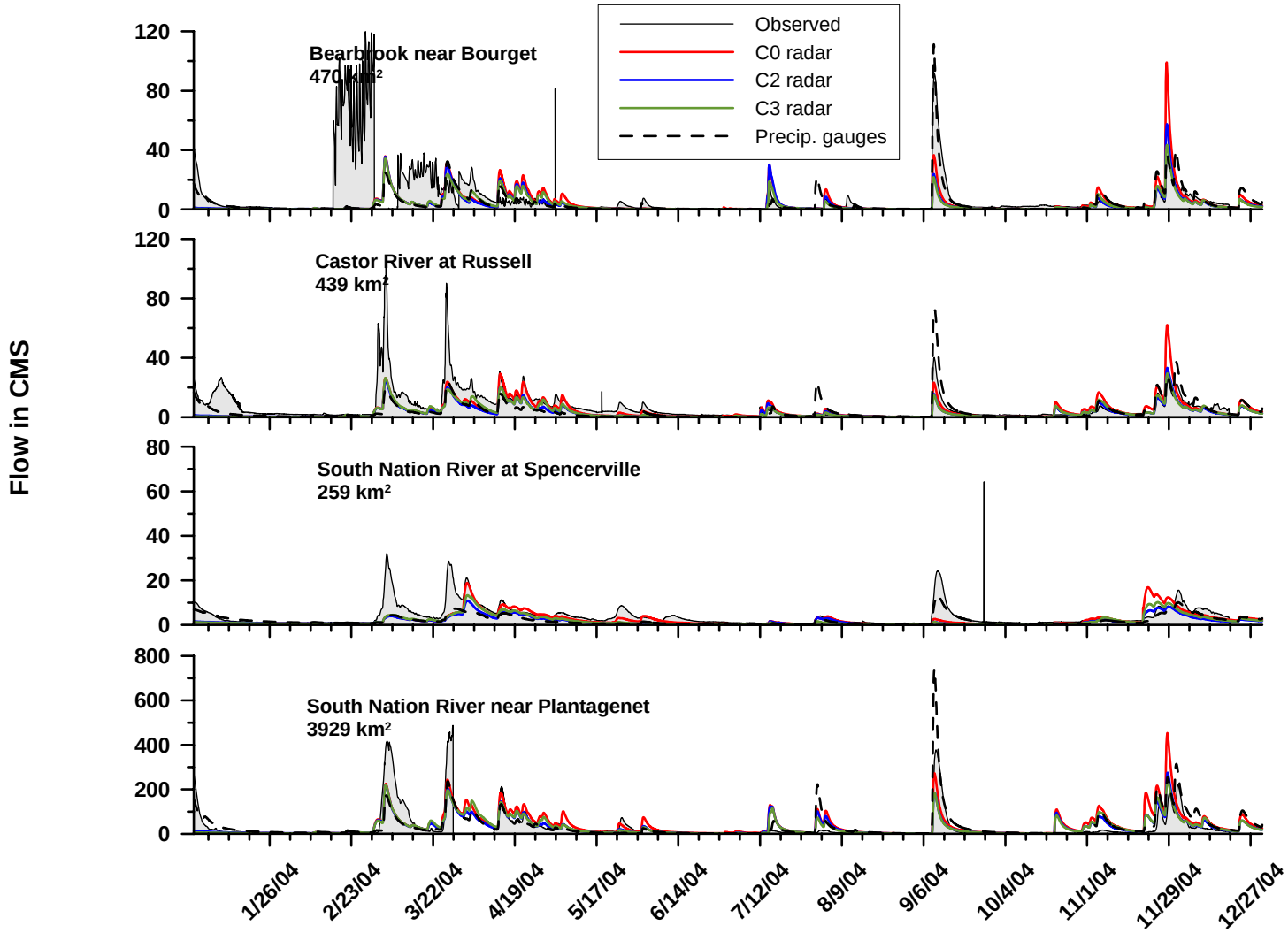

Figure C.6- Eastern Ontario streamflows: January to December 2004

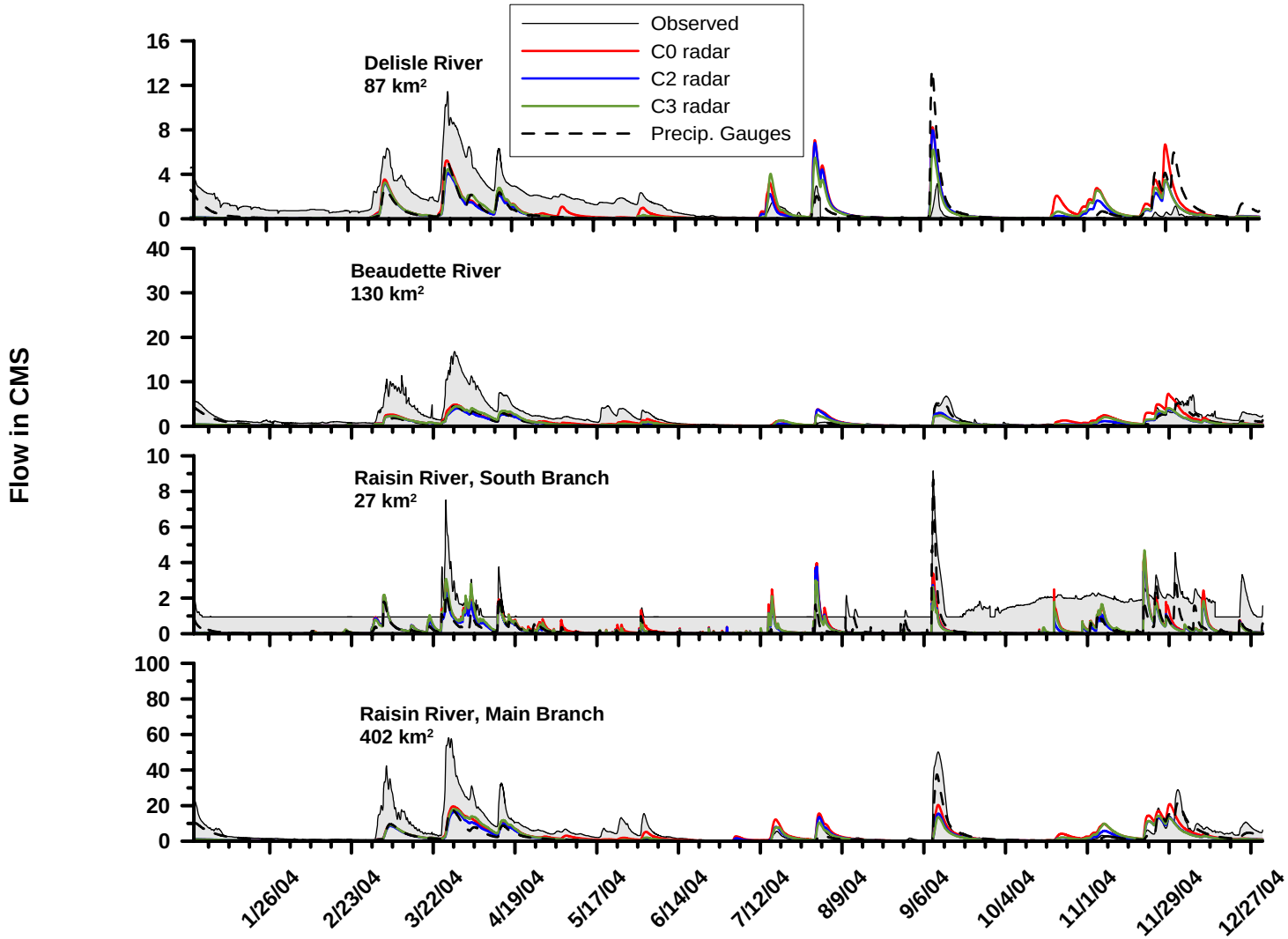

Figure C.7- Eastern Ontario streamflows: January to December 2004 (continued)

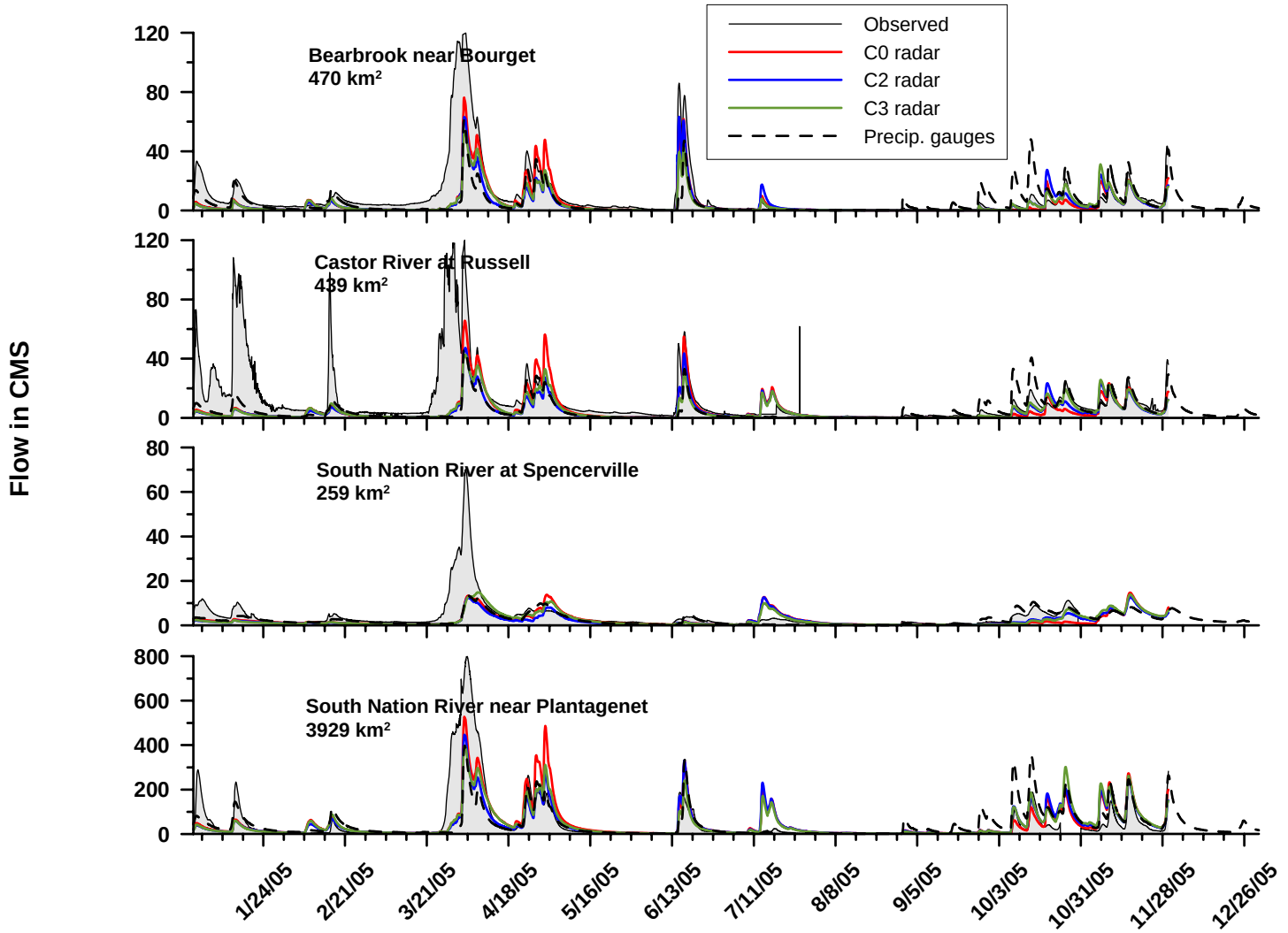

Figure C.8- Eastern Ontario streamflows: January to December 2005

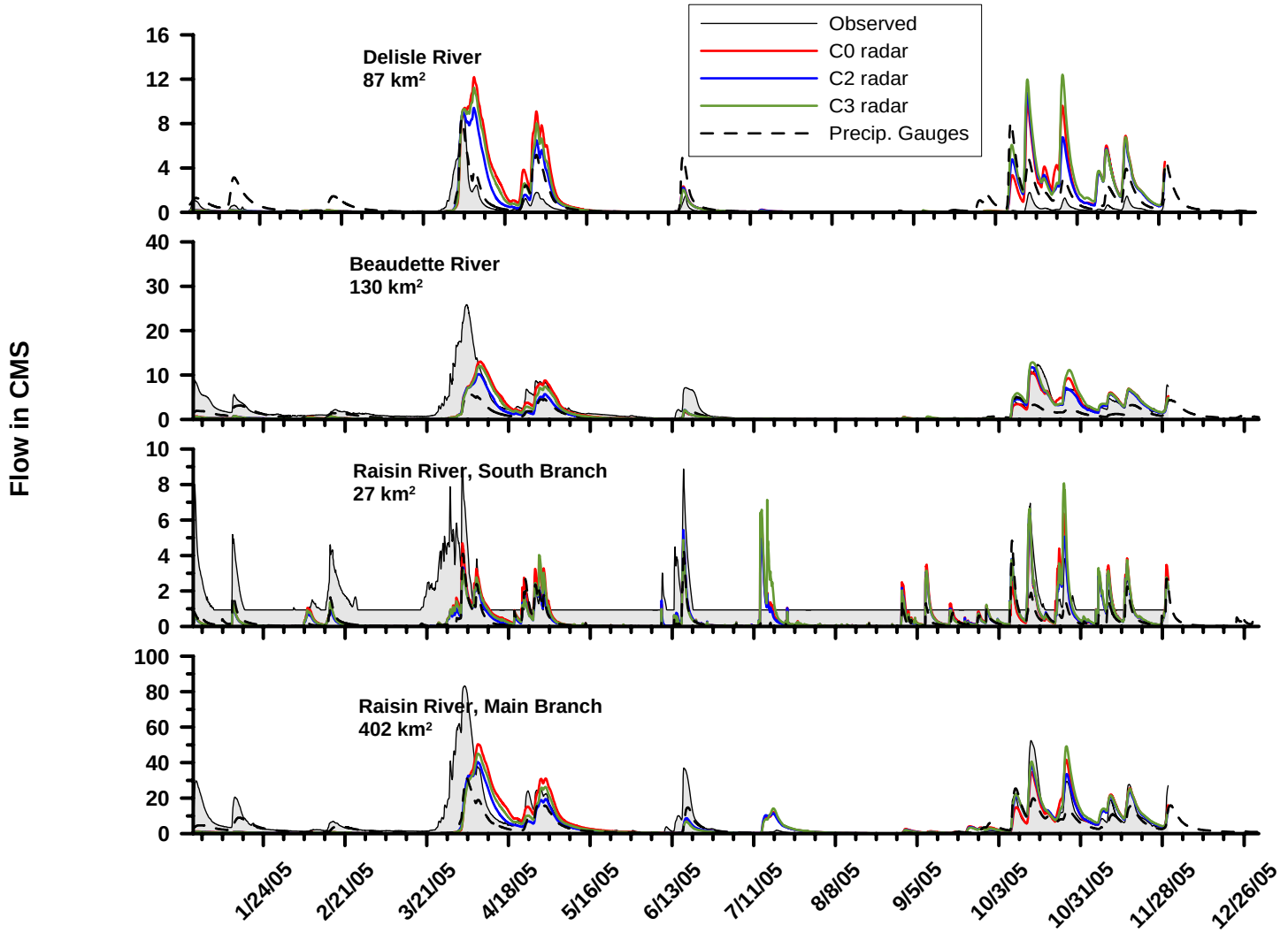

Figure C.9- Eastern Ontario streamflows: January to December 2005 (continued)

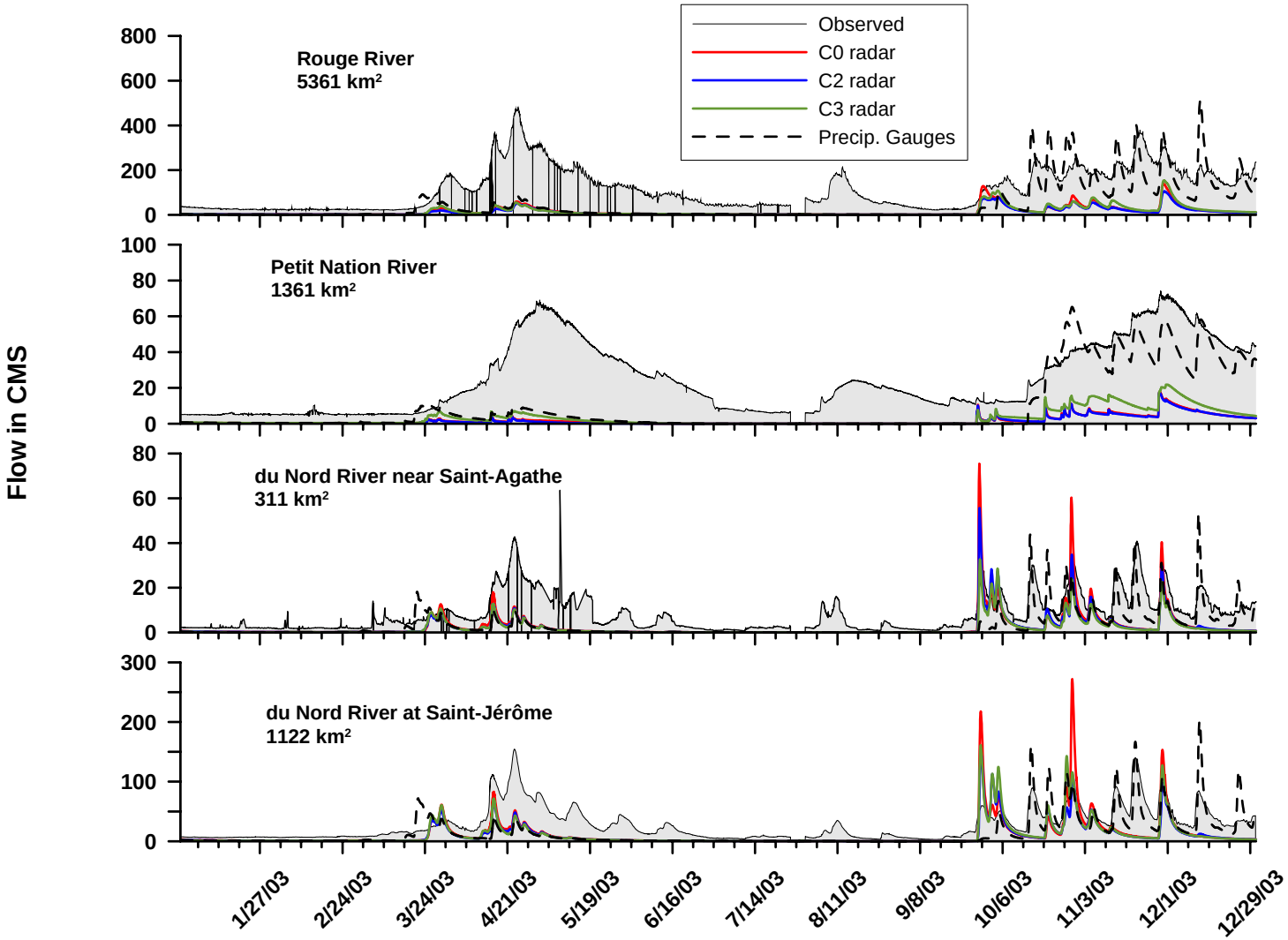

Figure C.10- Quebec, north of the St. Lawrence River streamflows: January to December 2003

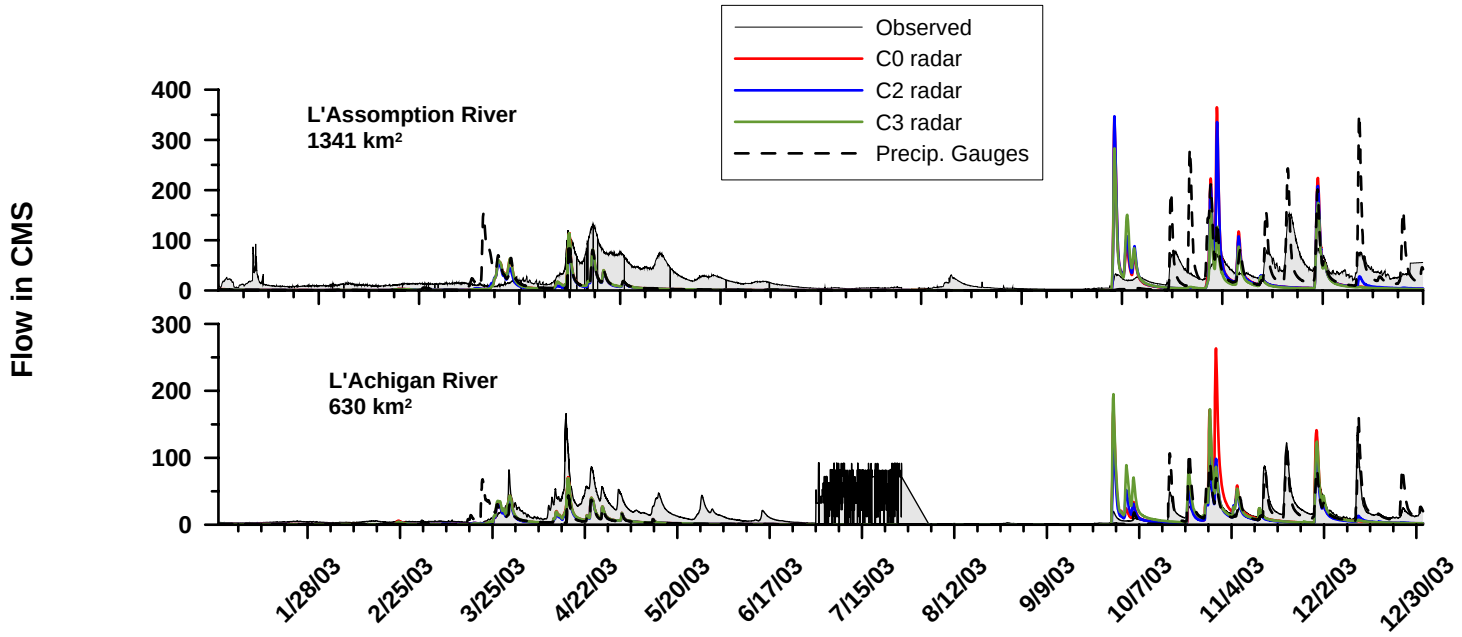

Figure C.11- Quebec, north of the St. Lawrence River streamflows: January to December 2003 (continued)

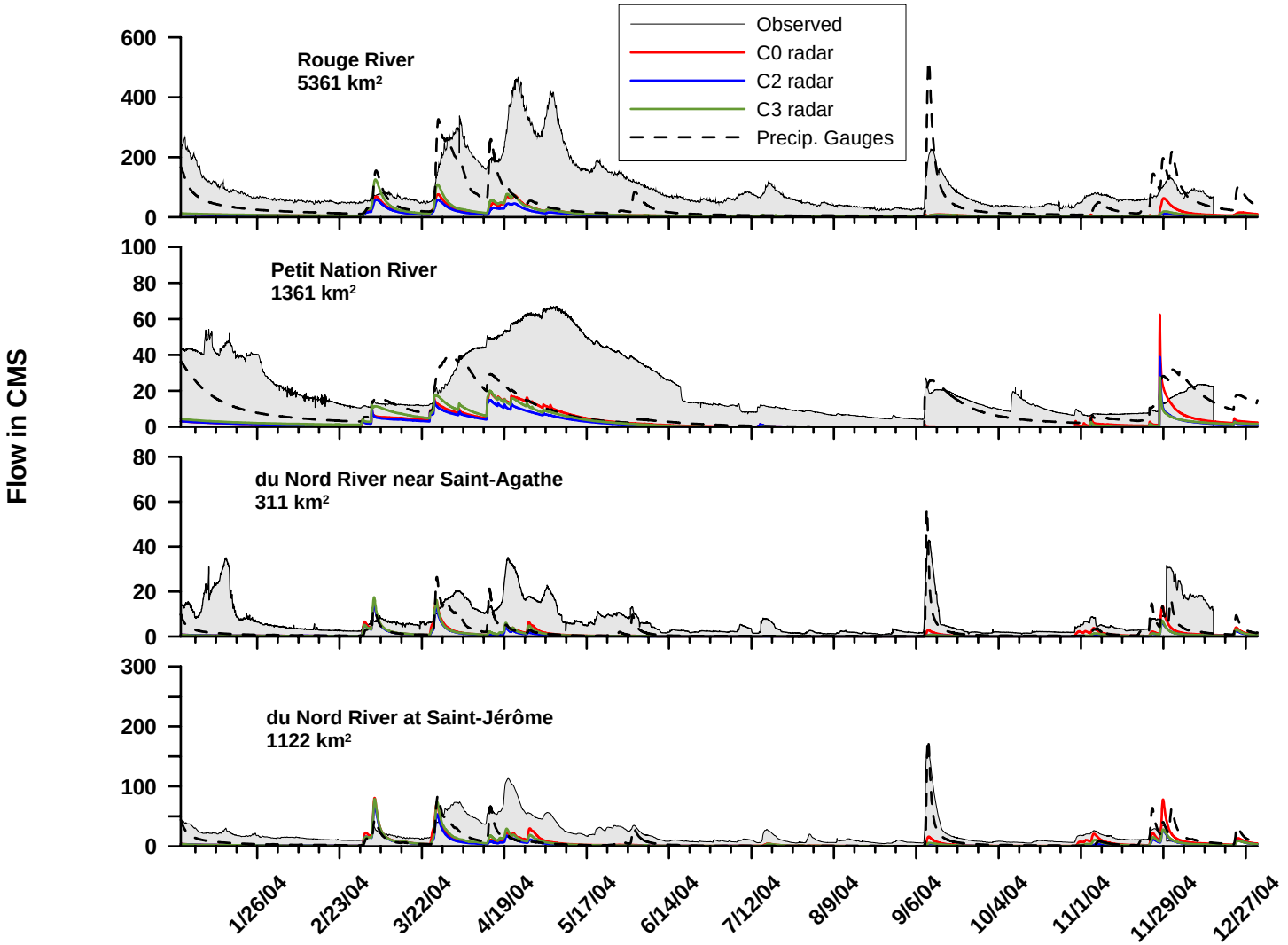

Figure C.12- Quebec, north of the St. Lawrence River streamflows: January to December 2004

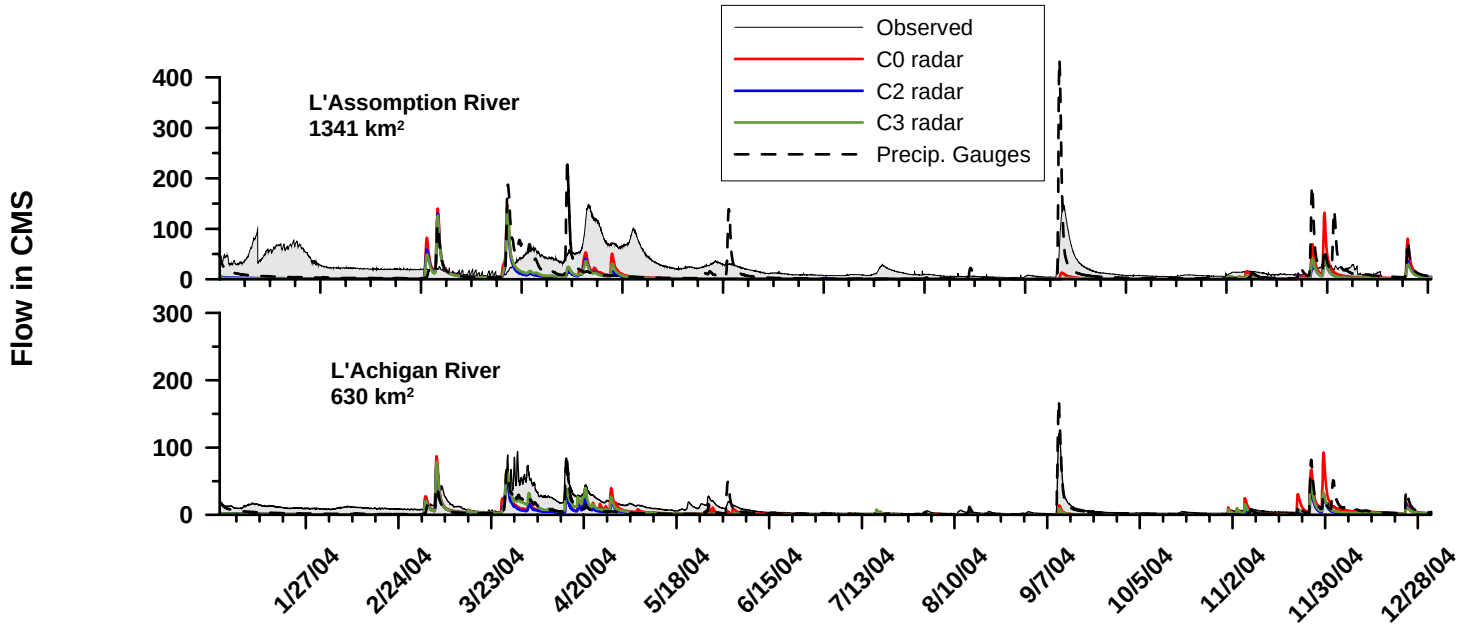

Figure C.13- Quebec, north of the St. Lawrence River streamflows: January to December 2004 (continued)

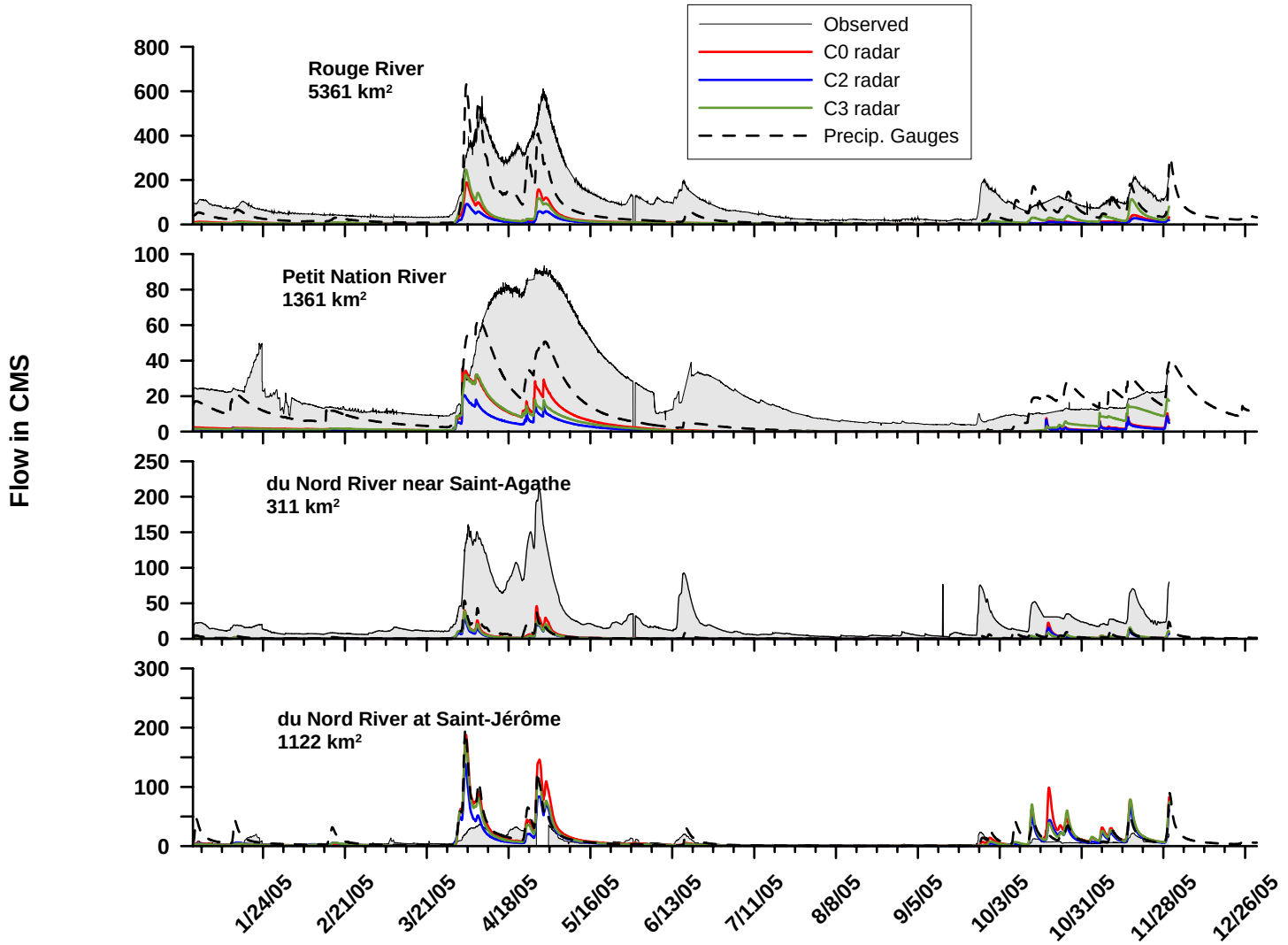

Figure C.14- Quebec, north of the St. Lawrence River streamflows: January to December 2005

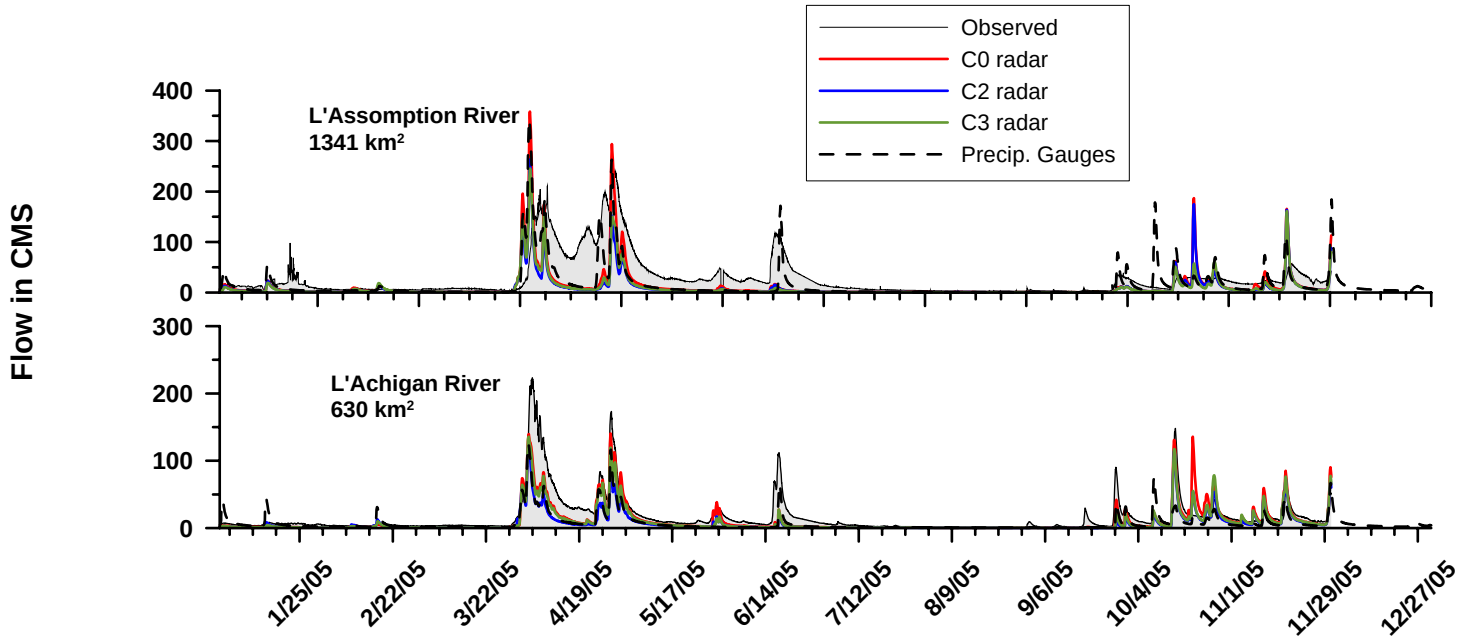

Figure C.15- Quebec, north of the St. Lawrence River streamflows: January to December 2005 (continued)

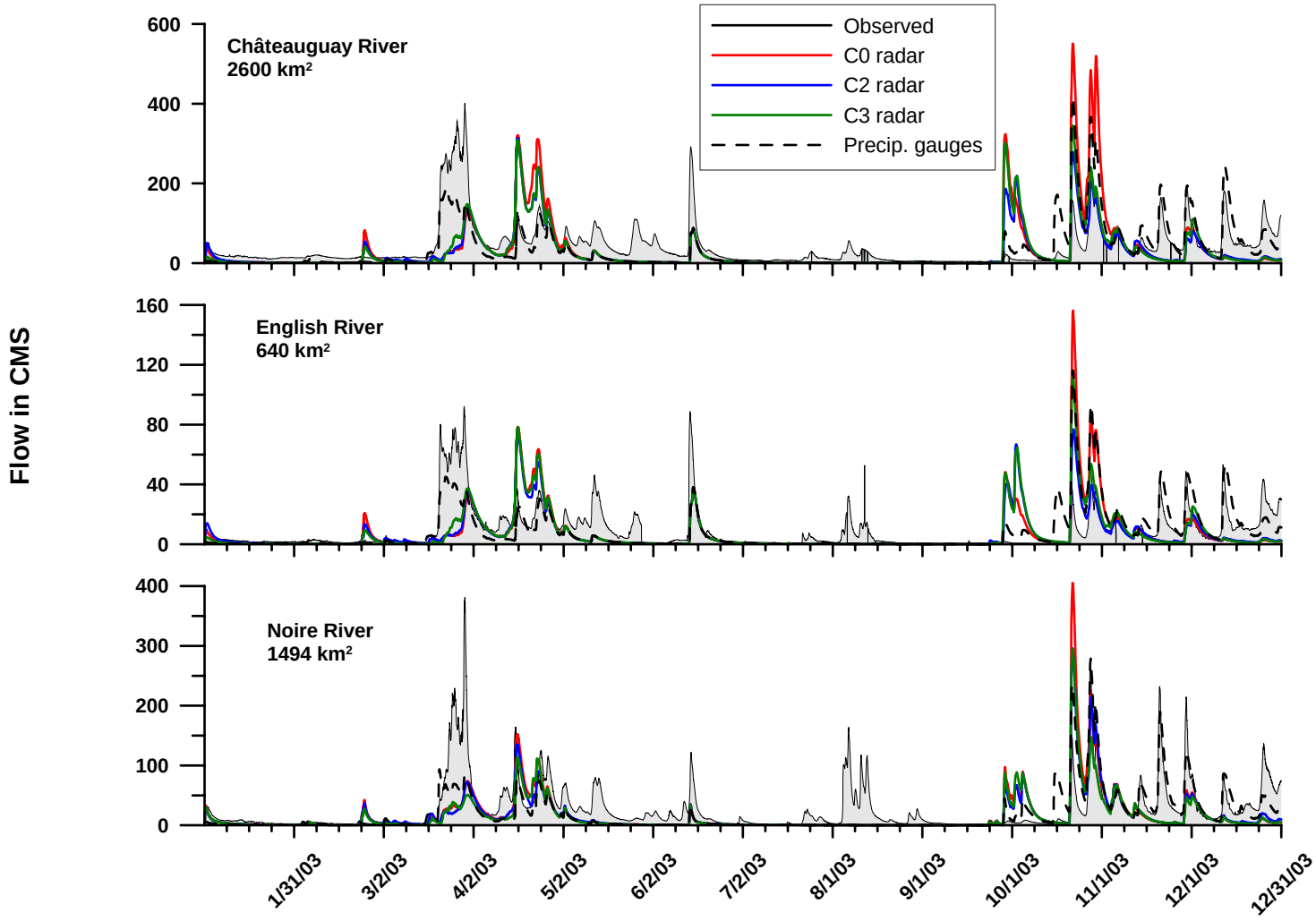

Figure C.16- Quebec, south of the St. Lawrence River streamflows: January to December 2003

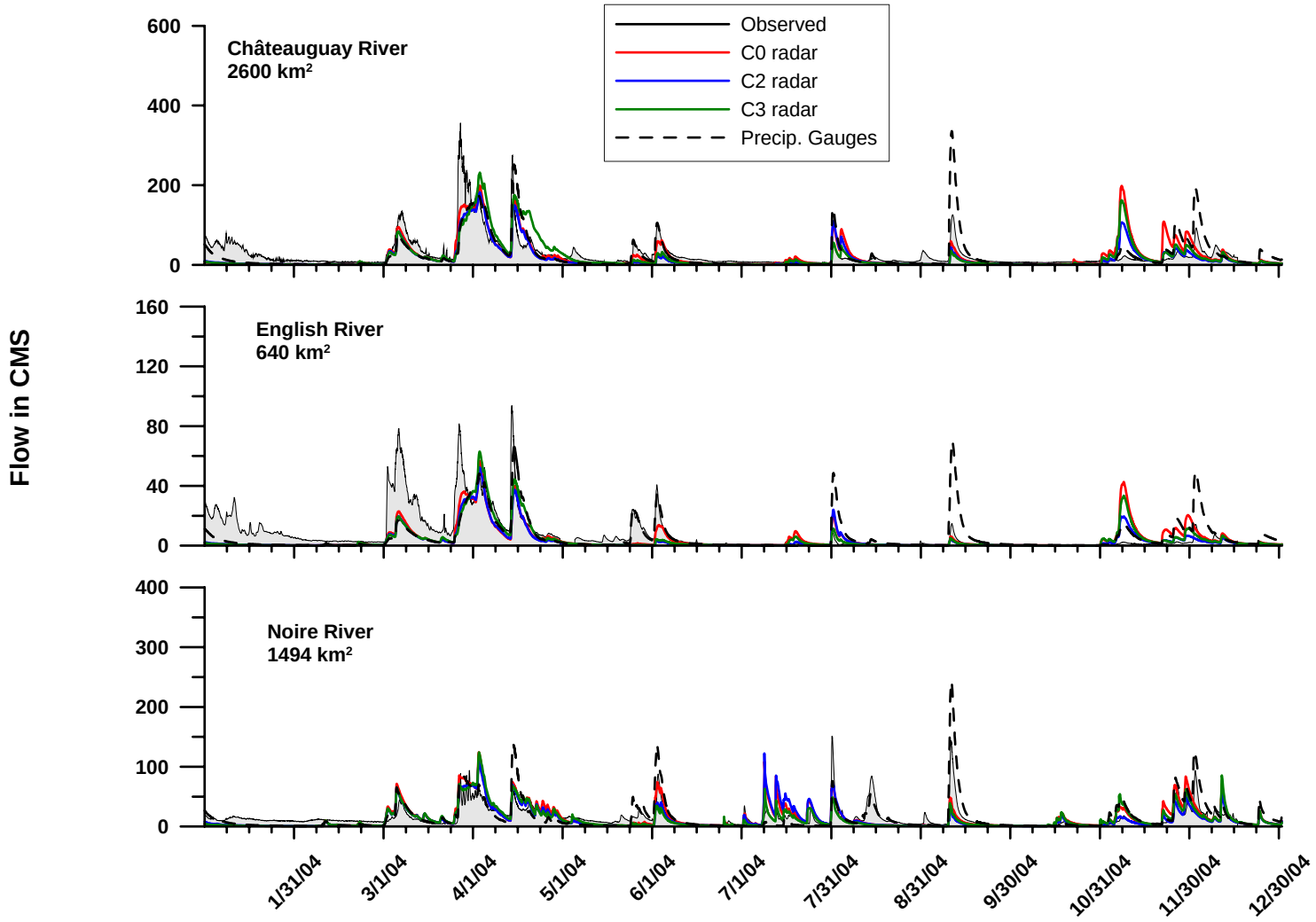

Figure C.17- Quebec, south of the St. Lawrence River streamflows: January to December 2004

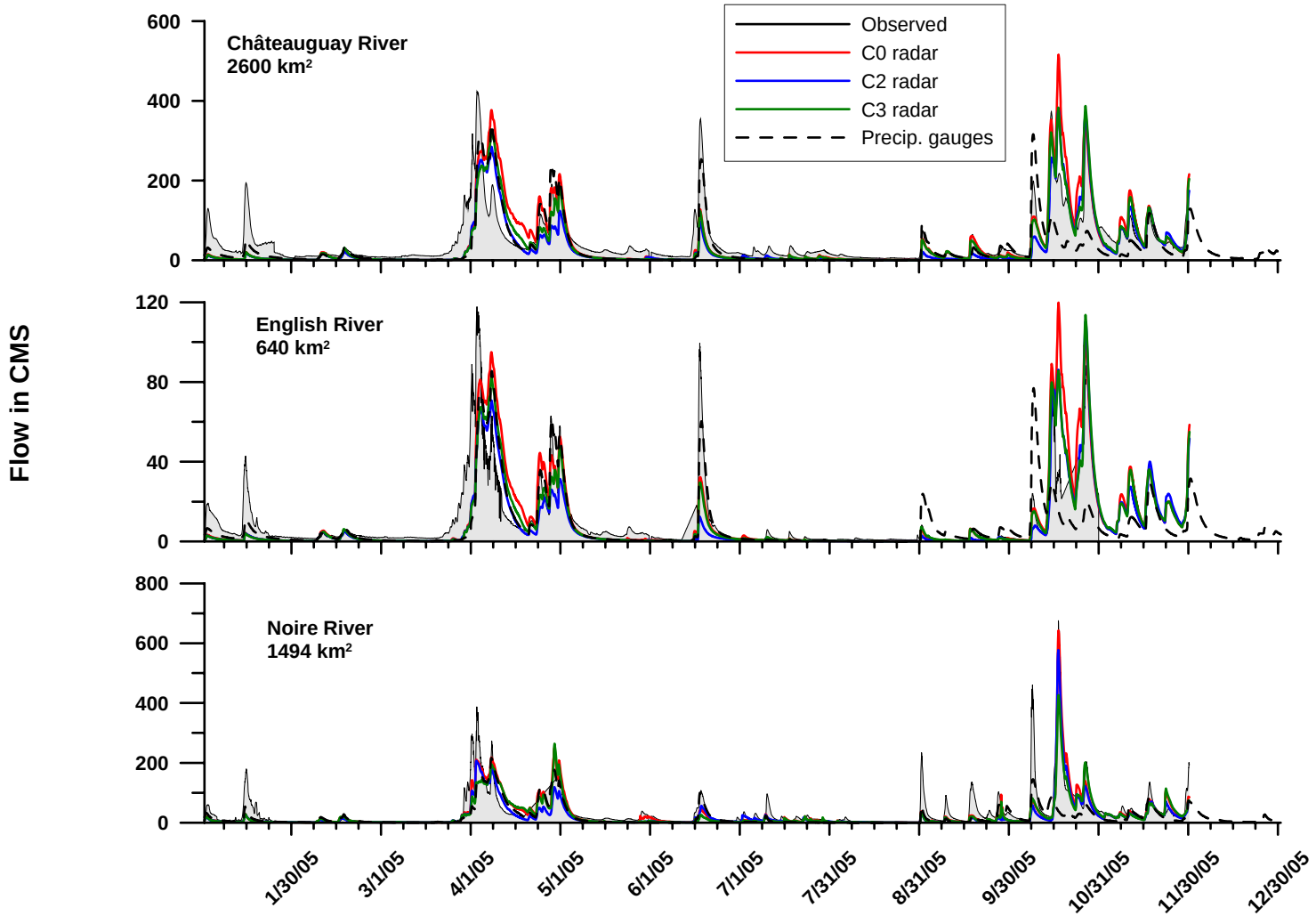

Figure C.18- Quebec, south of the St. Lawrence River streamflows: January to December 2005

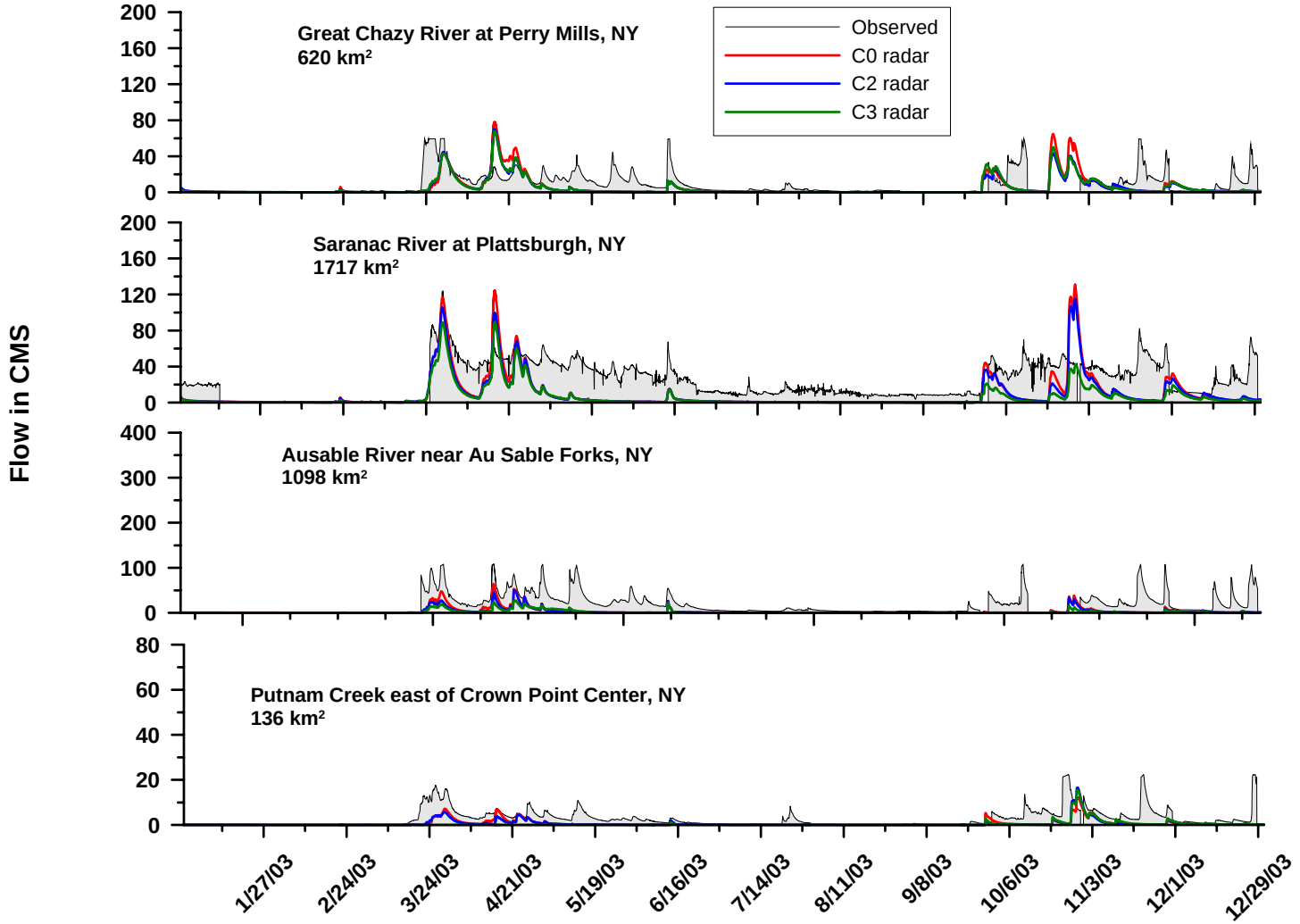

Figure C.19- Lake Champlain basin streamflows: January to December 2003

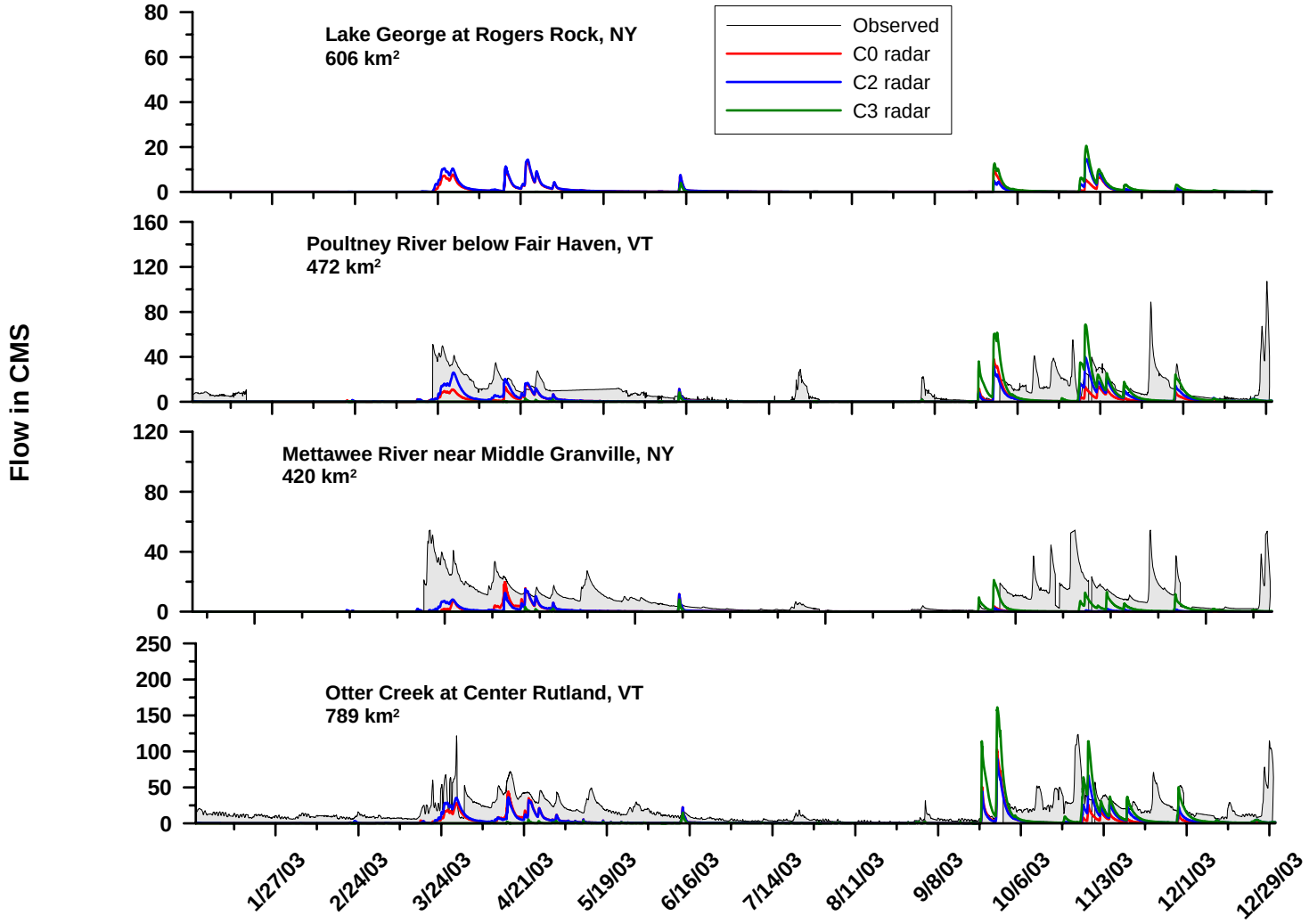

Figure C.20- Lake Champlain basin streamflows: January to December 2003 (continued)

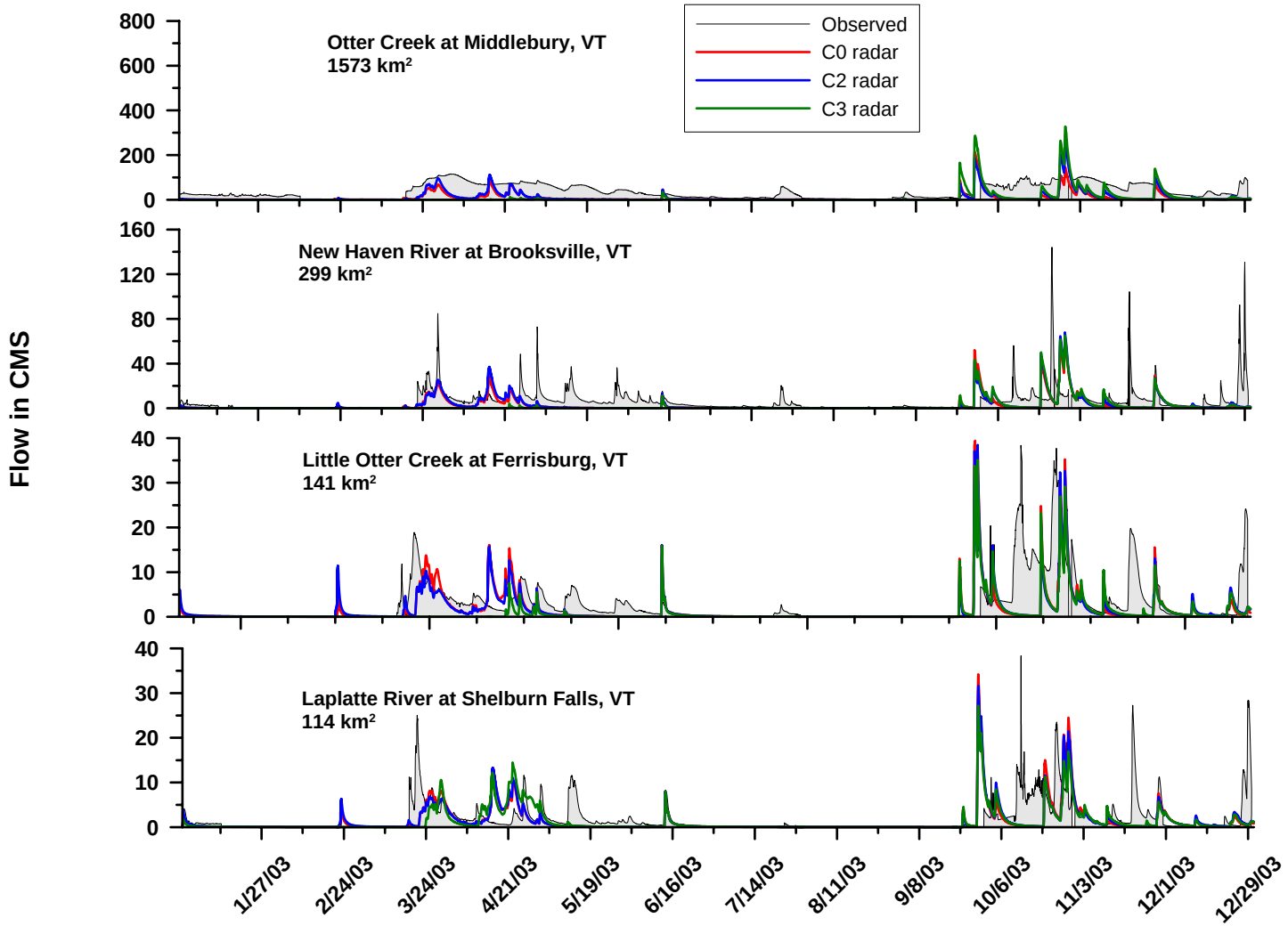

Figure C.21- Lake Champlain basin streamflows: January to December 2003 (continued)

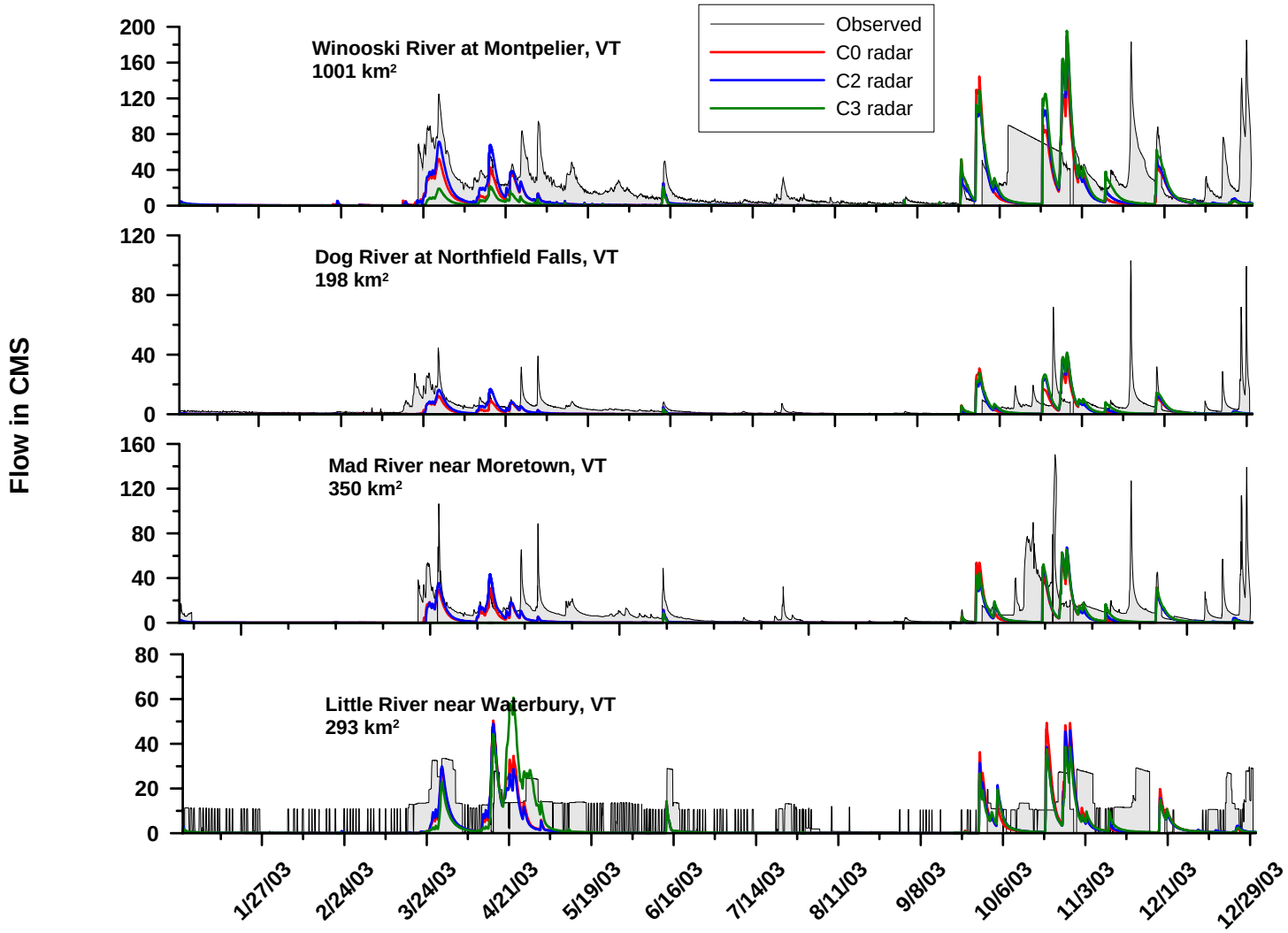

Figure C.22- Lake Champlain basin streamflows: January to December 2003 (continued)

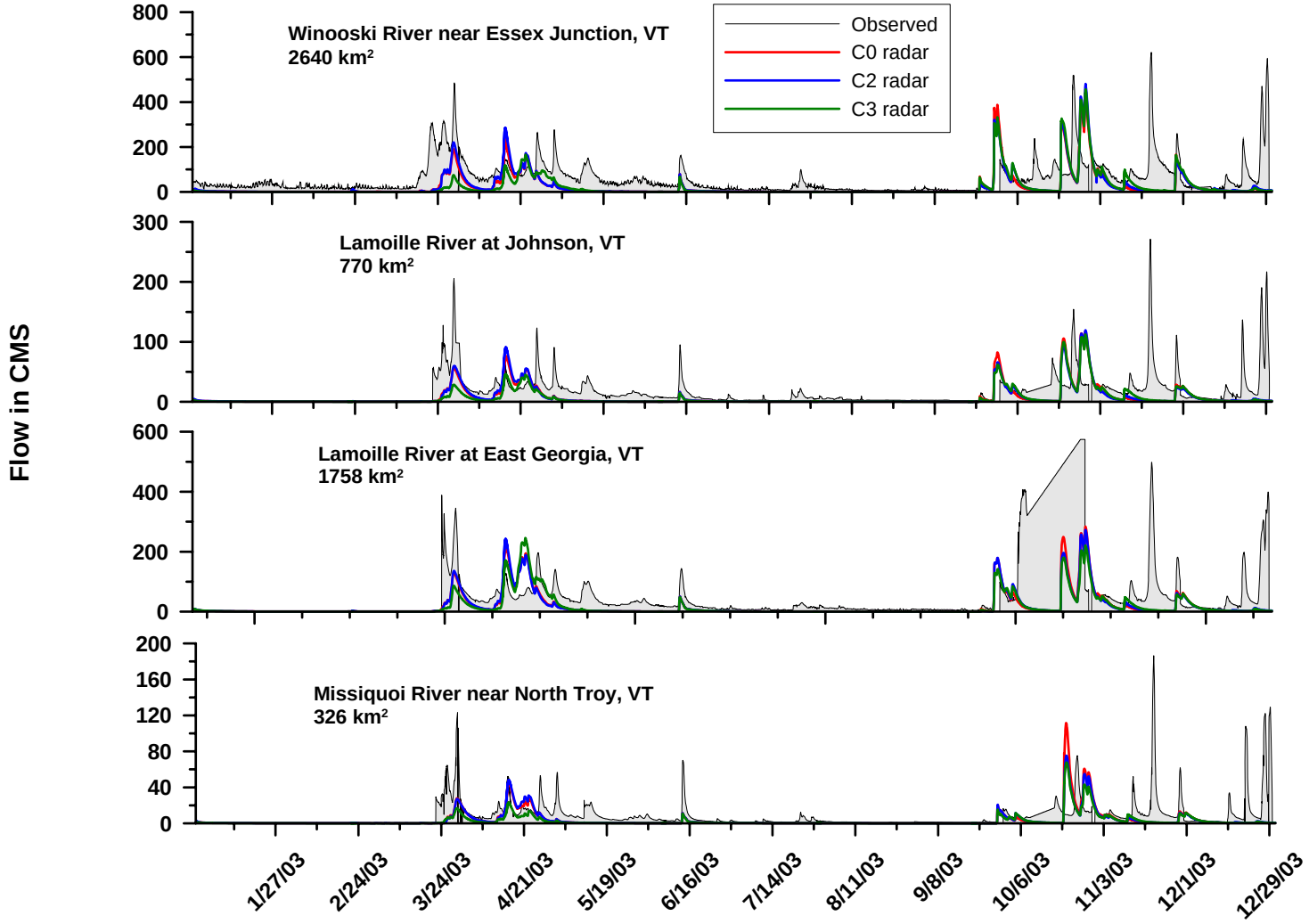

Figure C.23- Lake Champlain basin streamflows: January to December 2003 (continued)

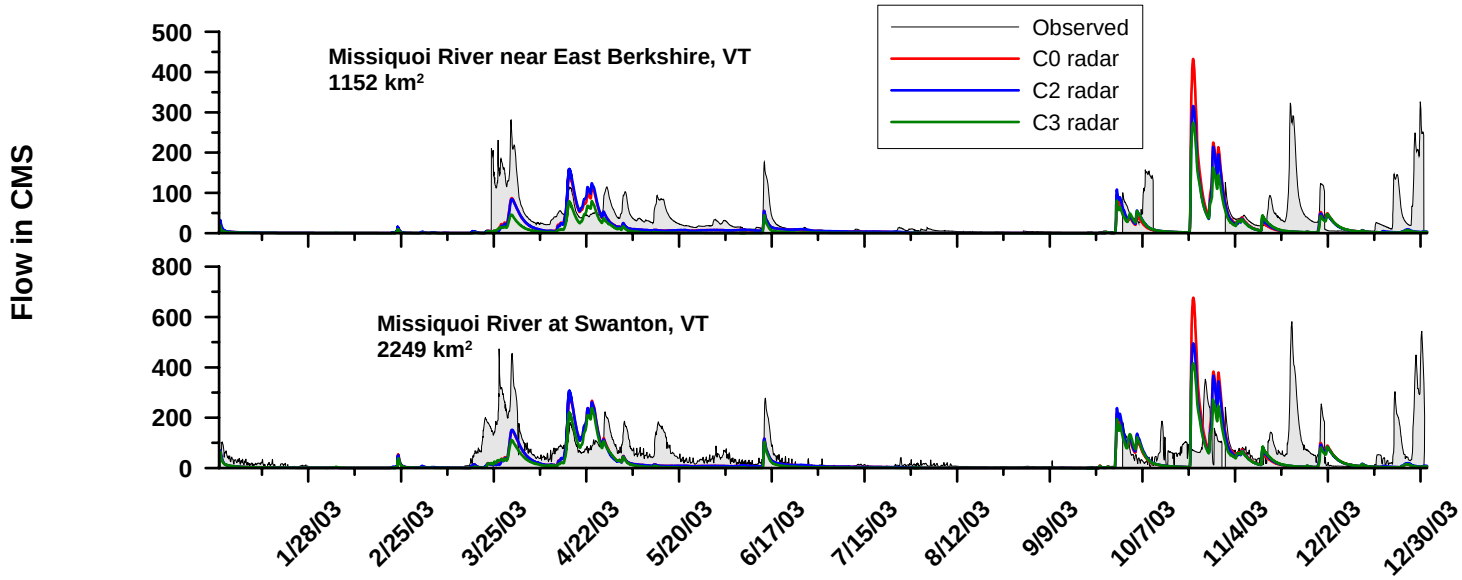

Figure C.24- Lake Champlain basin streamflows: January to December 2003 (continued)

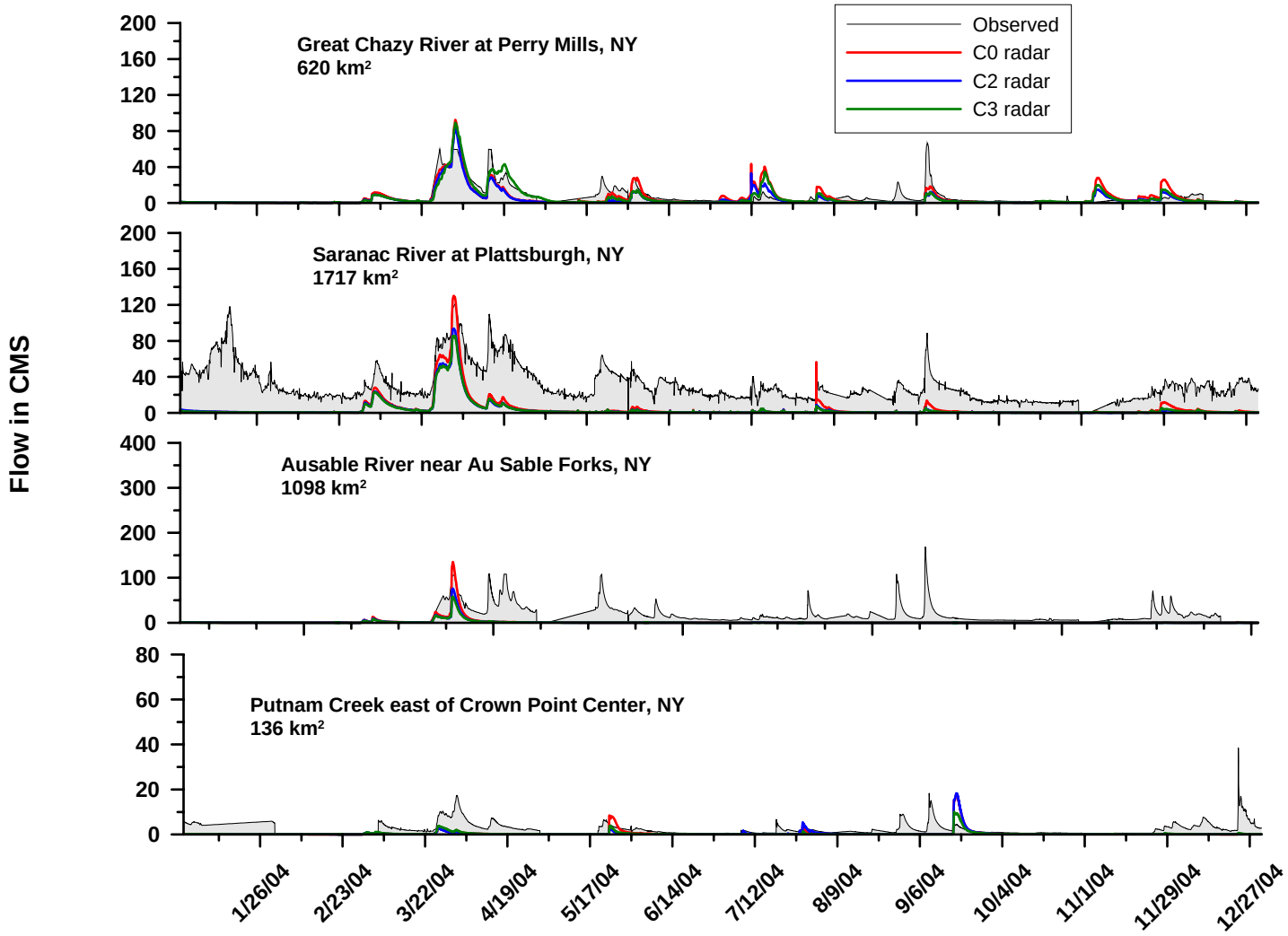

Figure C.25- Lake Champlain basin streamflows: January to December 2004

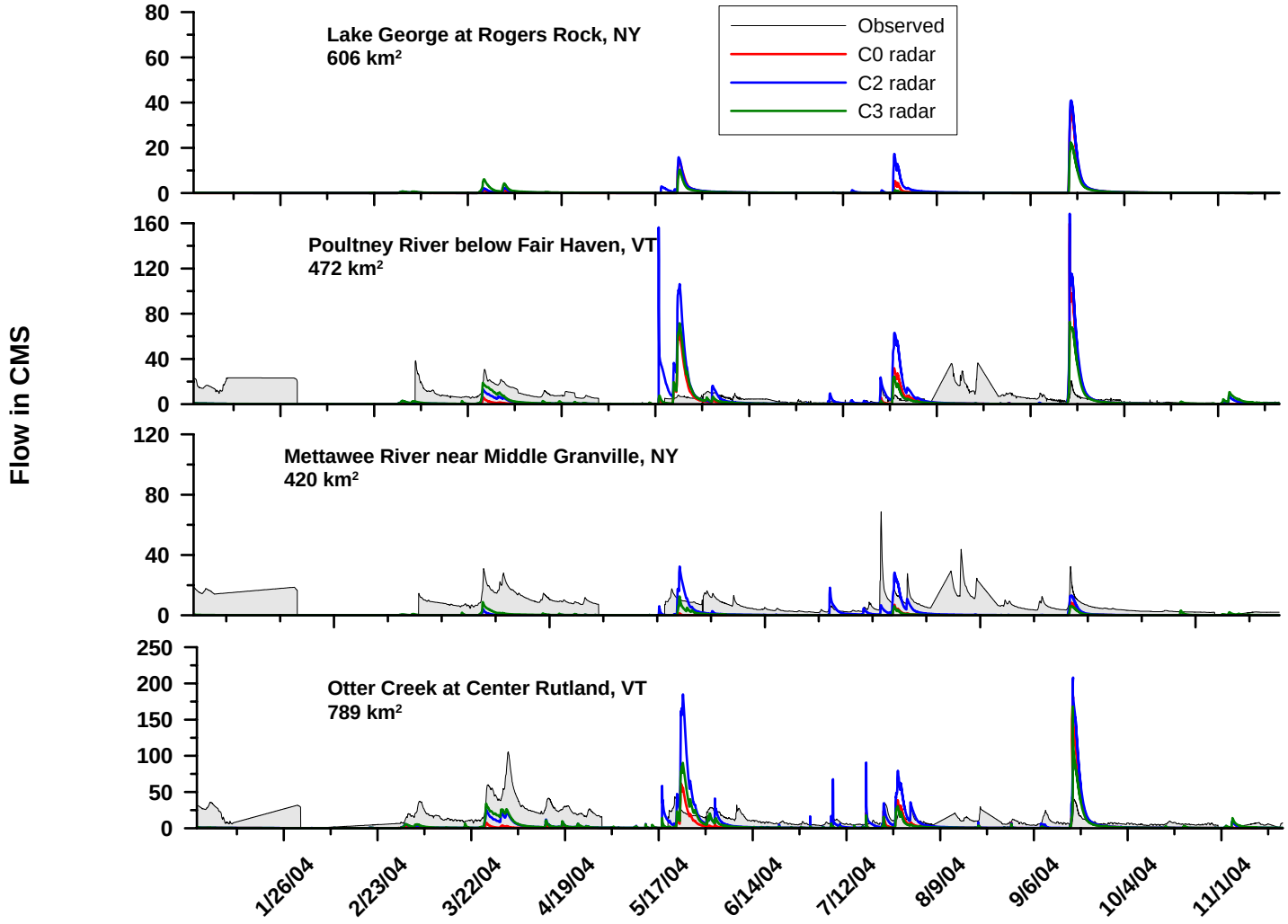

Figure C.26- Lake Champlain basin streamflows: January to December 2004 (continued)

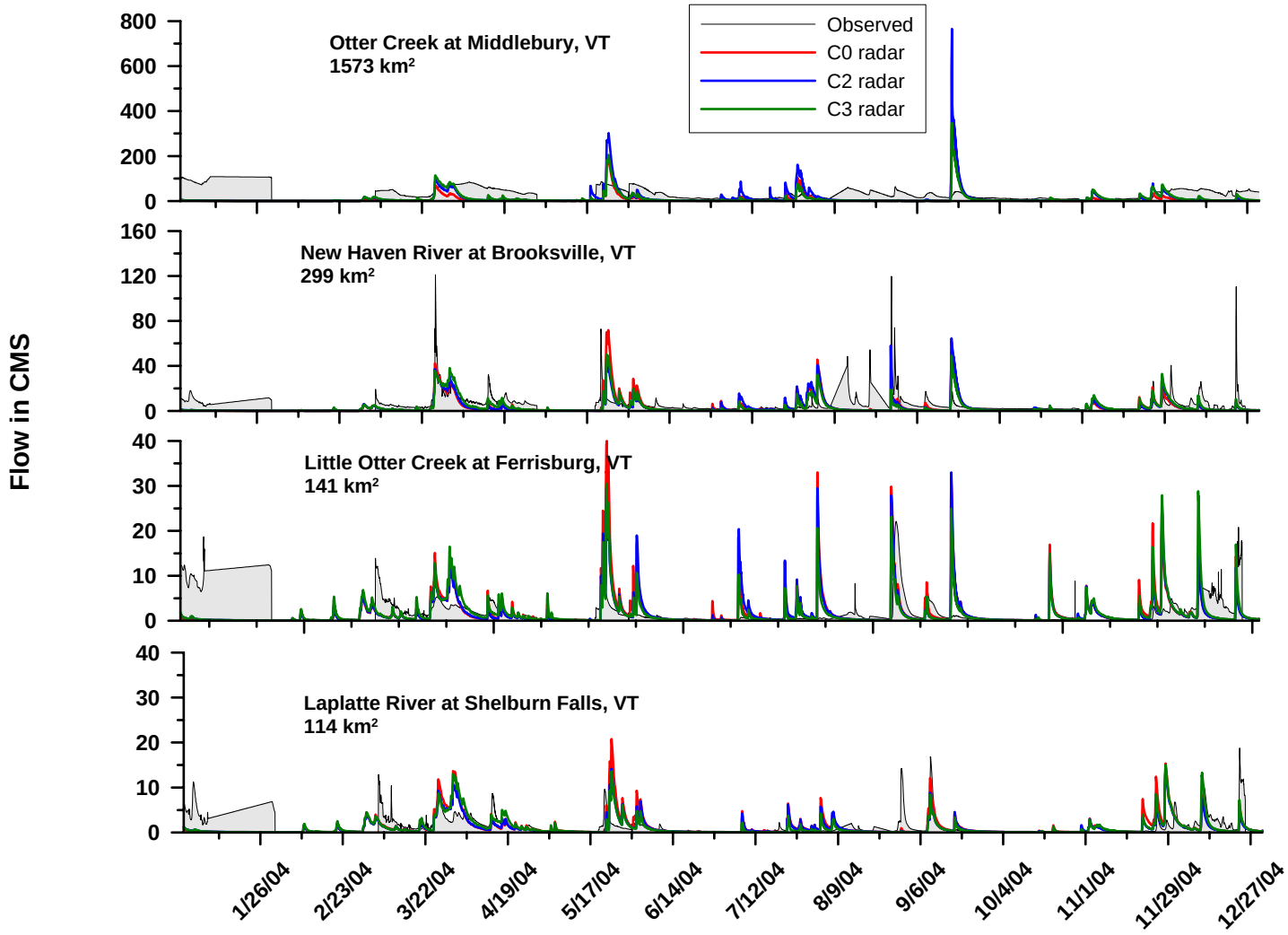

Figure C.27- Lake Champlain basin streamflows: January to December 2004 (continued)

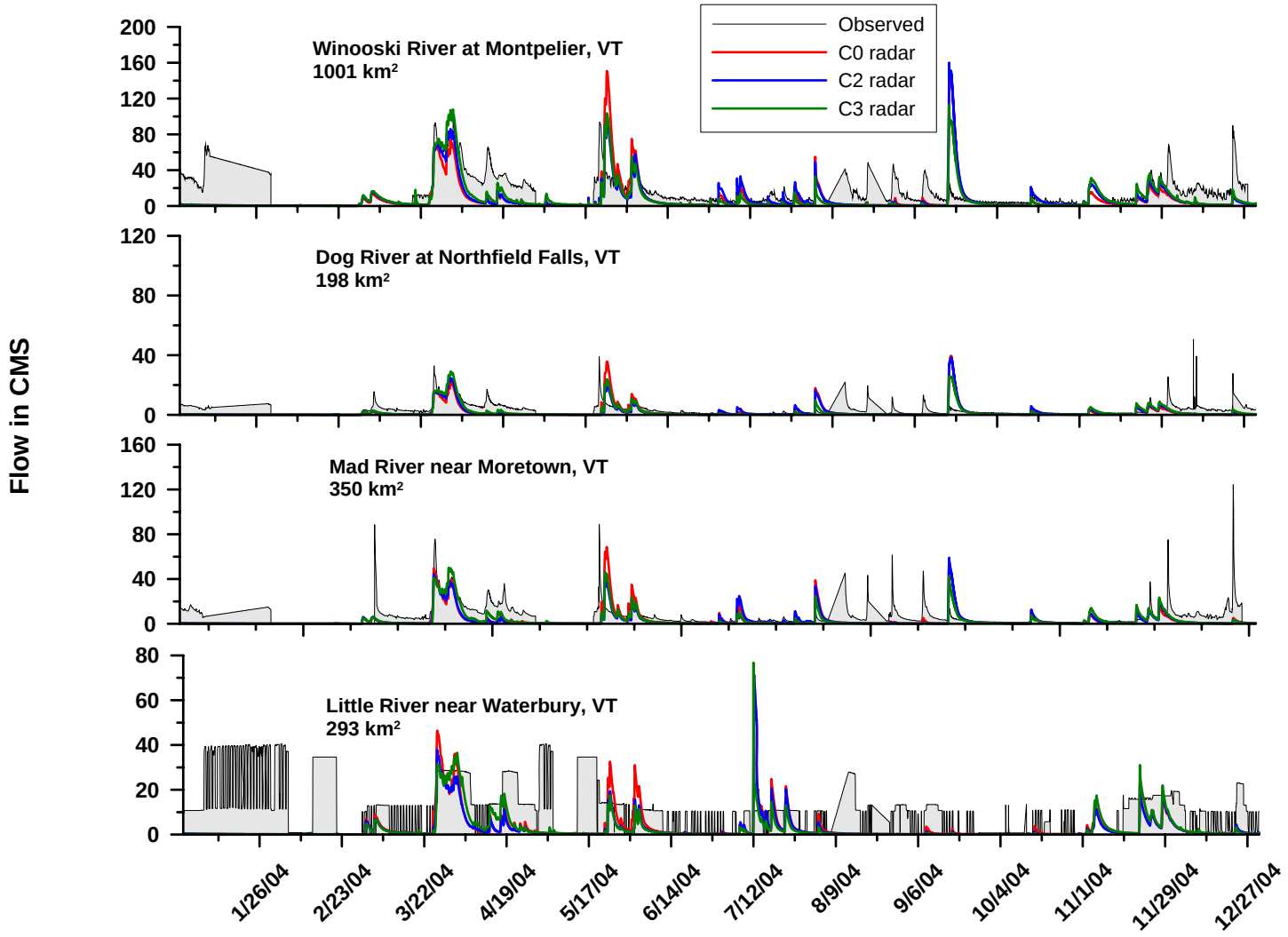

Figure C.28- Lake Champlain basin streamflows: January to December 2004 (continued)

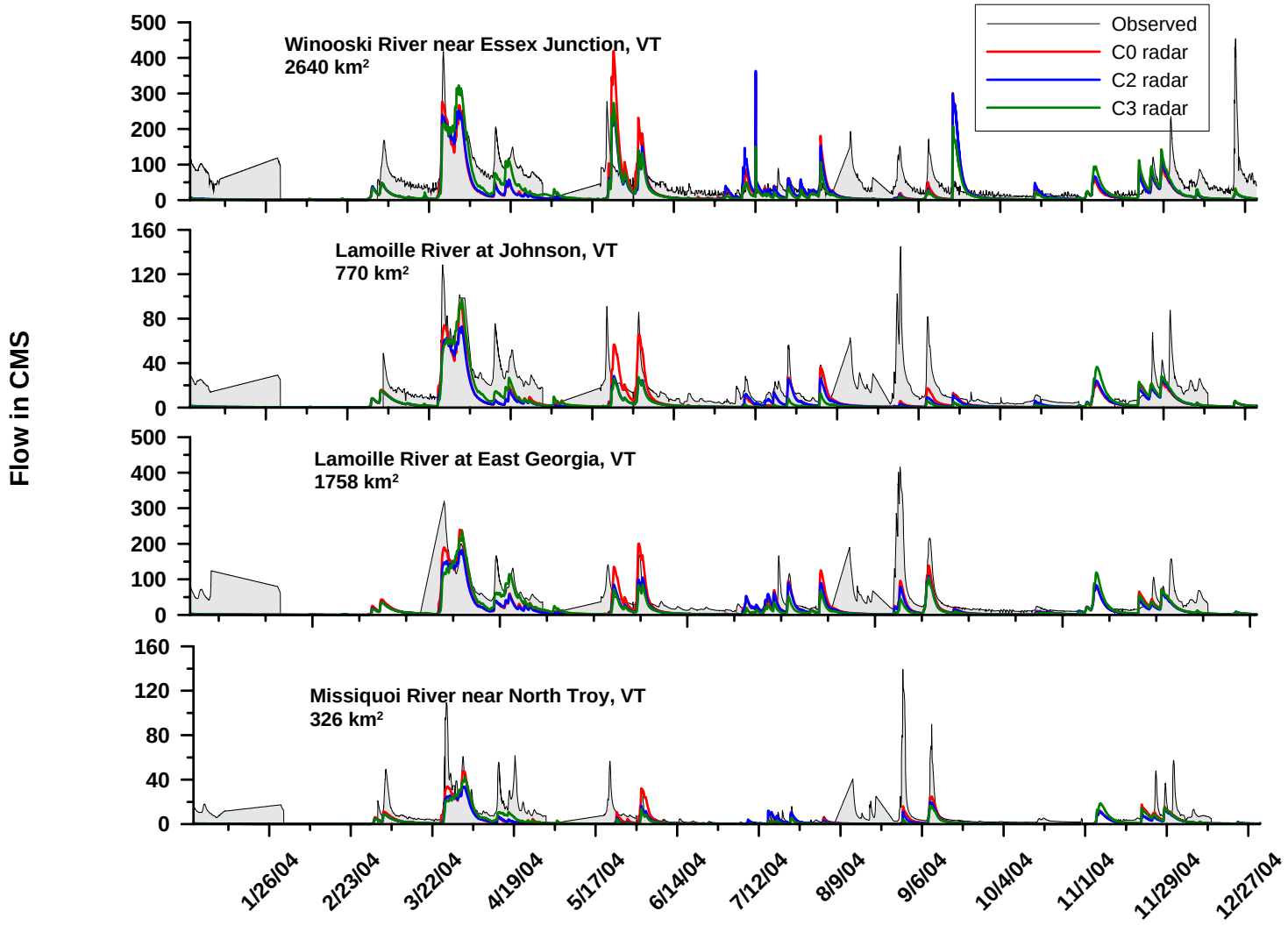

Figure C.29- Lake Champlain basin streamflows: January to December 2004 (continued)

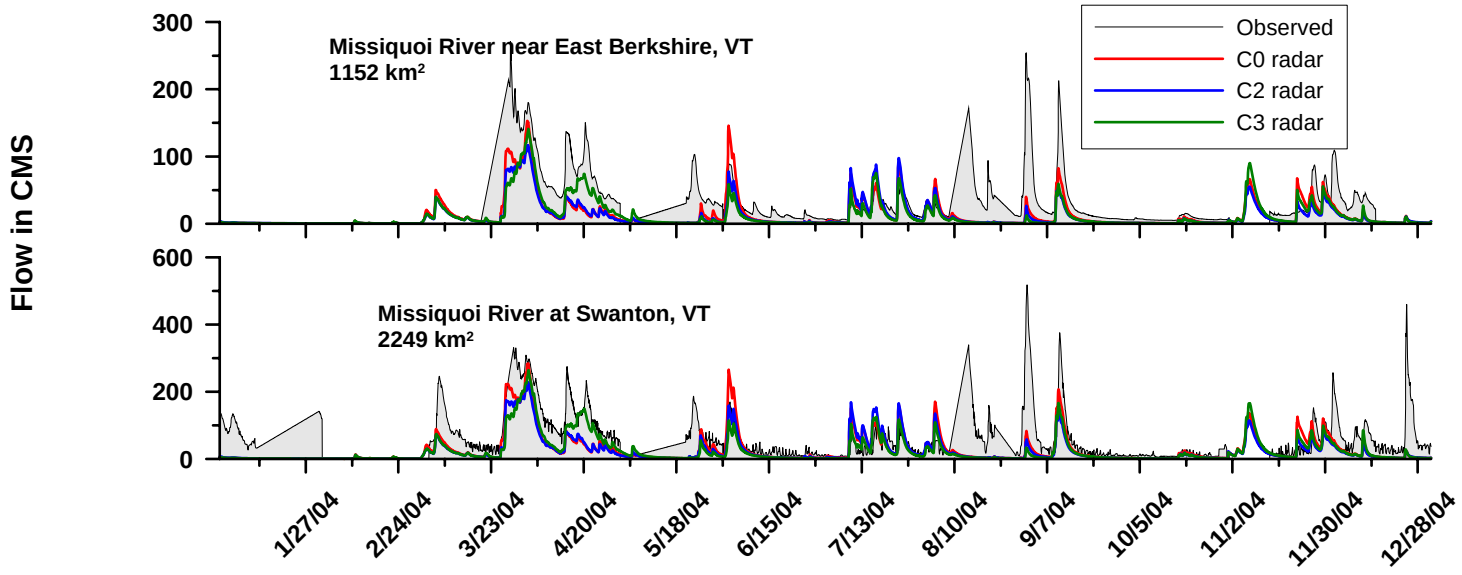

Figure C.30- Lake Champlain basin streamflows: January to December 2004 (continued)

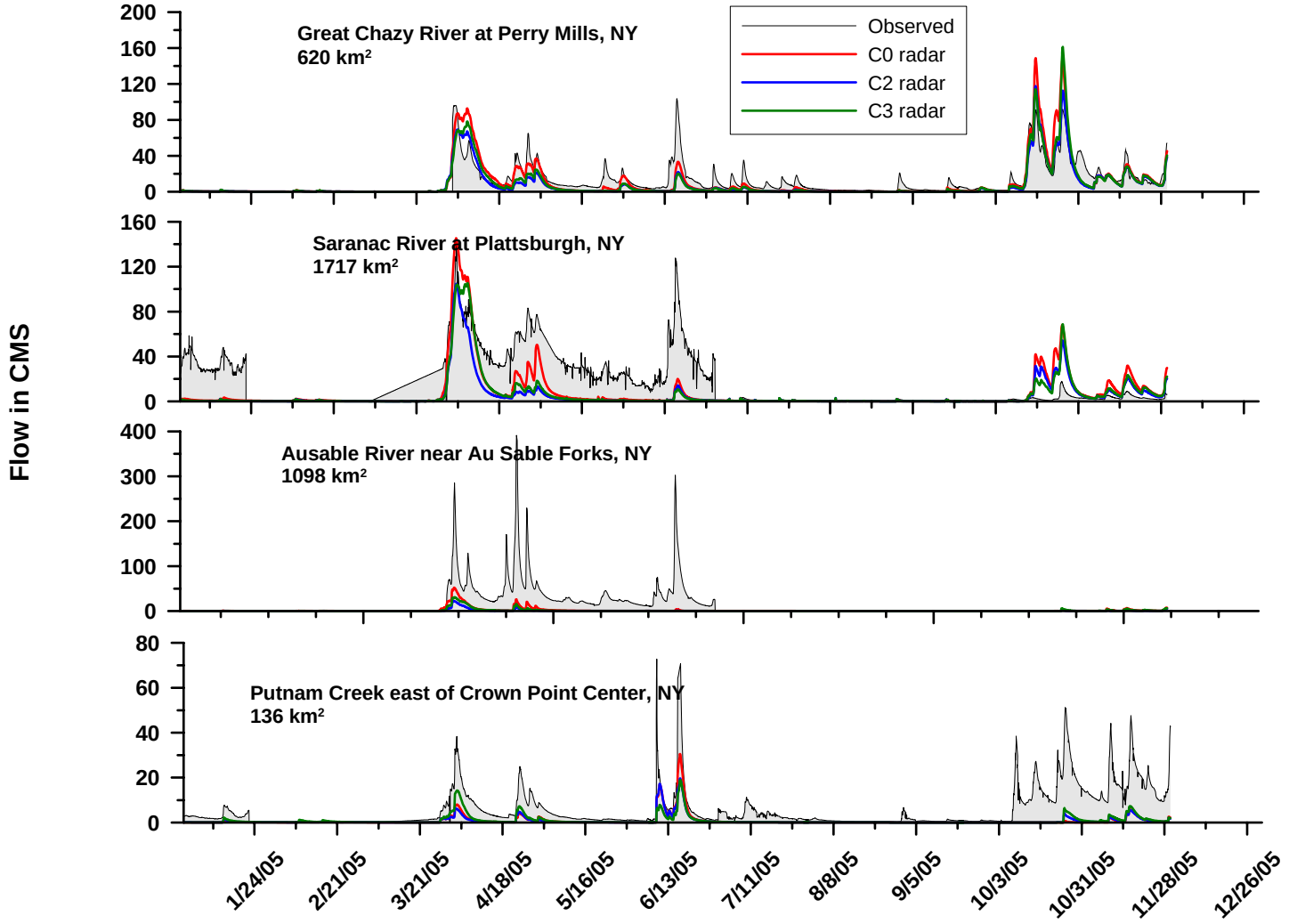

Figure C.31- Lake Champlain basin streamflows: January to December 2005

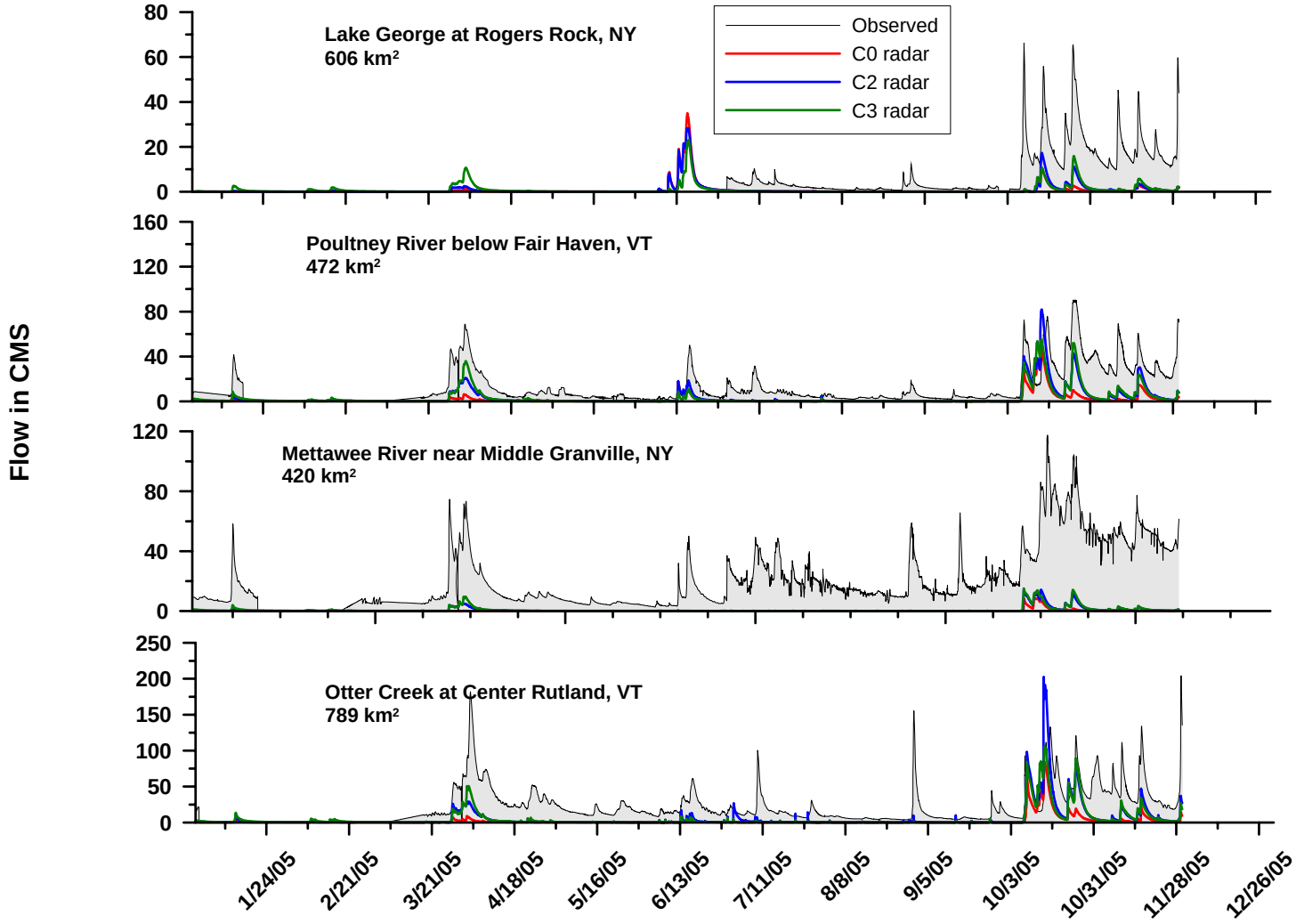

Figure C.32- Lake Champlain basin streamflows: January to December 2005 (continued)

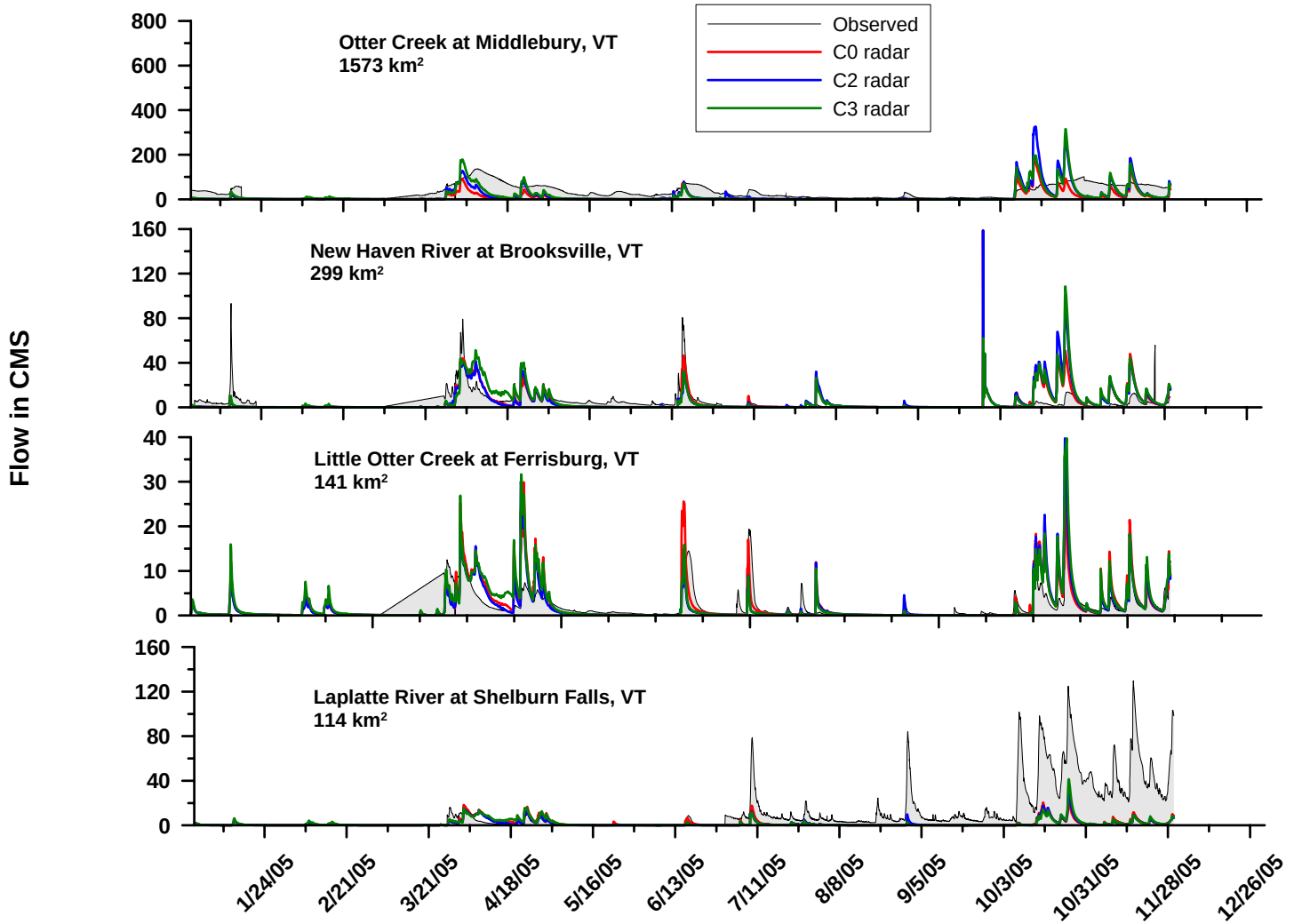

Figure C.33- Lake Champlain basin streamflows: January to December 2005 (continued)

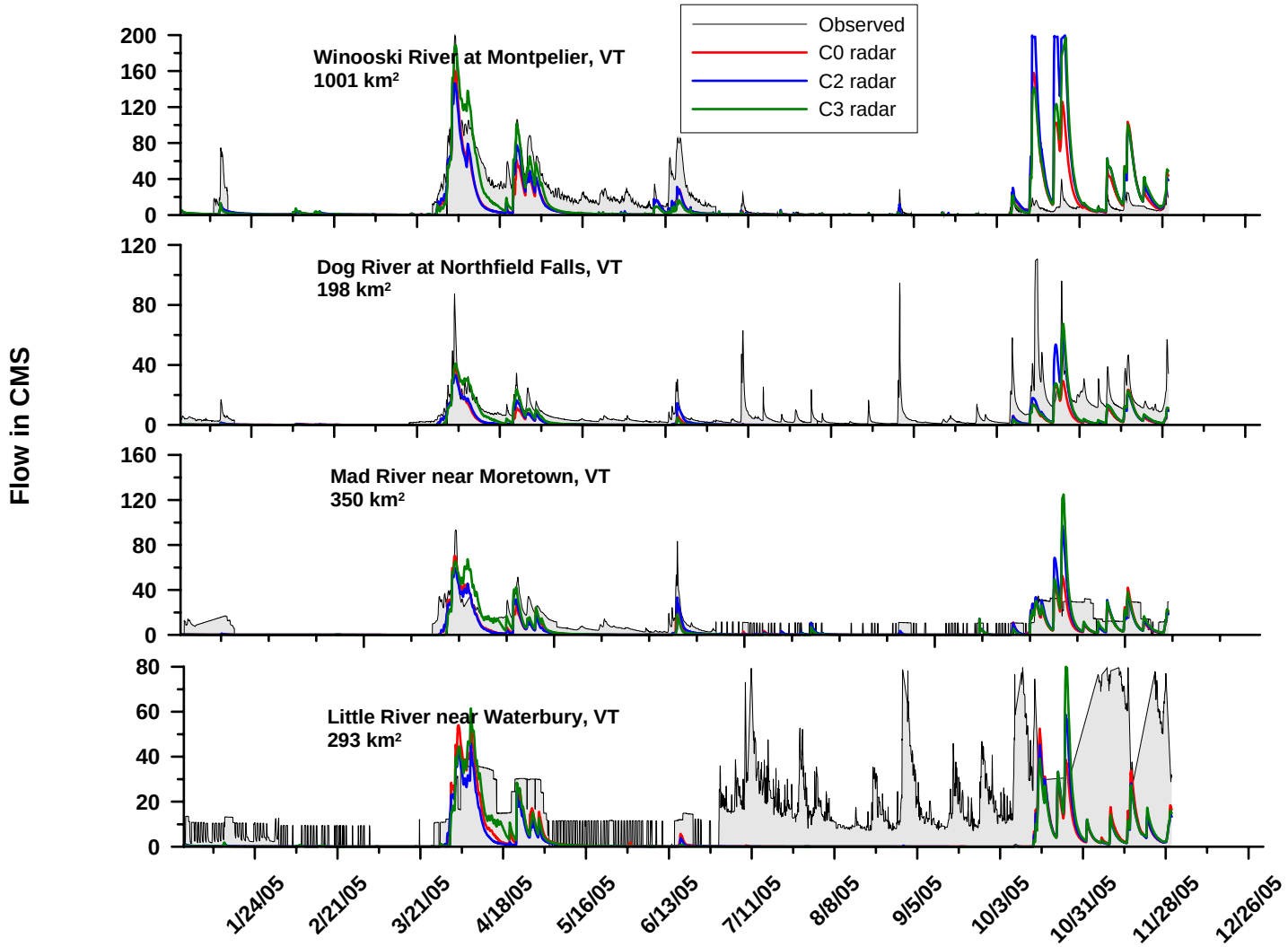

Figure C.34- Lake Champlain basin streamflows: January to December 2005 (continued)

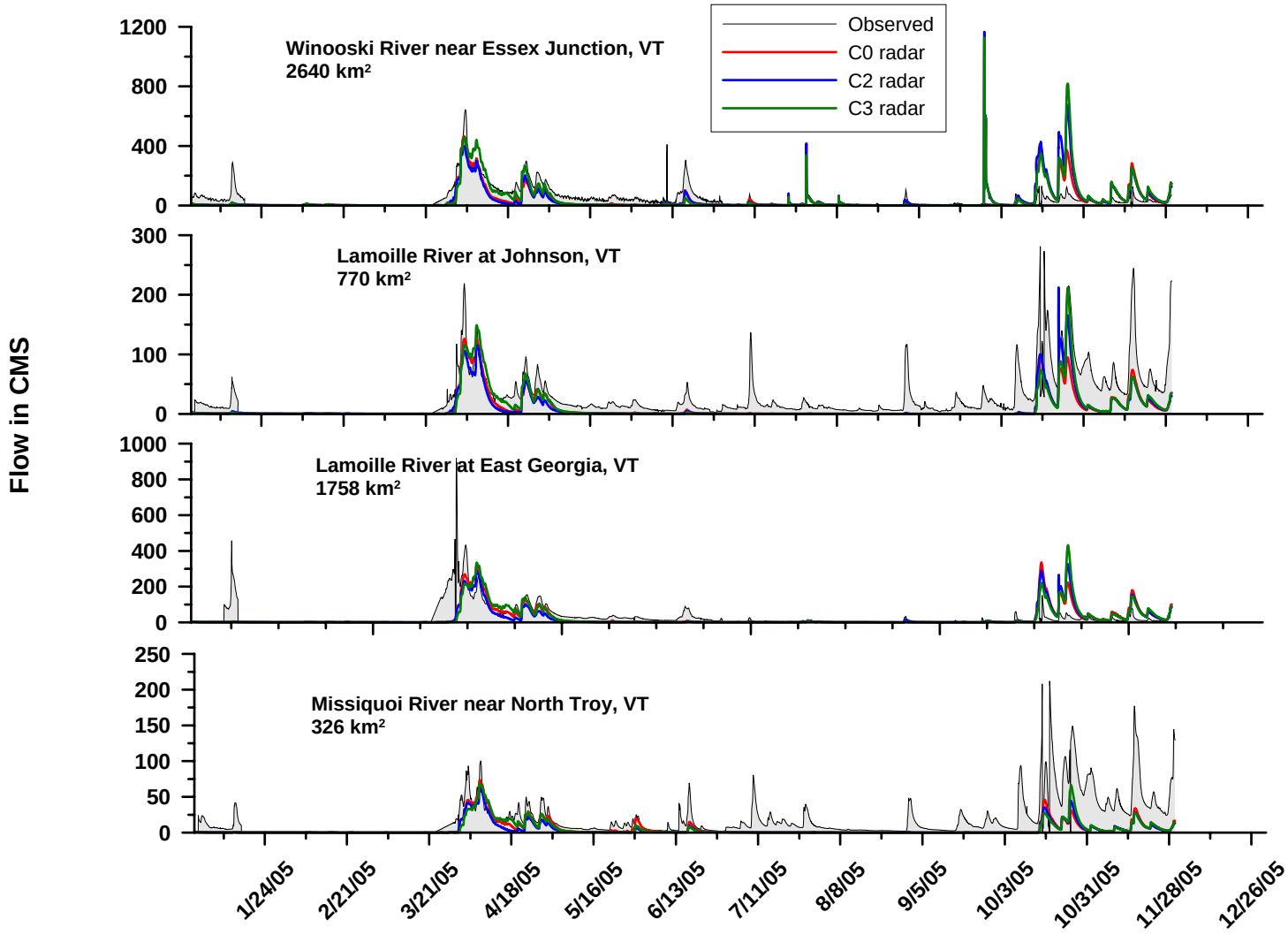

Figure C.35- Lake Champlain basin streamflows: January to December 2005 (continued)

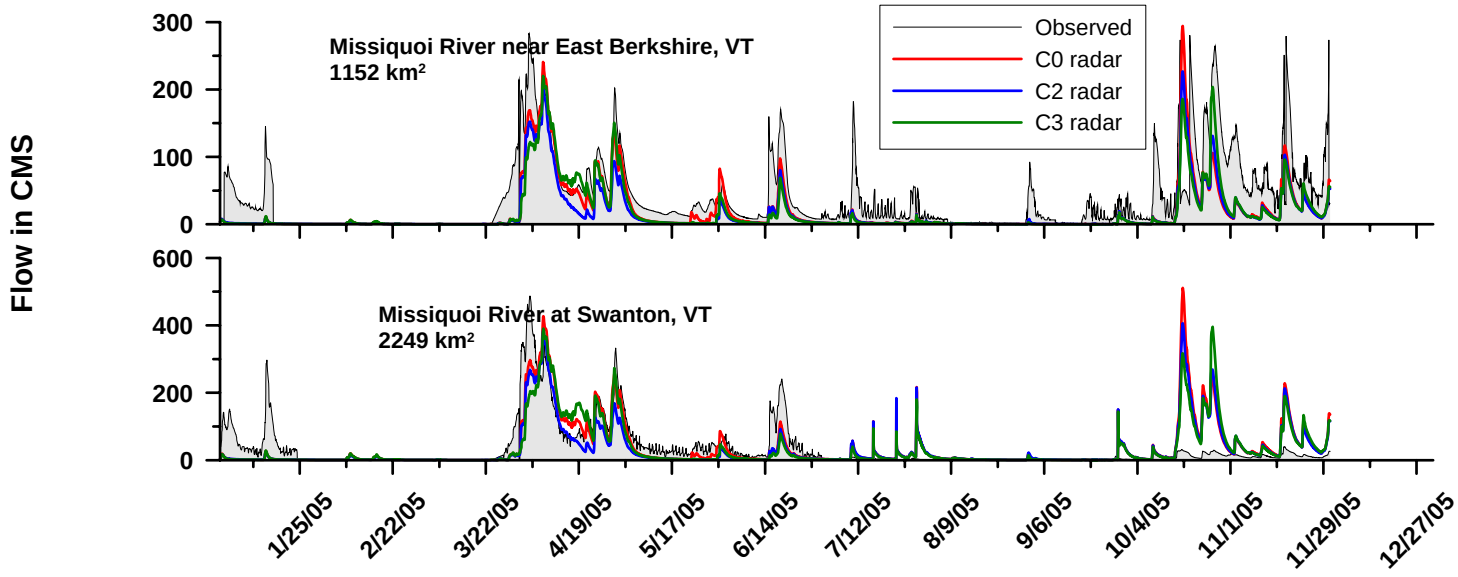

Figure C.36- Lake Champlain basin streamflows: January to December 2005 (continued)

Appendix D

Event Analysis

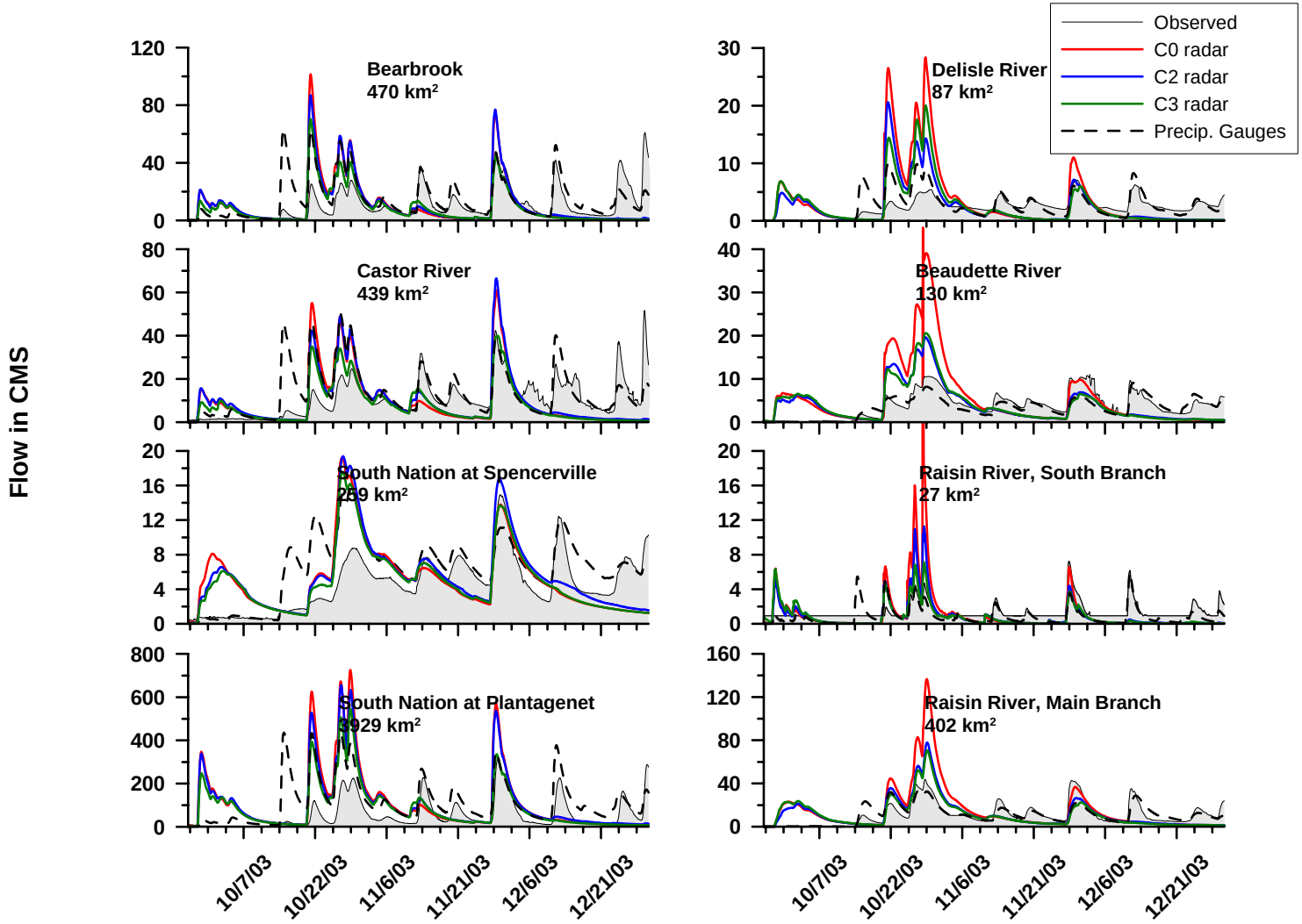

Figure D.1- Eastern Ontario, September 26th to December 31st 2003 (calibration period)

Table D.1- Statistical criteria for Eastern Ontario, September 26th to December 31st 2003 (calibration period)

	Statistical Criteria							
	Nash	R^2	RMSE	RMSE/qbar	%Dv	APB	Bias	MAE
	PRECIP. GAUGES							
Bearbrook	0.00	0.42	11.66	1.12	40.82	69.41	4.27	7.25
Castor	-0.28	0.34	10.00	0.94	26.68	56.38	2.85	6.01
SNC, Plantagenet	-0.86	0.49	96.03	1.72	110.76	117.39	61.72	65.42
SNC, Spencerville	-0.04	0.53	3.19	0.70	41.74	49.17	1.90	2.24
Beaudette	0.68	0.71	1.69	0.45	-13.14	31.13	-0.50	1.18
Delisle	-0.12	0.55	1.66	0.72	11.71	44.37	0.27	1.02
RR, S. Branch	0.07	0.45	0.96	0.71	-35.53	53.03	-0.48	0.72
RR, Main Branch	0.68	0.68	5.91	0.55	0.45	33.04	0.05	3.56
	C0 RADAR							
Bearbrook	-0.89	0.16	16.03	1.53	1.31	96.13	0.14	10.05
Castor	-0.82	0.18	11.94	1.12	-12.57	79.19	-1.34	8.45
SNC, Plantagenet	-2.84	0.27	137.84	2.47	97.15	154.18	54.14	85.92
SNC, Spencerville	-0.46	0.20	3.78	0.83	12.71	63.06	0.58	2.88
Beaudette	-3.90	0.32	6.63	1.75	43.22	111.53	1.64	4.22
Delisle	-10.12	0.15	5.22	2.28	44.97	139.53	1.03	3.20
RR, S. Branch	-5.63	0.23	2.55	1.89	-14.75	97.84	-0.20	1.33
RR, Main Branch	-1.96	0.40	17.95	1.67	39.12	105.41	4.21	11.35
	C2 RADAR							
Bearbrook	-0.65	0.18	14.98	1.43	1.47	91.59	0.15	9.57
Castor	-0.61	0.22	11.23	1.05	-9.09	76.37	-0.97	8.15
SNC, Plantagenet	-2.06	0.29	123.18	2.21	90.55	141.92	50.46	79.09
SNC, Spencerville	-0.31	0.31	3.59	0.79	20.13	59.49	0.92	2.71
Beaudette	-0.55	0.27	3.73	0.98	2.90	78.60	0.11	2.98
Delisle	-3.93	0.12	3.48	1.52	8.45	102.82	0.19	2.36
RR, S. Branch	-1.13	0.29	1.45	1.07	-36.10	77.97	-0.49	1.06
RR, Main Branch	-0.11	0.39	10.97	1.02	7.24	77.82	0.78	8.38
	C3 RADAR							
Bearbrook	-0.27	0.15	13.12	1.26	-17.77	79.32	-1.86	8.29
Castor	-0.24	0.19	9.85	0.92	-27.05	63.88	-2.89	6.81
SNC, Plantagenet	-0.91	0.27	97.15	1.74	59.63	117.27	33.23	65.35
SNC, Spencerville	-0.16	0.27	3.38	0.74	7.95	56.49	0.36	2.58
Beaudette	-0.68	0.25	3.88	1.03	4.41	82.38	0.17	3.12
Delisle	-4.23	0.12	3.58	1.56	12.76	110.14	0.29	2.52
RR, S. Branch	-0.71	0.23	1.30	0.96	-41.49	73.15	-0.56	0.99
RR, Main Branch	-0.13	0.31	11.08	1.03	1.98	78.24	0.21	8.42

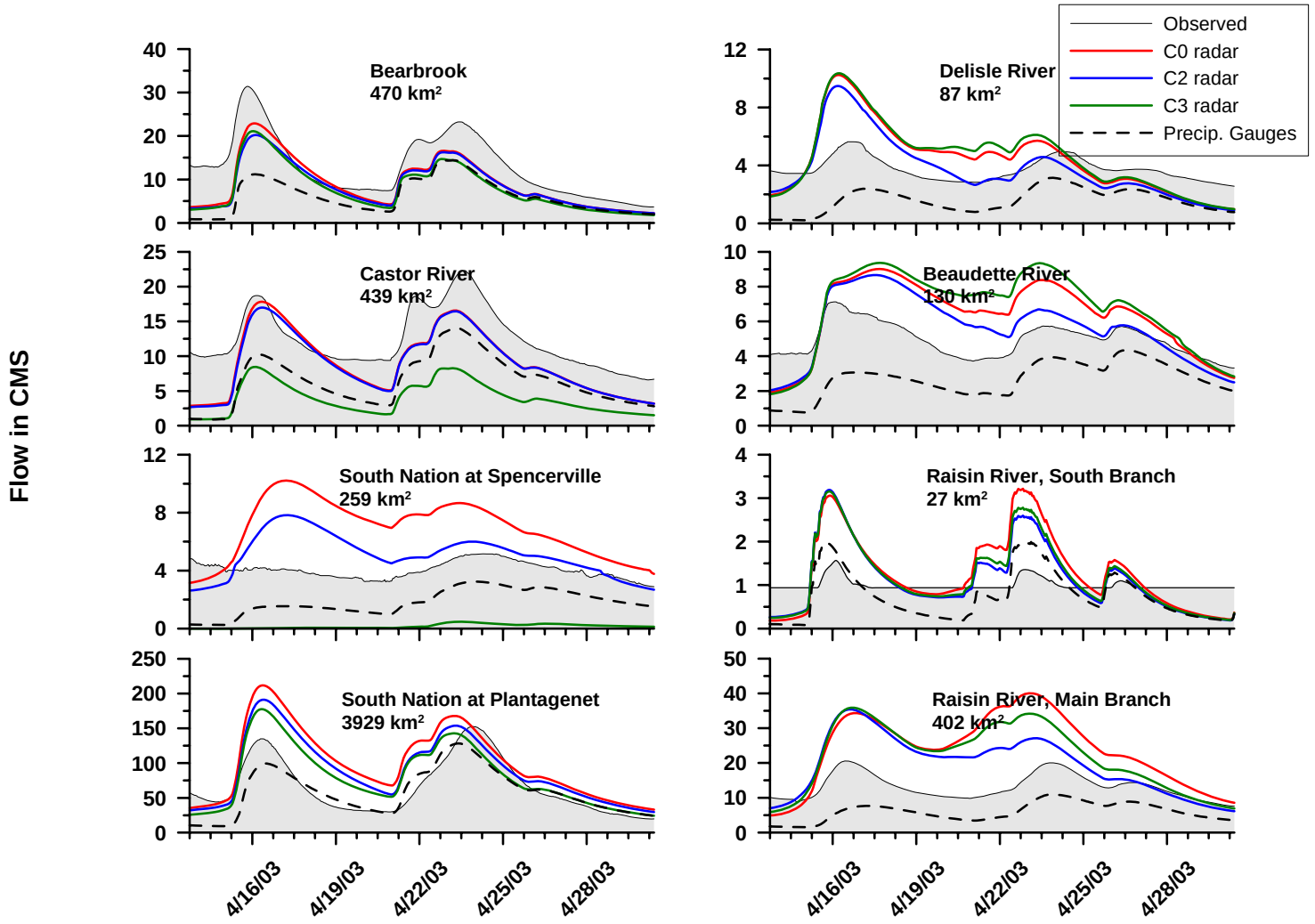

Figure D.2- Eastern Ontario, April 14th to May 1st 2003

Table D.2- Statistical criteria for Eastern Ontario,, April 14th to May 1st 2003

	Statistical Criteria							
	Nash	R^2	RMSE	RMSE/qbar	%Dv	APB	Bias	MAE
	PRECIP. GAUGES							
Bearbrook	-0.37	0.60	8.23	0.64	-52.09	52.09	-6.75	6.75
Castor	-1.25	0.79	6.23	0.50	-47.77	47.77	-5.94	5.94
SNC, Plantagenet	0.69	0.72	21.59	0.32	-11.06	24.25	-7.37	16.16
SNC, Spencerville	-16.15	0.27	2.34	0.58	-54.90	54.90	-2.22	2.22
Beaudette	-5.48	0.30	2.42	0.49	-45.32	45.32	-2.25	2.25
Delisle	-7.43	0.40	2.23	0.60	-57.12	57.12	-2.12	2.12
RR, S. Branch	-13.57	0.62	0.52	0.52	-24.63	44.91	-0.25	0.45
RR, Main Branch	-3.47	0.58	7.52	0.57	-54.34	54.34	-7.16	7.16
	C0 RADAR							
Bearbrook	0.48	0.77	5.06	0.39	-29.16	31.26	-3.78	4.05
Castor	0.08	0.73	3.99	0.32	-25.94	28.40	-3.23	3.53
SNC, Plantagenet	-0.40	0.63	45.69	0.69	51.62	55.30	34.39	36.85
SNC, Spencerville	-37.07	0.04	3.48	0.86	72.17	75.59	2.92	3.06
Beaudette	-3.73	0.50	2.07	0.42	28.77	36.98	1.43	1.83
Delisle	-6.03	0.45	2.03	0.55	20.30	46.20	0.76	1.72
RR, S. Branch	-35.32	0.57	0.82	0.82	30.07	63.67	0.30	0.64
RR, Main Branch	-13.42	0.49	13.50	1.03	83.86	87.62	11.04	11.54
	C2 RADAR							
Bearbrook	0.37	0.76	5.57	0.43	-33.29	33.90	-4.31	4.39
Castor	0.03	0.74	4.09	0.33	-27.50	29.07	-3.42	3.62
SNC, Plantagenet	0.14	0.66	35.68	0.54	36.16	43.98	24.09	29.30
SNC, Spencerville	-8.54	0.05	1.74	0.43	26.10	33.60	1.06	1.36
Beaudette	-1.37	0.57	1.47	0.30	14.48	24.40	0.72	1.21
Delisle	-3.47	0.56	1.62	0.44	2.37	34.50	0.09	1.28
RR, S. Branch	-24.85	0.64	0.69	0.69	15.25	54.30	0.15	0.54
RR, Main Branch	-5.39	0.52	8.98	0.68	50.04	54.26	6.59	7.14
	C3 RADAR							
Bearbrook	0.26	0.79	6.05	0.47	-38.83	38.84	-5.03	5.03
Castor	-3.44	0.81	8.77	0.71	-67.91	67.91	-8.45	8.45
SNC, Plantagenet	0.43	0.66	29.16	0.44	21.63	36.55	14.42	24.35
SNC, Spencerville	-47.21	0.32	3.92	0.97	-96.10	96.10	-3.89	3.89
Beaudette	-6.29	0.40	2.57	0.52	37.49	45.53	1.86	2.26
Delisle	-7.08	0.42	2.18	0.59	25.30	49.64	0.94	1.85
RR, S. Branch	-27.27	0.62	0.72	0.72	19.59	56.70	0.20	0.57
RR, Main Branch	-9.59	0.49	11.56	0.88	68.59	71.38	9.03	9.40

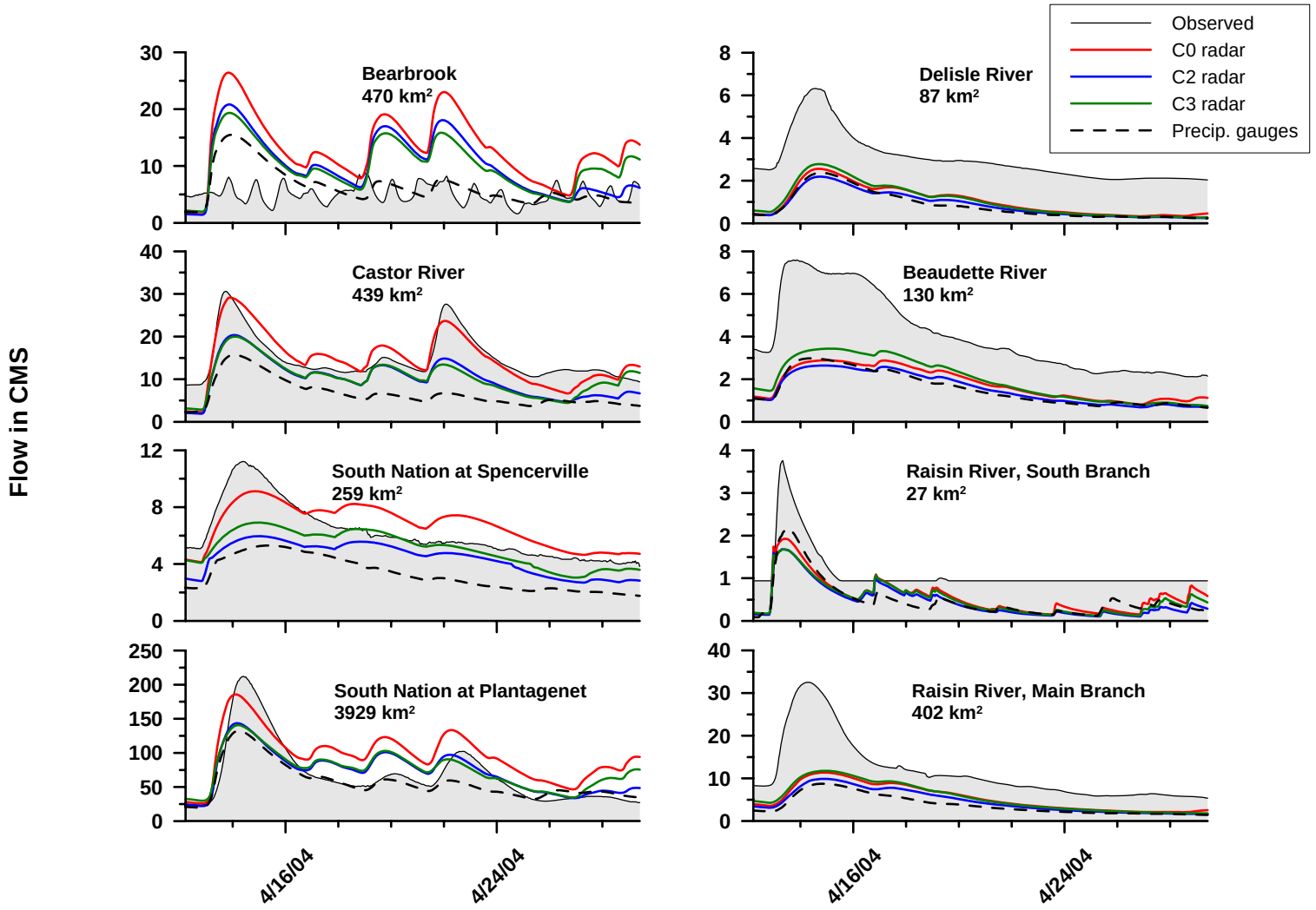

Figure D.3- Eastern Ontario, April 13th to April 30th 2004

Table D.3- Statistical criteria for Eastern Ontario, April 13th to April 30th 2004

	Statistical Criteria							
	Nash	R^2	RMSE	RMSE/qbar	%Dv	APB	Bias	MAE
	PRECIP. GAUGES							
Bearbrook	- Gauge malfunction -							
Castor	-1.94	0.51	8.96	0.60	-54.86	54.86	-8.17	8.17
SNC, Plantagenet	0.67	0.86	25.81	0.38	-16.87	24.39	-11.61	16.78
SNC, Spencerville	-1.53	0.82	3.08	0.50	-46.95	46.95	-2.91	2.91
Beaudette	-1.27	0.94	2.74	0.67	-61.85	61.85	-2.51	2.51
Delisle	-3.19	0.88	2.26	0.75	-72.51	72.51	-2.19	2.19
RR, S. Branch	-0.48	0.86	0.65	0.58	-55.05	55.07	-0.61	0.61
RR, Main Branch	-0.69	0.76	9.57	0.82	-67.33	67.33	-7.84	7.84
	C0 RADAR							
Bearbrook	- Gauge malfunction -							
Castor	0.71	0.78	2.80	0.19	-0.59	15.83	-0.09	2.36
SNC, Plantagenet	0.36	0.74	36.09	0.53	40.11	46.76	27.59	32.17
SNC, Spencerville	0.55	0.63	1.30	0.21	9.07	18.78	0.56	1.16
Beaudette	-0.98	0.82	2.56	0.63	-55.79	55.79	-2.27	2.27
Delisle	-2.52	0.83	2.07	0.69	-65.96	65.96	-2.00	2.00
RR, S. Branch	-0.34	0.68	0.61	0.55	-48.04	48.77	-0.54	0.54
RR, Main Branch	-0.19	0.70	8.03	0.69	-53.41	53.41	-6.22	6.22
	C2 RADAR							
Bearbrook	- Gauge malfunction -							
Castor	-0.12	0.69	5.54	0.37	-31.71	31.71	-4.72	4.72
SNC, Plantagenet	0.70	0.75	24.69	0.36	5.88	27.08	4.05	18.63
SNC, Spencerville	-0.26	0.63	2.17	0.35	-28.65	28.65	-1.77	1.77
Beaudette	-1.31	0.86	2.76	0.68	-61.49	61.49	-2.50	2.50
Delisle	-3.11	0.84	2.24	0.74	-71.21	71.21	-2.15	2.15
RR, S. Branch	-0.85	0.67	0.72	0.65	-58.77	59.13	-0.65	0.66
RR, Main Branch	-0.43	0.69	8.80	0.76	-60.07	60.07	-6.99	6.99
	C3 RADAR							
Bearbrook	- Gauge malfunction -							
Castor	-0.16	0.56	5.62	0.38	-29.79	30.64	-4.44	4.56
SNC, Plantagenet	0.63	0.71	27.58	0.40	10.08	32.41	6.93	22.30
SNC, Spencerville	0.33	0.67	1.59	0.26	-17.36	17.95	-1.08	1.11
Beaudette	-0.61	0.88	2.30	0.57	-51.44	51.44	-2.09	2.09
Delisle	-2.35	0.87	2.02	0.67	-64.93	64.93	-1.96	1.96
RR, S. Branch	-0.65	0.63	0.68	0.61	-53.75	54.23	-0.60	0.60
RR, Main Branch	-0.13	0.72	7.83	0.67	-52.49	52.49	-6.11	6.11

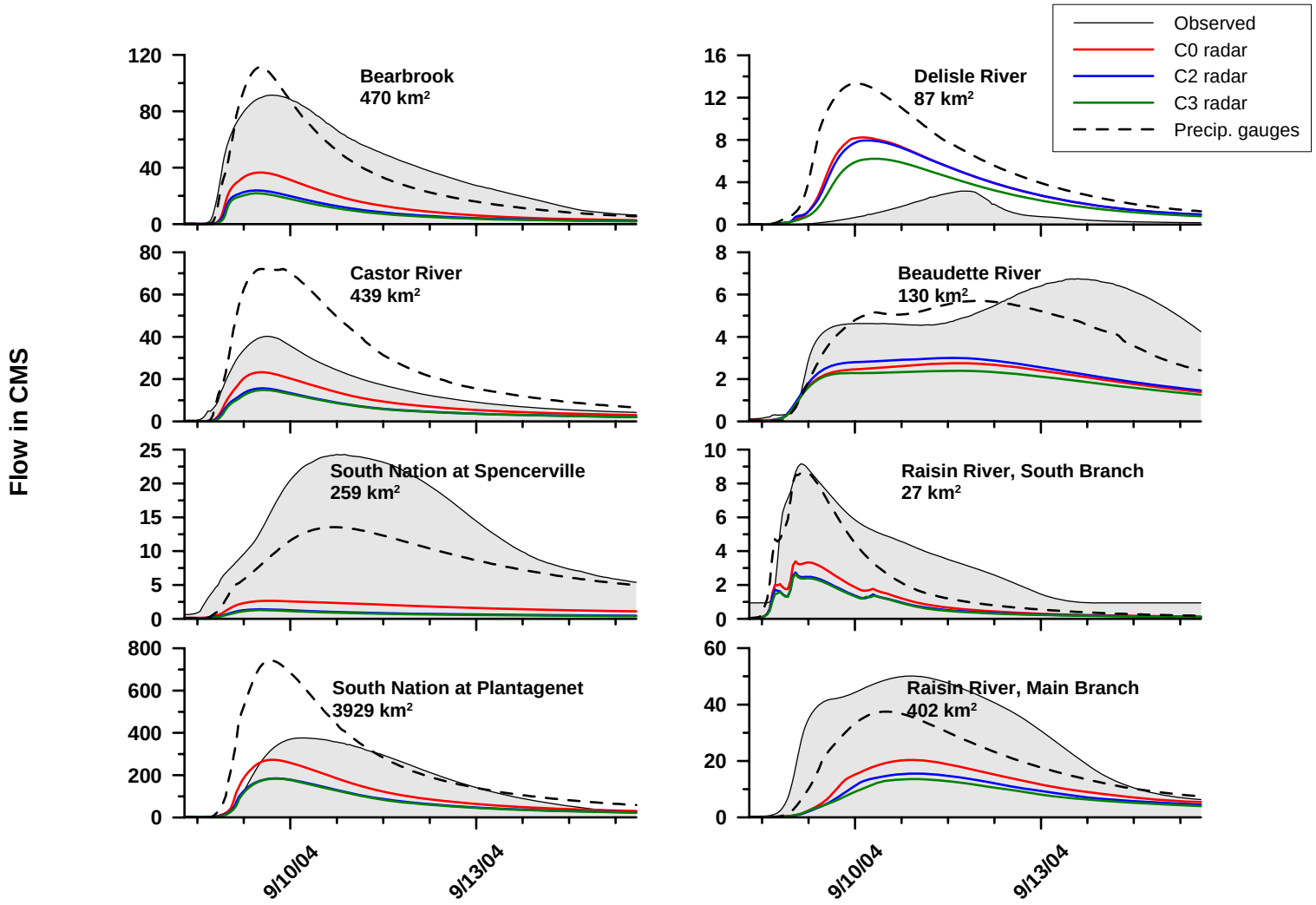

Figure D.4- Eastern Ontario, September 9th to September 16th 2004

Table D.4- Statistical criteria for Eastern Ontario, September 9th to September 16th 2004

	Statistical Criteria							
	Nash	**R^2**	**RMSE**	**RMSE/qbar**	**%Dv**	**APB**	**Bias**	**MAE**
	PRECIP. GAUGES							
Bearbrook	0.84	0.90	11.52	0.29	-16.16	24.49	-6.46	9.79
Castor	-1.19	0.97	17.03	1.10	81.74	83.13	12.66	12.87
SNC, Plantagenet	-0.57	0.65	159.95	0.92	46.77	50.88	81.04	88.16
SNC, Spencerville	0.10	0.92	6.86	0.49	-40.72	40.72	-5.71	5.71
Beaudette	0.41	0.59	1.40	0.30	-15.50	23.22	-0.74	1.10
Delisle	-36.37	0.23	5.89	6.32	482.78	482.78	4.50	4.50
RR, S. Branch	0.65	0.87	1.44	0.45	-35.95	38.81	-1.14	1.23
RR, Main Branch	0.46	0.87	12.49	0.43	-34.60	35.36	-10.00	10.22
	C0 RADAR							
Bearbrook	-0.32	0.93	33.01	0.83	-68.95	68.95	-27.55	27.55
Castor	0.48	0.98	8.30	0.54	-42.88	42.88	-6.64	6.64
SNC, Plantagenet	0.39	0.74	99.59	0.58	-40.63	44.00	-70.41	76.24
SNC, Spencerville	-2.76	0.64	14.03	1.00	-87.84	87.84	-12.31	12.31
Beaudette	-1.78	0.49	3.05	0.64	-57.06	57.24	-2.71	2.71
Delisle	-10.92	0.35	3.33	3.57	270.61	270.61	2.52	2.52
RR, S. Branch	-0.27	0.90	2.75	0.87	-71.30	71.46	-2.26	2.27
RR, Main Branch	-0.64	0.73	21.71	0.75	-62.56	62.56	-18.08	18.08
	C2 RADAR							
Bearbrook	-0.81	0.91	38.63	0.97	-79.56	79.56	-31.79	31.79
Castor	-0.09	0.97	12.01	0.78	-62.03	62.03	-9.60	9.60
SNC, Plantagenet	-0.05	0.76	130.94	0.76	-58.07	58.24	-100.63	100.93
SNC, Spencerville	-3.30	0.41	15.01	1.07	-94.60	94.60	-13.26	13.26
Beaudette	-1.52	0.44	2.90	0.61	-53.44	53.69	-2.53	2.55
Delisle	-10.05	0.38	3.20	3.43	264.07	264.07	2.46	2.46
RR, S. Branch	-0.55	0.89	3.04	0.96	-77.68	77.72	-2.47	2.47
RR, Main Branch	-1.06	0.70	24.32	0.84	-70.72	70.72	-20.44	20.44
	C3 RADAR							
Bearbrook	-0.92	0.90	39.77	1.00	-81.81	81.81	-32.69	32.69
Castor	-0.15	0.97	12.31	0.80	-63.41	63.41	-9.82	9.82
SNC, Plantagenet	-0.08	0.76	132.93	0.77	-59.35	59.35	-102.85	102.85
SNC, Spencerville	-3.35	0.41	15.10	1.08	-95.25	95.25	-13.35	13.35
Beaudette	-2.18	0.48	3.25	0.69	-61.48	61.64	-2.92	2.92
Delisle	-4.90	0.43	2.34	2.51	191.09	191.09	1.78	1.78
RR, S. Branch	-0.59	0.90	3.07	0.97	-78.69	78.69	-2.50	2.50
RR, Main Branch	-1.25	0.71	25.46	0.88	-74.31	74.31	-21.48	21.48

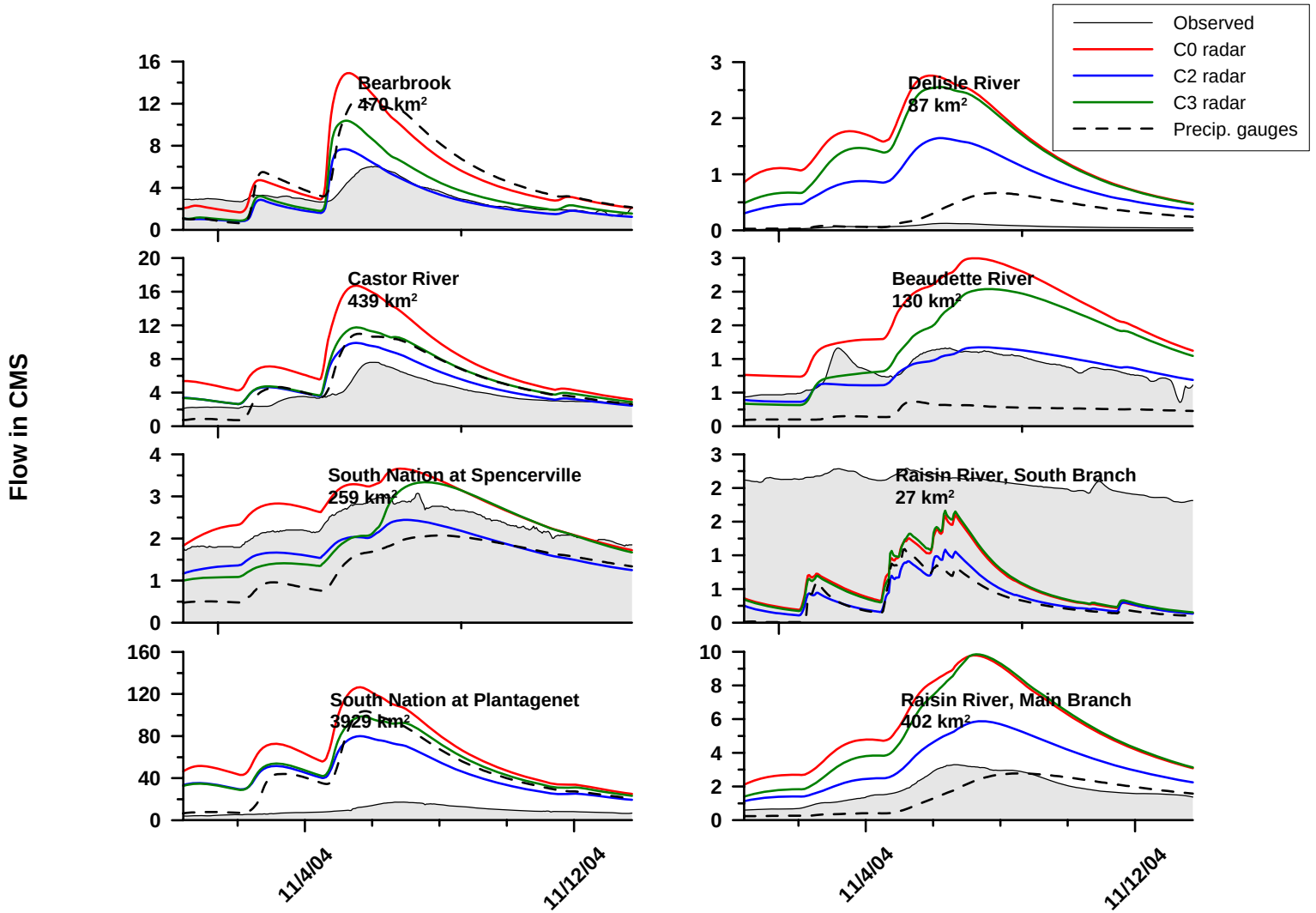

Figure D.5- Eastern Ontario, November 1st to November 13th 2004

Table D.5- Statistical criteria for Eastern Ontario, November 1st to November 13th 2004

	Statistical Criteria							
	Nash	**R^2**	**RMSE**	**RMSE/qbar**	**%Dv**	**APB**	**Bias**	**MAE**
	PRECIP. GAUGES							
Bearbrook	-7.23	0.69	3.44	1.12	73.10	92.59	2.24	2.83
Castor	-1.10	0.88	2.19	0.57	35.19	45.99	1.35	1.76
SNC, Plantagenet	-129.22	0.77	42.73	4.53	368.16	368.16	34.74	34.74
SNC, Spencerville	-5.73	0.50	0.99	0.43	-39.69	39.69	-0.92	0.92
Beaudette	-6.98	0.49	0.63	0.76	-72.94	72.94	-0.61	0.61
Delisle	-111.22	0.35	0.31	4.83	365.19	366.85	0.24	0.24
RR, S. Branch	- Gauge malfunction -							
RR, Main Branch	0.13	0.53	0.77	0.42	-20.57	34.42	-0.38	0.64
	C0 RADAR							
Bearbrook	-8.36	0.69	3.66	1.20	75.35	83.37	2.31	2.55
Castor	-8.91	0.77	4.75	1.24	101.60	101.60	3.89	3.89
SNC, Plantagenet	-259.66	0.44	60.45	6.41	576.76	576.76	54.43	54.43
SNC, Spencerville	-0.42	0.85	0.46	0.20	16.71	17.30	0.39	0.40
Beaudette	-14.41	0.73	0.88	1.06	95.01	95.01	0.79	0.79
Delisle	-	0.74	1.58	24.44	2230.22	2230.22	1.44	1.44
RR, S. Branch	- Gauge malfunction -							
RR, Main Branch	-23.08	0.94	4.03	2.18	201.94	201.94	3.73	3.73
	C2 RADAR							
Bearbrook	-0.02	0.64	1.21	0.40	-9.66	25.85	-0.30	0.79
Castor	-0.18	0.80	1.64	0.43	30.88	31.41	1.18	1.20
SNC, Plantagenet	-100.20	0.46	37.67	3.99	364.39	364.39	34.39	34.39
SNC, Spencerville	-1.12	0.92	0.56	0.24	-23.66	23.66	-0.55	0.55
Beaudette	0.49	0.62	0.16	0.19	-1.54	15.08	-0.01	0.13
Delisle	-924.92	0.93	0.90	13.86	1255.98	1255.98	0.81	0.81
RR, S. Branch	-	-	-	-	-	-	-	-
RR, Main Branch	-3.10	0.95	1.66	0.90	82.24	82.24	1.52	1.52
	C3 RADAR							
Bearbrook	-1.49	0.62	1.89	0.62	16.50	41.13	0.51	1.26
Castor	-1.79	0.85	2.52	0.66	51.52	51.52	1.97	1.97
SNC, Plantagenet	-158.87	0.65	47.34	5.02	452.63	452.63	42.72	42.72
SNC, Spencerville	-1.19	0.56	0.57	0.25	-9.67	21.28	-0.22	0.49
Beaudette	-6.22	0.56	0.60	0.72	51.15	61.45	0.43	0.51
Delisle	-	0.90	1.42	22.03	1968.72	1968.72	1.27	1.27
RR, S. Branch	- Gauge malfunction -							
RR, Main Branch	-20.26	0.96	3.79	2.05	182.02	182.02	3.36	3.36

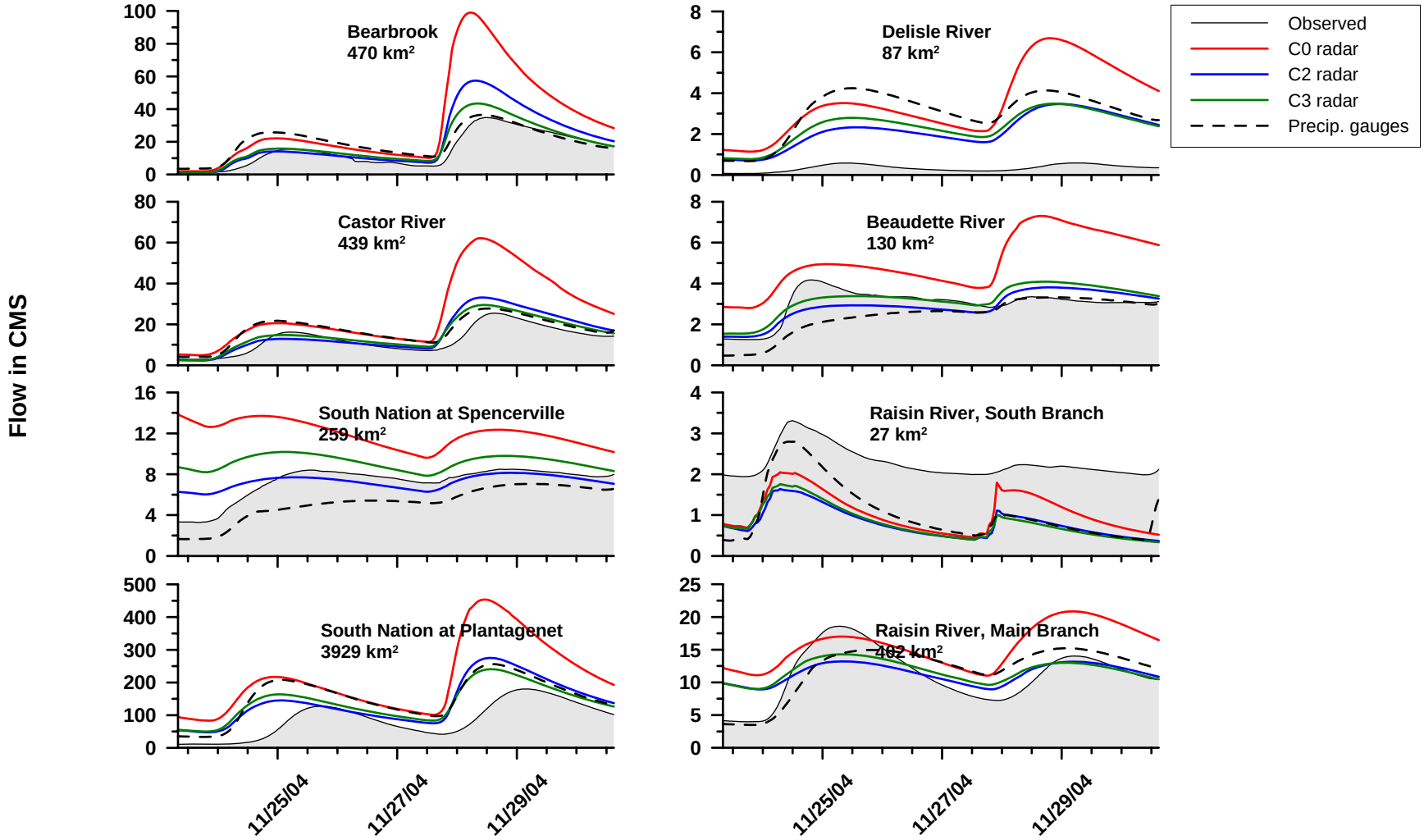

Figure D.6- Eastern Ontario, November 24th to December 6th 2004

Table D.6- Statistical criteria for Eastern Ontario, November 24th to December 6th 2004

	Statistical Criteria							
	Nash	R^2	RMSE	RMSE/qbar	%Dv	APB	Bias	MAE
	PRECIP. GAUGES							
Bearbrook	-0.25	0.54	8.90	0.62	43.49	46.09	6.25	6.62
Castor	-0.50	0.78	7.02	0.52	43.98	43.98	5.92	5.92
SNC, Plantagenet	-0.75	0.61	76.74	0.75	62.38	62.38	63.93	63.93
SNC, Spencerville	0.17	0.85	2.67	0.30	-26.30	26.32	-2.36	2.36
Beaudette	0.46	0.76	0.98	0.25	-18.36	19.06	-0.73	0.76
Delisle	-146.29	0.74	3.14	7.26	686.88	686.88	2.97	2.97
RR, S. Branch	-4.23	0.86	1.31	0.54	-52.76	52.76	-1.27	1.27
RR, Main Branch	0.71	0.77	3.61	0.25	-2.26	21.13	-0.32	3.00
	C0 RADAR							
Bearbrook	-5.17	0.71	19.79	1.38	69.67	78.90	10.01	11.34
Castor	-5.12	0.41	14.17	1.05	54.35	69.01	7.32	9.29
SNC, Plantagenet	-3.52	0.07	123.51	1.21	64.16	93.24	65.76	95.56
SNC, Spencerville	-1.86	0.32	4.96	0.55	12.21	49.23	1.10	4.42
Beaudette	-1.75	0.05	2.21	0.56	13.57	49.39	0.54	1.97
Delisle	-130.43	0.03	2.97	6.86	582.23	582.23	2.52	2.52
RR, S. Branch	-8.89	0.01	1.80	0.75	-68.35	68.35	-1.65	1.65
RR, Main Branch	-0.41	0.00	7.99	0.56	-7.38	45.59	-1.05	6.47
	C2 RADAR							
Bearbrook	-0.02	0.79	8.07	0.56	13.33	36.98	1.92	5.31
Castor	0.04	0.49	5.62	0.42	-2.78	32.99	-0.37	4.44
SNC, Plantagenet	-0.48	0.10	70.65	0.69	11.38	53.01	11.66	54.32
SNC, Spencerville	-1.19	0.10	4.34	0.48	-28.36	33.80	-2.54	3.03
Beaudette	-1.52	0.04	2.12	0.53	-34.11	39.90	-1.36	1.59
Delisle	-36.90	0.04	1.60	3.68	317.36	317.36	1.37	1.37
RR, S. Branch	-10.46	0.01	1.94	0.81	-75.82	75.82	-1.83	1.83
RR, Main Branch	-0.71	0.00	8.79	0.62	-33.20	42.58	-4.71	6.04
	C3 RADAR							
Bearbrook	0.58	0.76	5.15	0.36	0.24	27.57	0.03	3.96
Castor	0.18	0.45	5.19	0.39	-5.22	30.10	-0.70	4.05
SNC, Plantagenet	-0.42	0.06	69.27	0.68	9.61	52.87	9.85	54.18
SNC, Spencerville	-0.98	0.21	4.12	0.46	-11.61	36.37	-1.04	3.26
Beaudette	-1.40	0.08	2.07	0.52	-28.55	38.14	-1.14	1.52
Delisle	-43.04	0.02	1.72	3.97	343.16	343.16	1.49	1.49
RR, S. Branch	-10.39	0.01	1.93	0.80	-75.31	75.31	-1.81	1.81
RR, Main Branch	-0.75	0.01	8.91	0.63	-32.09	42.99	-4.56	6.10

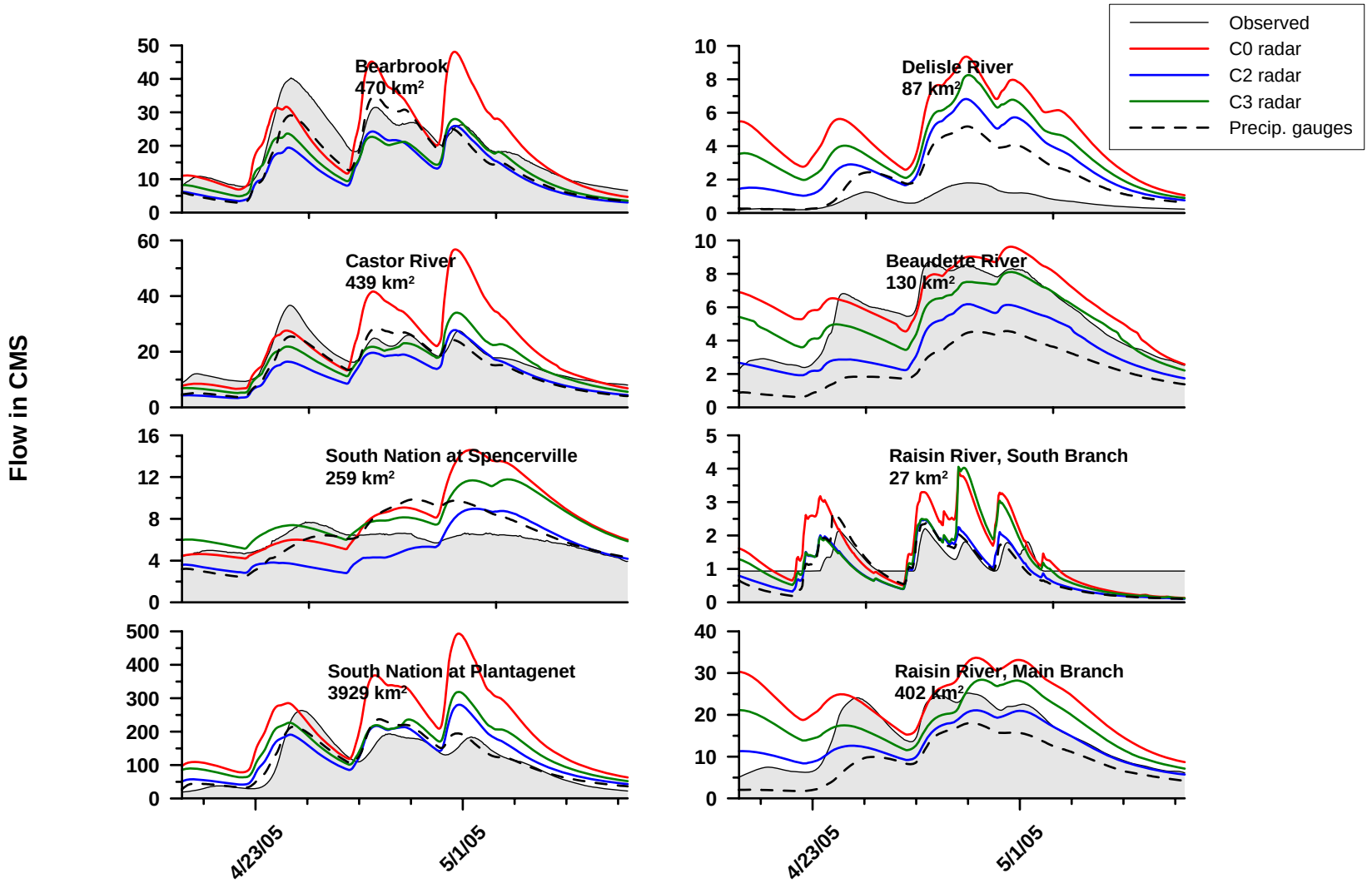

Figure D.7- Eastern Ontario, April 21st to May 7th 2005

Table D.7- Statistical criteria for Eastern Ontario, April 21st to May 7th 2005

	Statistical Criteria							
	Nash	R^2	RMSE	RMSE/qbar	%Dv	APB	Bias	MAE
	PRECIP. GAUGES							
Bearbrook	0.63	0.84	5.67	0.30	-21.43	25.83	-4.12	4.96
Castor	0.58	0.83	4.63	0.26	-18.02	22.90	-3.20	4.07
SNC, Plantagenet	0.84	0.85	27.87	0.25	6.52	18.93	7.33	21.26
SNC, Spencerville	-3.72	0.41	1.94	0.33	7.26	27.37	0.43	1.62
Beaudette	-1.33	0.75	3.28	0.60	-55.73	55.73	-3.05	3.05
Delisle	-11.52	0.91	1.72	2.28	177.19	177.79	1.34	1.34
RR, S. Branch	-1.20	0.69	0.53	0.45	-21.41	38.47	-0.25	0.45
RR, Main Branch	-0.02	0.77	6.93	0.46	-40.21	40.21	-6.06	6.06
	C0 RADAR							
Bearbrook	0.19	0.55	8.38	0.44	10.76	31.76	2.07	6.10
Castor	-1.32	0.49	10.90	0.61	28.08	43.36	4.99	7.71
SNC, Plantagenet	-2.43	0.49	128.64	1.15	89.22	93.69	100.20	105.22
SNC, Spencerville	-15.90	0.13	3.66	0.62	37.15	46.85	2.19	2.77
Beaudette	0.39	0.62	1.68	0.31	18.78	23.60	1.03	1.29
Delisle	-83.20	0.68	4.47	5.92	541.14	541.14	4.09	4.09
RR, S. Branch	-5.06	0.46	0.87	0.74	23.20	58.28	0.27	0.69
RR, Main Branch	-1.02	0.38	9.73	0.65	51.04	51.66	7.69	7.78
	C2 RADAR							
Bearbrook	0.10	0.66	8.84	0.46	-36.36	36.59	-6.99	7.03
Castor	0.00	0.60	7.15	0.40	-30.64	31.78	-5.45	5.65
SNC, Plantagenet	0.52	0.62	47.95	0.43	16.12	34.15	18.11	38.35
SNC, Spencerville	-4.70	0.05	2.13	0.36	-13.07	30.52	-0.77	1.80
Beaudette	0.00	0.76	2.15	0.39	-33.64	33.72	-1.84	1.84
Delisle	-27.09	0.85	2.58	3.42	289.67	289.67	2.19	2.19
RR, S. Branch	-1.24	0.57	0.53	0.45	-21.77	40.70	-0.26	0.48
RR, Main Branch	0.55	0.66	4.61	0.31	-14.12	22.02	-2.13	3.32
	C3 RADAR							
Bearbrook	0.37	0.70	7.37	0.38	-27.57	28.78	-5.30	5.53
Castor	0.48	0.61	5.17	0.29	-10.44	22.35	-1.86	3.97
SNC, Plantagenet	0.16	0.59	63.63	0.57	37.87	49.30	42.53	55.37
SNC, Spencerville	-8.43	0.18	2.74	0.46	35.04	37.00	2.07	2.19
Beaudette	0.65	0.66	1.28	0.23	-4.50	18.47	-0.25	1.01
Delisle	-48.92	0.78	3.44	4.56	407.54	407.54	3.08	3.08
RR, S. Branch	-3.46	0.42	0.75	0.64	1.19	50.19	0.01	0.59
RR, Main Branch	0.23	0.42	6.03	0.40	17.69	33.81	2.66	5.09

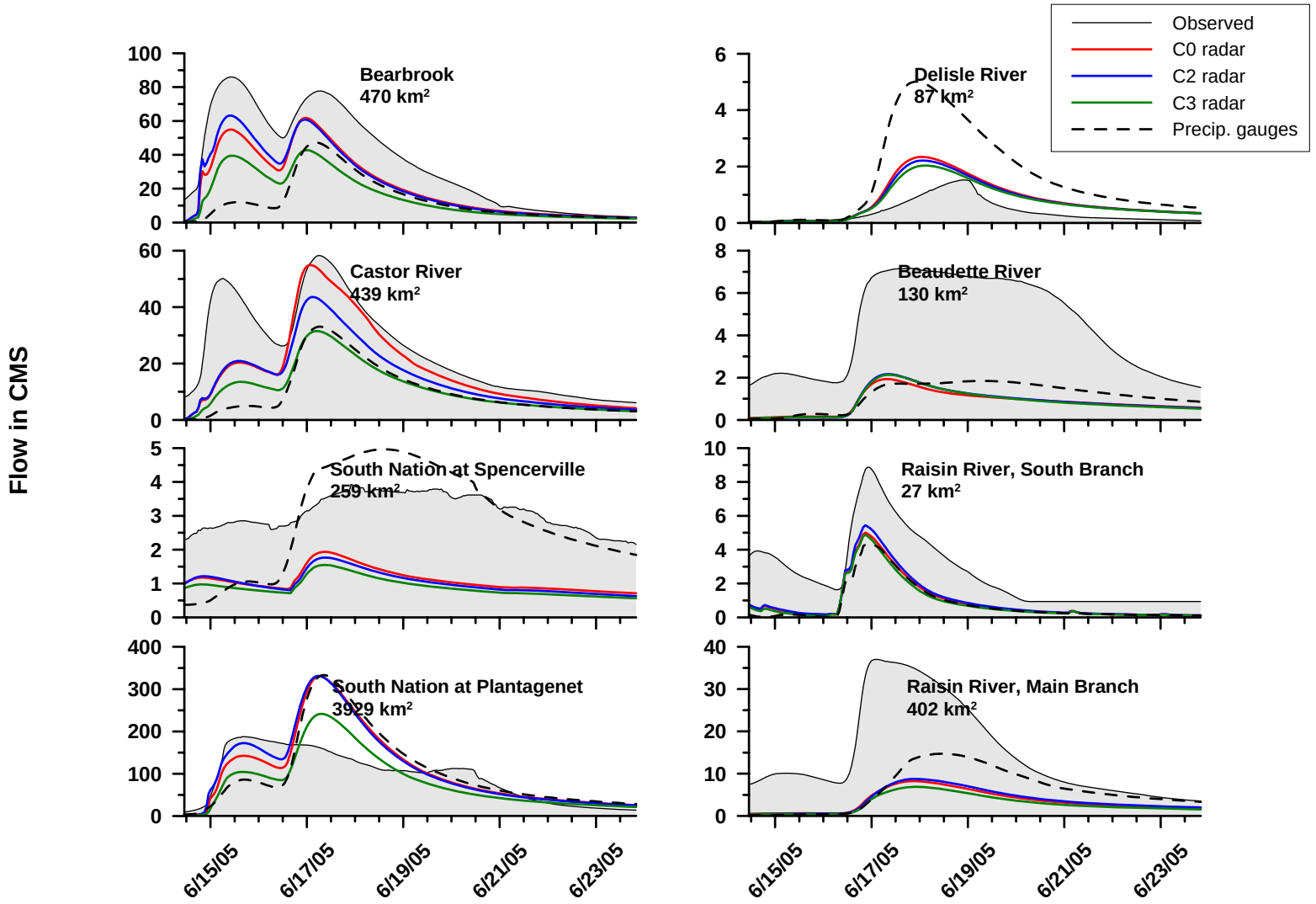

Figure D.8- Eastern Ontario, June 15th to June 24th 2005

Table D.8- Statistical criteria for Eastern Ontario, June 15th to June 24th 2005

	Statistical Criteria							
	Nash	R^2	RMSE	RMSE/qbar	%Dv	APB	Bias	MAE
	PRECIP. GAUGES							
Bearbrook	-0.26	0.46	31.46	0.86	-62.88	62.88	-23.00	23.00
Castor	-0.35	0.50	18.74	0.75	-58.57	58.57	-14.70	14.70
SNC, Plantagenet	- Gauge malfunction -							
SNC, Spencerville	-3.43	0.77	1.09	0.35	-5.53	28.45	-0.17	0.89
Beaudette	-1.87	0.75	3.71	0.83	-74.01	74.01	-3.31	3.31
Delisle	-15.94	0.80	1.74	4.42	317.64	317.96	1.25	1.25
RR, S. Branch	-0.06	0.82	2.19	0.82	-69.24	69.24	-1.84	1.84
RR, Main Branch	-0.28	0.39	12.55	0.83	-58.48	58.48	-8.83	8.83
	C0 RADAR							
Bearbrook	0.60	0.93	17.73	0.49	-38.53	38.53	-14.09	14.09
Castor	0.58	0.73	10.44	0.42	-25.31	26.29	-6.35	6.60
SNC, Plantagenet	- Gauge malfunction -							
SNC, Spencerville	-14.83	0.36	2.05	0.66	-64.61	64.61	-2.01	2.01
Beaudette	-2.39	0.76	4.03	0.90	-81.06	81.06	-3.62	3.62
Delisle	-0.77	0.83	0.56	1.43	108.01	108.94	0.43	0.43
RR, S. Branch	0.10	0.86	2.02	0.76	-64.47	64.47	-1.71	1.71
RR, Main Branch	-0.76	0.71	14.74	0.98	-76.71	76.71	-11.58	11.58
	C2 RADAR							
Bearbrook	0.66	0.94	16.36	0.45	-36.36	36.36	-13.30	13.30
Castor	0.43	0.82	12.21	0.49	-38.34	38.34	-9.62	9.62
SNC, Plantagenet	- Gauge malfunction -							
SNC, Spencerville	-15.93	0.32	2.12	0.68	-66.83	66.83	-2.08	2.08
Beaudette	-2.29	0.75	3.97	0.89	-80.26	80.26	-3.59	3.59
Delisle	-0.45	0.83	0.51	1.29	98.52	99.89	0.39	0.39
RR, S. Branch	0.19	0.86	1.91	0.72	-61.73	61.76	-1.64	1.64
RR, Main Branch	-0.71	0.66	14.53	0.96	-75.23	75.23	-11.35	11.35
	C3 RADAR							
Bearbrook	0.14	0.92	25.96	0.71	-56.87	56.87	-20.80	20.80
Castor	-0.10	0.76	16.88	0.67	-54.78	54.78	-13.75	13.75
SNC, Plantagenet	- Gauge malfunction -							
SNC, Spencerville	-18.07	0.36	2.25	0.72	-71.15	71.15	-2.22	2.22
Beaudette	-2.32	0.75	3.99	0.89	-80.64	80.64	-3.60	3.60
Delisle	-0.10	0.84	0.44	1.13	87.26	88.82	0.34	0.35
RR, S. Branch	0.00	0.83	2.12	0.80	-67.60	67.60	-1.79	1.79
RR, Main Branch	-0.93	0.69	15.41	1.02	-80.68	80.68	-12.18	12.18

Table D.9- Eastern Ontario event summary, best-performing precipitation product

	Apr 14 to May 1/03				Apr 13 to Apr 30/04				Sept 9 to Sept 16/04				Nov 1 to Nov 13/04				Nov 24 to Dec 6/04			
	RAG	C0	C2	C3	RAG	C0	C2	C3	RAG	C0	C2	C3	RAG	C0	C2	C3	RAG	C0	C2	C3
Bearbrook		X			-	-	-	-	X						X					X
Castor		X				X				X					X					X
SNC, Plantagenet	X						X			X					X					X
SNC, Spencerville			X			X			X					X			X			
Beaudette			X					X	X						X		X			
Delisle			X					X				X	X						X	
RR, S. Branch	X					X			X				-	-	-	-	X			
RR, Main Branch	X							X	X				X				X			

	Apr 21 to May 7/05				Jun 15 to Jun 24/05				SUM			
	RAG	C0	C2	C3	RAG	C0	C2	C3	RAG	C0	C2	C3
Bearbrook	X						X		2	1	2	3
Castor	X					X			1	4	1	3
SNC, Plantagenet	X							-	4	1	2	1
SNC, Spencerville	X				X				6	2	1	0
Beaudette				X	X				3	0	4	2
Delisle	X							X	4	0	2	3
RR, S. Branch	X						X		6	1	1	0
RR, Main Branch			X		X				5	0	1	1
									31	**9**	**14**	**13**

Table D.10- Eastern Ontario event summary, best-performing radar precipitation product

	Apr 14 to May 1/03			Sept 26 to Dec 31/03			Apr 13 to Apr 30/04			Sept 9 to Sept 16/04			Nov 1 to Nov 13/04			Nov 24 to Dec 6/04		
	C0	C2	C3	C0	C2	C3	C0	C2	C3	C0	C2	C3	C0	C2	C3	C0	C2	C3
Bearbrook	X					X	-	-	-		X			X				X
Castor	X					X	X				X			X				X
SNC, Plantagenet			X			X		X		X				X				X
SNC, Spencerville		X				X	X			X			X					X
Beaudette		X			X						X			X				X
Delisle		X			X					X		X		X			X	
RR, S. Branch		X				X		X		X			-	-	-	X		
RR, Main Branch		X			X					X				X		X		

	Apr 21 to May 7/05			Jun 15 to Jun 24/05			SUM		
	C0	C2	C3	C0	C2	C3	C0	C2	C3
Bearbrook			X		X		2	2	3
Castor			X	X			4	1	3
SNC, Plantagenet		X				-	1	3	3
SNC, Spencerville		X		X			4	2	2
Beaudette			X		X		0	5	3
Delisle		X				X	0	5	3
RR, S. Branch		X			X		2	4	1
RR, Main Branch		X			X		2	5	1
							15	**27**	**19**

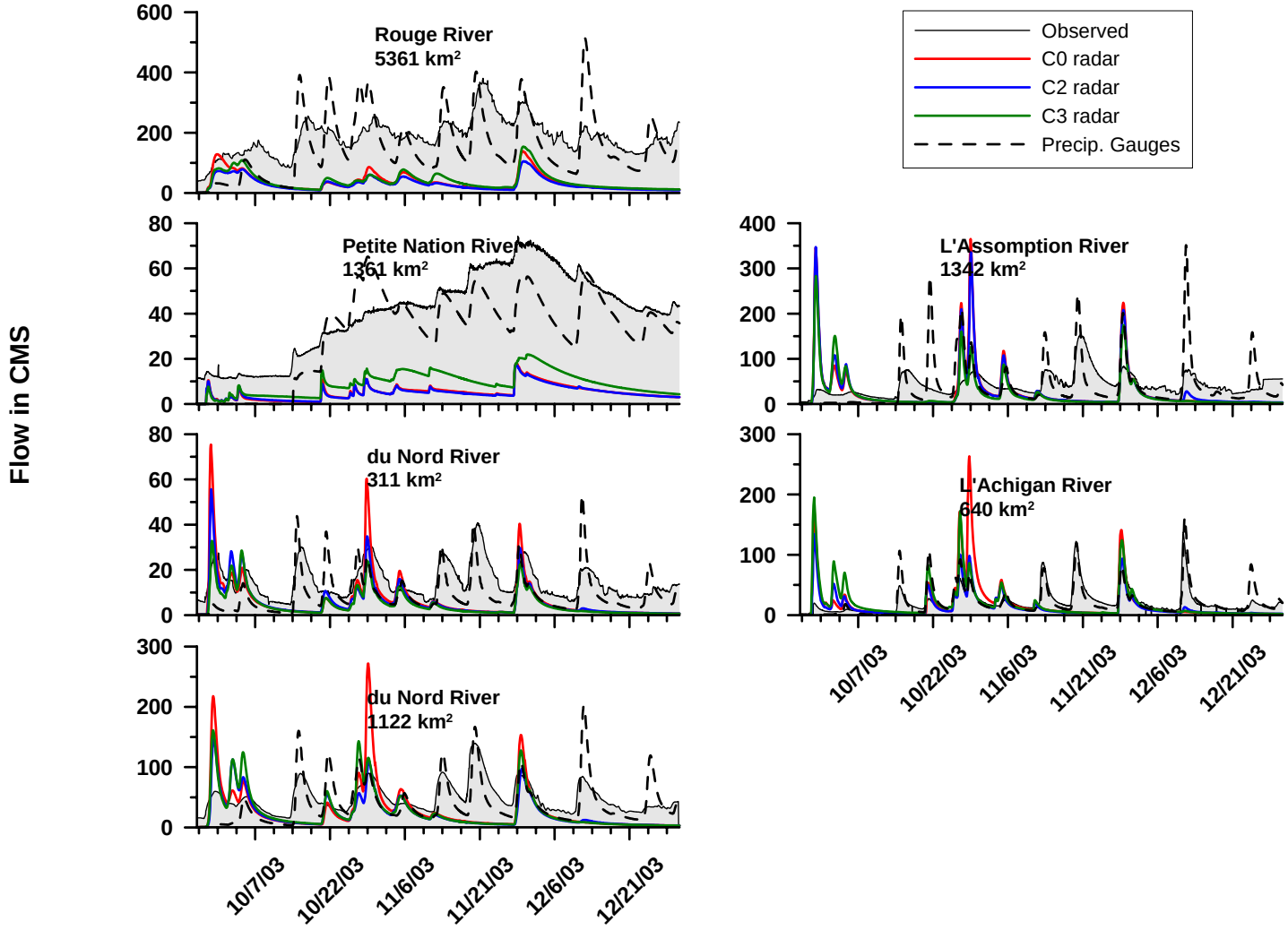

Figure D.9- Quebec, north of the St. Lawrence River, September 26th to December 31st 2003 (calibration period)

Table D.11- Statistical criteria for Quebec, north of the St. Lawrence River, September 26th to December 31st 2003 (calibration period)

	Statistical Criteria							
	Nash	R^2	RMSE	RMSE/qbar	%Dv	APB	Bias	MAE
	PRECIP. GAUGES							
Rouge	-1.22	0.40	88.40	0.48	-18.04	40.75	-33.51	75.69
Petite Nation	0.37	0.67	14.41	0.35	-22.44	29.85	-9.14	12.16
du Nord (311 km^2)	-0.33	0.46	28.59	0.59	-17.90	45.63	-8.66	22.08
du Nord (1122 km^2)	-0.56	0.32	9.30	0.64	-36.73	52.53	-5.34	7.64
L'Assomption	-2.64	0.25	47.36	1.12	-4.54	72.39	-1.91	30.50
L'Achigan	0.58	0.67	14.67	0.66	-4.71	38.67	-1.05	8.66
	C0 RADAR							
Rouge	-6.59	0.00	163.51	0.88	-80.84	81.11	-150.15	150.65
Petite Nation	-3.67	0.54	39.07	0.96	-87.58	87.58	-35.69	35.69
du Nord (311 km^2)	-2.34	0.08	45.22	0.94	-41.89	67.72	-20.27	32.77
du Nord (1122 km^2)	-1.95	0.13	12.77	0.88	-55.39	68.26	-8.05	9.92
L'Assomption	-4.18	0.01	56.52	1.34	-36.81	91.25	-15.51	38.45
L'Achigan	-1.17	0.13	33.36	1.49	-17.86	83.39	-4.00	18.67
	C2 RADAR							
Rouge	-6.98	0.01	167.62	0.90	-83.93	83.93	-155.88	155.88
Petite Nation	-3.72	0.51	39.31	0.97	-88.00	88.00	-35.86	35.86
du Nord (311 km^2)	-1.73	0.04	40.93	0.85	-51.92	64.64	-25.12	31.28
du Nord (1122 km^2)	-1.73	0.11	12.28	0.85	-60.12	67.62	-8.74	9.83
L'Assomption	-3.83	0.01	54.56	1.30	-37.09	89.05	-15.63	37.52
L'Achigan	-0.30	0.11	25.83	1.15	-40.18	70.57	-8.99	15.80
	C3 RADAR							
Rouge	-6.20	0.02	159.21	0.86	-78.83	78.83	-146.42	146.42
Petite Nation	-2.73	0.60	34.91	0.86	-77.93	77.93	-31.75	31.75
du Nord (311 km^2)	-1.89	0.05	42.08	0.87	-45.95	66.33	-22.24	32.10
du Nord (1122 km^2)	-1.78	0.11	12.39	0.85	-66.66	69.51	-9.69	10.11
L'Assomption	-2.86	0.00	48.78	1.16	-48.34	85.91	-20.37	36.19
L'Achigan	-0.84	0.07	30.77	1.37	-19.18	80.52	-4.29	18.02

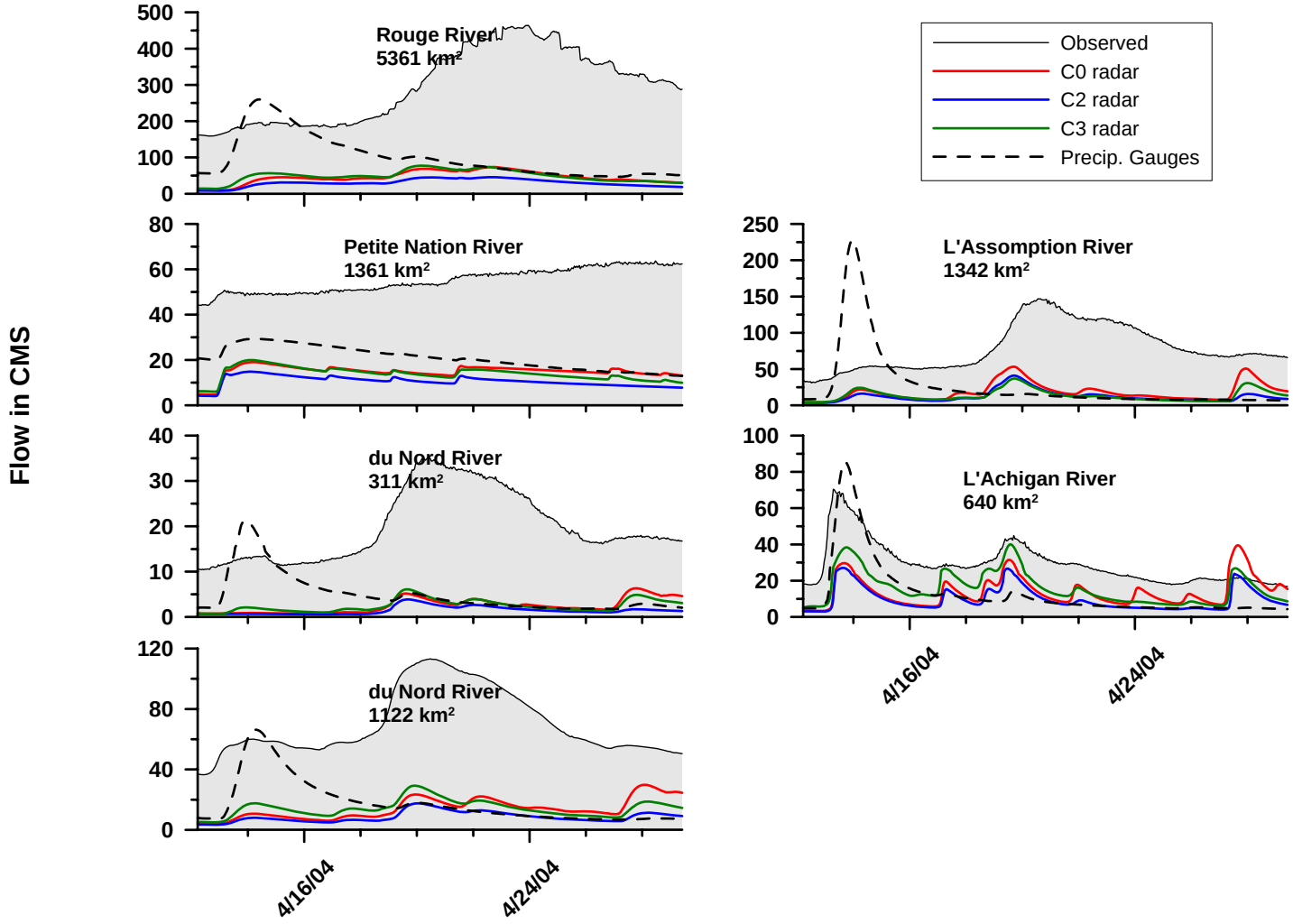

Figure D.10- Quebec, north of the St. Lawrence River, April 13th to April 30th 2004

Table D.12- Statistical criteria for Quebec, north of the St. Lawrence River, April 13th to April 30th 2004

	Statistical Criteria							
	Nash	**R^2**	**RMSE**	**RMSE/qbar**	**%Dv**	**APB**	**Bias**	**MAE**
	PRECIP. GAUGES							
Rouge	-4.89	0.39	245.10	0.82	-66.28	69.41	-197.31	206.64
Petite Nation	-43.52	0.78	35.58	0.65	-62.05	62.05	-34.15	34.15
du Nord (311 km^2)	-6.64	0.02	59.29	0.84	-74.39	74.94	-52.35	52.73
du Nord (1122 km^2)	-4.50	0.14	18.11	0.91	-74.93	78.69	-14.92	15.67
L'Assomption	-5.52	0.11	81.24	1.02	-65.38	89.54	-51.89	71.06
L'Achigan	-1.45	0.74	18.27	0.62	-54.33	58.91	-15.99	17.33
	C0 RADAR							
Rouge	-6.03	0.45	267.87	0.90	-84.66	84.66	-252.03	252.03
Petite Nation	-56.43	0.01	40.42	0.73	-72.70	72.70	-40.02	40.02
du Nord (311 km^2)	-6.70	0.21	59.54	0.85	-80.02	80.02	-56.31	56.31
du Nord (1122 km^2)	-4.92	0.33	18.80	0.94	-87.76	87.76	-17.48	17.48
L'Assomption	-3.48	0.18	67.36	0.85	-76.72	76.72	-60.89	60.89
L'Achigan	-1.73	0.13	19.29	0.66	-52.54	57.16	-15.46	16.82
	C2 RADAR							
Rouge	-6.89	0.40	283.78	0.95	-89.83	89.83	-267.43	267.43
Petite Nation	-69.68	0.14	44.84	0.82	-80.59	80.59	-44.36	44.36
du Nord (311 km^2)	-8.04	0.72	64.50	0.92	-87.76	87.76	-61.75	61.75
du Nord (1122 km^2)	-5.54	0.81	19.76	0.99	-92.85	92.85	-18.49	18.49
L'Assomption	-4.22	0.34	72.67	0.92	-84.52	84.52	-67.07	67.07
L'Achigan	-2.39	0.43	21.50	0.73	-66.52	66.69	-19.57	19.62
	C3 RADAR							
Rouge	-5.94	0.19	266.19	0.89	-83.51	83.51	-248.62	248.62
Petite Nation	-59.84	0.13	41.60	0.76	-74.52	74.52	-41.02	41.02
du Nord (311 km^2)	-6.48	0.58	58.67	0.83	-79.48	79.48	-55.93	55.93
du Nord (1122 km^2)	-4.88	0.49	18.74	0.94	-87.55	87.55	-17.44	17.44
L'Assomption	-4.16	0.11	72.27	0.91	-82.80	82.80	-65.71	65.71
L'Achigan	-0.75	0.56	15.43	0.52	-45.38	46.20	-13.35	13.59

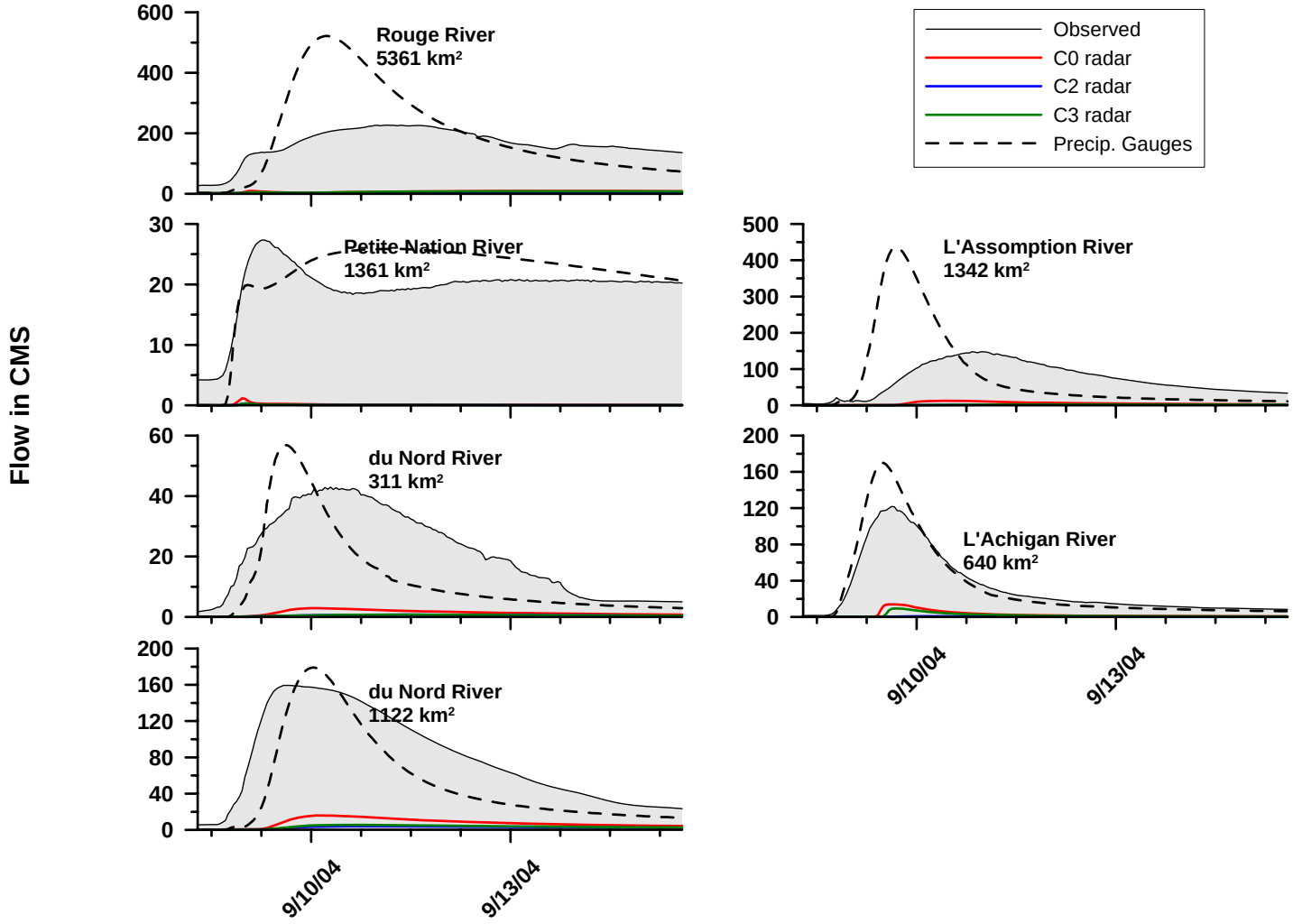

Figure D.11- Quebec, north of the St. Lawrence River, September 9th to September 16th 2004

Table D.13- Statistical criteria for Quebec, north of the St. Lawrence River, September 9th to September 16th 2004

	Statistical Criteria							
	Nash	**R^2**	**RMSE**	**RMSE/qbar**	**%Dv**	**APB**	**Bias**	**MAE**
	PRECIP. GAUGES							
Rouge	-5.42	0.52	126.92	0.77	22.52	53.29	37.29	88.27
Petite Nation	-0.03	0.58	4.55	0.23	11.27	20.40	2.21	4.00
du Nord (311 km^2)	0.46	0.78	36.47	0.45	-34.30	37.50	-27.55	30.12
du Nord (1122 km^2)	0.06	0.53	13.33	0.63	-37.57	51.29	-8.00	10.92
L'Assomption	-6.02	0.05	115.38	1.58	9.38	104.85	6.84	76.49
L'Achigan	0.83	0.95	13.94	0.43	5.68	23.87	1.84	7.75
	C0 RADAR							
Rouge	-10.00	0.15	166.10	1.00	-95.79	95.79	-158.66	158.66
Petite Nation	-18.89	0.08	19.94	1.02	-99.29	99.29	-19.44	19.44
du Nord (311 km^2)	-1.99	0.61	85.93	1.07	-90.25	90.25	-72.49	72.49
du Nord (1122 km^2)	-2.00	0.73	23.76	1.12	-93.31	93.31	-19.87	19.87
L'Assomption	-2.26	0.88	78.64	1.08	-92.75	92.75	-67.66	67.66
L'Achigan	-0.62	0.70	42.91	1.32	-91.79	91.79	-29.80	29.80
	C2 RADAR							
Rouge	-10.58	0.00	170.44	1.03	-98.37	98.37	-162.93	162.93
Petite Nation	-19.05	0.19	20.02	1.02	-99.70	99.70	-19.52	19.52
du Nord (311 km^2)	-2.42	0.18	91.83	1.14	-96.55	96.55	-77.55	77.55
du Nord (1122 km^2)	-2.28	0.23	24.83	1.17	-97.54	97.54	-20.77	20.77
L'Assomption	-2.67	0.08	83.49	1.14	-97.84	97.84	-71.37	71.37
L'Achigan	-0.90	0.18	46.45	1.43	-98.63	98.63	-32.02	32.02
	C3 RADAR							
Rouge	-10.08	0.26	166.68	1.01	-96.18	96.18	-159.30	159.30
Petite Nation	-19.05	0.24	20.02	1.02	-99.70	99.70	-19.52	19.52
du Nord (311 km^2)	-2.36	0.29	91.00	1.13	-95.61	95.61	-76.79	76.79
du Nord (1122 km^2)	-2.28	0.22	24.83	1.17	-97.54	97.54	-20.77	20.77
L'Assomption	-2.65	0.18	83.23	1.14	-97.56	97.56	-71.16	71.16
L'Achigan	-0.73	0.56	44.41	1.37	-94.44	94.44	-30.66	30.66

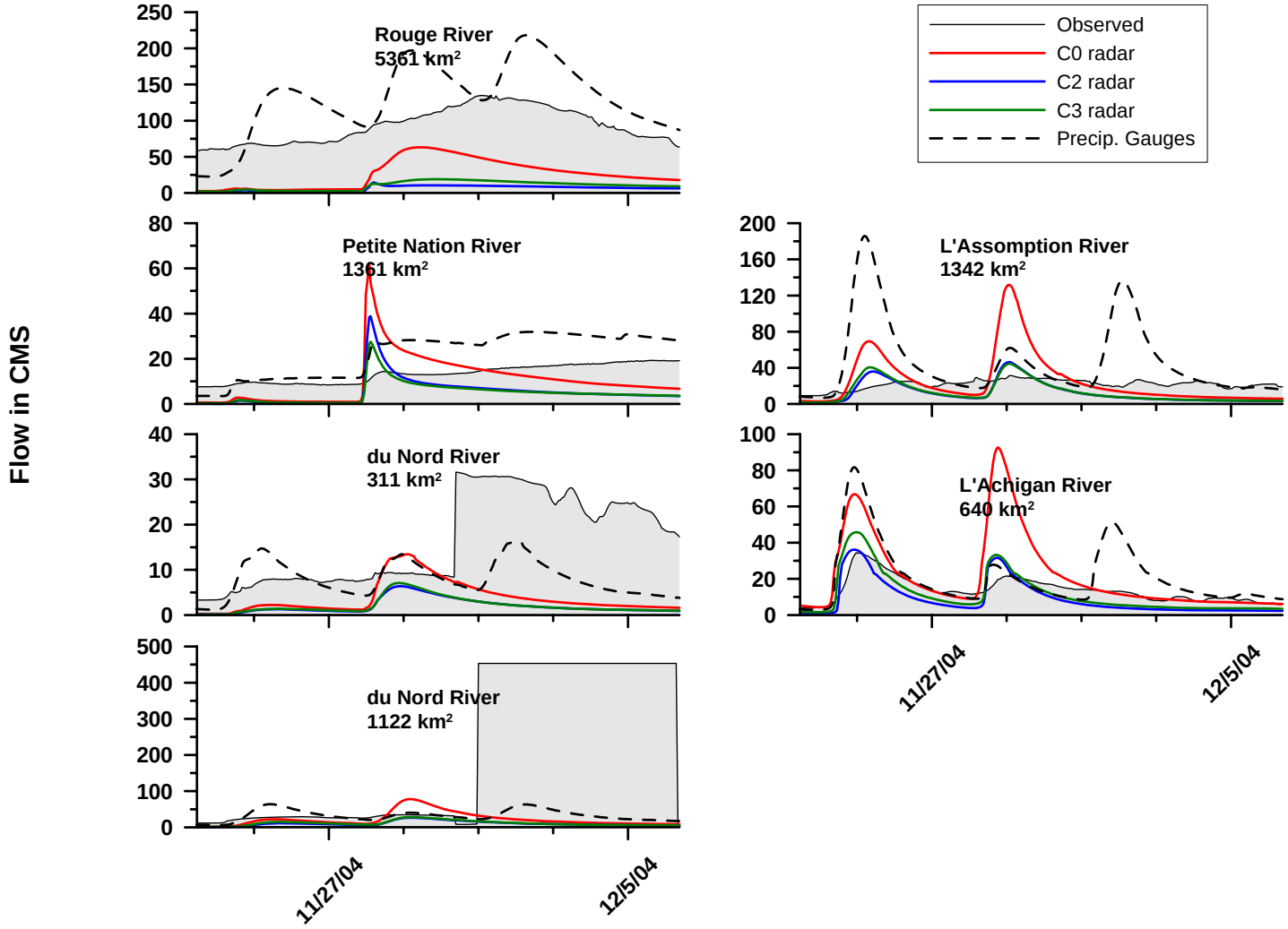

Figure D.12- Quebec, north of the St. Lawrence River, November 24th to December 6th 2004

Table D.14- Statistical criteria for Quebec, north of the St. Lawrence River, November 24th to December 6th 2004

	Statistical Criteria							
	Nash	**R^2**	**RMSE**	**RMSE/qbar**	**%Dv**	**APB**	**Bias**	**MAE**
	PRECIP. GAUGES							
Rouge	-3.78	0.53	52.49	0.56	41.45	48.59	38.68	45.34
Petite Nation	-6.37	0.83	10.75	0.80	65.82	69.98	8.84	9.40
du Nord (311 km^2)	- Gauge malfunction -							
du Nord (1122 km^2)	- Gauge malfunction -							
L'Assomption	-90.71	0.00	49.12	2.24	114.53	125.79	25.09	27.55
L'Achigan	-3.96	0.49	15.44	1.11	53.55	67.08	7.47	9.35
	C0 RADAR							
Rouge	-7.15	0.67	68.56	0.74	-71.98	71.98	-67.17	67.17
Petite Nation	-5.81	0.08	10.33	0.77	-21.26	61.84	-2.86	8.31
du Nord (311 km^2)	- Gauge malfunction -							
du Nord (1122 km^2)	- Gauge malfunction -							
L'Assomption	-25.79	0.21	26.55	1.21	17.89	79.89	3.92	17.50
L'Achigan	-6.27	0.54	18.68	1.34	58.37	66.70	8.14	9.30
	C2 RADAR							
Rouge	-12.84	0.68	89.34	0.96	-93.03	93.03	-86.82	86.82
Petite Nation	-5.93	0.05	10.42	0.78	-60.41	71.01	-8.12	9.54
du Nord (311 km^2)	- Gauge malfunction -							
du Nord (1122 km^2)	- Gauge malfunction -							
L'Assomption	-6.13	0.22	13.69	0.63	-42.08	57.79	-9.22	12.66
L'Achigan	-0.04	0.71	7.07	0.51	-34.59	47.12	-4.82	6.57
	C3 RADAR							
Rouge	-11.59	0.78	85.21	0.91	-89.02	89.02	-83.07	83.07
Petite Nation	-5.39	0.09	10.01	0.75	-64.13	69.41	-8.61	9.32
du Nord (311 km^2)	- Gauge malfunction -							
du Nord (1122 km^2)	- Gauge malfunction -							
L'Assomption	-6.22	0.17	13.78	0.63	-39.69	57.92	-8.69	12.69
L'Achigan	0.08	0.75	6.66	0.48	-16.50	40.62	-2.30	5.66

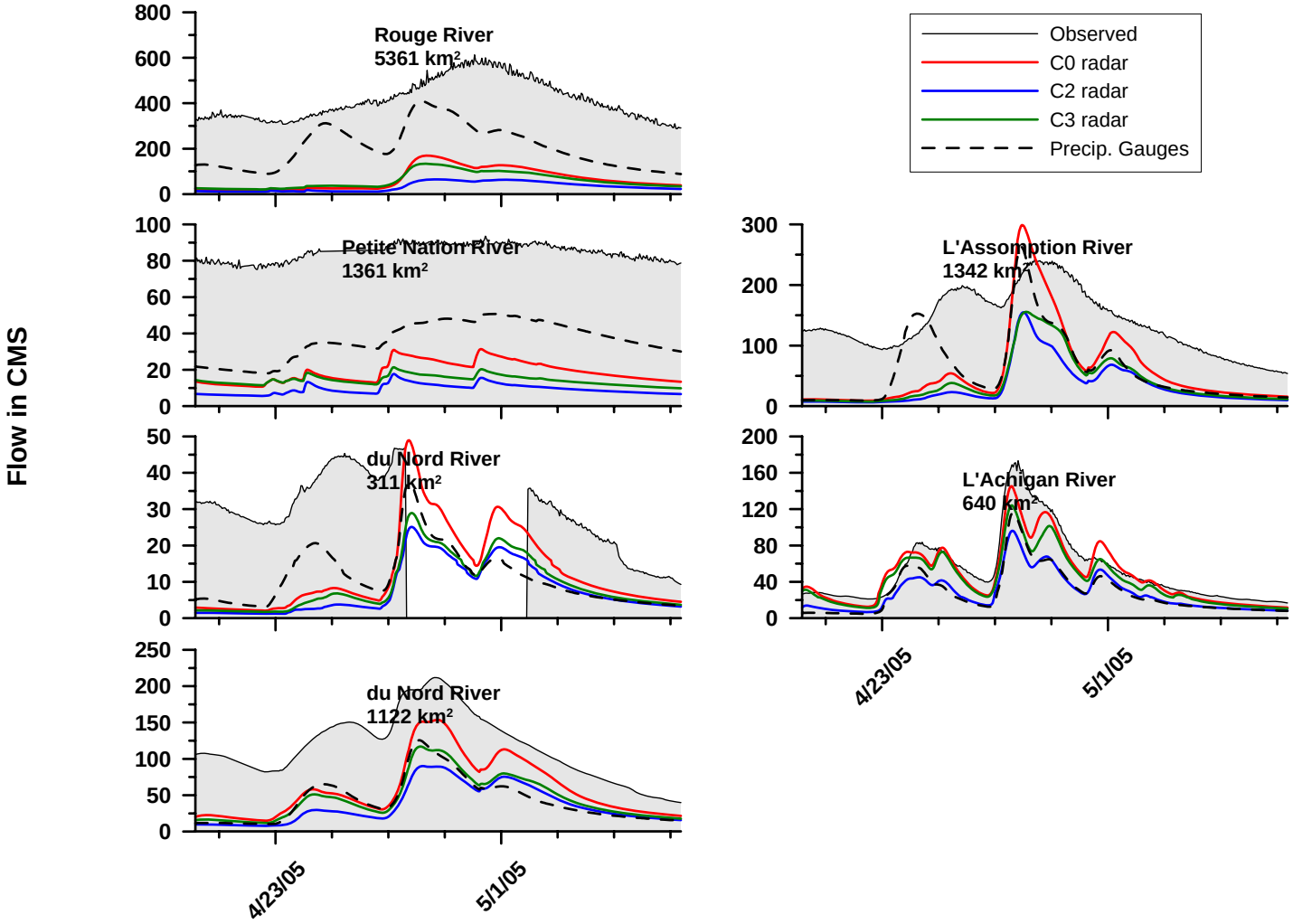

Figure D.13- Quebec, north of the St. Lawrence River, April 21st to May 7th 2005

Table D.15- Statistical criteria for Quebec, north of the St. Lawrence River, April 21st to May 7th 2005

	Statistical Criteria							
	Nash	**R^2**	**RMSE**	**RMSE/qbar**	**%Dv**	**APB**	**Bias**	**MAE**
	PRECIP. GAUGES							
Rouge	-5.27	0.52	220.27	0.53	-50.51	50.51	-209.73	209.73
Petite Nation	-117.11	0.85	48.73	0.58	-57.02	57.02	-48.32	48.32
du Nord (311 km^2)	- Gauge malfunction -							
du Nord (1122 km^2)	-0.96	0.06	21.64	0.99	-48.82	92.42	-10.72	20.29
L'Assomption	-2.03	0.45	89.23	0.65	-56.11	59.24	-77.41	81.72
L'Achigan	0.35	0.90	30.52	0.57	-47.94	47.95	-25.60	25.60
	C0 RADAR							
Rouge	-15.11	0.76	353.19	0.85	-84.14	84.14	-349.37	349.37
Petite Nation	-216.01	0.77	66.05	0.78	-77.88	77.88	-65.99	65.99
du Nord (311 km^2)	- Gauge malfunction -							
du Nord (1122 km^2)	-1.67	0.31	25.29	1.15	-42.12	105.66	-9.25	23.20
L'Assomption	-2.19	0.52	91.57	0.66	-57.41	60.70	-79.20	83.74
L'Achigan	0.86	0.89	14.36	0.27	-11.86	20.11	-6.33	10.73
	C2 RADAR							
Rouge	-18.56	0.77	389.16	0.94	-92.15	92.15	-382.64	382.64
Petite Nation	-282.33	0.70	75.47	0.89	-89.01	89.01	-75.43	75.43
du Nord (311 km^2)	- Gauge malfunction -							
du Nord (1122 km^2)	-1.58	0.42	24.89	1.13	-64.15	104.63	-14.08	22.97
L'Assomption	-3.73	0.51	111.49	0.81	-76.52	76.52	-105.56	105.56
L'Achigan	0.28	0.92	31.98	0.60	-48.17	48.17	-25.72	25.72
	C3 RADAR							
Rouge	-15.77	0.80	360.35	0.87	-85.62	85.62	-355.53	355.53
Petite Nation	-246.46	0.52	70.53	0.83	-83.15	83.15	-70.46	70.46
du Nord (311 km^2)	- Gauge malfunction -							
du Nord (1122 km^2)	-1.46	0.36	24.29	1.11	-58.05	102.82	-12.74	22.57
L'Assomption	-3.04	0.61	103.07	0.75	-71.07	71.07	-98.04	98.04
L'Achigan	0.74	0.89	19.13	0.36	-22.85	25.77	-12.20	13.76

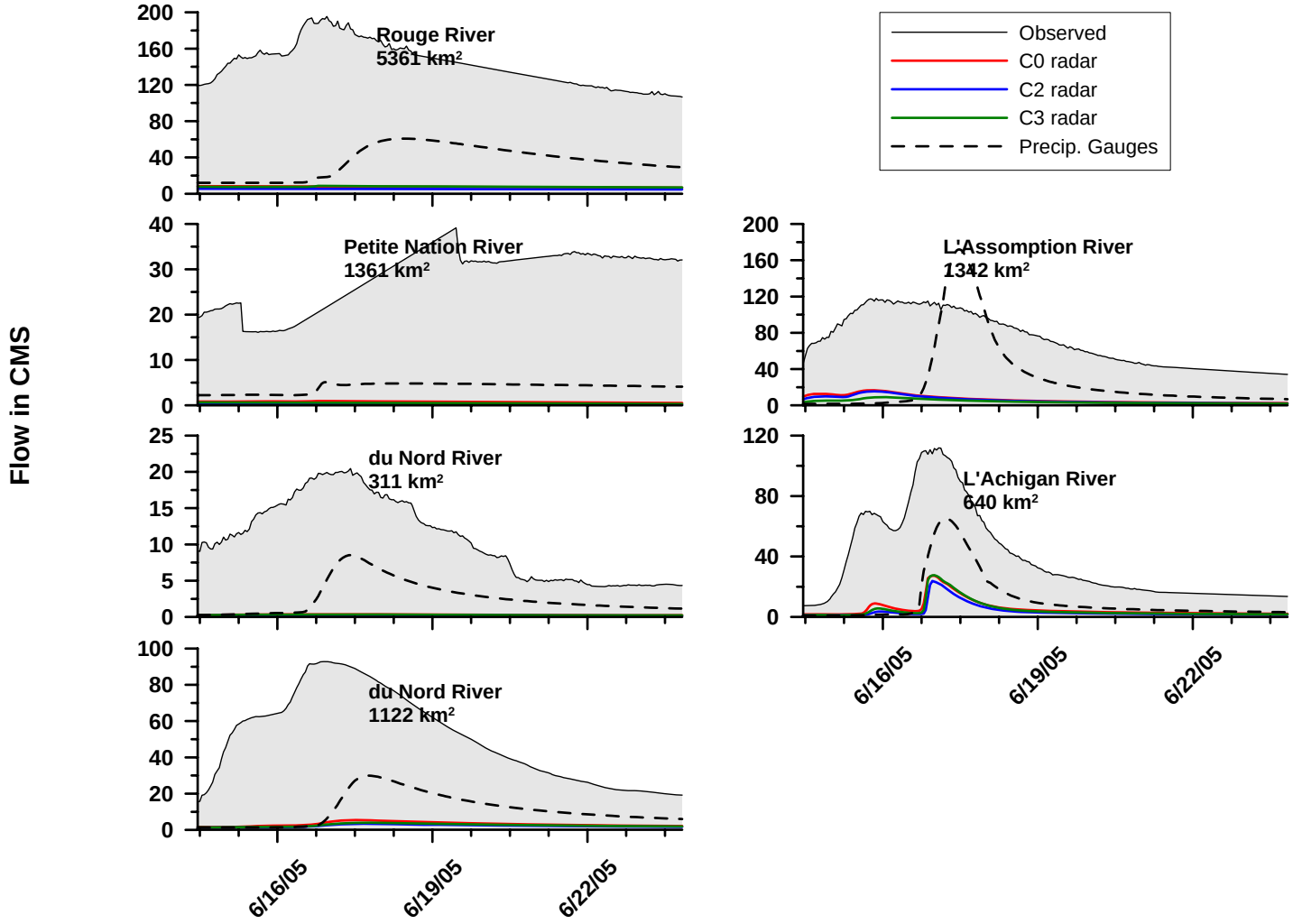

Figure D.14- Quebec, north of the St. Lawrence River, June 15th to June 24th 2005

Table D.16- Statistical criteria for Quebec, north of the St. Lawrence River, June 15th to June 24th 2005

	Statistical Criteria							
	Nash	**R^2**	**RMSE**	**RMSE/qbar**	**%Dv**	**APB**	**Bias**	**MAE**
	PRECIP. GAUGES							
Rouge	-20.71	0.00	111.13	0.78	-74.83	74.83	-107.00	107.00
Petite Nation	- Gauge malfunction -							
du Nord (311 km^2)	-2.56	0.15	45.88	0.90	-78.08	78.08	-40.01	40.01
du Nord (1122 km^2)	-1.93	0.32	9.32	0.86	-75.13	75.13	-8.12	8.12
L'Assomption	-3.14	0.17	58.84	0.82	-60.16	70.59	-43.37	50.89
L'Achigan	-0.35	0.53	34.63	0.90	-71.09	71.09	-27.43	27.43
	C0 RADAR							
Rouge	-32.22	0.53	137.47	0.96	-94.73	94.73	-135.45	135.45
Petite Nation	- Gauge malfunction -							
du Nord (311 km^2)	-3.85	0.43	53.54	1.05	-93.77	93.77	-48.05	48.05
du Nord (1122 km^2)	-3.71	0.94	11.81	1.09	-97.12	97.12	-10.50	10.50
L'Assomption	-4.90	0.67	70.26	0.98	-90.81	90.81	-65.47	65.47
L'Achigan	-0.98	0.66	41.95	1.09	-86.20	86.20	-33.26	33.26
	C2 RADAR							
Rouge	-33.39	0.56	139.86	0.98	-96.40	96.40	-137.84	137.84
Petite Nation	- Gauge malfunction -							
du Nord (311 km^2)	-4.04	0.25	54.58	1.07	-95.66	95.66	-49.02	49.02
du Nord (1122 km^2)	-3.76	0.92	11.88	1.10	-97.78	97.78	-10.57	10.57
L'Assomption	-5.03	0.73	71.03	0.99	-91.88	91.88	-66.24	66.24
L'Achigan	-1.17	0.53	43.89	1.14	-90.31	90.31	-34.84	34.84
	C3 RADAR							
Rouge	-32.13	0.71	137.27	0.96	-94.59	94.59	-135.24	135.24
Petite Nation	- Gauge malfunction -							
du Nord (311 km^2)	-3.97	0.26	54.22	1.06	-94.95	94.95	-48.66	48.66
du Nord (1122 km^2)	-3.73	0.93	11.84	1.10	-97.43	97.43	-10.54	10.54
L'Assomption	-5.38	0.87	73.08	1.01	-94.20	94.20	-67.91	67.91
L'Achigan	-1.04	0.58	42.55	1.10	-87.84	87.84	-33.89	33.89

Table D.17- Quebec, north of the St. Lawrence River event summary, best-performing precipitation product

	Apr 13 to Apr 30/04				Sept 9 to Sept 16/04				Nov 1 to Nov 13/04				Nov 24 to Dec 6/04			
	RAG	C0	C2	C3	RAG	C0	C2	C3	RAG	C0	C2	C3	RAG	C0	C2	C3
Rouge	X				X				X				X			
Petite Nation	X				X					X			X			
du Nord (311 km2)	X				X				-	-	-	-	-	-	-	-
du Nord (1122 km2)	X				X				-	-	-	-	X			
L'Assomption		X				X					X		X			
L'Achigan				X	X							X		X		

	Apr 21 to May 7/05				SUM			
	RAG	C0	C2	C3	RAG	C0	C2	C3
Rouge	X				7	0	0	0
Petite Nation	-	-	-	-	3	1	0	0
du Nord (311 km2)	X				5	0	0	0
du Nord (1122 km2)	X				6	0	0	0
L'Assomption	X				2	4	1	0
L'Achigan	X				2	1	0	2
					25	**6**	**1**	**2**

Table D.18- Quebec, north of the St. Lawrence River event summary, best-performing radar precipitation product

	Sep 26 to Dec 31/03			Apr 13 to Apr 30/04			Sept 9 to Sept 16/04			Nov 1 to Nov 13/04			Nov 24 to Dec 6/04		
	C0	C2	C3	C0	C2	C3	C0	C2	C3	C0	C2	C3	C0	C2	C3
Rouge			1			1	1			1			1		
Petite Nation			1	1			1			1			1		
du Nord (311 km2)		1				1	1			-	-	-	-	-	-
du Nord (1122 km2)		1				1	1			-	-	-			1
L'Assomption			1	1			1				1		1		
L'Achigan		1				1	1					1	1		

	Apr 21 to May 7/05			SUM		
	C0	C2	C3	C0	C2	C3
Rouge			X	3	0	3
Petite Nation	-	-	-	4	0	1
du Nord (311 km2)	X			2	1	1
du Nord (1122 km2)	X			2	1	2
L'Assomption	X			4	1	1
L'Achigan	X			3	1	2
				18	**4**	**10**

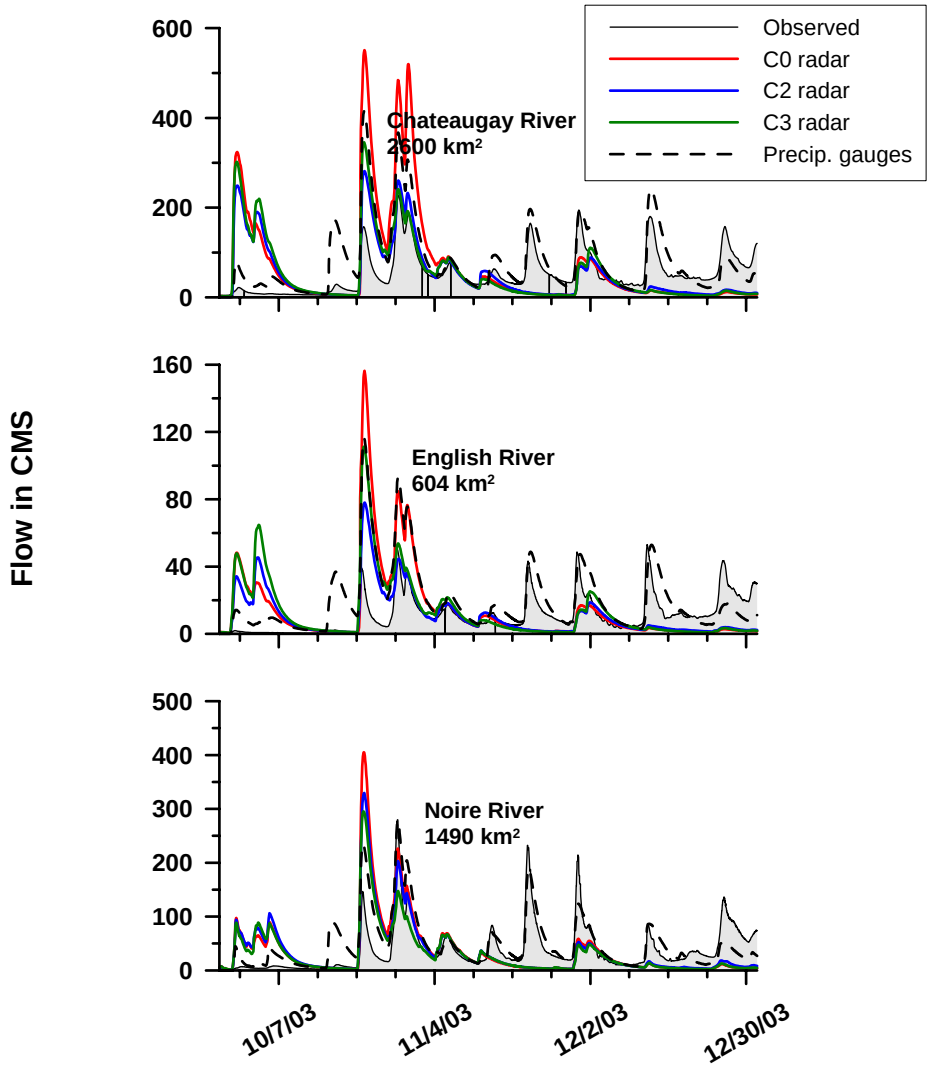

Figure D.15- Quebec, south of the St. Lawrence River, September 26th to December 31st 2003 (calibration period)

Table D.19- Statistical criteria for Quebec, south of the St. Lawrence River, September 26th to December 31st 2003

	Statistical Criteria							
	Nash	**R^2**	**RMSE**	**RMSE/qbar**	**%Dv**	**APB**	**Bias**	**MAE**
	PRECIP. GAUGES							
Chateauguay	-0.54	0.62	57.46	1.07	49.82	68.58	26.66	36.70
English	-1.49	0.38	17.83	1.56	71.46	99.12	8.15	11.30
Noire	0.52	0.65	30.80	0.80	23.71	53.32	9.17	20.63
	C0 RADAR							
Chateauguay	-3.85	0.19	102.07	1.91	29.96	122.07	16.03	65.33
English	-3.33	0.07	23.52	2.06	23.65	123.70	2.70	14.11
Noire	-0.72	0.15	58.08	1.50	-6.53	91.47	-2.53	35.39
	C2 RADAR							
Chateauguay	-1.07	0.10	66.66	1.25	-2.88	85.64	-1.54	45.83
English	-1.01	0.03	16.04	1.41	-5.30	92.33	-0.60	10.53
Noire	-0.43	0.15	53.07	1.37	-10.22	87.16	-3.95	33.72
	C3 RADAR							
Chateauguay	-1.64	0.06	75.30	1.41	1.60	93.88	0.86	50.24
English	-2.28	0.02	20.48	1.80	15.04	115.63	1.72	13.19
Noire	-0.38	0.11	52.08	1.35	-20.45	87.68	-7.91	33.92

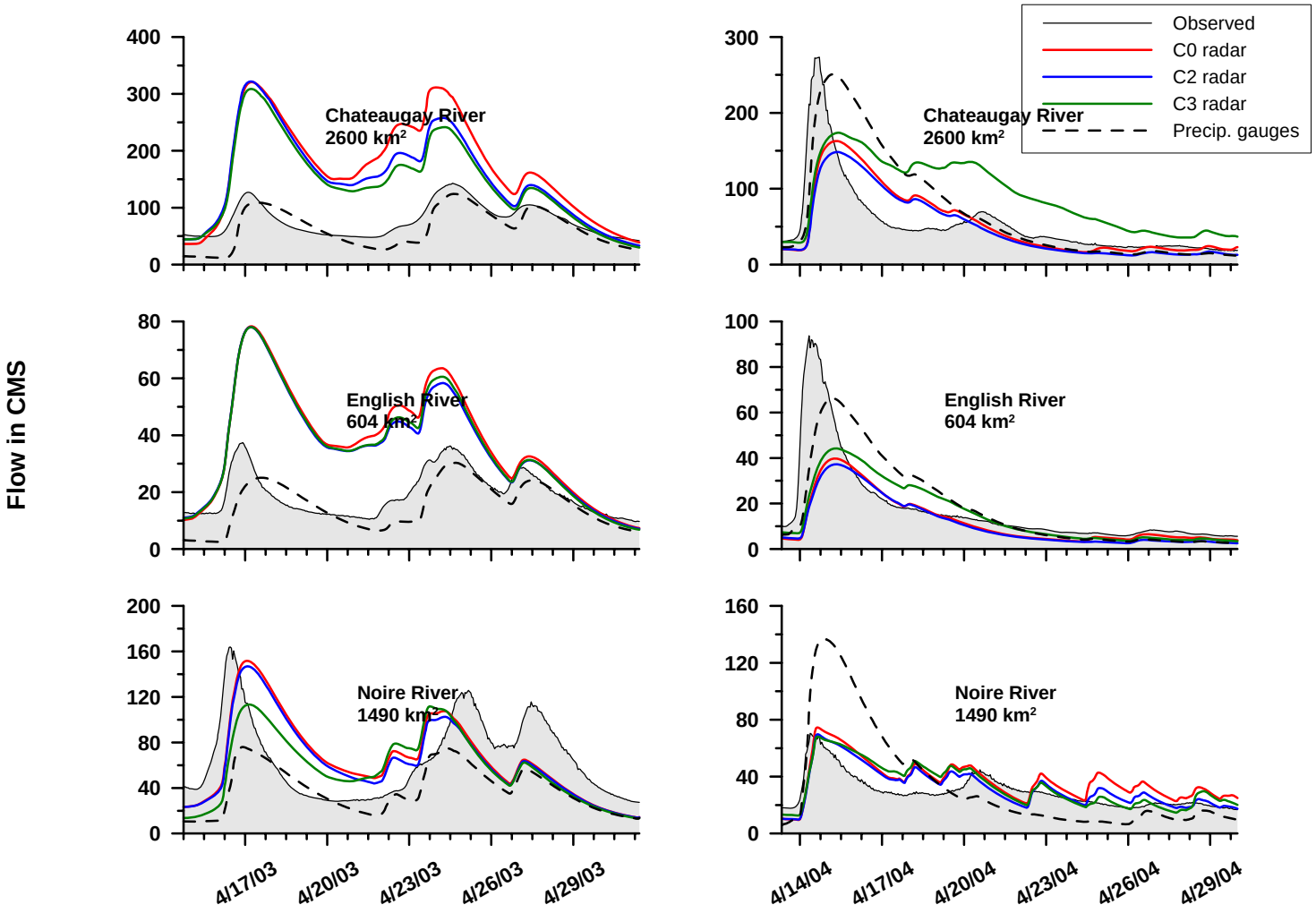

Figure D.16- Quebec, south of the St. Lawrence River, April 14th to May 1st 2003

Figure D.17- Quebec, south of the St. Lawrence River, April 13th to April 30th 2004

Table D.20- Statistical criteria for Quebec, south of the St. Lawrence River, April 14th to May 1st 2003

	Statistical Criteria							
	Nash	R^2	RMSE	RMSE/qbar	%Dv	APB	Bias	MAE
	PRECIP. GAUGES							
Chateauguay	0.35	0.70	22.64	0.29	-17.70	23.38	-13.68	18.08
English	0.23	0.55	6.89	0.36	-20.36	27.12	-3.94	5.24
Noire	-0.20	0.40	37.26	0.57	-40.35	42.77	-26.36	27.94
	C0 RADAR							
Chateauguay	-16.46	0.47	117.36	1.52	124.12	125.79	95.96	97.25
English	-8.77	0.37	24.44	1.26	97.64	99.35	18.88	19.21
Noire	-0.12	0.21	36.00	0.55	0.87	49.46	0.57	32.32
	C2 RADAR							
Chateauguay	-11.46	0.43	99.14	1.28	100.50	101.91	77.70	78.78
English	-7.42	0.36	22.69	1.17	88.41	90.42	17.10	17.48
Noire	-0.05	0.22	34.84	0.53	-3.29	47.34	-2.15	30.93
	C3 RADAR							
Chateauguay	-9.13	0.44	89.37	1.16	88.30	90.44	68.27	69.92
English	-7.77	0.37	23.16	1.20	90.29	92.74	17.46	17.93
Noire	-0.05	0.18	34.94	0.54	-10.70	47.64	-6.99	31.13

Table D.21- Statistical criteria for Quebec, south of the St. Lawrence River, April 13th to April 30th 2004

	Statistical Criteria							
	Nash	R^2	RMSE	RMSE/qbar	%Dv	APB	Bias	MAE
	PRECIP. GAUGES							
Chateauguay	-0.01	0.55	50.59	0.93	28.74	60.62	15.66	33.03
English	0.49	0.55	13.87	0.78	4.03	48.63	0.72	8.65
Noire	-5.07	0.64	28.77	0.98	17.09	70.56	5.03	20.76
	C0 RADAR							
Chateauguay	0.42	0.46	38.21	0.70	-0.57	42.86	-0.31	23.35
English	0.40	0.50	15.10	0.85	-31.84	36.37	-5.67	6.47
Noire	-0.06	0.56	12.00	0.41	26.36	36.25	7.76	10.67
	C2 RADAR							
Chateauguay	0.40	0.45	38.86	0.71	-10.70	45.26	-5.83	24.66
English	0.35	0.49	15.65	0.88	-37.60	41.37	-6.69	7.36
Noire	0.38	0.61	9.19	0.31	10.53	25.75	3.10	7.58
	C3 RADAR							
Chateauguay	-0.32	0.31	57.72	1.06	65.53	89.47	35.70	48.74
English	0.43	0.45	14.61	0.82	-14.78	41.64	-2.63	7.41
Noire	0.20	0.59	10.41	0.35	13.94	27.93	4.10	8.22

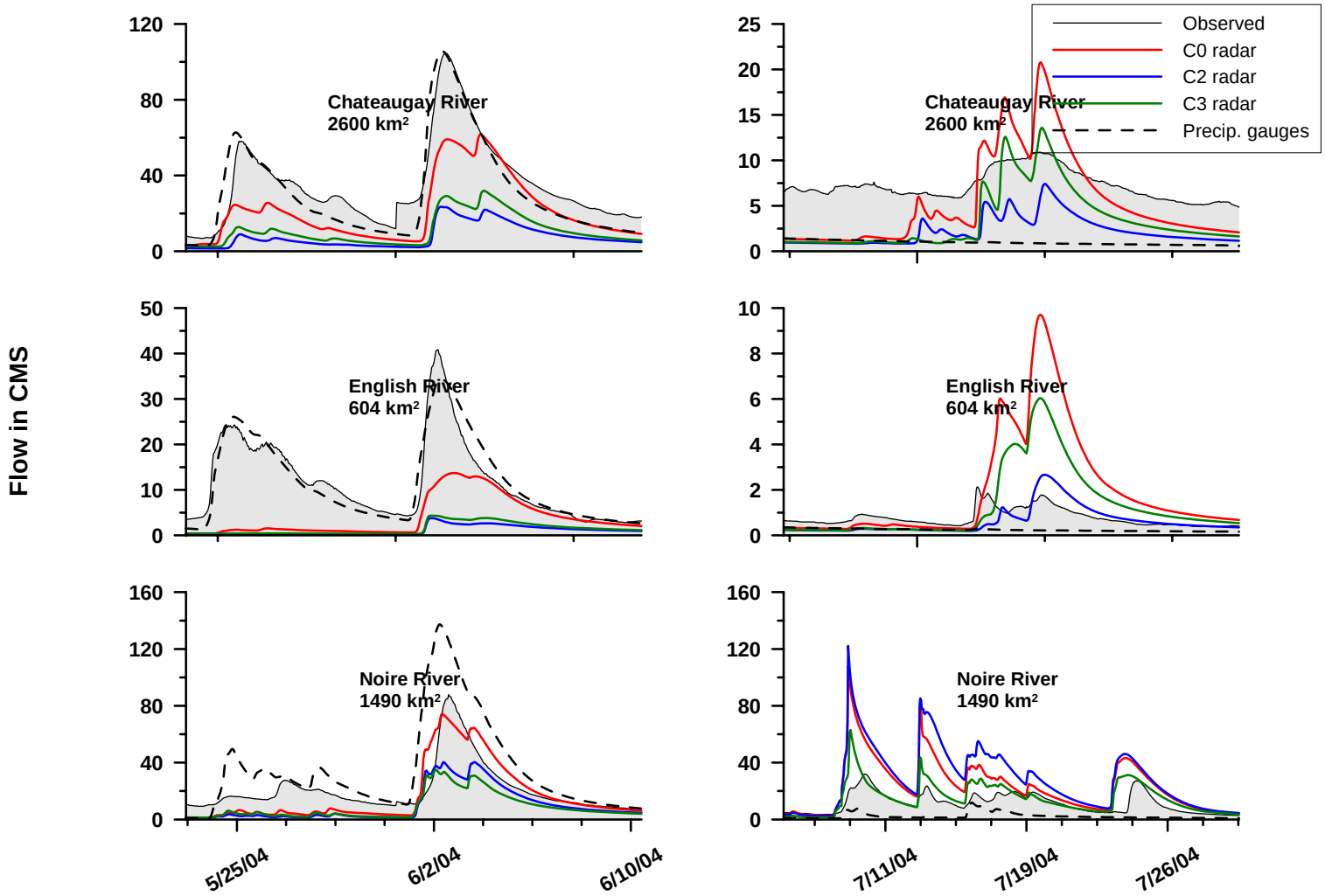

Figure D.18- Quebec, south of the St. Lawrence River, May 23rd to June 10th 2004

Figure D.19- Quebec, south of the St. Lawrence River, July 5th to July 30th 2004

Table D.22- Statistical criteria for Quebec, south of the St. Lawrence River, May 23rd to June 10th 2004

	Statistical Criteria							
	Nash	R^2	RMSE	RMSE/qbar	%Dv	APB	Bias	MAE
	PRECIP. GAUGES							
Chateauguay	0.82	0.89	9.55	0.27	-11.93	21.50	-4.23	7.62
English	0.90	0.90	2.78	0.24	0.69	17.81	0.08	2.10
Noire	-0.98	0.75	24.28	1.17	69.18	74.16	14.42	15.46
	C0 RADAR							
Chateauguay	0.38	0.78	17.50	0.49	-39.07	39.57	-13.85	14.02
English	-0.58	0.21	11.06	0.94	-66.71	66.76	-7.85	7.85
Noire	0.60	0.75	10.96	0.53	-18.69	42.10	-3.89	8.77
	C2 RADAR							
Chateauguay	-1.17	0.71	32.71	0.92	-78.21	78.21	-27.71	27.71
English	-1.40	0.14	13.64	1.16	-90.81	90.81	-10.68	10.68
Noire	0.23	0.64	15.10	0.73	-51.80	54.13	-10.80	11.28
	C3 RADAR							
Chateauguay	-0.74	0.69	29.31	0.83	-69.06	69.06	-24.47	24.47
English	-1.30	0.14	13.33	1.13	-88.01	88.01	-10.35	10.35
Noire	0.08	0.64	16.58	0.80	-58.19	59.83	-12.13	12.47

Table D.23- Statistical criteria for Quebec, south of the St. Lawrence River, July 5th to July 30th 2004

	Statistical Criteria							
	Nash	R^2	RMSE	RMSE/qbar	%Dv	APB	Bias	MAE
	PRECIP. GAUGES							
Chateauguay	-14.89	0.01	6.47	0.90	-86.81	86.81	-6.26	6.26
English	-1.85	0.03	0.65	0.85	-68.61	68.61	-0.52	0.52
Noire	-1.43	0.23	11.08	0.97	-79.15	79.15	-9.08	9.08
	C0 RADAR							
Chateauguay	-5.21	0.76	4.04	0.56	-24.79	49.25	-1.79	3.55
English	-39.16	0.54	2.42	3.18	155.50	188.23	1.19	1.44
Noire	-5.40	0.57	17.99	1.57	102.87	103.94	11.80	11.92
	C2 RADAR							
Chateauguay	-8.78	0.63	5.07	0.70	-68.92	68.92	-4.97	4.97
English	-0.68	0.36	0.50	0.65	-17.31	49.01	-0.13	0.37
Noire	-10.05	0.59	23.64	2.06	145.83	147.73	16.73	16.95
	C3 RADAR							
Chateauguay	-6.05	0.74	4.31	0.60	-52.20	55.00	-3.76	3.97
English	-12.60	0.46	1.41	1.85	69.80	122.49	0.53	0.93
Noire	-0.24	0.57	7.92	0.69	31.03	41.54	3.56	4.77

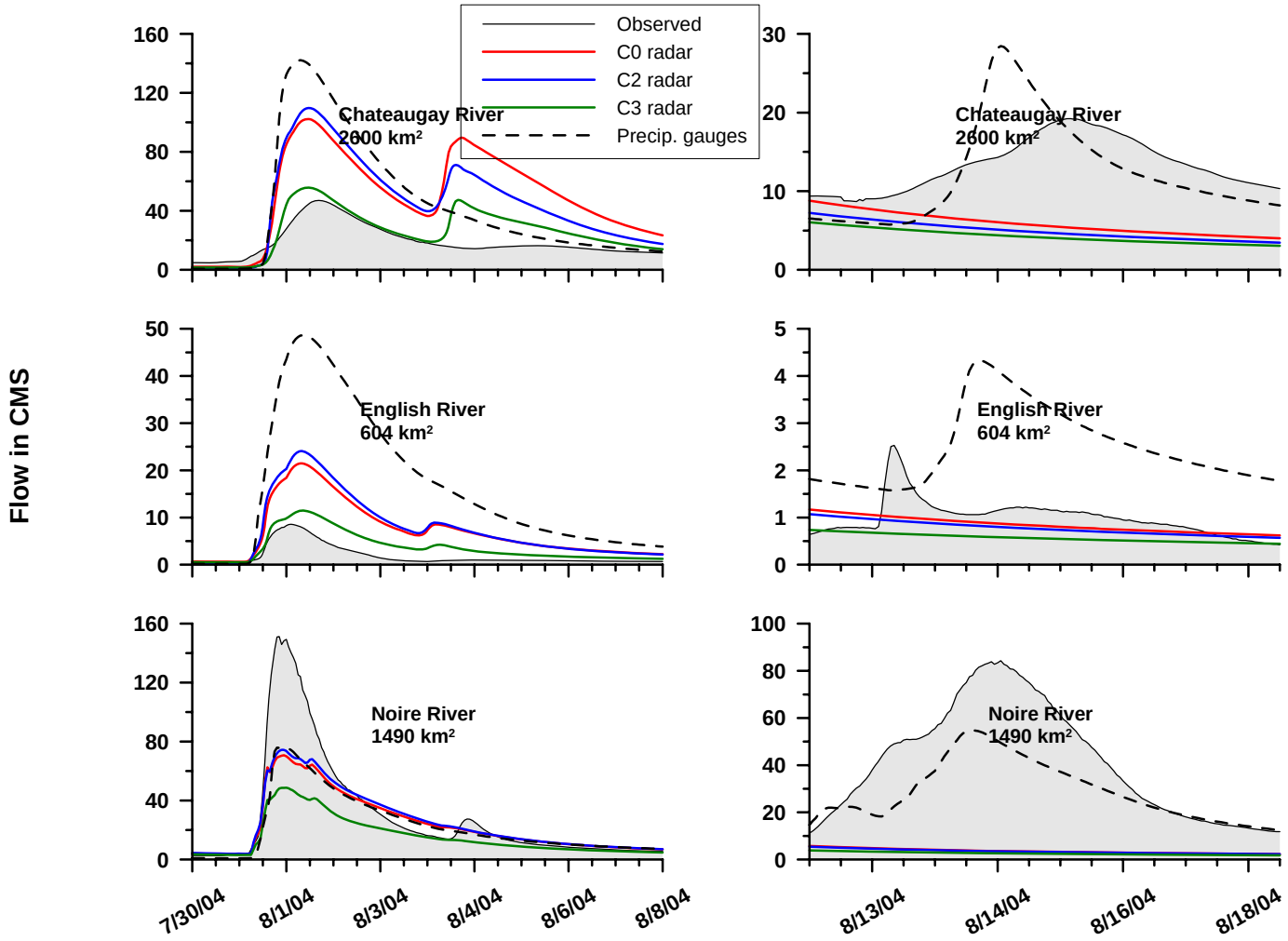

Figure D.20- Quebec, south of the St. Lawrence River, July 30th to August 8th 2004

Figure D.21- Quebec, south of the St. Lawrence River, August 12th to August 18th 2004

Table D.24- Statistical criteria for Quebec, south of the St. Lawrence River, July 30th to August 8th 2004

	Statistical Criteria							
	Nash	R^2	RMSE	RMSE/qbar	%Dv	APB	Bias	MAE
	PRECIP. GAUGES							
Chateauguay	-12.25	0.88	40.07	2.09	128.82	138.00	24.72	26.49
English	-81.60	0.71	19.73	10.59	790.48	794.70	14.74	14.81
Noire	0.69	0.88	21.01	0.70	-24.25	34.31	-7.24	10.24
	C0 RADAR							
Chateauguay	-11.40	0.55	38.78	2.02	164.64	171.18	31.60	32.85
English	-8.30	0.81	6.62	3.55	284.08	284.08	5.30	5.30
Noire	0.68	0.87	21.24	0.71	-19.60	33.03	-5.85	9.86
	C2 RADAR							
Chateauguay	-8.61	0.79	34.13	1.78	139.48	148.18	26.77	28.44
English	-11.03	0.82	7.53	4.04	312.82	314.59	5.83	5.87
Noire	0.71	0.86	20.26	0.68	-15.79	32.36	-4.71	9.66
	C3 RADAR							
Chateauguay	-0.14	0.61	11.74	0.61	36.24	45.42	6.96	8.72
English	-0.11	0.84	2.29	1.23	97.53	97.77	1.82	1.82
Noire	0.40	0.91	29.21	0.98	-47.76	48.06	-14.26	14.35

Table D.25- Statistical criteria for Quebec, south of the St. Lawrence River, August 12th to August 18th 2004

	Statistical Criteria							
	Nash	R^2	RMSE	RMSE/qbar	%Dv	APB	Bias	MAE
	PRECIP. GAUGES							
Chateauguay	-1.13	0.49	4.80	0.36	-7.06	29.30	-0.95	3.92
English	-18.93	0.02	1.72	1.72	149.04	155.67	1.49	1.56
Noire	0.43	0.88	17.85	0.43	-30.57	32.33	-12.81	13.54
	C0 RADAR							
Chateauguay	-5.82	0.25	8.58	0.64	-56.29	56.29	-7.53	7.53
English	-0.01	0.16	0.39	0.39	-15.78	29.28	-0.16	0.29
Noire	-2.64	0.04	44.93	1.07	-91.58	91.58	-38.37	38.37
	C2 RADAR							
Chateauguay	-7.03	0.24	9.31	0.70	-63.14	63.14	-8.45	8.45
English	-0.19	0.16	0.42	0.42	-22.73	32.07	-0.23	0.32
Noire	-2.66	0.05	45.03	1.08	-91.85	91.85	-38.48	38.48
	C3 RADAR							
Chateauguay	-8.05	0.23	9.89	0.74	-68.33	68.33	-9.14	9.14
English	-1.14	0.17	0.56	0.56	-43.50	43.75	-0.44	0.44
Noire	-2.78	0.06	45.77	1.09	-93.85	93.85	-39.32	39.32

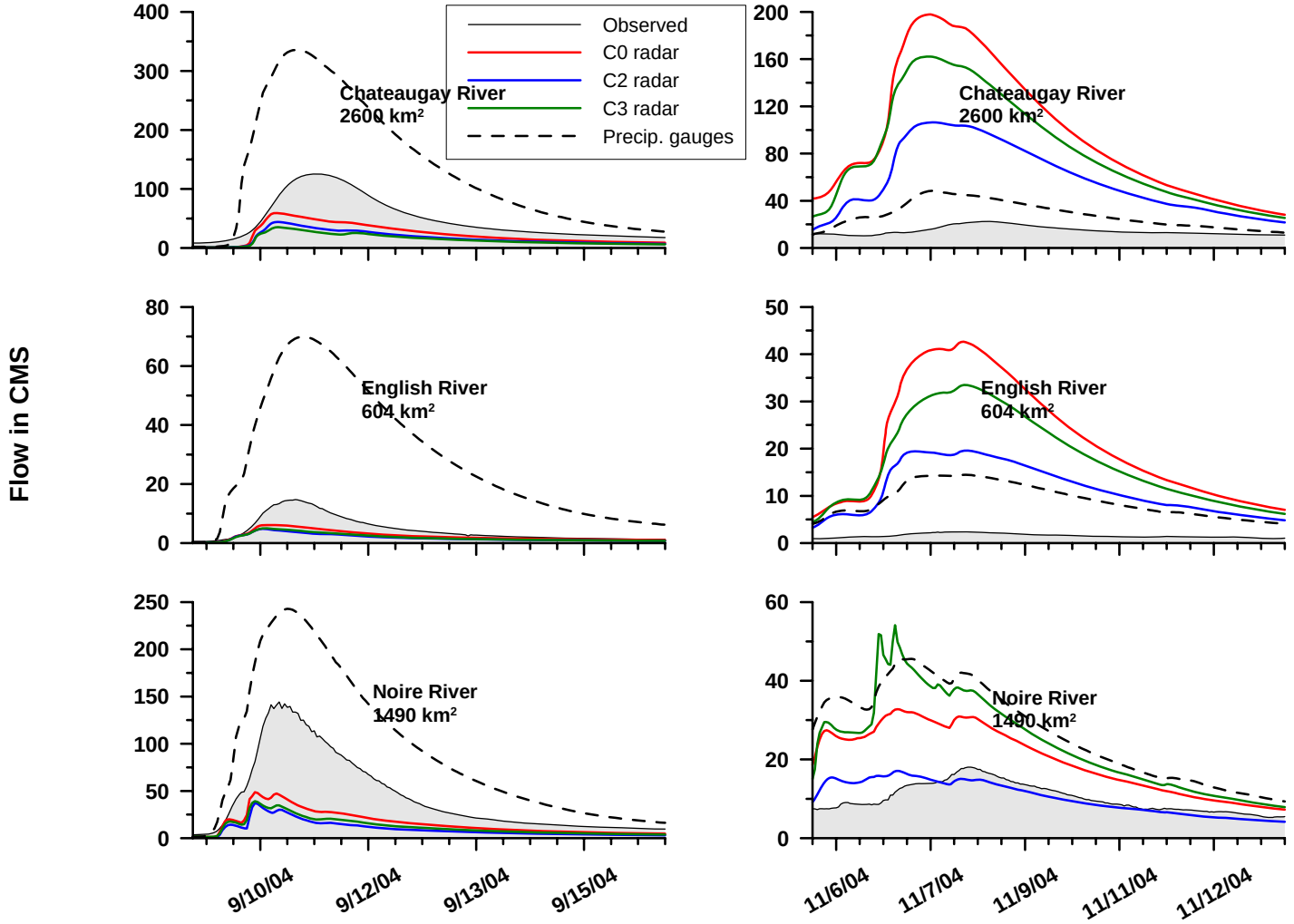

Figure D.22- Quebec, south of the St. Lawrence River, September 9th to September 16th 2004

Figure D.23- Quebec, south of the St. Lawrence River, November 5th to November 13th 2004

Table D.26- Statistical criteria for Quebec, south of the St. Lawrence River, September 9th to September 16th 2004

	Statistical Criteria							
	Nash	R^2	RMSE	RMSE/qbar	%Dv	APB	Bias	MAE
	PRECIP. GAUGES							
Chateauguay	-8.95	0.89	113.77	2.33	177.97	180.32	86.87	88.02
English	-54.77	0.88	30.55	6.68	542.17	542.45	24.80	24.82
Noire	-1.12	0.96	59.58	1.35	109.79	110.07	48.41	48.53
	C0 RADAR							
Chateauguay	0.14	0.85	33.42	0.69	-52.01	52.01	-25.39	25.39
English	0.34	0.91	3.34	0.73	-46.54	46.72	-2.13	2.14
Noire	0.00	0.88	40.91	0.93	-63.58	63.58	-28.03	28.03
	C2 RADAR							
Chateauguay	-0.31	0.83	41.20	0.84	-65.58	65.58	-32.01	32.01
English	-0.04	0.82	4.16	0.91	-61.43	61.52	-2.81	2.81
Noire	-0.38	0.81	48.09	1.09	-77.58	77.58	-34.21	34.21
	C3 RADAR							
Chateauguay	-0.52	0.81	44.49	0.91	-70.86	70.86	-34.59	34.59
English	0.07	0.88	3.95	0.86	-58.55	58.57	-2.68	2.68
Noire	-0.25	0.83	45.69	1.04	-72.22	72.22	-31.84	31.84

Table D.27- Statistical criteria for Quebec, south of the St. Lawrence River, November 5th to November 13th 2004

	Statistical Criteria							
	Nash	R^2	RMSE	RMSE/qbar	%Dv	APB	Bias	MAE
	PRECIP. GAUGES							
Chateauguay	-18.06	0.64	15.76	1.07	91.86	91.87	13.49	13.49
English	-379.97	0.92	8.12	5.21	484.09	484.09	7.54	7.54
Noire	-26.80	0.61	18.97	1.85	162.42	162.42	16.65	16.65
	C0 RADAR							
Chateauguay	-730.78	0.57	97.63	6.65	560.11	560.11	82.26	82.26
English	-Infinity	0.92	23.40	15.02	1288.98	1288.98	20.08	20.08
Noire	-9.29	0.61	11.54	1.13	96.46	96.46	9.89	9.89
	C2 RADAR							
Chateauguay	195.39	0.66	50.58	3.44	295.55	295.55	43.41	43.41
English	712.20	0.89	11.11	7.13	642.04	642.04	10.00	10.00
Noire	0.31	0.50	2.99	0.29	2.34	22.16	0.24	2.27
	C3 RADAR							
Chateauguay	-496.18	0.55	80.47	5.48	465.57	465.57	68.38	68.38
English	-Infinity	0.93	18.53	11.90	1045.44	1045.44	16.28	16.28
Noire	-21.08	0.55	16.90	1.65	136.73	136.73	14.02	14.02

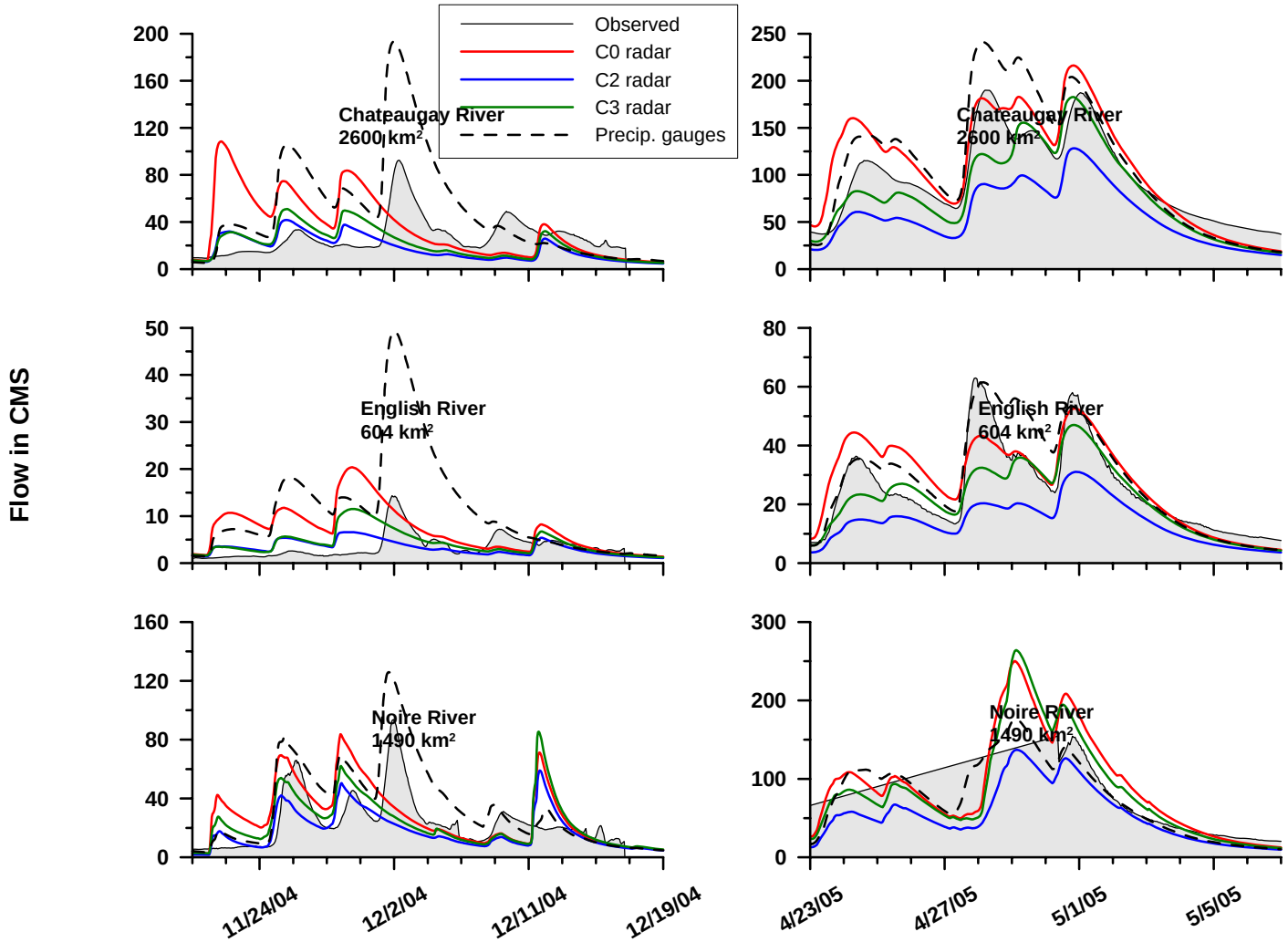

Figure D.24- Quebec, south of the St. Lawrence River, November 20th to December 19th 2004

Figure D.25- Quebec, south of the St. Lawrence River, April 23rd to May 7th 2005

Table D.28- Statistical criteria for Quebec, south of the St. Lawrence River, November 20th to December 19th 2004

	Statistical Criteria							
	Nash	R^2	RMSE	RMSE/qbar	%Dv	APB	Bias	MAE
	PRECIP. GAUGES							
Chateauguay	-4.72	0.56	41.34	1.62	94.63	120.51	24.21	30.84
English	-20.68	0.54	12.45	3.87	257.53	262.18	8.29	8.44
Noire	-0.15	0.78	19.81	0.89	56.07	64.26	12.55	14.39
	C0 RADAR							
Chateauguay	-2.95	0.00	34.33	1.34	37.88	101.66	9.69	26.01
English	-5.04	0.01	6.57	2.04	120.47	142.35	3.88	4.58
Noire	-0.21	0.24	20.28	0.91	24.22	65.74	5.42	14.72
	C2 RADAR							
Chateauguay	-0.52	0.00	21.28	0.83	-30.83	62.23	-7.89	15.92
English	-0.12	0.03	2.83	0.88	1.86	67.58	0.06	2.17
Noire	0.17	0.26	16.82	0.75	-19.98	49.25	-4.47	11.03
	C3 RADAR							
Chateauguay	-0.42	0.01	20.56	0.80	-12.28	62.80	-3.14	16.07
English	-0.64	0.09	3.42	1.06	41.05	77.51	1.32	2.49
Noire	-0.52	0.12	22.76	1.02	15.63	63.21	3.50	14.15

Table D.29- Statistical criteria for Quebec, south of the St. Lawrence River, April 23rd to May 7th 2005

	Statistical Criteria							
	Nash	R^2	RMSE	RMSE/qbar	%Dv	APB	Bias	MAE
	PRECIP. GAUGES							
Chateauguay	0.47	0.90	32.69	0.34	17.59	27.06	17.02	26.18
English	0.74	0.86	7.35	0.29	14.42	21.66	3.67	5.52
Noire	-	-	-	-	-	-	-	-
	C0 RADAR							
Chateauguay	0.62	0.83	27.83	0.29	14.51	22.16	14.04	21.44
English	0.68	0.73	8.20	0.32	11.39	25.03	2.90	6.38
Noire	-	-	-	-	-	-	-	-
	C2 RADAR							
Chateauguay	0.09	0.88	43.03	0.45	-39.85	39.85	-38.56	38.56
English	0.02	0.74	14.29	0.56	-43.43	43.43	-11.06	11.06
Noire	-	-	-	-	-	-	-	-
	C3 RADAR							
Chateauguay	0.63	0.68	27.33	0.28	1.08	19.93	1.04	19.28
English	0.68	0.68	8.17	0.32	-0.94	22.37	-0.24	5.70
Noire	-	-	-	-	-	-	-	-

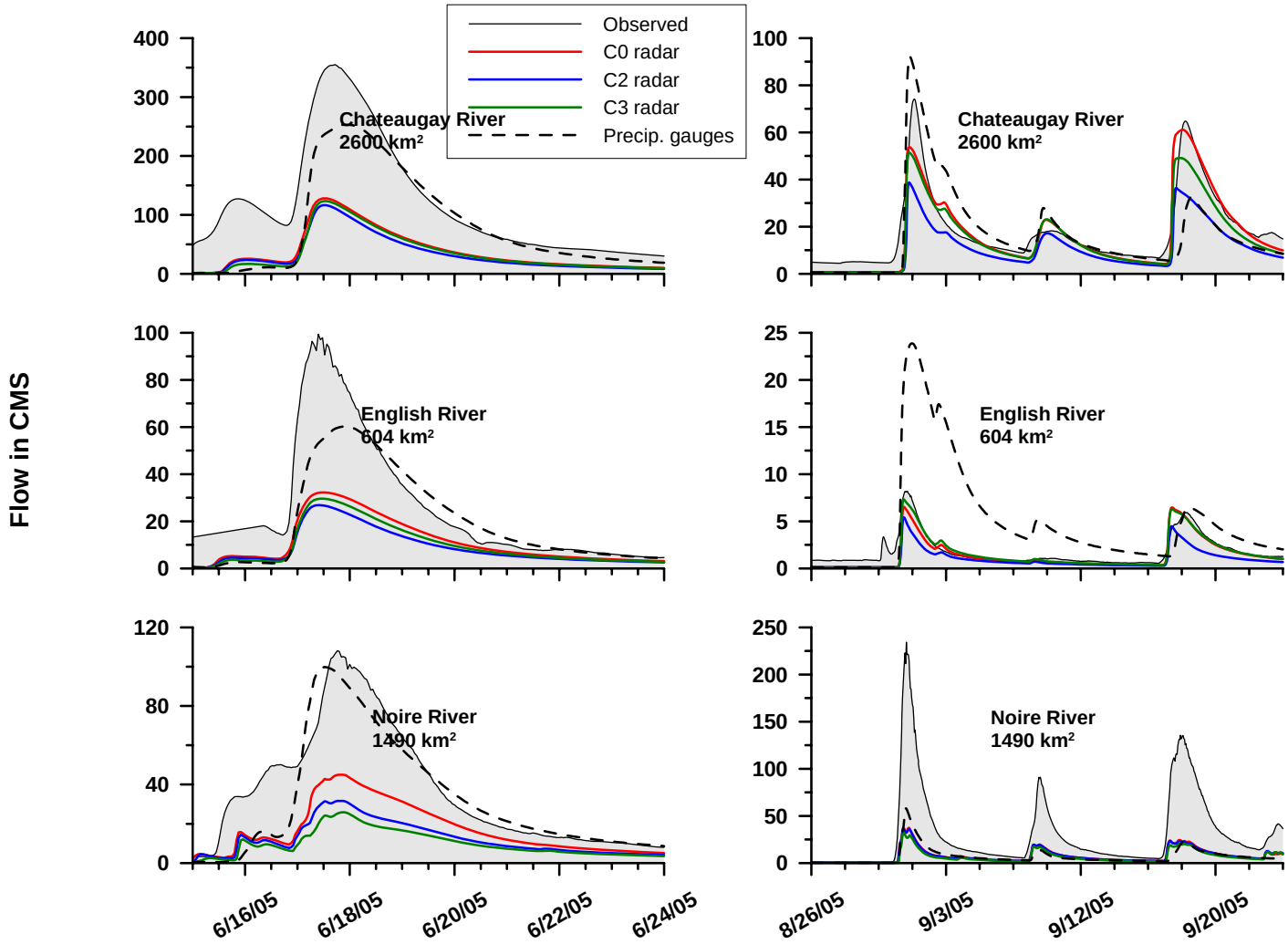

Figure D.26- Quebec, south of the St. Lawrence River, June 15th to June 24th 2005

Figure D.27- Quebec, south of the St. Lawrence River, August 26th to September 24th 2005

Table D.30- Statistical criteria for Quebec, south of the St. Lawrence River, June 15th to June 24th 2005

	Statistical Criteria							
	Nash	R^2	RMSE	RMSE/qbar	%Dv	APB	Bias	MAE
	PRECIP. GAUGES							
Chateauguay	0.62	0.77	59.04	0.49	-31.06	33.80	-37.48	40.77
English	0.69	0.74	14.71	0.56	-22.73	35.60	-5.93	9.28
Noire	0.78	0.81	13.83	0.37	-12.85	24.60	-4.77	9.14
	C0 RADAR							
Chateauguay	-0.16	0.93	103.53	0.86	-68.05	68.05	-82.09	82.09
English	0.24	0.90	22.89	0.88	-56.95	56.95	-14.85	14.85
Noire	0.17	0.87	27.09	0.73	-53.37	53.54	-19.84	19.90
	C2 RADAR							
Chateauguay	-0.32	0.93	110.20	0.91	-72.65	72.65	-87.65	87.65
English	0.03	0.93	25.79	0.99	-66.46	66.46	-17.32	17.32
Noire	-0.24	0.88	33.08	0.89	-66.52	66.62	-24.72	24.76
	C3 RADAR							
Chateauguay	-0.24	0.90	107.02	0.89	-70.61	70.61	-85.19	85.19
English	0.13	0.90	24.46	0.94	-62.62	62.62	-16.32	16.32
Noire	-0.47	0.87	36.00	0.97	-73.07	73.07	-27.16	27.16

Table D.31- Statistical criteria for Quebec, south of the St. Lawrence River, August 26th to September 24th 2005

	Statistical Criteria							
	Nash	R^2	RMSE	RMSE/qbar	%Dv	APB	Bias	MAE
	PRECIP. GAUGES							
Chateauguay	0.41	0.57	11.94	0.66	-7.30	44.44	-1.33	8.07
English	-10.93	0.40	5.65	3.17	170.76	198.50	3.04	3.54
Noire	0.02	0.86	41.70	1.34	-77.03	77.03	-24.00	24.00
	C0 RADAR							
Chateauguay	0.85	0.87	6.07	0.34	-8.75	21.42	-1.59	3.89
English	0.77	0.82	0.79	0.44	-21.19	28.22	-0.38	0.50
Noire	0.00	0.94	42.10	1.35	-76.01	76.01	-23.68	23.68
	C2 RADAR							
Chateauguay	0.53	0.86	10.66	0.59	-41.47	41.76	-7.53	7.58
English	0.48	0.81	1.18	0.66	-46.57	46.91	-0.83	0.84
Noire	-0.01	0.93	42.36	1.36	-76.43	76.43	-23.82	23.82
	C3 RADAR							
Chateauguay	0.82	0.87	6.58	0.36	-18.47	25.46	-3.35	4.62
English	0.82	0.85	0.70	0.40	-14.62	24.97	-0.26	0.45
Noire	-0.08	0.92	43.83	1.41	-80.00	80.00	-24.93	24.93

Table D.32- Quebec, south of the St. Lawrence River event summary, best-performing precipitation product

	Apr 14 to May 1/03				Apr 13 to Apr 30/04				May 23 to Jun 10/04				Jul 5 to Jul 30/04			
	RAG	C0	C2	C3	RAG	C0	C2	C3	RAG	C0	C2	C3	RAG	C0	C2	C3
Chateauguay	X					X			X					X		
English			X		X				X				X			
Noire	X						X			X						X

	Jul 30 to Aug 8/04				Aug 12 to Aug 18/04				Sept 9 to Sept 16/04				Nov 5 to Nov 13/04			
	RAG	C0	C2	C3	RAG	C0	C2	C3	RAG	C0	C2	C3	RAG	C0	C2	C3
Chateauguay				X	X					X			X			
English				X		X				X			X			
Noire	X				X					X					X	

	Nov 20 to Dec 19/04				Apr 23 to May 7/05				Jun 15 to Jun 24/05				Aug 26 to Sept 24/05			
	RAG	C0	C2	C3	RAG	C0	C2	C3	RAG	C0	C2	C3	RAG	C0	C2	C3
Chateauguay			X					X	X					X		
English			X		X				X							X
Noire			X						X				X			

	SUM			
	RAG	C0	C2	C3
Chateauguay	5	4	1	2
English	6	2	2	2
Noire	5	2	3	1
	16	**8**	**6**	**5**

Table D.33- Quebec, south of the St. Lawrence River event summary, best-performing radar precipitation product

	Apr 14 to May 1/03			Sept 26 to Dec 31/03			Apr 13 to Apr 30/04			May 23 to Jun 10/04			Jul 5 to Jul 30/04		
	C0	C2	C3	C0	C2	C3	C0	C2	C3	C0	C2	C3	C0	C2	C3
Chateauguay			X		X		X			X			X		
English		X			X				X	X				X	
Noire		X			X			X		X					X

	Jul 30 to Aug 8/04			Aug 12 to Aug 18/04			Sept 9 to Sept 16/04			Nov 5 to Nov 13/04			Nov 20 to Dec 19/04		
	C0	C2	C3	C0	C2	C3	C0	C2	C3	C0	C2	C3	C0	C2	C3
Chateauguay			X	X			X				X			X	
English			X	X			X				X			X	
Noire		X		X			X				X			X	

	Apr 23 to May 7/05			Jun 15 to Jun 24/05			Aug 26 to Sept 24/05			SUM		
	C0	C2	C3	C0	C2	C3	C0	C2	C3	C0	C2	C3
Chateauguay			X	X			X			7	3	3
English			X	X					X	4	5	4
Noire	-	-	-	X			X			5	6	1
										16	**14**	**8**

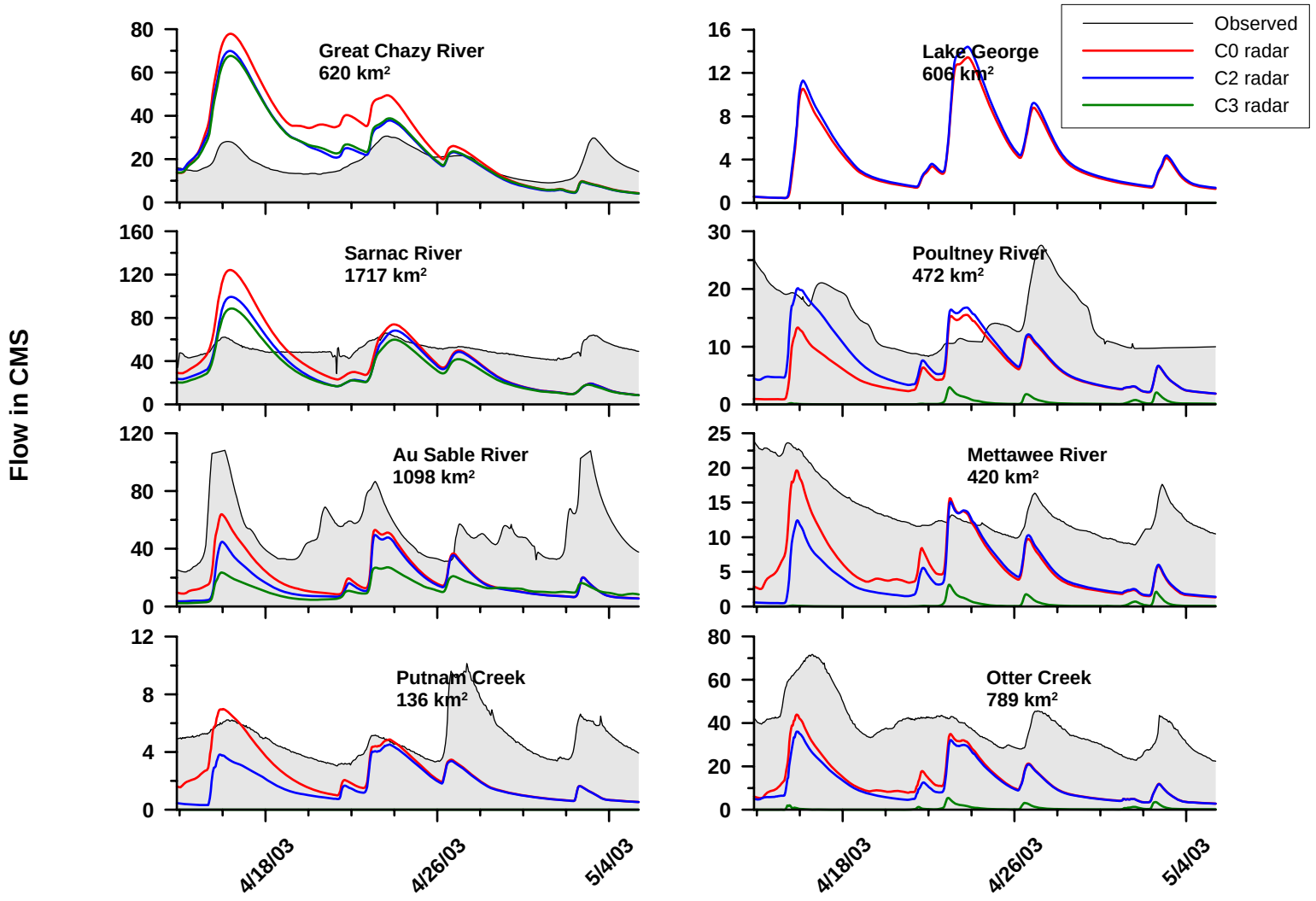

Figure D.28- Lake Champlain Basin, April 14th to May 5th 2003

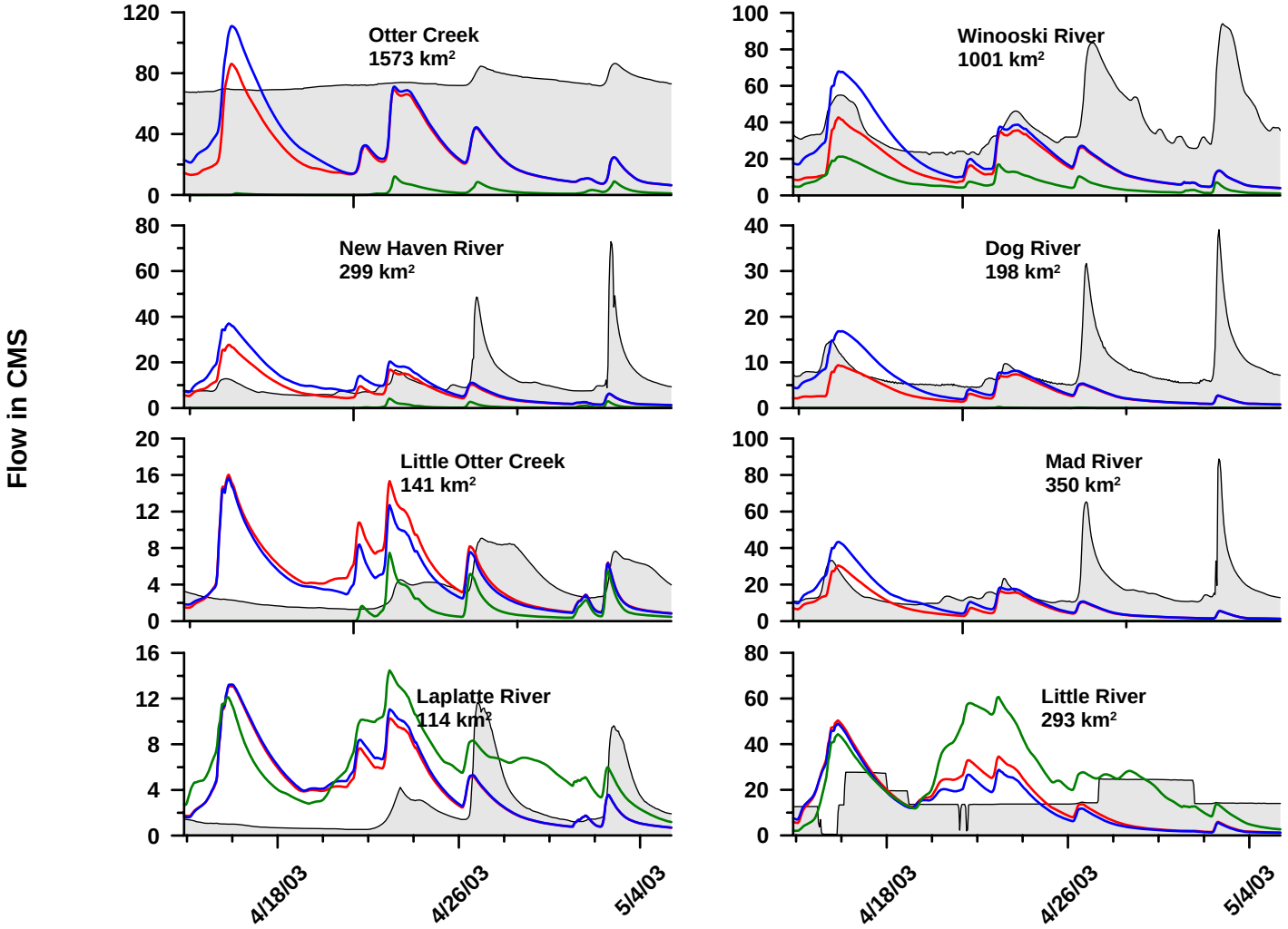

Figure D.29- Lake Champlain Basin, April 14th to May 5th 2003 (continued)

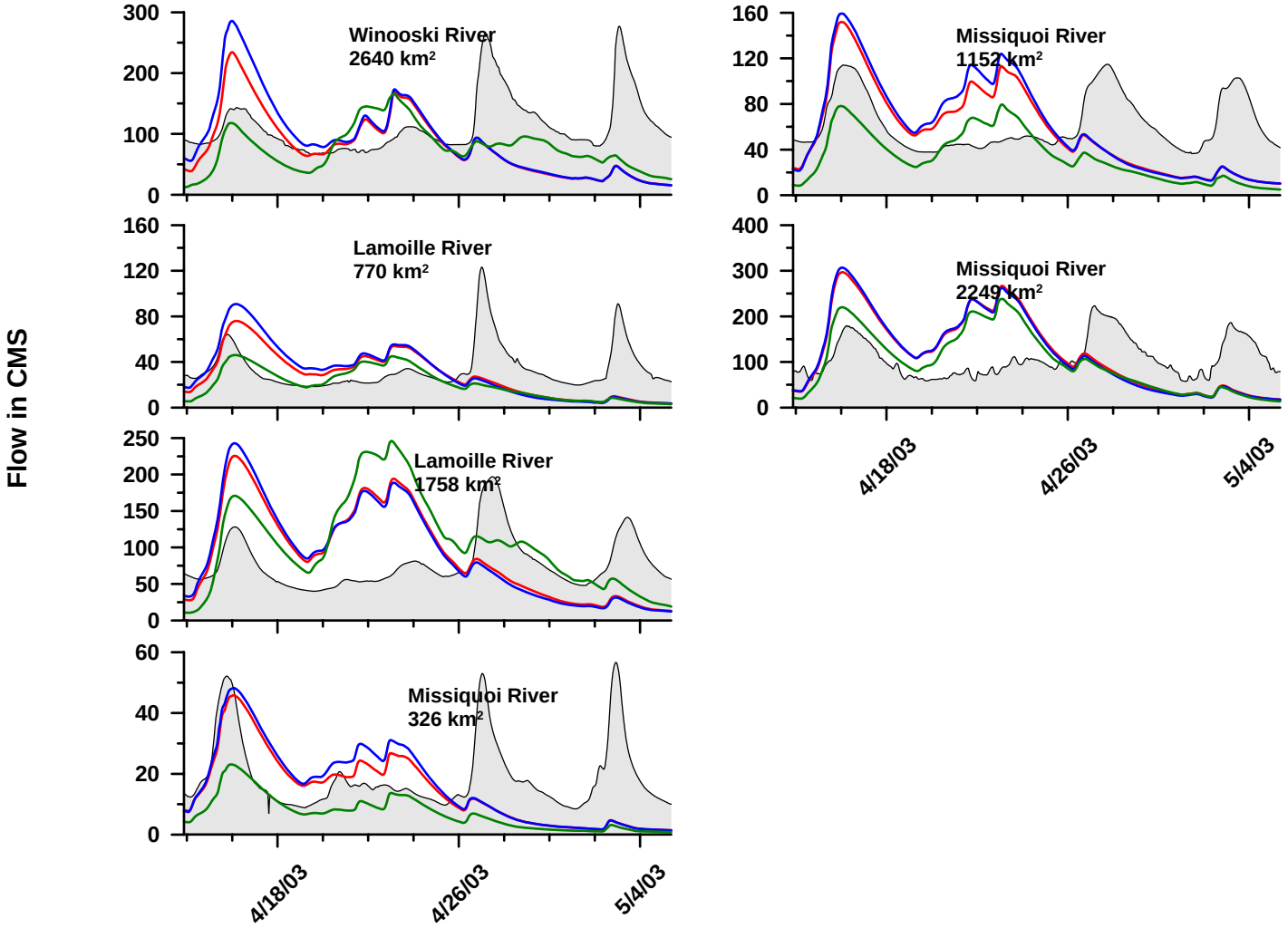

Figure D.30- Lake Champlain Basin, April 14th to May 5th 2003 (continued)

Table D.34- Lake Champlain Basin, April 14th to May 5th 2003

	Statistical Criteria							
	Nash	R^2	RMSE	RMSE/qbar	%Dv	APB	Bias	MAE
	C0 RADAR							
Great Chazy River	-10.74	0.24	20.58	1.13	57.99	84.83	10.57	15.46
Saranac River	-19.74	0.22	28.24	0.55	-18.73	45.60	-9.56	23.26
Ausable	-2.39	0.22	38.23	0.72	-62.24	62.34	-33.17	33.22
Putnam Creek	-3.35	0.09	3.16	0.64	-51.34	52.57	-2.55	2.61
Lake George	-	-	-	-	-	-	-	-
Poultney River	-3.03	0.03	10.36	0.72	-59.35	63.26	-8.50	9.06
Mettawee River	-4.29	0.23	9.09	0.66	-58.27	59.25	-8.08	8.21
Otter Creek (789 km^2)	-4.58	0.50	27.20	0.70	-66.34	66.34	-25.90	25.90
Otter Creek (1573 km^2)	142.75	0.04	50.78	0.69	-62.92	64.04	-46.29	47.11
New Haven River	-0.71	0.00	11.78	1.00	-36.09	64.57	-4.25	7.61
Little Otter Creek	-4.44	0.11	5.24	1.39	37.92	114.34	1.43	4.30
Laplatte River	-2.58	0.03	4.76	1.97	78.05	156.20	1.89	3.78
Winooski River	-2.14	0.02	30.43	0.76	-59.78	59.78	-24.03	24.03
Dog River	-1.09	0.02	7.57	0.88	-61.69	61.80	-5.29	5.30
Mad River	-0.90	0.02	15.68	0.90	-55.77	61.34	-9.68	10.65
Little River	-	-	-	-	-	-	-	-
Winooski River	-1.84	0.00	78.74	0.70	-28.25	53.09	-31.90	59.97
Lamoille River(770 km^2)	-1.10	0.00	27.90	0.82	-16.53	64.79	-5.64	22.11
Lamoille River (1758 km^2)	-3.50	0.00	74.54	0.96	18.83	84.78	14.68	66.09
Missisquoi River(326 km^2)	-0.70	0.05	15.05	0.79	-22.69	60.68	-4.32	11.56
Missisquoi River (1152 km^2)	-1.96	0.03	41.37	0.66	-9.35	57.75	-5.84	36.09
Missisquoi River (2249 km^2)	-3.94	0.00	93.13	0.86	12.46	76.18	13.49	82.47
	C2 RADAR							
Great Chazy River	-5.98	0.24	15.87	0.87	30.81	60.29	5.61	10.99
Saranac River	-16.71	0.26	26.10	0.51	-30.05	44.66	-15.32	22.78
Ausable	-3.00	0.17	41.51	0.78	-69.09	69.15	-36.82	36.85
Putnam Creek	-4.50	0.11	3.56	0.72	-64.31	64.31	-3.19	3.19
Lake George	-	-	-	-	-	-	-	-
Poultney River	-2.00	0.12	8.94	0.62	-47.66	53.46	-6.83	7.66
Mettawee River	-6.15	0.01	10.57	0.76	-66.76	67.69	-9.25	9.38
Otter Creek (789 km^2)	-5.37	0.39	29.05	0.74	-70.70	70.70	-27.60	27.60
Otter Creek (1573 km^2)	-132.77	0.12	48.99	0.67	-56.25	61.34	-41.38	45.12
New Haven River	-1.08	0.01	12.99	1.10	-15.58	77.86	-1.84	9.17

Little Otter Creek	-3.27	0.09	4.64	1.24	19.46	99.94	0.73	3.76
Laplatte River	-2.90	0.04	4.97	2.05	86.15	163.49	2.09	3.96
Winooski River	-1.96	0.00	29.52	0.73	-46.41	55.36	-18.66	22.25
Dog River	-1.01	0.01	7.42	0.87	-44.76	58.90	-3.84	5.05
Mad River	-0.98	0.01	15.99	0.92	-40.58	63.50	-7.04	11.02
Little River	-	-	-	-	-	-	-	-
Winooski River	-2.27	0.01	84.46	0.75	-19.31	59.70	-21.81	67.43
Lamoille River(770 km^2)	-1.49	0.00	30.36	0.89	-9.60	72.38	-3.28	24.70
Lamoille River (1758 km^2)	-3.83	0.00	77.22	0.99	19.19	88.18	14.96	68.74
Missisquoi River(326 km^2)	-0.86	0.04	15.76	0.83	-15.36	66.47	-2.93	12.67
Missisquoi River (1152 km^2)	-2.50	0.02	44.98	0.72	-3.51	63.79	-2.19	39.87
Missisquoi River (2249 km^2)	-4.14	0.00	94.97	0.88	11.71	77.95	12.68	84.39
	C3 RADAR							
Great Chazy River	-5.61	0.24	15.44	0.85	31.42	59.83	5.72	10.90
Saranac River	-16.79	0.26	26.16	0.51	-36.83	46.13	-18.79	23.53
Ausable	-3.78	0.19	45.41	0.85	-77.47	77.47	-41.29	41.29
Putnam Creek	-10.70	0.01	5.18	1.05	-99.96	99.96	-4.96	4.96
Lake George	-	-	-	-	-	-	-	-
Poultney River	-7.40	0.02	14.97	1.05	-97.84	97.84	-14.01	14.01
Mettawee River	-11.86	0.01	14.18	1.02	-98.04	98.04	-13.59	13.59
Otter Creek (789 km^2)	-11.19	0.00	40.21	1.03	-98.64	98.64	-38.51	38.51
Otter Creek (1573 km^2)	285.61	0.38	71.71	0.98	-97.36	97.36	-71.63	71.63
New Haven River	-1.51	0.25	14.28	1.21	-96.23	96.23	-11.34	11.34
Little Otter Creek	-1.50	0.10	3.55	0.95	-73.10	78.17	-2.75	2.94`
Laplatte River	-3.59	0.00	5.39	2.22	157.75	191.26	3.82	4.63
Winooski River	-3.85	0.00	37.81	0.94	-83.07	83.07	-33.39	33.39
Dog River	-2.67	0.11	10.03	1.17	-99.83	99.83	-8.56	8.56
Mad River	-2.33	0.00	20.75	1.20	-99.98	99.98	-17.35	17.35
Little River	-	-	-	-	-	-	-	-
Winooski River	-1.18	0.00	68.91	0.61	-31.63	46.77	-35.73	52.82
Lamoille River(770 km^2)	-0.96	0.00	26.92	0.79	-38.57	55.41	-13.16	18.91
Lamoille River (1758 km^2)	-3.78	0.00	76.85	0.99	37.85	76.95	29.50	59.98
Missisquoi River(326 km^2)	-1.02	0.08	16.42	0.86	-62.67	62.88	-11.94	11.98
Missisquoi River (1152 km^2)	-2.02	0.01	41.78	0.67	-45.66	55.15	-28.53	34.47
Missisquoi River (2249 km^2)	-2.56	0.00	79.10	0.73	-6.23	61.55	-6.74	66.63

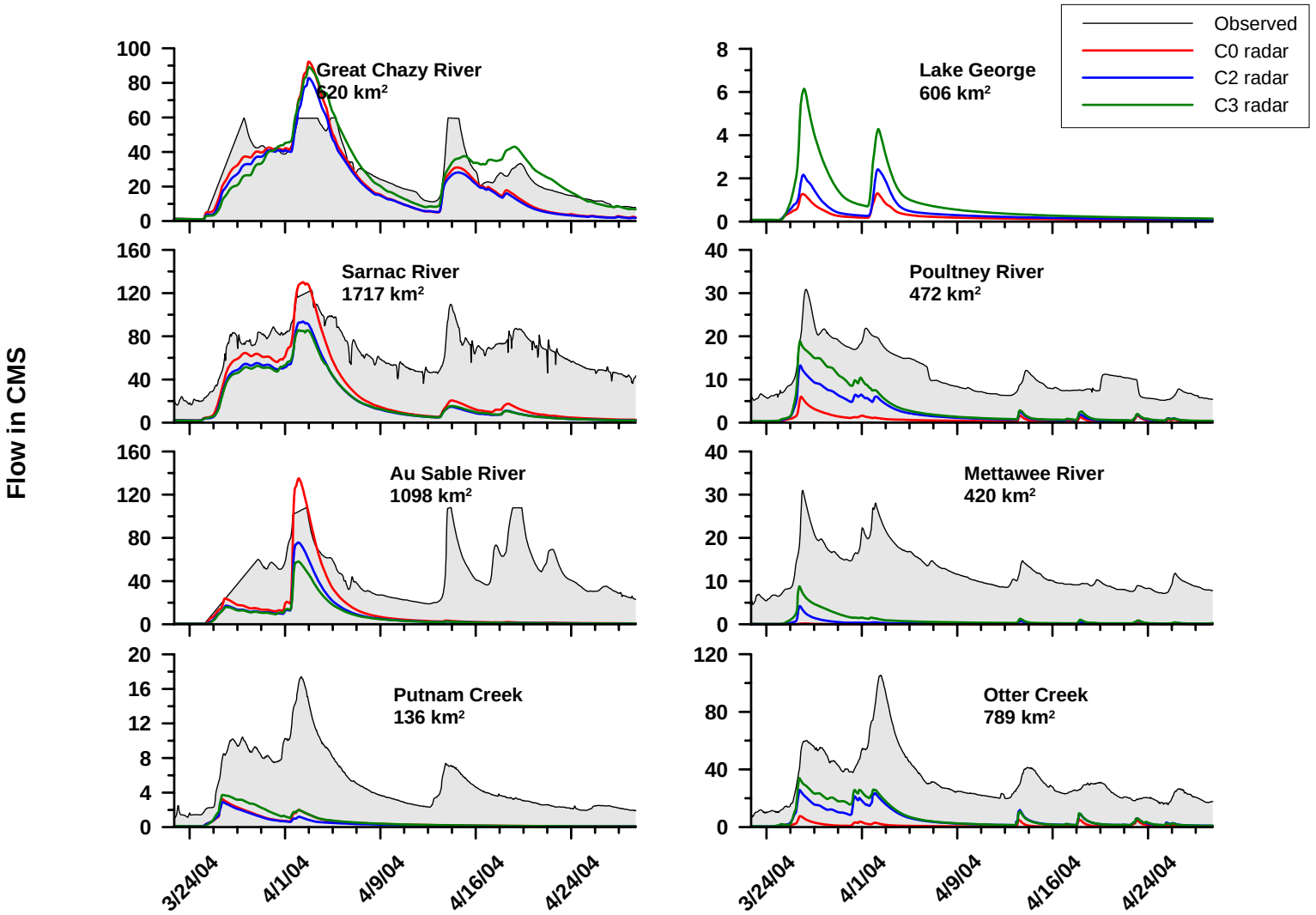

Figure D.31- Lake Champlain Basin, March 23rd to April 30th 2004

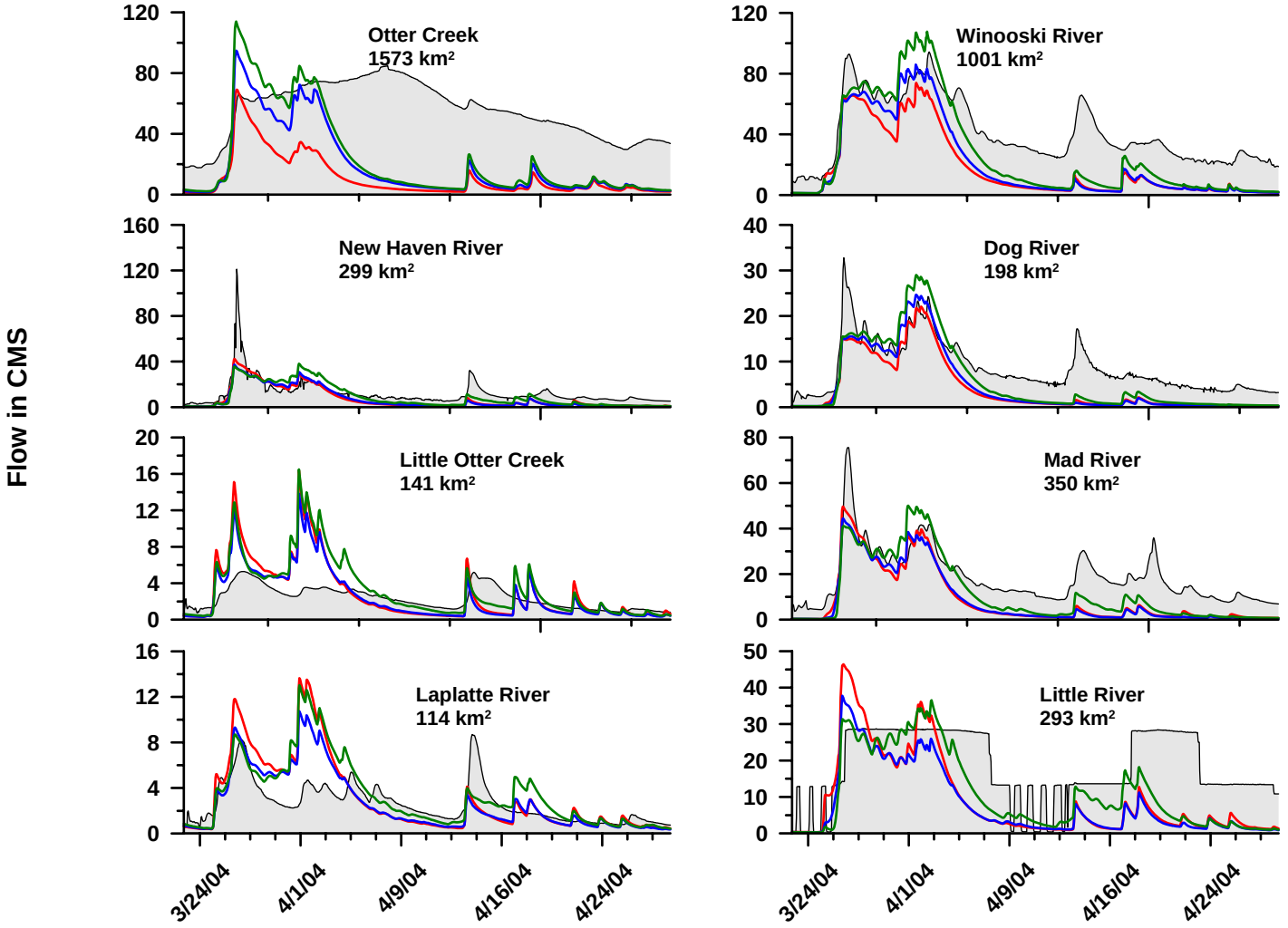

Figure D.32- Lake Champlain Basin, March 23rd to April 30th 2004 (continued)

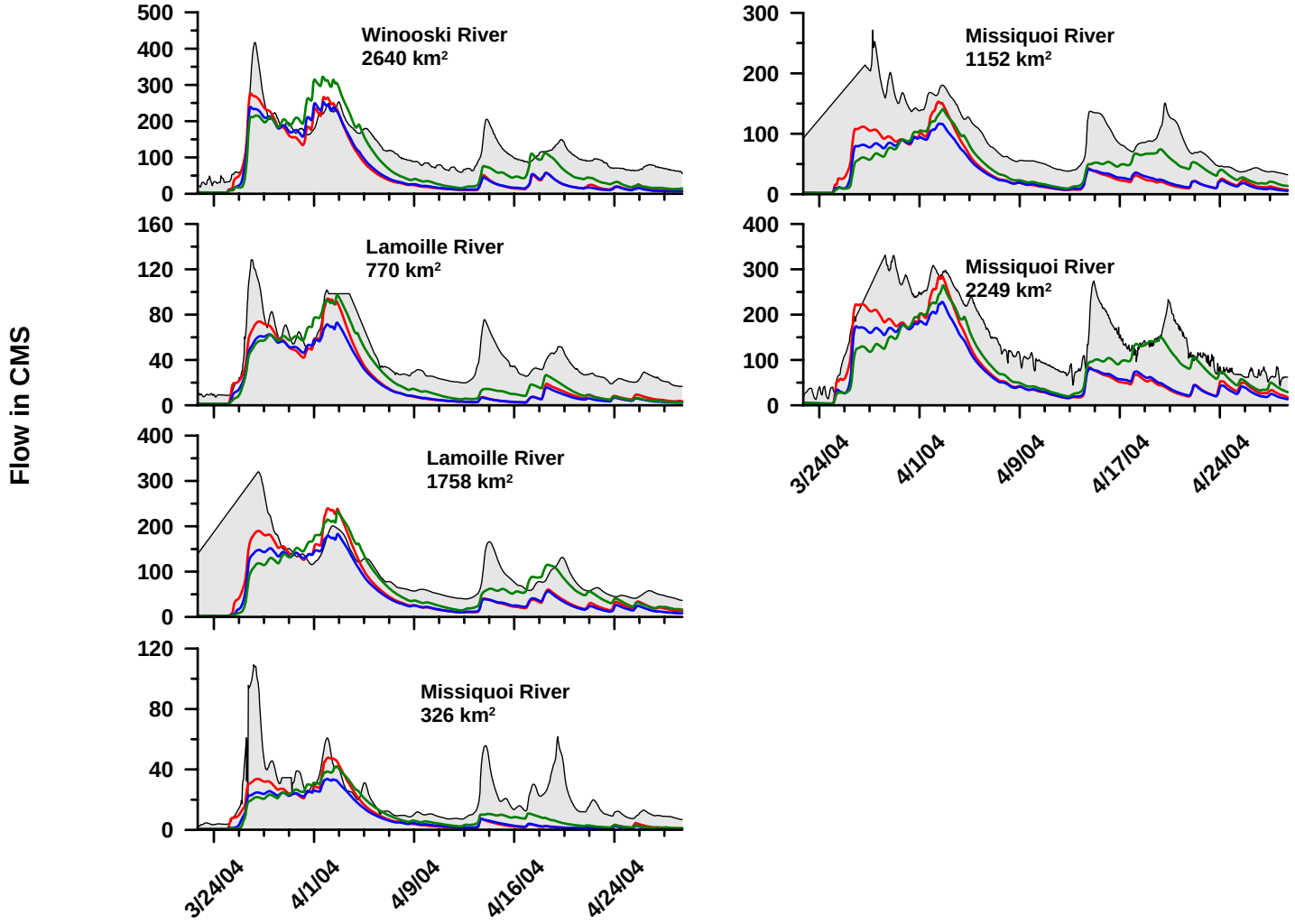

Figure D.33- Lake Champlain Basin, March 23rd to April 30th 2004 (continued)

Table D.35- Statistical criteria for Lake Champlain Basin, March 23rd to April 30th 2004

	Statistical Criteria							
	Nash	R^2	RMSE	RMSE/qbar	%Dv	APB	Bias	MAE
	C0 RADAR							
Great Chazy River	-	-	-	-	-	-	-	-
Saranac River	-	-	-	-	-	-	-	-
Ausable	-1.30	0.24	41.21	0.92	-70.40	73.71	-31.41	32.89
Putnam Creek	-1.41	0.58	5.45	1.07	-89.25	89.25	-4.53	4.53
Lake George	-	-	-	-	-	-	-	-
Poultney River	-3.11	0.60	11.21	1.03	-92.88	92.88	-10.10	10.10
Mettawee River	-5.62	0.04	13.25	1.08	-99.72	99.72	-12.21	12.21
Otter Creek (789 km^2)	-2.81	0.18	35.62	1.11	-96.22	96.22	-30.88	30.88
Otter Creek (1573 km^2)	-5.88	0.09	48.37	0.88	-80.24	80.47	-44.25	44.38
New Haven River	0.42	0.63	8.70	0.71	-42.90	49.96	-5.23	6.09
Little Otter Creek	-3.92	0.38	2.73	1.17	22.52	76.15	0.53	1.78
Laplatte River	-1.17	0.41	2.57	0.98	16.85	64.85	0.44	1.69
Winooski River	-0.37	0.78	25.41	0.62	-56.73	56.73	-23.15	23.15
Dog River	0.15	0.78	5.22	0.61	-51.89	53.33	-4.42	4.54
Mad River	0.05	0.76	11.55	0.63	-52.55	54.11	-9.71	9.99
Little River	-	-	-	-	-	-	-	-
Winooski River	0.06	0.79	66.94	0.55	-46.11	48.58	-56.06	59.07
Lamoille River(770 km^2)	0.19	0.77	24.16	0.58	-48.70	48.99	-20.37	20.49
Lamoille River (1758 km^2)	-	-	-	-	-	-	-	-
Missisquoi River(326 km^2)	0.05	0.46	18.39	0.83	-54.89	57.04	-12.12	12.59
Missisquoi River (1152 km^2)	-	-	-	-	-	-	-	-
Missisquoi River (2249 km^2)	0.07	0.75	80.67	0.54	-45.85	46.27	-68.89	69.51
	C2 RADAR							
Great Chazy River	-	-	-	-	-	-	-	-
Saranac River	-	-	-	-	-	-	-	-
Ausable	-1.53	0.23	43.22	0.97	-80.79	80.96	-36.04	36.12
Putnam Creek	-1.55	0.42	5.60	1.10	-91.06	91.06	-4.62	4.62
Lake George	-	-	-	-	-	-	-	-
Poultney River	-1.78	0.83	9.23	0.85	-79.48	79.48	-8.64	8.64
Mettawee River	-5.24	0.37	12.87	1.05	-97.34	97.34	-11.92	11.92
Otter Creek (789 km^2)	-1.68	0.69	29.88	0.93	-82.80	82.80	-26.57	26.57

Otter Creek (1573 km^2)	-4.46	0.16	43.09	0.78	-65.70	68.96	-36.23	38.03
New Haven River	0.34	0.56	9.30	0.76	-43.52	52.58	-5.31	6.41
Little Otter Creek	-2.43	0.37	2.28	0.97	9.73	65.84	0.23	1.54
Laplatte River	-0.32	0.41	2.00	0.77	2.54	52.75	0.07	1.38
Winooski River	-0.20	0.78	23.72	0.58	-49.91	51.40	-20.37	20.97
Dog River	0.17	0.75	5.15	0.61	-45.37	52.04	-3.86	4.43
Mad River	-0.01	0.73	11.93	0.65	-54.09	55.58	-9.99	10.27
Little River	-	-	-	-	-	-	-	-
Winooski River	0.02	0.76	68.39	0.56	-46.83	49.57	-56.94	60.27
Lamoille River(770 km^2)	0.00	0.74	26.76	0.64	-54.93	55.17	-22.97	23.08
Lamoille River (1758 km^2)	-	-	-	-	-	-	-	-
Missisquoi River(326 km^2)	-0.12	0.44	19.88	0.90	-62.53	62.59	-13.80	13.81
Missisquoi River (1152 km^2)	-	-	-	-	-	-	-	-
Missisquoi River (2249 km^2)	-0.08	0.81	87.00	0.58	-51.85	51.85	-77.91	77.91
	C3 RADAR							
Great Chazy River	-	-	-	-	-	-	-	-
Saranac River	-	-	-	-	-	-	-	-
Ausable	-1.65	0.23	44.23	0.99	-83.48	83.62	-37.24	37.31
Putnam Creek	-1.26	0.51	5.27	1.04	-86.41	86.41	-4.38	4.38
Lake George	-	-	-	-	-	-	-	-
Poultney River	-1.12	0.81	8.05	0.74	-70.47	70.47	-7.66	7.66
Mettawee River	-4.55	0.48	12.14	0.99	-92.63	92.63	-11.34	11.34
Otter Creek (789 km^2)	-1.41	0.61	28.30	0.88	-78.55	78.55	-25.21	25.21
Otter Creek (1573 km^2)	-4.23	0.16	42.16	0.76	-58.51	67.10	-32.26	37.00
New Haven River	0.37	0.48	9.07	0.74	-26.19	50.14	-3.19	6.11
Little Otter Creek	-4.18	0.38	2.80	1.20	41.56	71.72	0.97	1.68
Laplatte River	-0.93	0.37	2.42	0.93	28.42	56.60	0.74	1.48
Winooski River	0.08	0.81	20.84	0.51	-35.65	45.03	-14.55	18.38
Dog River	0.24	0.74	4.95	0.58	-32.90	50.32	-2.80	4.28
Mad River	0.24	0.70	10.37	0.56	-37.98	47.72	-7.01	8.81
Little River	-	-	-	-	-	-	-	-
Winooski River	0.30	0.72	57.92	0.48	-27.61	41.39	-33.57	50.33
Lamoille River(770 km^2)	0.33	0.73	21.98	0.53	-40.11	43.21	-16.78	18.07
Lamoille River (1758 km^2)	-	-	-	-	-	-	-	-
Missisquoi River(326 km^2)	-0.01	0.36	18.90	0.86	-51.95	54.78	-11.47	12.09
Missisquoi River (1152 km^2)	-	-	-	-	-	-	-	-
Missisquoi River (2249 km^2)	0.27	0.75	71.41	0.48	-37.89	38.31	-56.93	57.56

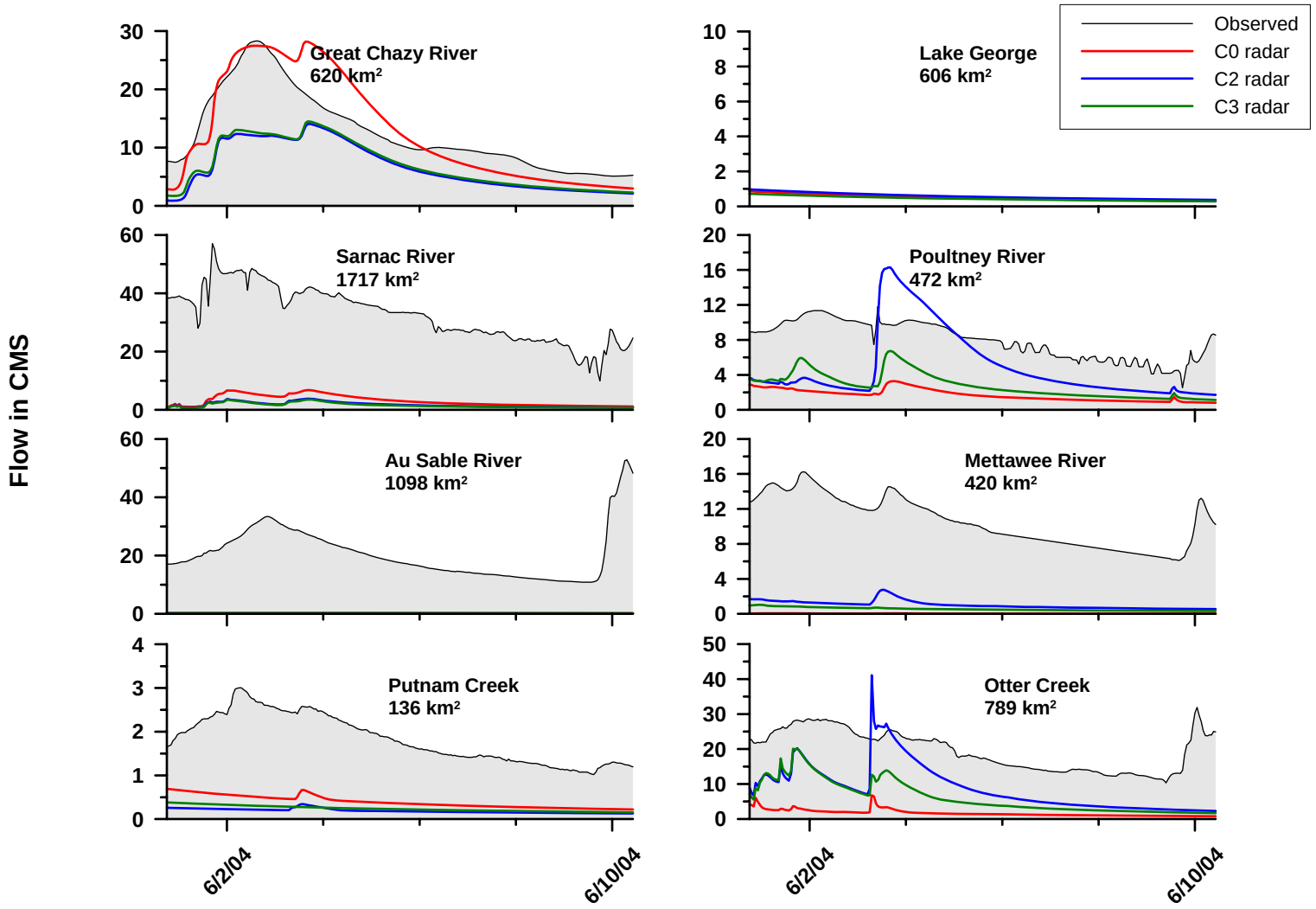

Figure D.34- Lake Champlain Basin, May 31st to June 10th 2004

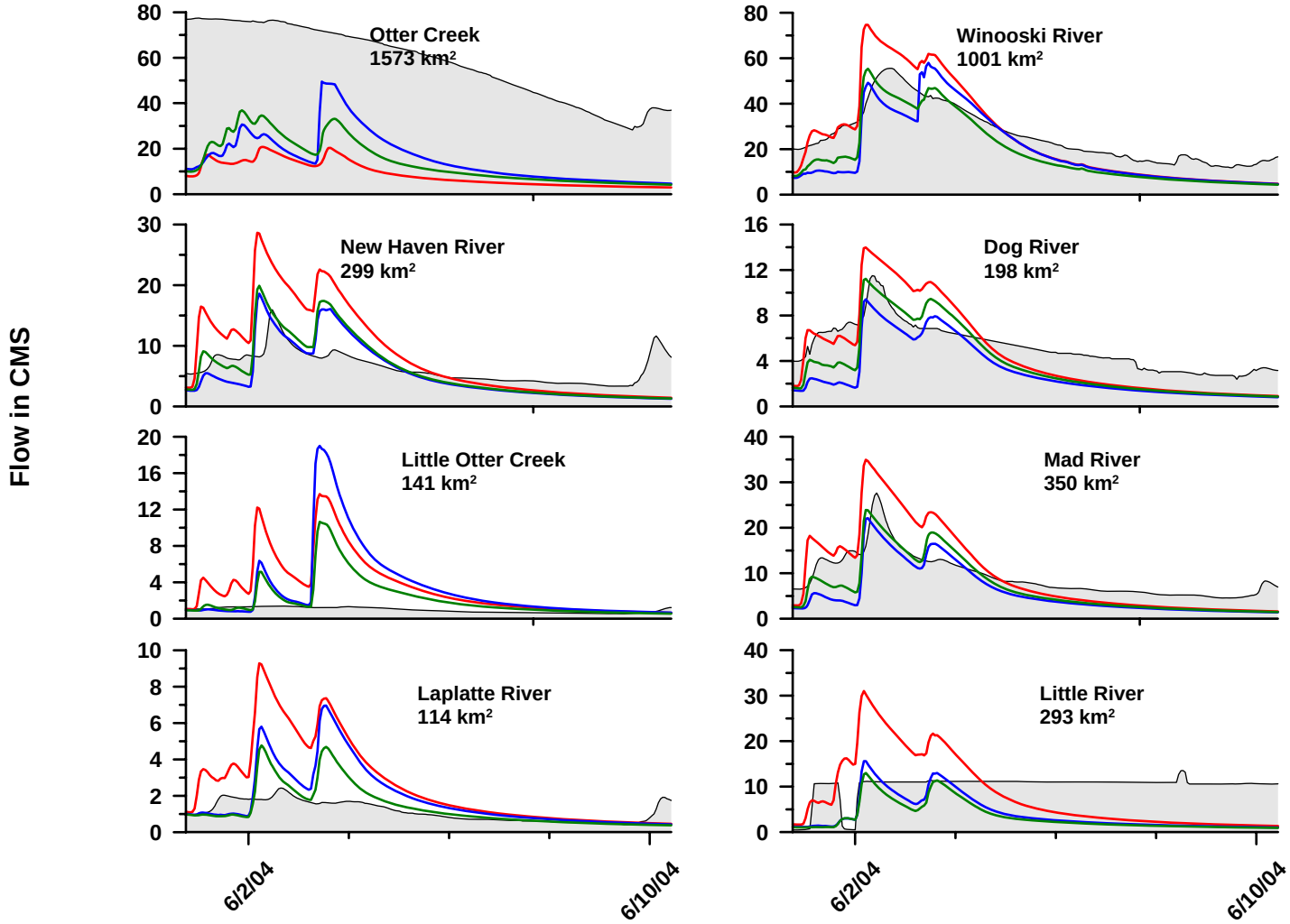

Figure D.35- Lake Champlain Basin, May 31st to June 10th 2004 (continued)

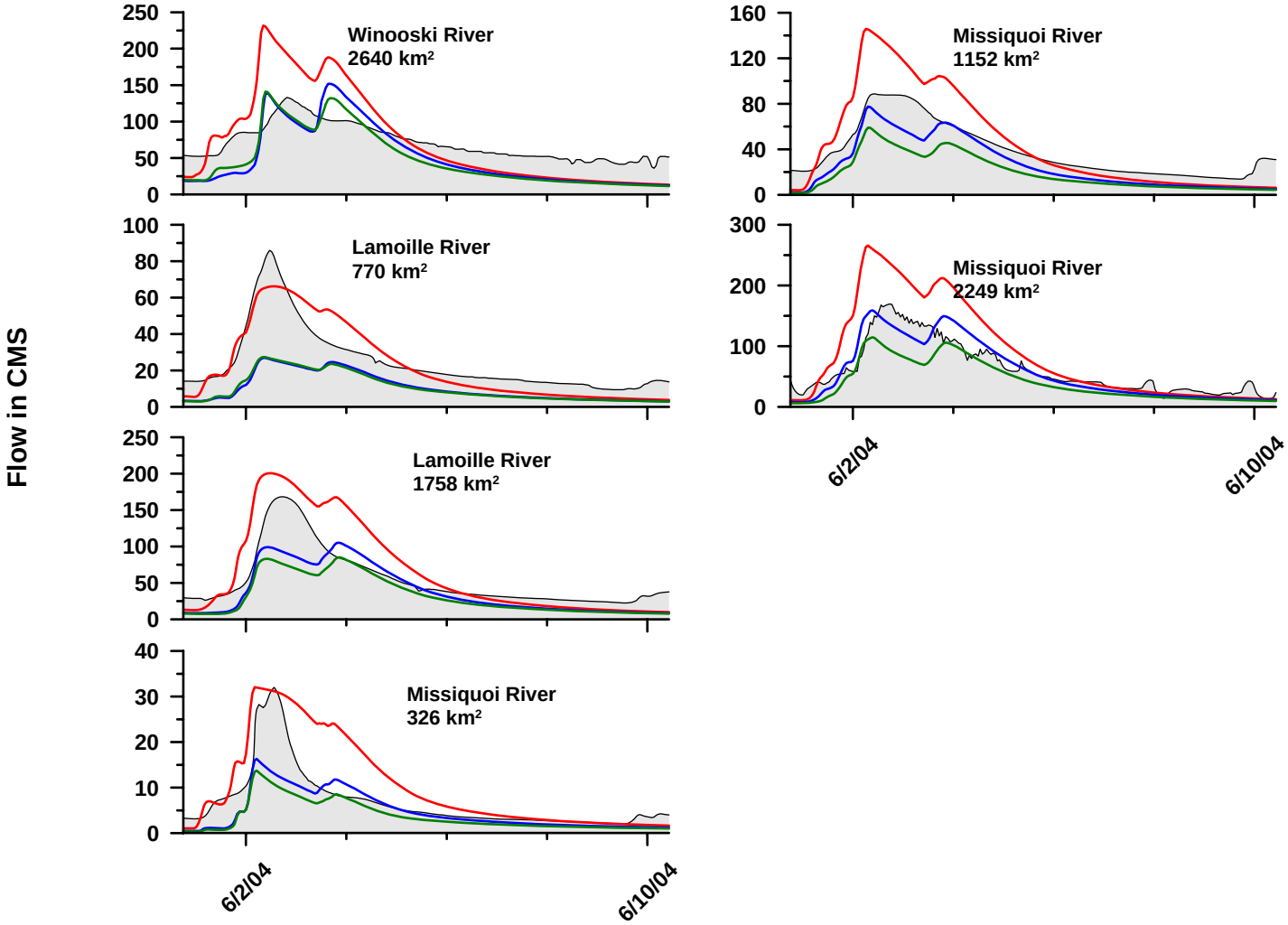

Figure D.36- Lake Champlain Basin, May 31st to June 10th 2004 (continued)

Table D.36- Statistical criteria for Lake Champlain Basin, May 31st to June 10th 2004

	Statistical Criteria							
	Nash	R^2	RMSE	RMSE/qbar	%Dv	APB	Bias	MAE
	C0 RADAR							
Great Chazy River	0.67	0.85	3.88	0.31	3.04	24.06	0.39	3.05
Saranac River	-9.74	0.63	30.61	0.94	-90.45	90.45	-29.55	29.55
Ausable	-5.39	0.08	22.04	1.08	-98.90	98.90	-20.24	20.24
Putnam Creek	-6.41	0.68	1.51	0.82	-78.49	78.49	-1.44	1.44
Lake George	-	-	-	-	-	-	-	-
Poultney River	-8.05	0.63	6.47	0.82	-78.77	78.77	-6.25	6.25
Mettawee River	-13.30	0.63	10.88	1.03	-99.65	99.65	-10.50	10.50
Otter Creek (789 km^2)	-9.44	0.31	18.59	0.95	-91.26	91.26	-17.82	17.82
Otter Creek (1573 km^2)	-8.76	0.75	50.13	0.87	-84.58	84.58	-48.75	48.75
New Haven River	-4.59	0.56	6.17	0.97	37.08	69.15	2.37	4.42
Little Otter Creek	-189.23	0.52	4.00	4.20	271.33	273.83	2.58	2.60
Laplatte River	-17.68	0.65	2.40	2.11	131.87	140.13	1.51	1.60
Winooski River	0.39	0.93	9.56	0.37	-1.28	30.16	-0.33	7.84
Dog River	-0.19	0.85	2.19	0.42	-9.53	38.43	-0.49	1.99
Mad River	-0.19	0.85	5.15	0.56	8.55	43.60	0.79	4.03
Little River	-	-	-	-	-	-	-	-
Little River	-9.45	0.00	8.57	0.84	-17.55	75.52	-1.80	7.74
Winooski River	-1.97	0.87	42.20	0.60	7.30	48.13	5.15	33.97
Lamoille River(770 km^2)	0.79	0.84	8.23	0.33	-6.28	28.37	-1.55	7.00
Lamoille River (1758 km^2)	0.31	0.86	33.37	0.61	25.20	44.66	13.78	24.42
Missisquoi River(326 km^2)	0.14	0.75	6.28	0.91	51.45	58.62	3.55	4.05
Missisquoi River (1152 km^2)	0.07	0.94	22.38	0.59	20.36	43.27	7.78	16.53
Missisquoi River (2249 km^2)	-0.32	0.89	49.27	0.80	43.34	53.92	26.59	33.08
	C2 RADAR							
Great Chazy River	-0.10	0.76	7.03	0.56	-47.18	47.18	-5.97	5.97
Saranac River	-10.83	0.60	32.13	0.98	-94.70	94.70	-30.94	30.94
Ausable	-5.41	0.06	22.07	1.08	-99.08	99.08	-20.28	20.28
Putnam Creek	-8.68	0.67	1.72	0.94	-89.68	89.68	-1.64	1.64
Lake George	-	-	-	-	-	-	-	-
Poultney River	-3.70	0.20	4.67	0.59	-38.47	51.04	-3.05	4.05
Mettawee River	-10.70	0.56	9.84	0.93	-90.24	90.24	-9.51	9.51
Otter Creek (789 km^2)	-3.28	0.37	11.91	0.61	-53.99	55.95	-10.54	10.93
Otter Creek (1573 km^2)	-6.22	0.50	43.11	0.75	-72.14	72.14	-41.58	41.58

New Haven River	-0.78	0.46	3.48	0.55	-13.57	41.04	-0.87	2.62
Little Otter Creek	-257.72	0.21	4.66	4.90	254.50	265.68	2.42	2.53
Laplatte River	-6.65	0.39	1.54	1.35	63.07	84.49	0.72	0.96
Winooski River	0.36	0.76	9.85	0.38	-24.13	33.33	-6.27	8.66
Dog River	-0.50	0.71	2.45	0.47	-40.12	42.34	-2.08	2.19
Mad River	0.16	0.71	4.33	0.47	-35.30	40.35	-3.26	3.73
Little River	-	-	-	-	-	-	-	-
Winooski River	-0.50	0.77	30.03	0.43	-27.21	39.52	-19.20	27.89
Lamoille River(770 km^2)	-0.07	0.73	18.48	0.75	-57.27	57.27	-14.13	14.13
Lamoille River (1758 km^2)	0.59	0.73	25.74	0.47	-27.94	34.96	-15.27	19.11
Missisquoi River(326 km^2)	0.54	0.68	4.59	0.67	-31.30	37.96	-2.16	2.62
Missisquoi River (1152 km^2)	0.64	0.89	13.98	0.37	-31.21	31.29	-11.93	11.96
Missisquoi River (2249 km^2)	0.82	0.85	18.27	0.30	-5.11	23.72	-3.13	14.56
	C3 RADAR							
Great Chazy River	0.01	0.78	6.69	0.53	-44.28	44.28	-5.61	5.61
Saranac River	-10.98	0.59	32.33	0.99	-95.30	95.30	-31.13	31.13
Ausable	-5.41	0.06	22.08	1.08	-99.11	99.11	-20.29	20.29
Putnam Creek	-8.12	0.66	1.67	0.91	-86.97	86.97	-1.59	1.59
Lake George	-	-	-	-	-	-	-	-
Poultney River	-5.12	0.65	5.33	0.67	-65.04	65.04	-5.16	5.16
Mettawee River	-11.96	0.72	10.36	0.98	-94.87	94.87	-9.99	9.99
Otter Creek (789 km^2)	-4.74	0.58	13.78	0.71	-67.98	67.98	-13.28	13.28
Otter Creek (1573 km^2)	-6.60	0.69	44.24	0.77	-74.92	74.92	-43.19	43.19
New Haven River	-0.88	0.50	3.58	0.56	-3.50	40.52	-0.22	2.59
Little Otter Creek	-66.53	0.27	2.38	2.50	129.42	137.47	1.23	1.31
Laplatte River	-1.58	0.43	0.89	0.78	21.00	45.25	0.24	0.52
Winooski River	0.52	0.90	8.52	0.33	-27.35	30.60	-7.11	7.95
Dog River	-0.03	0.79	2.04	0.39	-26.71	36.32	-1.38	1.88
Mad River	0.40	0.77	3.65	0.40	-23.98	34.43	-2.22	3.18
Little River	-	-	-	-	-	-	-	-
Winooski River	-0.38	0.84	28.80	0.41	-31.46	38.56	-22.20	27.21
Lamoille River(770 km^2)	-0.06	0.79	18.33	0.74	-57.87	57.87	-14.28	14.28
Lamoille River (1758 km^2)	0.40	0.74	31.21	0.57	-40.57	40.63	-22.18	22.21
Missisquoi River(326 km^2)	0.37	0.75	5.35	0.78	-47.08	47.15	-3.25	3.26
Missisquoi River (1152 km^2)	0.16	0.89	21.27	0.56	-49.23	49.23	-18.81	18.81
Missisquoi River (2249 km^2)	0.61	0.83	26.93	0.44	-32.04	32.89	-19.66	20.18

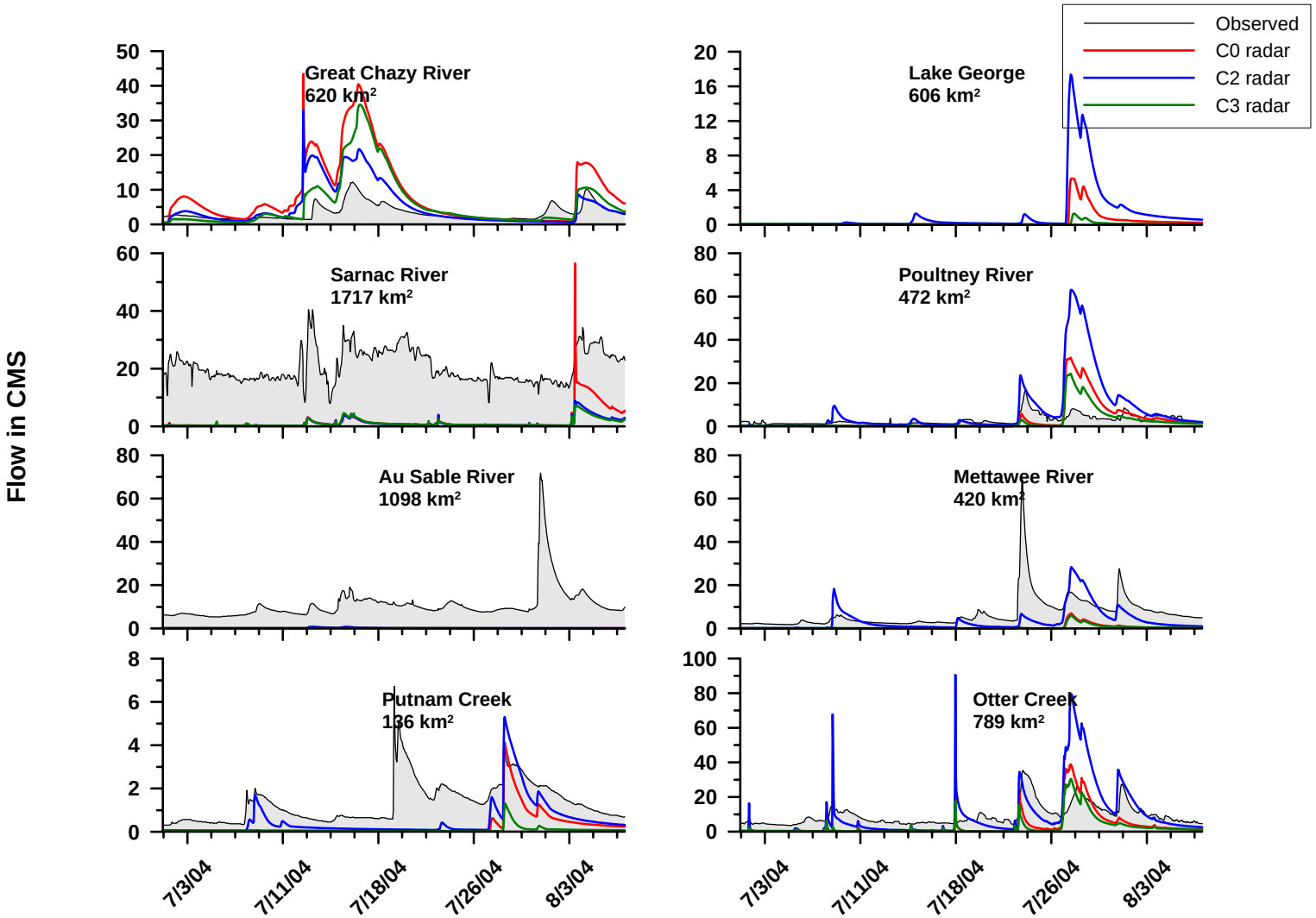

Figure D.37- Lake Champlain Basin, July 1st to August 8th 2004

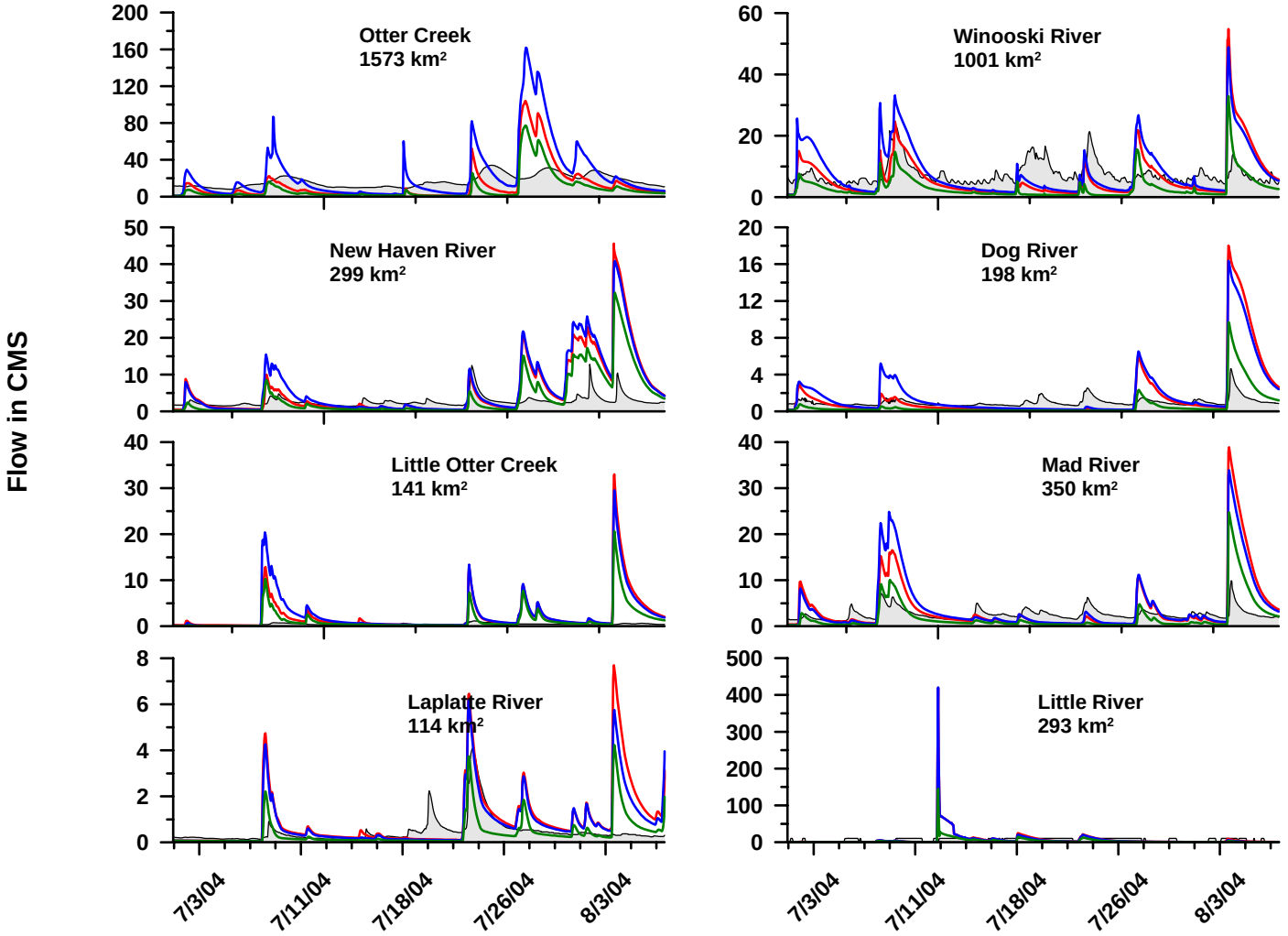

Figure D.38- Lake Champlain Basin, July 1st to August 8th 2004 (continued)

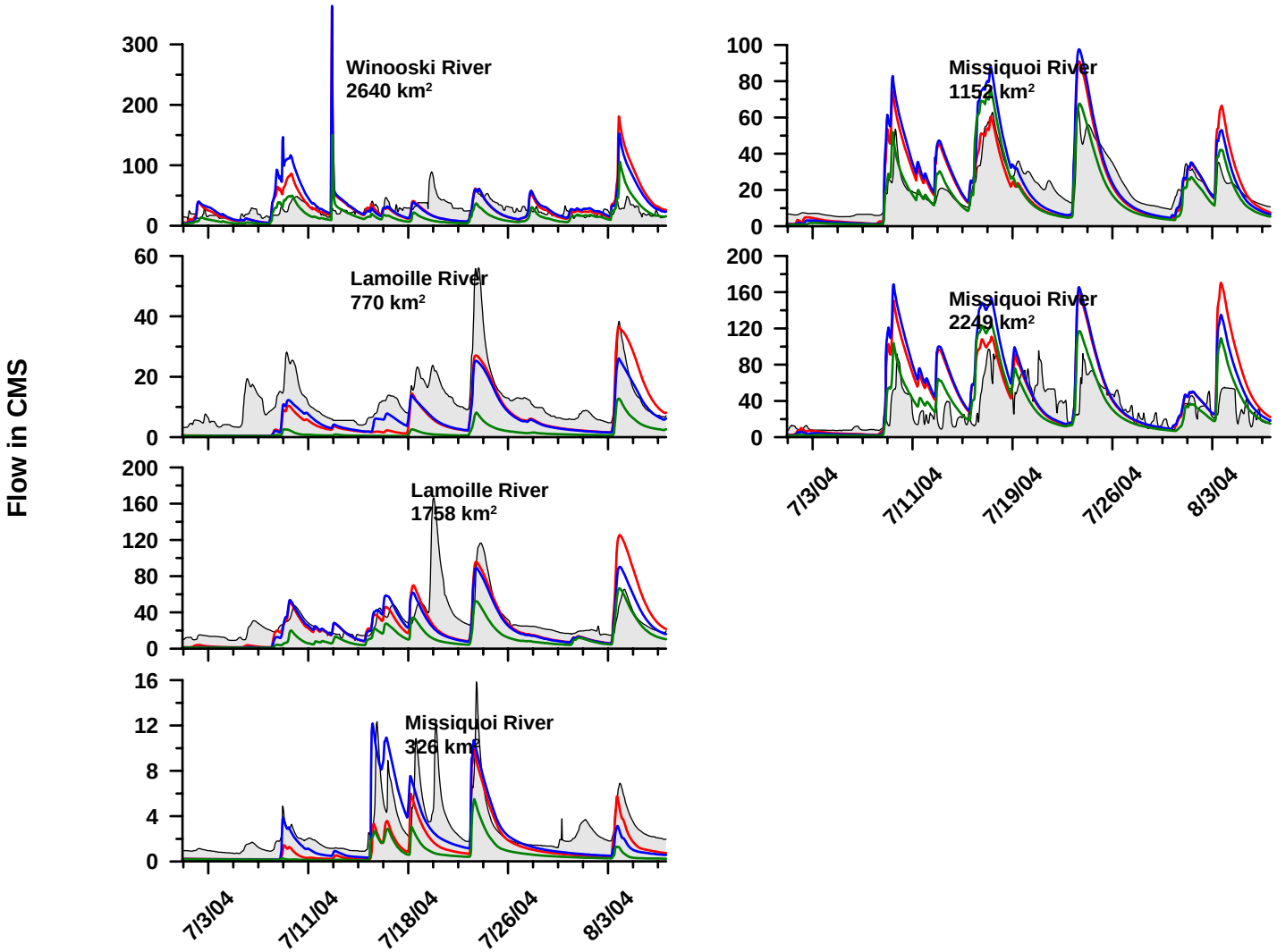

Figure D.39- Lake Champlain Basin, July 1st to August 8th 2004 (continued)

Table D.37- Statistical criteria for Lake Champlain Basin, July 1st to August 8th 2004

	Statistical Criteria							
	Nash	R^2	RMSE	RMSE/qbar	%Dv	APB	Bias	MAE
	C0 RADAR							
Great Chazy River	-15.28	0.62	9.39	2.77	157.12	175.63	5.32	5.95
Saranac River	-11.20	0.20	19.49	0.95	-91.27	91.63	-18.80	18.88
Ausable	-1.86	0.00	13.39	1.22	-98.35	98.35	-10.80	10.80
Putnam Creek	-1.08	0.23	1.34	1.01	-79.61	80.22	-1.05	1.06
Lake George	-	-	-	-	-	-	-	-
Poultney River	-5.13	0.22	5.70	1.97	4.79	108.08	0.14	3.12
Mettawee River	-0.67	0.10	9.72	1.40	-93.45	93.45	-6.48	6.48
Otter Creek (789 km^2)	-1.01	0.30	8.72	0.94	-62.80	77.14	-5.84	7.18
Otter Creek (1573 km^2)	-5.97	0.22	18.05	1.08	-24.81	74.08	-4.15	12.38
New Haven River	-25.97	0.27	7.82	2.87	107.07	156.74	2.92	4.27
Little Otter Creek	-457.93	0.08	4.26	10.44	428.14	439.16	1.75	1.79
Laplatte River	-3.45	0.18	1.23	2.61	91.21	132.43	0.43	0.62
Winooski River	-2.90	0.09	7.07	0.95	-13.95	66.12	-1.04	4.92
Dog River	-36.12	0.45	2.91	2.93	61.59	136.63	0.61	1.36
Mad River	-20.64	0.36	5.63	2.18	50.32	114.02	1.30	2.94
Little River	-	-	-	-	-	-	-	-
Winooski River	-4.84	0.05	29.19	1.09	15.56	63.81	4.16	17.07
Lamoille River(770 km^2)	0.05	0.52	8.44	0.70	-46.86	57.63	-5.65	6.95
Lamoille River (1758 km^2)	-0.09	0.27	25.30	0.81	-17.15	50.64	-5.34	15.76
Missisquoi River(326 km^2)	0.17	0.54	2.15	0.78	-51.98	56.28	-1.44	1.56
Missisquoi River (1152 km^2)	0.23	0.66	12.05	0.57	5.50	42.53	1.16	9.01
Missisquoi River (2249 km^2)	-	-	-	-	-	-	-	-
	C2 RADAR							
Great Chazy River	-3.48	0.47	4.93	1.45	54.89	83.38	1.86	2.83
Saranac River	-12.00	0.34	20.12	0.98	-94.77	94.77	-19.52	19.52
Ausable	-1.86	0.00	13.41	1.22	-98.48	98.48	-10.82	10.82
Putnam Creek	-0.65	0.28	1.19	0.90	-62.28	66.81	-0.82	0.88
Lake George	-	-	-	-	-	-	-	-
Poultney River	-27.50	0.33	12.29	4.26	141.38	170.53	4.08	4.93
Mettawee River	-0.12	0.18	7.95	1.15	-50.06	68.16	-3.47	4.73
Otter Creek (789 km^2)	-2.69	0.43	11.81	1.27	-0.06	76.16	-0.01	7.08
Otter Creek (1573 km^2)	-16.08	0.27	28.25	1.69	38.24	88.80	6.39	14.84
New Haven River	-27.87	0.29	8.09	2.97	127.33	171.83	3.47	4.68

Little Otter Creek	-509.45	0.11	4.50	11.02	486.27	500.73	1.99	2.04
Laplatte River	-1.72	0.23	0.96	2.04	61.34	109.93	0.29	0.52
Winooski River	-3.12	0.15	7.27	0.98	8.74	72.68	0.65	5.40
Dog River	-30.02	0.46	2.66	2.68	83.33	140.26	0.83	1.40
Mad River	-20.16	0.46	5.57	2.16	59.32	119.01	1.53	3.07
Little River	-	-	-	-	-	-	-	-
Winooski River	-5.18	0.04	30.01	1.12	21.84	69.20	5.84	18.51
Lamoille River(770 km^2)	0.17	0.67	7.91	0.66	-50.31	51.23	-6.06	6.17
Lamoille River (1758 km^2)	0.11	0.32	22.90	0.74	-25.41	44.91	-7.90	13.97
Missisquoi River(326 km^2)	0.27	0.52	2.01	0.73	-26.14	51.33	-0.72	1.42
Missisquoi River (1152 km^2)	-0.03	0.74	13.93	0.66	16.42	48.33	3.48	10.23
Missisquoi River (2249 km^2)	-	-	-	-	-	-	-	-
	C3 RADAR							
Great Chazy River	-6.47	0.66	6.36	1.88	76.19	102.43	2.58	3.47
Saranac River	-12.06	0.39	20.17	0.98	-94.98	94.98	-19.57	19.57
Ausable	-1.89	0.02	13.46	1.23	-99.10	99.10	-10.88	10.88
Putnam Creek	-1.72	0.14	1.53	1.15	-94.14	94.14	-1.25	1.25
Lake George	-	-	-	-	-	-	-	-
Poultney River	-2.17	0.20	4.10	1.42	-27.96	91.26	-0.81	2.64
Mettawee River	-0.69	0.09	9.78	1.41	-93.81	93.81	-6.51	6.51
Otter Creek (789 km^2)	-1.12	0.23	8.95	0.96	-72.68	79.11	-6.76	7.36
Otter Creek (1573 km^2)	-3.96	0.17	15.23	0.91	-52.24	75.92	-8.73	12.69
New Haven River	-11.74	0.25	5.37	1.97	39.70	122.03	1.08	3.32
Little Otter Creek	-161.13	0.06	2.53	6.21	215.66	253.00	0.88	1.03
Laplatte River	-0.30	0.15	0.66	1.41	-19.00	78.70	-0.09	0.37
Winooski River	-2.04	0.07	6.25	0.84	-59.09	67.80	-4.39	5.04
Dog River	-4.48	0.49	1.12	1.13	-39.18	83.85	-0.39	0.83
Mad River	-4.95	0.40	2.95	1.14	-24.64	77.98	-0.64	2.01
Little River	-	-	-	-	-	-	-	-
Winooski River	-1.74	0.05	19.99	0.75	-36.65	56.70	-9.80	15.16
Lamoille River(770 km^2)	-1.17	0.48	12.80	1.06	-86.73	86.73	-10.45	10.45
Lamoille River (1758 km^2)	-0.34	0.26	28.06	0.90	-60.55	62.49	-18.84	19.44
Missisquoi River(326 km^2)	-0.37	0.56	2.76	1.00	-75.69	75.74	-2.09	2.09
Missisquoi River (1152 km^2)	0.54	0.78	9.29	0.44	-16.25	35.13	-3.44	7.44
Missisquoi River (2249 km^2)	-	-	-	-	-	-	-	-

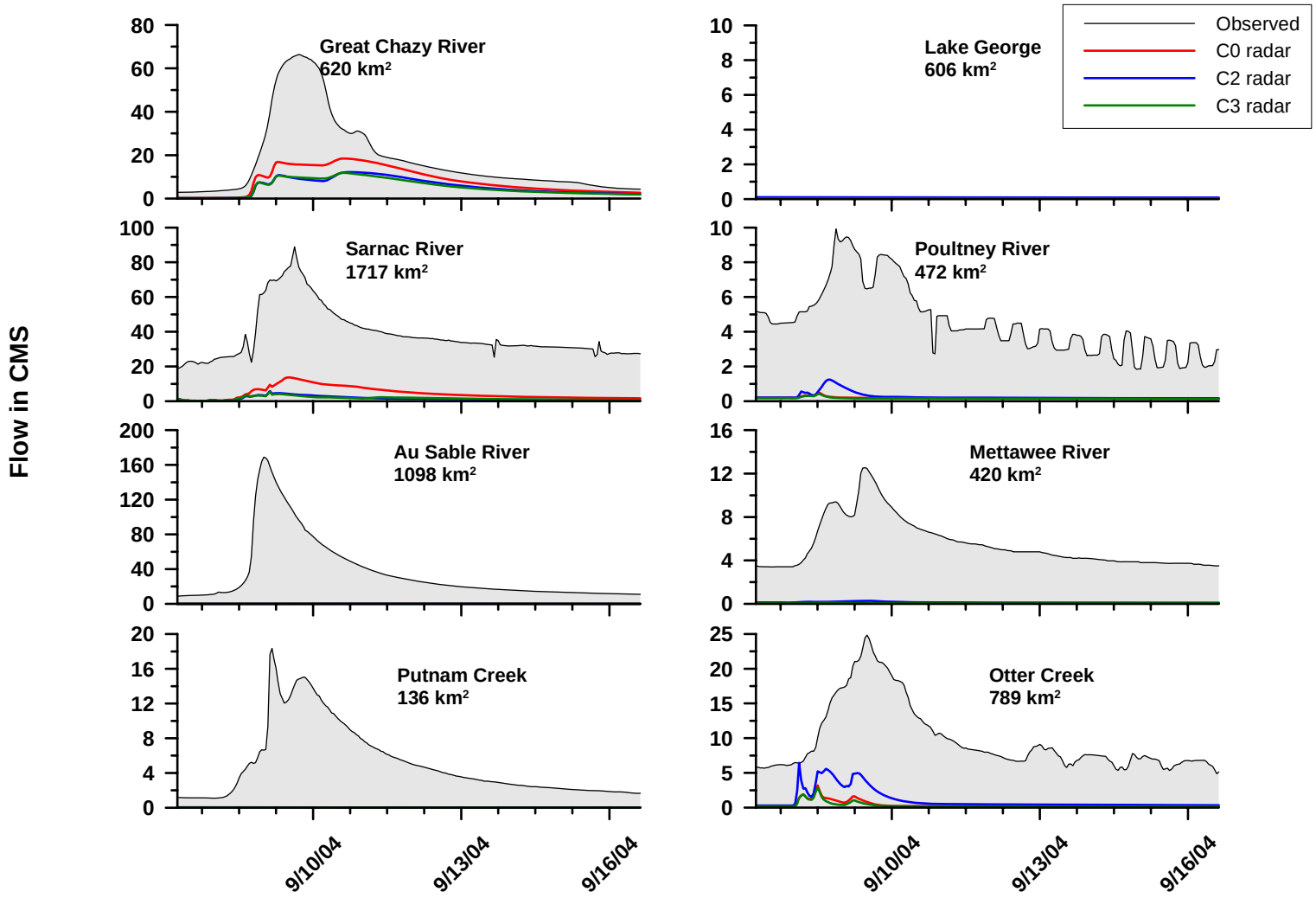

Figure D.40- Lake Champlain Basin, September 8th to September 17th 2004

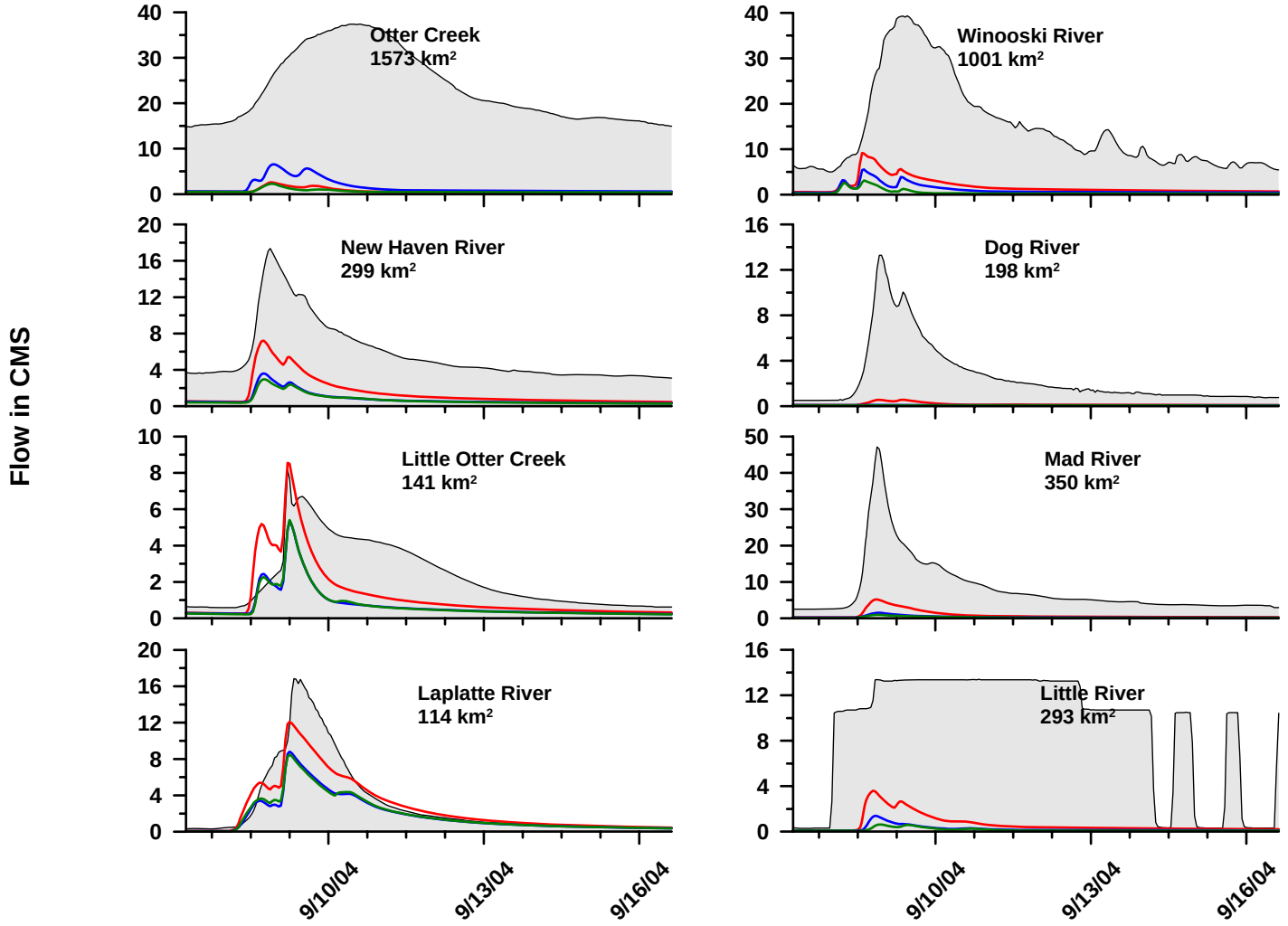

Figure D.41- Lake Champlain Basin, September 8th to September 17th 2004 (continued)

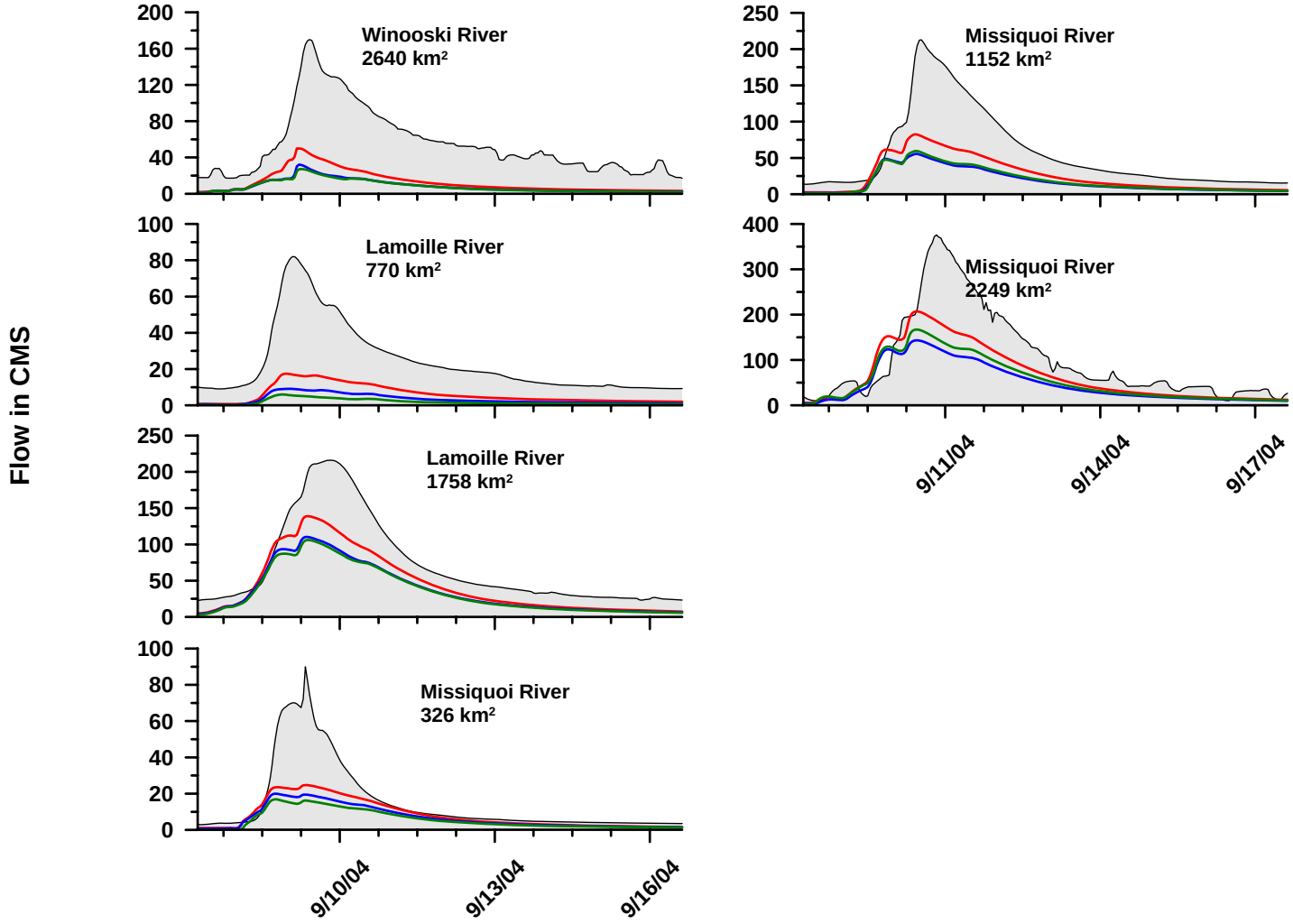

Figure D.42- Lake Champlain Basin, September 8th to September 17th 2004 (continued)

Table D.38- Statistical criteria for Lake Champlain Basin, September 8th to September 17th 2004

	Statistical Criteria							
	Nash	R^2	RMSE	RMSE/qbar	%Dv	APB	Bias	MAE
	C0 RADAR							
Great Chazy River	0.10	0.62	17.19	0.94	-55.16	55.16	-10.12	10.12
Saranac River	-4.90	0.86	35.57	0.93	-87.99	87.99	-33.68	33.68
Ausable	-0.92	0.62	52.37	1.44	-99.78	99.78	-36.22	36.22
Putnam Creek	-1.48	0.14	6.56	1.29	-99.26	99.26	-5.07	5.07
Lake George	-	-	-	-	-	-	-	-
Poultney River	-	-	-	-	-	-	-	-
Mettawee River	-5.98	0.28	5.87	1.07	-99.00	99.00	-5.44	5.44
Otter Creek (789 km^2)	-3.57	0.13	10.54	1.08	-96.02	96.02	-9.40	9.40
Otter Creek (1573 km^2)	-8.41	0.20	23.92	1.02	-96.95	96.95	-22.69	22.69
New Haven River	-0.93	0.91	4.67	0.82	-74.29	74.29	-4.25	4.25
Little Otter Creek	0.13	0.46	1.69	0.75	-43.31	58.67	-0.98	1.33
Laplatte River	0.84	0.91	1.67	0.54	-13.35	27.68	-0.41	0.85
Winooski River	-1.42	0.44	15.57	1.07	-87.49	87.49	-12.76	12.76
Dog River	-0.64	0.93	3.57	1.41	-93.43	93.43	-2.37	2.37
Mad River	-0.54	0.95	10.34	1.26	-89.35	89.35	-7.36	7.36
Little River	-	-	-	-	-	-	-	-
Winooski River	-0.85	0.85	50.30	0.90	-76.84	76.84	-42.89	42.89
Lamoille River(770 km^2)	-0.44	0.92	23.13	0.96	-74.52	74.52	-18.02	18.02
Lamoille River (1758 km^2)	0.66	0.91	35.39	0.50	-36.81	38.11	-26.33	27.26
Missisquoi River(326 km^2)	0.43	0.81	15.15	0.98	-45.59	47.34	-7.05	7.32
Missisquoi River (1152 km^2)	0.32	0.86	44.81	0.80	-53.69	55.25	-30.21	31.09
Missisquoi River (2249 km^2)	0.59	0.79	62.82	0.61	-34.30	42.01	-35.15	43.05
	C2 RADAR							
Great Chazy River	-0.25	0.47	20.26	1.10	-69.69	69.69	-12.78	12.78
Saranac River	-6.15	0.85	39.14	1.02	-95.93	95.93	-36.71	36.71
Ausable	-0.92	0.20	52.39	1.44	-99.84	99.84	-36.24	36.24
Putnam Creek	-1.48	0.13	6.55	1.28	-99.15	99.15	-5.06	5.06
Lake George	-	-	-	-	-	-	-	-
Poultney River	-	-	-	-	-	-	-	-
Mettawee River	-5.76	0.79	5.78	1.05	-97.43	97.43	-5.35	5.35
Otter Creek (789 km^2)	-2.83	0.40	9.65	0.99	-88.81	88.81	-8.69	8.69
Otter Creek (1573 km^2)	-7.75	0.25	23.06	0.99	-93.68	93.68	-21.93	21.93
New Haven River	-1.82	0.90	5.65	0.99	-86.56	86.56	-4.95	4.95

Little Otter Creek	-0.28	0.49	2.05	0.90	-68.07	69.33	-1.54	1.57
Laplatte River	0.59	0.90	2.68	0.87	-40.40	41.33	-1.24	1.27
Winooski River	-1.73	0.34	16.51	1.13	-92.90	92.90	-13.55	13.55
Dog River	-0.77	0.38	3.70	1.46	-96.54	96.54	-2.45	2.45
Mad River	-0.83	0.97	11.29	1.37	-95.98	95.98	-7.91	7.91
Little River	-	-	-	-	-	-	-	-
Winooski River	-1.33	0.84	56.41	1.01	-84.94	84.94	-47.41	47.41
Lamoille River(770 km^2)	-0.93	0.91	26.75	1.11	-86.18	86.18	-20.84	20.84
Lamoille River (1758 km^2)	0.41	0.89	46.32	0.65	-48.12	48.40	-34.42	34.62
Missisquoi River(326 km^2)	0.27	0.80	17.06	1.10	-55.60	56.61	-8.59	8.75
Missisquoi River (1152 km^2)	-0.06	0.80	55.66	0.99	-68.10	68.50	-38.32	38.54
Missisquoi River (2249 km^2)	0.26	0.74	84.68	0.83	-52.31	56.52	-53.61	57.92
	C3 RADAR							
Great Chazy River	-0.25	0.60	20.25	1.10	-71.43	71.43	-13.10	13.10
Saranac River	-6.15	0.71	39.16	1.02	-95.72	95.72	-36.63	36.63
Ausable	-0.92	0.21	52.40	1.44	-99.86	99.86	-36.25	36.25
Putnam Creek	-1.49	0.14	6.57	1.29	-99.56	99.56	-5.08	5.08
Lake George	-	-	-	-	-	-	-	-
Poultney River	-	-	-	-	-	-	-	-
Mettawee River	-5.96	0.27	5.87	1.07	-98.84	98.84	-5.43	5.43
Otter Creek (789 km^2)	-3.66	0.05	10.64	1.09	-96.77	96.77	-9.47	9.47
Otter Creek (1573 km^2)	-8.52	0.12	24.07	1.03	-97.47	97.47	-22.81	22.81
New Haven River	-1.91	0.94	5.74	1.00	-87.73	87.73	-5.02	5.02
Little Otter Creek	-0.27	0.51	2.04	0.90	-68.44	69.29	-1.55	1.57
Laplatte River	0.58	0.88	2.71	0.88	-39.73	41.20	-1.22	1.27
Winooski River	-1.97	0.06	17.23	1.18	-96.81	96.81	-14.12	14.12
Dog River	-0.78	0.18	3.71	1.47	-97.06	97.06	-2.46	2.46
Mad River	-0.87	0.96	11.41	1.39	-96.97	96.97	-7.99	7.99
Little River	-	-	-	-	-	-	-	-
Winooski River	-1.38	0.82	57.05	1.02	-85.72	85.72	-47.84	47.84
Lamoille River(770 km^2)	-1.19	0.92	28.52	1.18	-92.24	92.24	-22.31	22.31
Lamoille River (1758 km^2)	0.37	0.89	48.08	0.67	-50.40	50.49	-36.05	36.11
Missisquoi River(326 km^2)	0.15	0.79	18.42	1.19	-63.02	63.32	-9.74	9.78
Missisquoi River (1152 km^2)	0.00	0.83	54.25	0.96	-66.46	66.85	-37.40	37.62
Missisquoi River (2249 km^2)	0.40	0.77	76.41	0.75	-45.48	50.89	-46.61	52.15

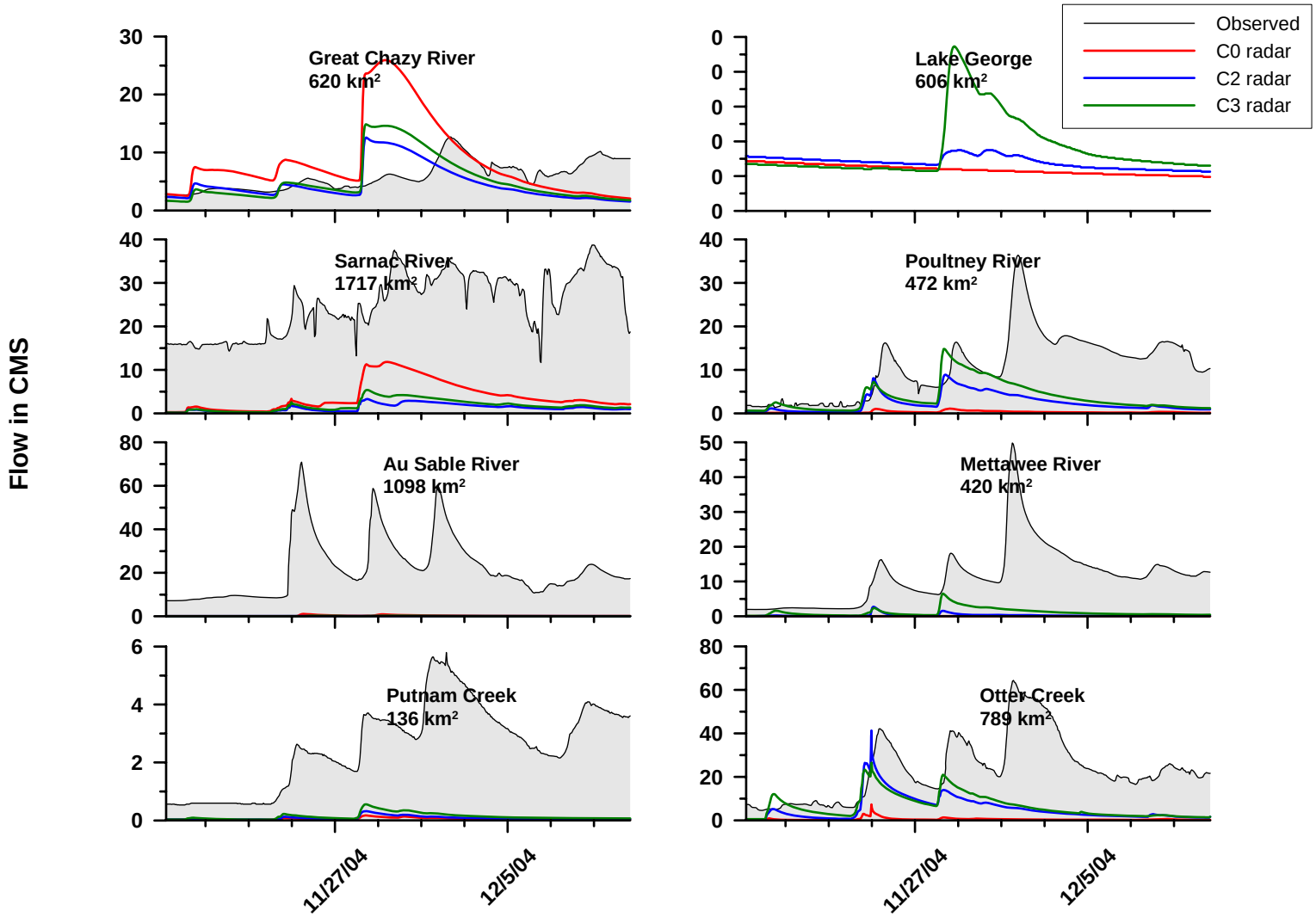

Figure D.43- Lake Champlain Basin, November 20th to December 11th 2004

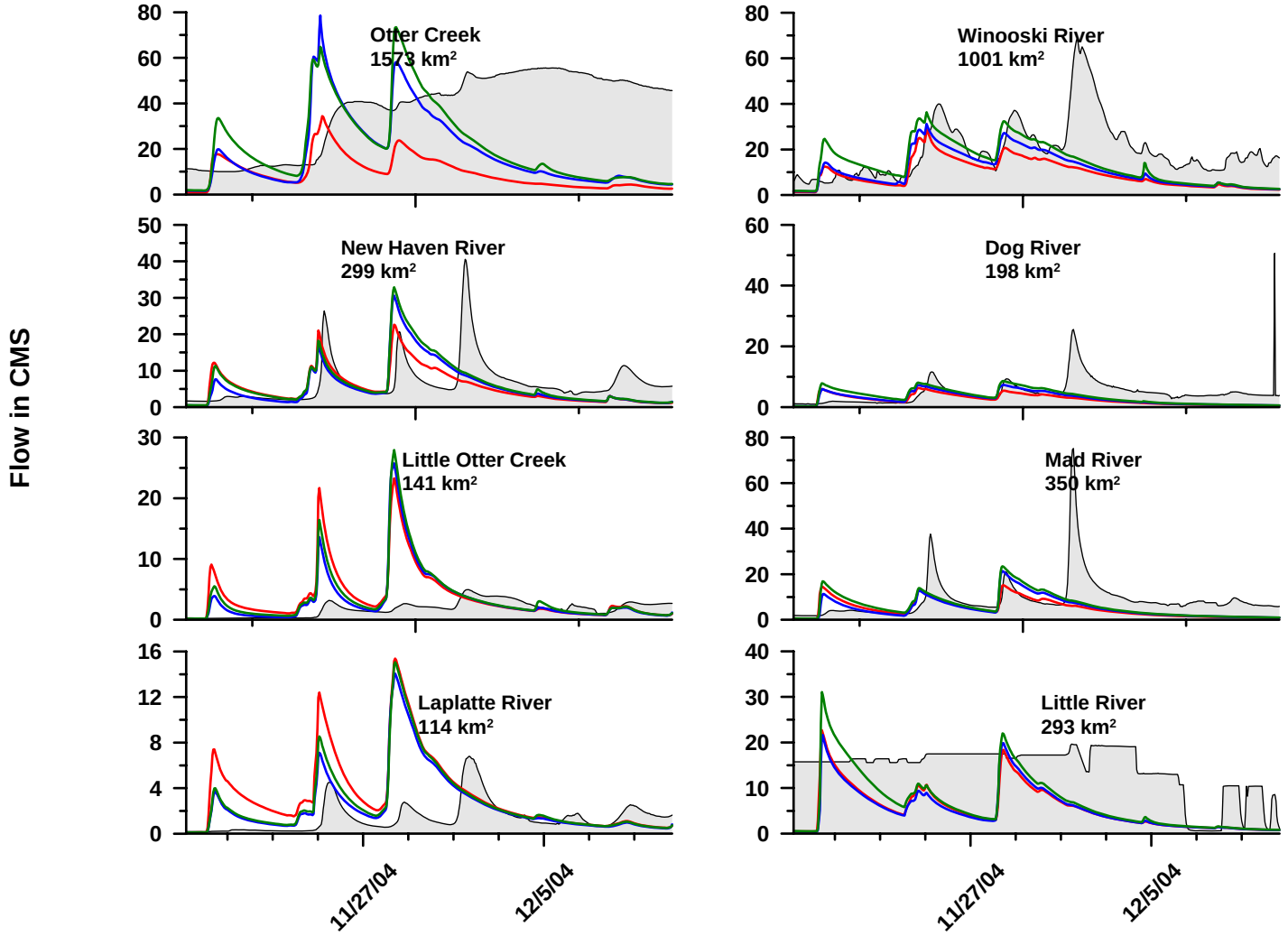

Figure D.44- Lake Champlain Basin, November 20th to December 11th 2004 (continued)

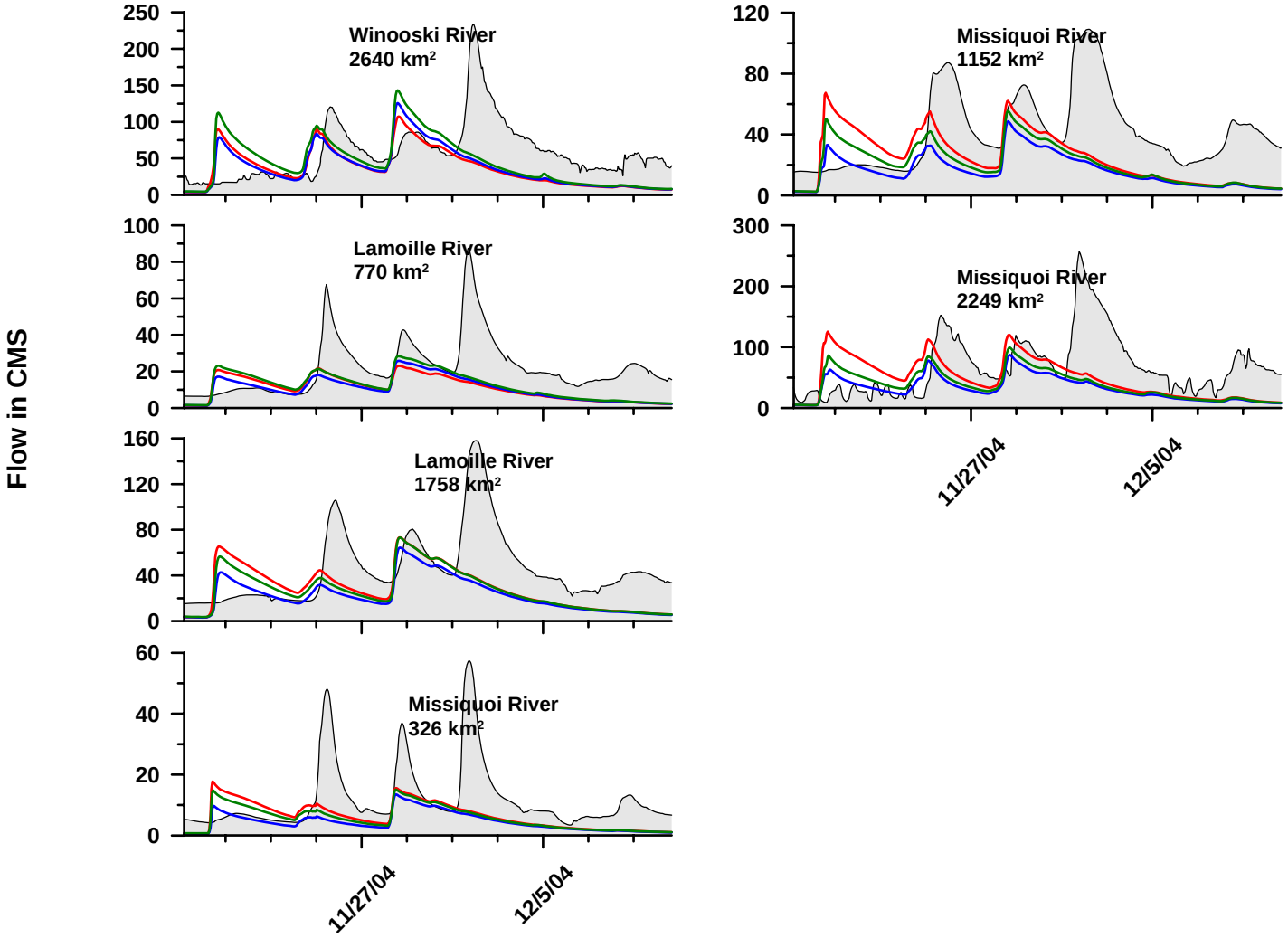

Figure D.45- Lake Champlain Basin, November 20th to December 11th 2004 (continued)

Table D.39- Statistical criteria for Lake Champlain Basin, November 20th to December 11th 2004

	Statistical Criteria							
	Nash	R^2	RMSE	RMSE/qbar	%Dv	APB	Bias	MAE
	C0 RADAR							
Great Chazy River	-8.33	0.00	7.49	1.27	45.62	83.78	2.69	4.95
Saranac River	-	-	-	-	-	-	-	-
Ausable	-2.45	0.52	25.66	1.17	-98.99	98.99	-21.72	21.72
Putnam Creek	-3.01	0.19	2.90	1.13	-97.91	97.91	-2.52	2.52
Lake George	-	-	-	-	-	-	-	-
Poultney River	-2.00	0.09	12.76	1.19	-97.20	97.20	-10.46	10.46
Mettawee River	-1.79	0.02	14.22	1.25	-99.76	99.76	-11.39	11.39
Otter Creek (789 km^2)	-2.44	0.04	27.26	1.16	-97.88	97.88	-23.02	23.02
Otter Creek (1573 km^2)	-3.07	0.07	33.99	0.91	-74.22	78.03	-27.61	29.03
New Haven River	-0.11	0.11	6.29	0.94	-17.65	63.20	-1.18	4.22
Little Otter Creek	-14.58	0.01	4.81	2.66	108.98	158.51	1.97	2.87
Laplatte River	-7.05	0.03	3.82	2.73	140.43	181.56	1.97	2.54
Winooski River	-0.49	0.19	15.57	0.78	-53.09	57.47	-10.55	11.42
Dog River	-0.35	0.02	4.83	1.01	-47.45	62.84	-2.28	3.01
Mad River	-0.18	0.05	9.93	1.11	-45.11	64.03	-4.06	5.76
Little River	-	-	-	-	-	-	-	-
Little River	-2.78	0.19	10.17	0.71	-61.09	63.06	-8.71	8.99
Winooski River	-0.44	0.04	47.79	0.82	-35.92	59.81	-20.90	34.80
Lamoille River(770 km^2)	-0.43	0.10	18.19	0.82	-49.81	61.49	-11.00	13.57
Lamoille River (1758 km^2)	-0.36	0.05	36.48	0.80	-36.34	61.23	-16.61	27.98
Missisquoi River(326 km^2)	-0.21	0.07	12.02	1.01	-46.27	65.61	-5.52	7.82
Missisquoi River (1152 km^2)	-0.68	0.03	32.39	0.78	-39.89	63.49	-16.60	26.42
Missisquoi River (2249 km^2)	-	-	-	-	-	-	-	-
	C2 RADAR							
Great Chazy River	-1.60	0.00	3.95	0.67	-22.57	52.38	-1.33	3.09
Saranac River	-	-	-	-	-	-	-	-
Ausable	-2.50	0.17	25.86	1.18	-99.69	99.69	-21.88	21.88
Putnam Creek	-2.92	0.20	2.87	1.12	-96.88	96.88	-2.49	2.49
Lake George	-	-	-	-	-	-	-	-
Mettawee River	-1.70	0.04	13.99	1.23	-97.62	97.62	-11.15	11.15
Otter Creek (789 km^2)	-1.44	0.08	22.94	0.98	-76.73	78.26	-18.05	18.41
Otter Creek (1573 km^2)	-2.19	0.00	30.12	0.81	-50.04	65.98	-18.61	24.55
New Haven River	-0.24	0.14	6.64	0.99	-13.57	65.55	-0.91	4.38

Little Otter Creek	-12.85	0.03	4.54	2.51	80.67	128.80	1.46	2.33
Laplatte River	-4.00	0.05	3.01	2.15	80.73	126.67	1.13	1.77
Winooski River	-0.30	0.19	14.52	0.73	-43.86	51.87	-8.71	10.31
Dog River	-0.25	0.03	4.66	0.97	-38.31	59.75	-1.84	2.87
Mad River	-0.12	0.09	9.67	1.08	-41.60	63.23	-3.74	5.69
Little River	-	-	-	-	-	-	-	-
Winooski River	-0.38	0.07	46.72	0.80	-34.61	59.16	-20.14	34.42
Lamoille River(770 km^2)	-0.38	0.18	17.89	0.81	-51.81	57.49	-11.44	12.69
Lamoille River (1758 km^2)	-0.41	0.14	37.10	0.81	-50.22	57.77	-22.95	26.40
Missisquoi River(326 km^2)	-0.32	0.16	12.56	1.05	-62.29	64.42	-7.43	7.68
Missisquoi River (1152 km^2)	-0.86	0.15	34.10	0.82	-60.21	63.00	-25.06	26.22
Missisquoi River (2249 km^2)	-	-	-	-	-	-	-	-
	C3 RADAR							
Great Chazy River	-2.11	0.03	4.33	0.73	-11.92	55.09	-0.70	3.25
Saranac River	-	-	-	-	-	-	-	-
Ausable	-2.50	0.25	25.84	1.18	-99.59	99.59	-21.85	21.85
Putnam Creek	-2.76	0.23	2.80	1.09	-94.63	94.63	-2.43	2.43
Lake George	-	-	-	-	-	-	-	-
Poultney River	-0.84	0.10	9.98	0.93	-65.55	69.58	-7.05	7.49
Mettawee River	-1.40	0.10	13.18	1.16	-90.24	90.24	-10.30	10.30
Otter Creek (789 km^2)	-1.29	0.06	22.23	0.95	-72.10	74.75y	-16.96	17.58
Otter Creek (1573 km^2)	-2.10	0.01	29.67	0.80	-42.00	66.11	-15.63	24.60
New Haven River	-0.35	0.13	6.94	1.04	-2.62	69.79	-0.18	4.66
Little Otter Creek	-15.62	0.02	4.97	2.75	101.74	145.58	1.84	2.63
Laplatte River	-4.83	0.05	3.25	2.32	96.64	139.49	1.35	1.95
Winooski River	-0.23	0.12	14.15	0.71	-30.49	50.69	-6.06	10.07
Dog River	-0.27	0.02	4.69	0.98	-27.11	64.60	-1.30	3.10
Mad River	-0.15	0.05	9.79	1.09	-30.44	68.82	-2.74	6.19
Little River	-	-	-	-	-	-	-	-
Winooski River	-0.48	0.03	48.50	0.83	-21.75	64.56	-12.66	37.57
Lamoille River(770 km^2)	-0.31	0.12	17.41	0.79	-43.64	58.13	-9.63	12.83
Lamoille River (1758 km^2)	-0.34	0.09	36.13	0.79	-41.16	58.82	-18.81	26.88
Missisquoi River(326 km^2)	-0.24	0.09	12.18	1.02	-52.14	64.40	-6.22	7.68
Missisquoi River (1152 km^2)	-0.71	0.06	32.69	0.79	-50.04	61.83	-20.83	25.73
Missisquoi River (2249 km^2)	-	-	-	-	-	-	-	-

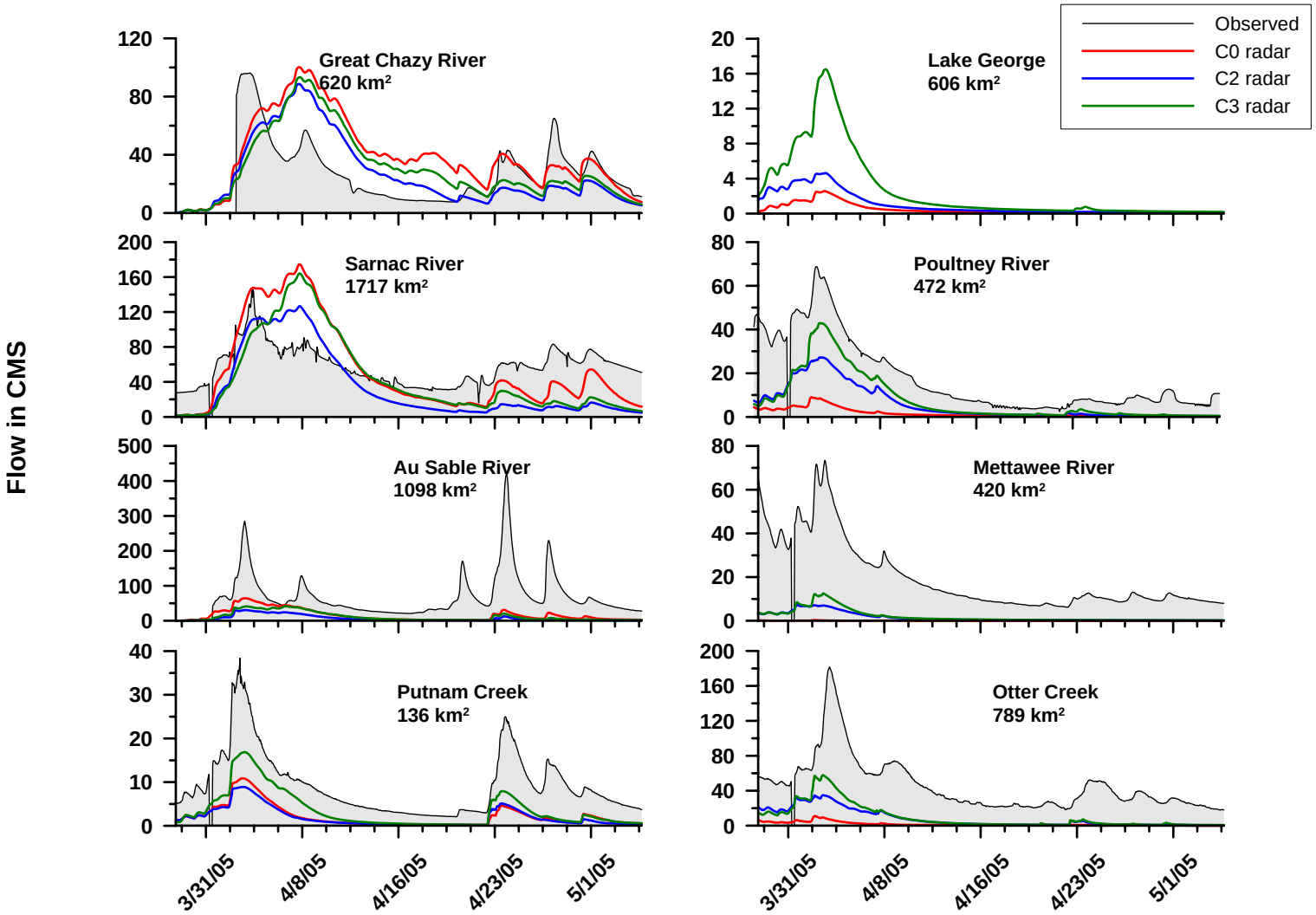

Figure D.46- Lake Champlain Basin, March 29th to May 5th 2005

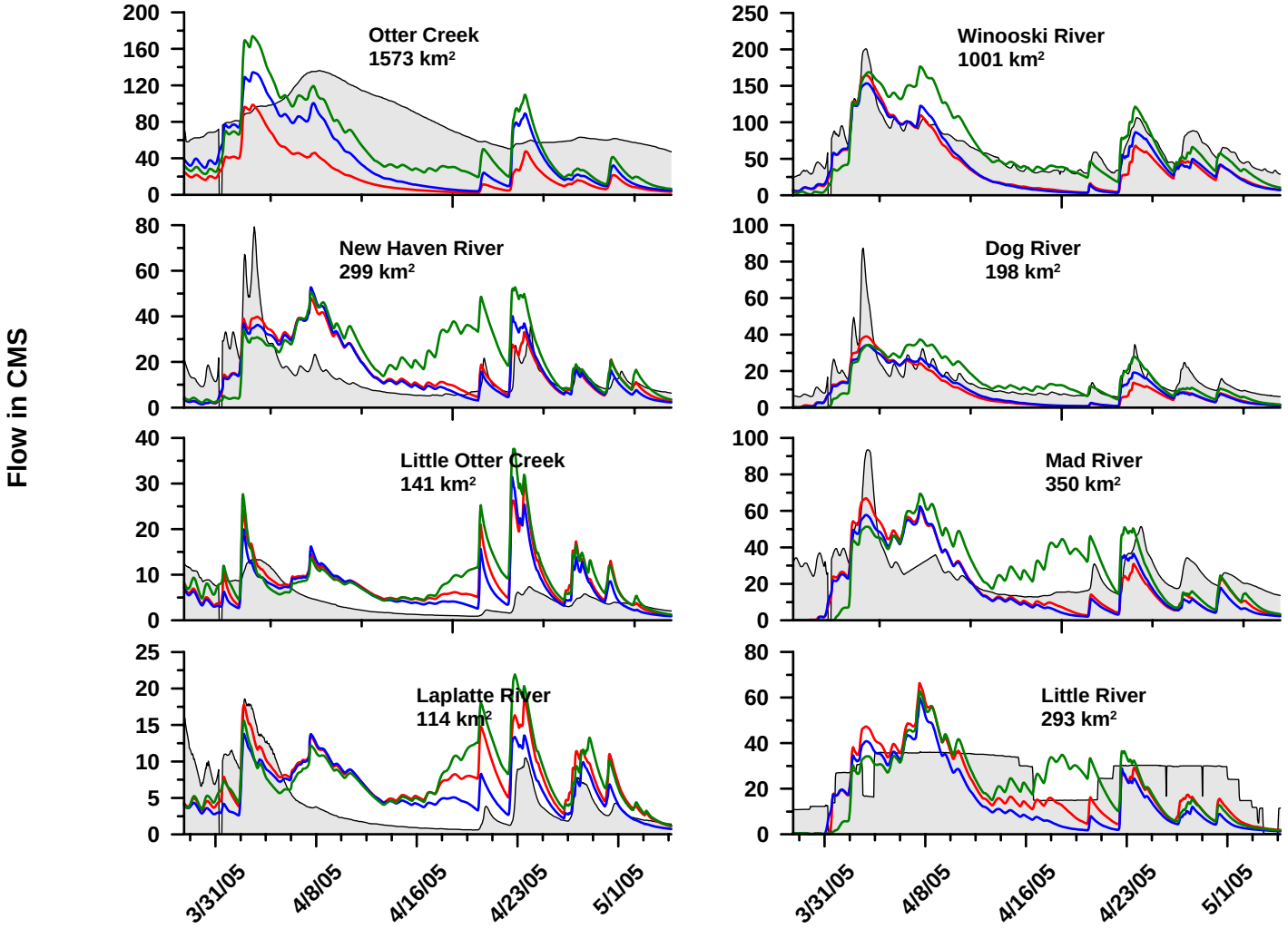

Figure D.47- Lake Champlain Basin, March 29th to May 5th 2005 (continued)

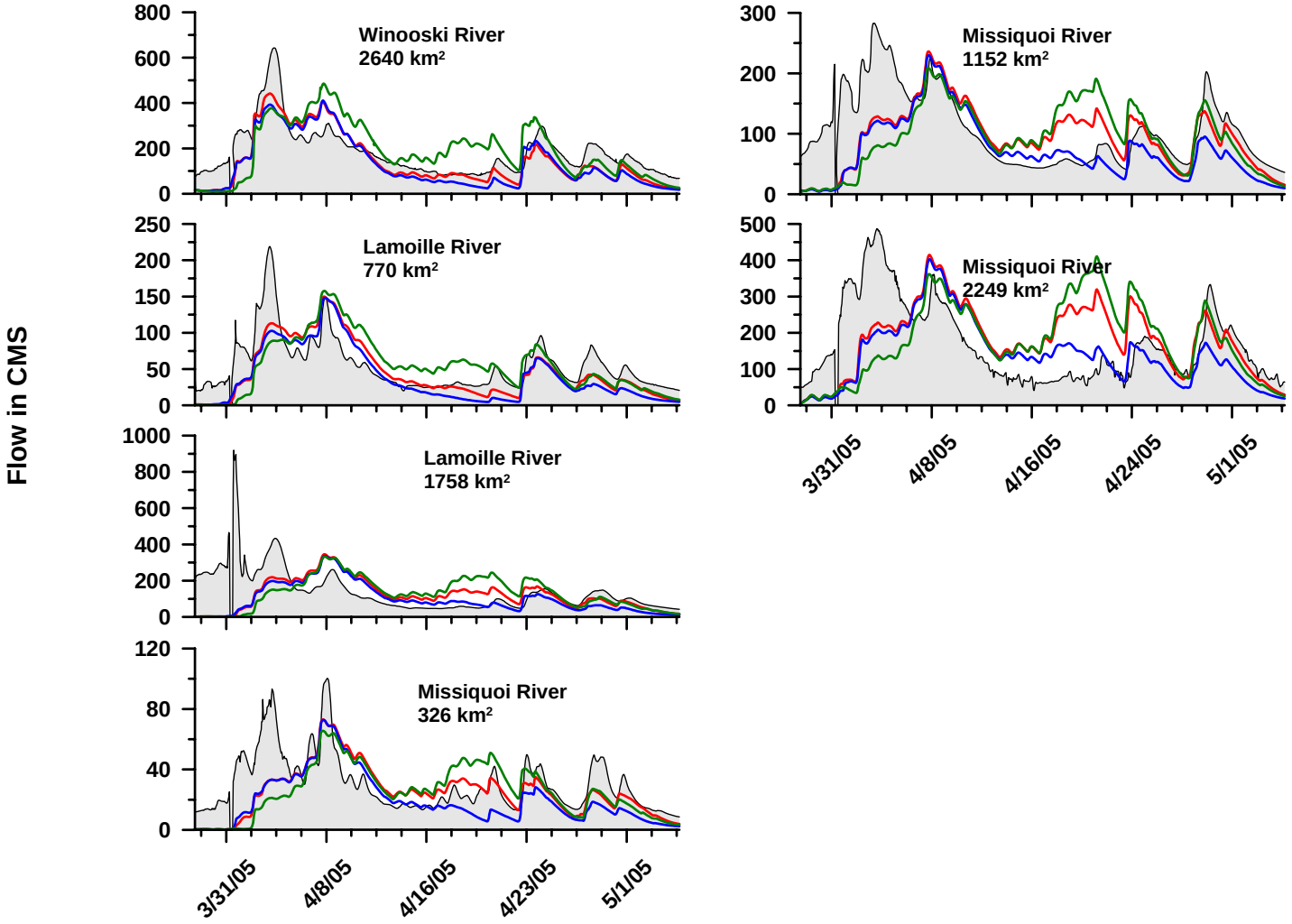

Figure D.48- Lake Champlain Basin, March 29th to May 5th 2005 (continued)

Table D.40- Statistical criteria for Lake Champlain Basin, March 29th to May 5th 2005

	Statistical Criteria							
	Nash	R^2	RMSE	RMSE/qbar	%Dv	APB	Bias	MAE
	C0 RADAR							
Great Chazy River	-0.41	0.30	26.44	1.03	52.54	78.03	13.45	19.98
Saranac River	-1.71	0.56	36.55	0.64	-6.17	52.53	-3.55	30.25
Ausable	-0.45	0.26	77.00	1.15	-76.72	77.61	-51.39	51.99
Putnam Creek	-0.43	0.85	8.55	0.94	-76.40	76.91	-6.97	7.02
Lake George	-	-	-	-	-	-	-	-
Poultney River	-0.71	0.89	21.86	1.24	-91.14	91.47	-16.08	16.14
Mettawee River	-1.48	0.53	25.07	1.29	-99.86	99.86	-19.39	19.39
Otter Creek (789 km^2)	-1.94	0.54	52.34	1.16	-96.43	96.56	-43.62	43.68
Otter Creek (1573 km^2)	-4.59	0.15	63.53	0.80	-71.82	72.59	-57.32	57.94
New Haven River	0.12	0.35	10.82	0.75	15.52	54.47	2.24	7.86
Little Otter Creek	-2.48	0.09	6.34	1.39	78.48	105.23	3.59	4.81
Laplatte River	-0.58	0.17	5.24	1.18	69.47	102.39	3.10	4.57
Winooski River	0.37	0.87	26.80	0.42	-34.16	38.07	-22.06	24.58
Dog River	0.46	0.73	8.44	0.56	-39.76	45.79	-5.98	6.88
Mad River	-0.19	0.44	15.06	0.57	-24.05	47.96	-6.31	12.58
Little River	-	-	-	-	-	-	-	-
Winooski River	0.57	0.72	71.85	0.40	-20.56	32.88	-37.13	59.38
Lamoille River(770 km^2)	0.45	0.57	27.27	0.50	-15.49	38.74	-8.41	21.03
Lamoille River (1758 km^2)	-0.37	0.01	136.29	0.99	-10.80	63.19	-14.93	87.36
Missisquoi River(326 km^2)	0.22	0.35	16.74	0.56	-15.93	40.65	-4.81	12.26
Missisquoi River (1152 km^2)	0.03	0.21	60.17	0.57	-10.72	43.90	-11.34	46.41
Missisquoi River (2249 km^2)	-0.21	0.10	119.64	0.72	9.57	57.74	16.01	96.61
	C2 RADAR							
Great Chazy River	0.07	0.33	21.42	0.84	5.68	65.79	1.46	16.85
Saranac River	-1.79	0.50	37.08	0.64	-41.46	57.60	-23.87	33.16
Ausable	-0.80	0.17	85.63	1.28	-89.90	90.10	-60.22	60.35
Putnam Creek	-0.54	0.86	8.88	0.97	-78.93	79.42	-7.20	7.25
Lake George	-	-	-	-	-	-	-	-
Poultney River	0.14	0.87	15.47	0.88	-67.25	68.41	-11.86	12.07
Mettawee River	-1.05	0.85	22.79	1.17	-92.35	92.69	-17.93	18.00
Otter Creek (789 km^2)	-1.08	0.63	43.98	0.97	-82.25	82.93	-37.20	37.51
Otter Creek (1573 km^2)	-2.67	0.23	51.52	0.65	-50.11	57.83	-39.99	46.16
New Haven River	-0.01	0.31	11.60	0.80	12.11	57.51	1.75	8.30

Little Otter Creek	-1.81	0.08	5.70	1.25	52.89	90.98	2.42	4.16
Laplatte River	-0.11	0.16	4.39	0.99	33.01	81.53	1.47	3.64
Winooski River	0.43	0.86	25.52	0.40	-31.39	35.73	-20.27	23.07
Dog River	0.46	0.69	8.40	0.56	-36.23	41.80	-5.45	6.28
Mad River	-0.28	0.41	15.67	0.60	-28.37	50.53	-7.45	13.26
Little River	-	-	-	-	-	-	-	-
Winooski River	0.45	0.70	80.74	0.45	-27.13	38.42	-48.99	69.38
Lamoille River(770 km^2)	0.36	0.59	29.48	0.54	-27.99	42.95	-15.19	23.31
Lamoille River (1758 km^2)	-0.31	0.04	133.36	0.97	-28.82	59.22	-39.85	81.87
Missisquoi River(326 km^2)	0.13	0.47	17.70	0.59	-34.67	45.50	-10.46	13.73
Missisquoi River (1152 km^2)	0.04	0.37	59.97	0.57	-31.10	41.63	-32.89	44.01
Missisquoi River (2249 km^2)	0.05	0.22	106.34	0.64	-15.68	50.04	-26.23	83.71
	C3 RADAR							
Great Chazy River	-0.19	0.23	24.29	0.95	21.22	73.93	5.43	18.93
Saranac River	-2.17	0.33	39.52	0.69	-23.87	59.23	-13.74	34.11
Ausable	-0.64	0.15	81.85	1.22	-83.00	83.31	-55.60	55.80
Putnam Creek	0.10	0.82	6.77	0.74	-61.44	62.17	-5.61	5.67
Lake George	-	-	-	-	-	-	-	-
Poultney River	0.40	0.81	12.90	0.73	-55.80	56.92	-9.84	10.04
Mettawee River	-0.91	0.85	21.98	1.13	-90.12	90.41	-17.50	17.56
Otter Creek (789 km^2)	-0.79	0.74	40.82	0.90	-78.67	79.30	-35.59	35.87
Otter Creek (1573 km^2)	-1.61	0.31	43.40	0.54	-33.70	49.33	-26.89	39.37
New Haven River	-1.36	0.04	17.76	1.23	55.80	98.44	8.05	14.20
Little Otter Creek	-4.61	0.03	8.05	1.76	103.46	126.23	4.73	5.77
Laplatte River	-1.23	0.04	6.23	1.40	77.73	117.96	3.47	5.26
Winooski River	0.39	0.72	26.39	0.41	2.03	31.00	1.31	20.02
Dog River	0.43	0.48	8.66	0.58	-5.48	39.85	-0.82	5.99
Mad River	-0.94	0.09	19.29	0.74	4.29	63.12	1.13	16.56
Little River	-	-	-	-	-	-	-	-
Winooski River	0.07	0.34	105.33	0.58	5.18	47.76	9.35	86.24
Lamoille River(770 km^2)	0.07	0.29	35.55	0.66	0.41	50.48	0.22	27.40
Lamoille River (1758 km^2)	-0.75	0.02	154.00	1.11	-4.41	78.14	-6.09	108.03
Missisquoi River(326 km^2)	-0.15	0.15	20.33	0.67	-15.24	51.10	-4.60	15.42
Missisquoi River (1152 km^2)	-0.56	0.02	76.37	0.72	-11.33	54.48	-11.98	57.60
Missisquoi River (2249 km^2)	-0.92	0.00	150.86	0.90	7.93	69.31	13.26	115.97

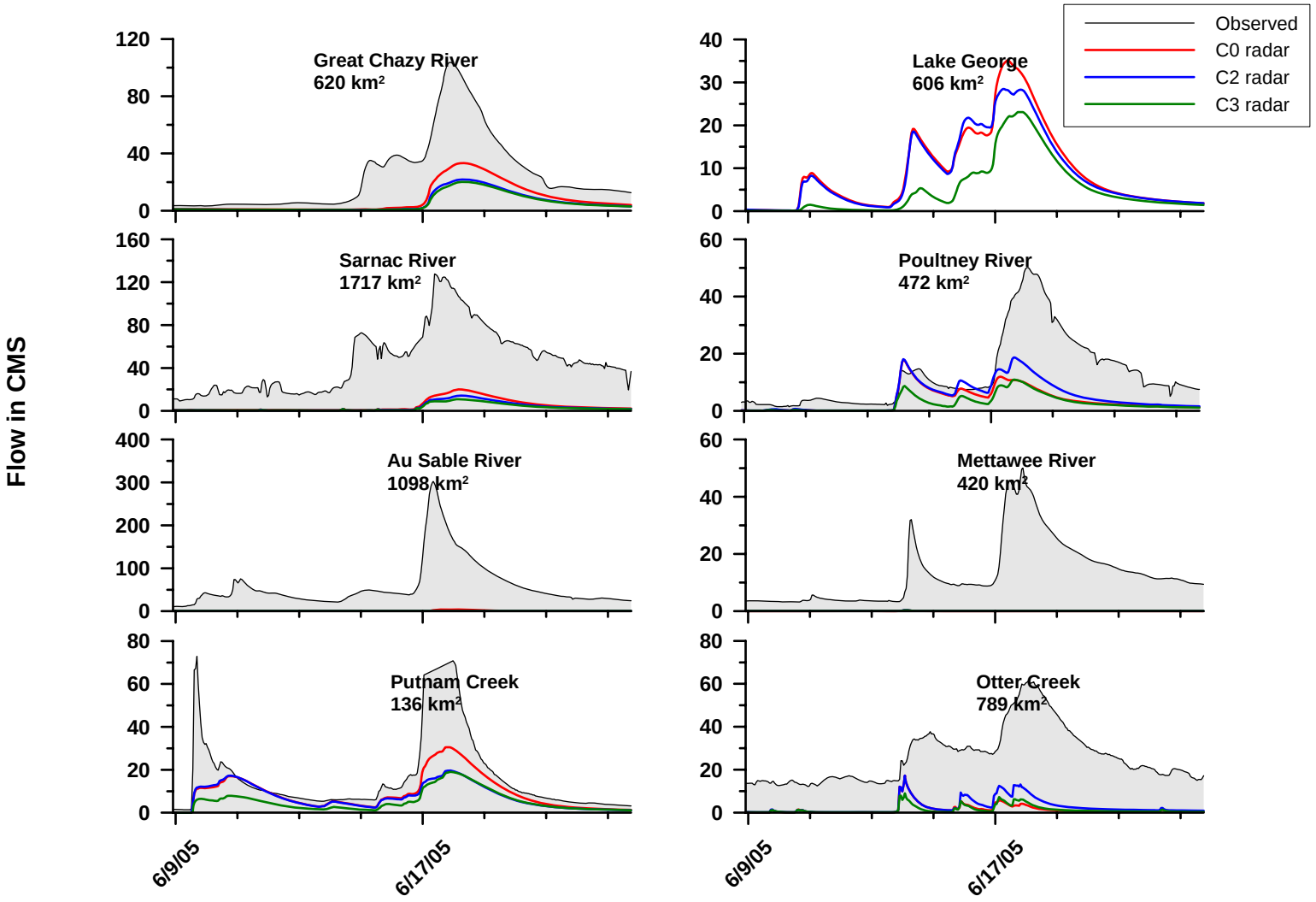

Figure D.49- Lake Champlain Basin, June 9th to June 23rd 2005

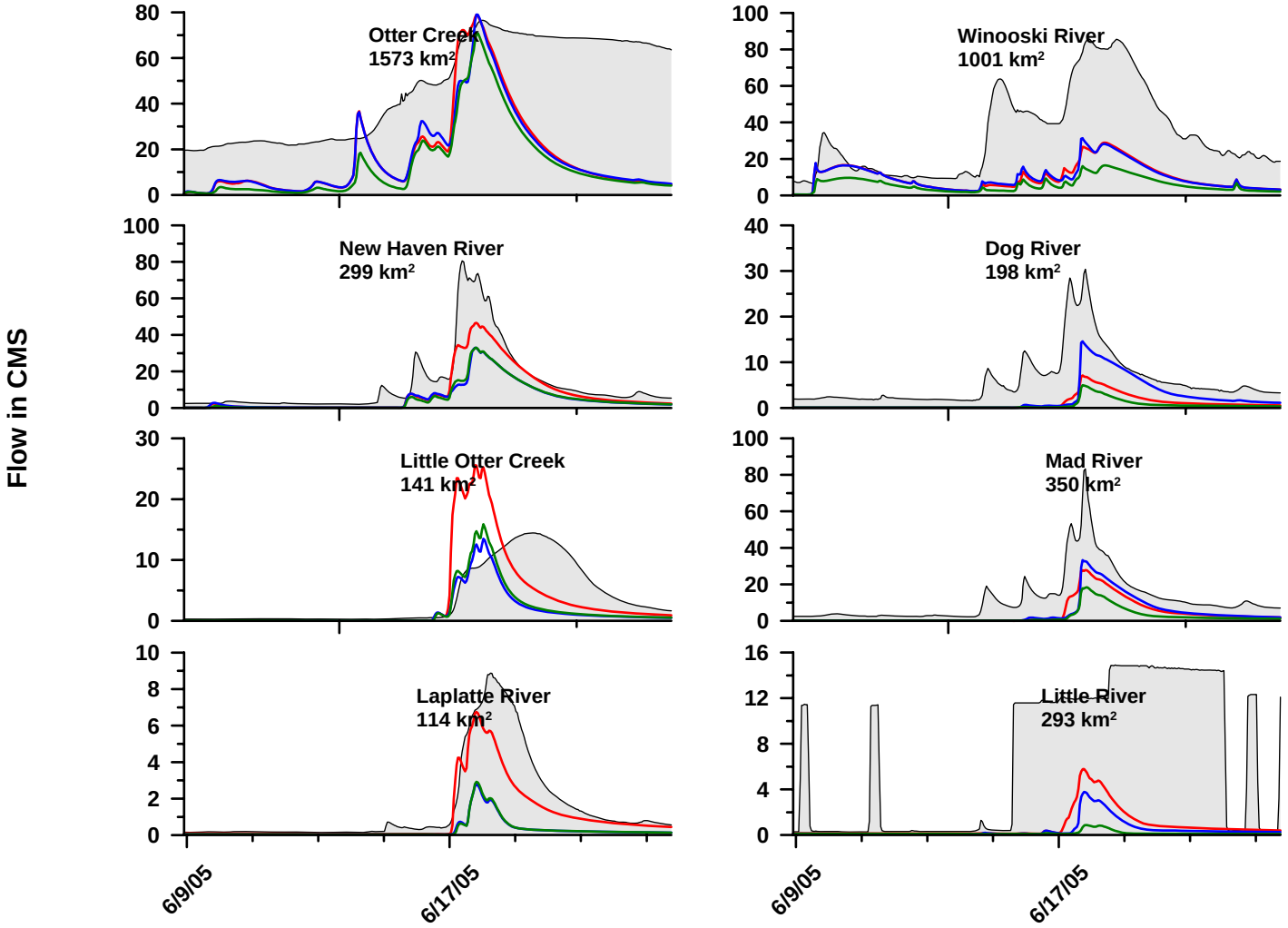

Figure D.50- Lake Champlain Basin, June 9th to June 23rd 2005 (continued)

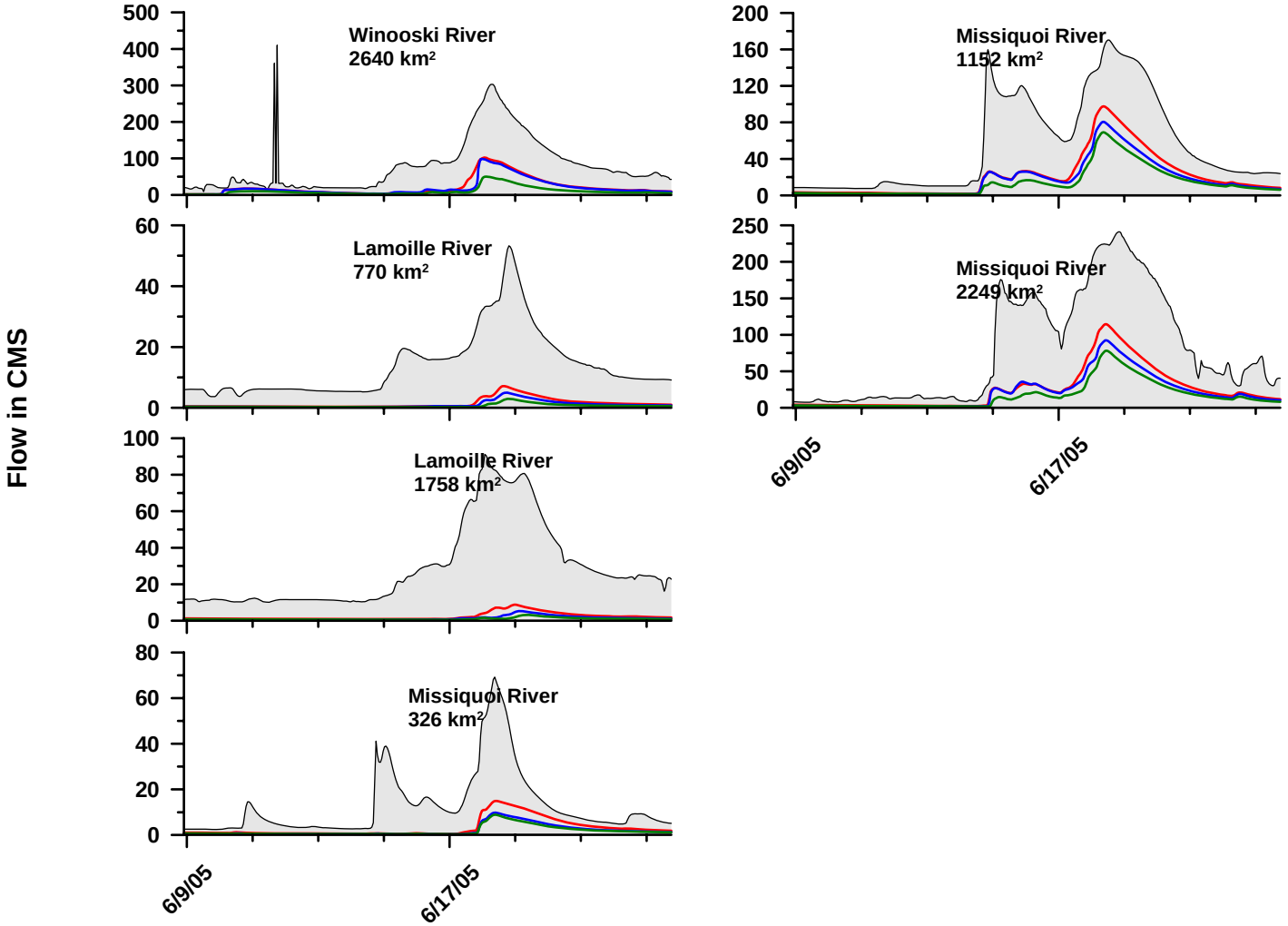

Figure D.51- Lake Champlain Basin, June 9th to June 23rd 2005 (continued)

Table D.41- Statistical criteria for Lake Champlain Basin, June 9th to June 23rd 2005

	Statistical Criteria							
	Nash	R^2	RMSE	RMSE/qbar	%Dv	APB	Bias	MAE
	C0 RADAR							
Great Chazy River	0.11	0.79	24.77	0.99	-68.51	68.51	-17.20	17.20
Saranac River	-1.76	0.72	49.08	1.05	-90.12	90.12	-42.32	42.32
Ausable	-1.09	0.57	80.18	1.35	-98.73	98.73	-58.62	58.62
Putnam Creek	0.40	0.77	14.27	0.85	-45.32	46.18	-7.61	7.75
Lake George	-	-	-	-	-	-	-	-
Poultney River	-0.30	0.33	14.26	1.09	-71.54	72.70	-9.38	9.54
Mettawee River	-1.41	0.00	17.33	1.31	-99.83	99.83	-13.26	13.26
Otter Creek (789 km^2)	-3.57	0.12	27.57	1.06	-94.45	94.45	-24.69	24.69
Otter Creek (1573 km^2)	-1.78	0.30	35.72	0.76	-63.48	64.65	-29.83	30.39
New Haven River	0.72	0.87	9.48	0.71	-40.11	40.38	-5.35	5.39
Little Otter Creek	-0.29	0.31	5.56	1.45	-10.83	82.07	-0.41	3.14
Laplatte River	0.73	0.85	1.24	0.80	-38.21	40.99	-0.59	0.64
Winooski River	-0.66	0.53	30.66	0.90	-70.27	70.67	-23.86	24.00
Dog River	-0.36	0.63	6.85	1.16	-83.46	83.46	-4.94	4.94
Mad River	0.28	0.80	11.81	0.97	-67.85	67.85	-8.26	8.26
Little River	-	-	-	-	-	-	-	-
Winooski River	-0.18	0.78	80.25	0.99	-74.04	74.07	-59.81	59.83
Lamoille River(770 km^2)	-1.13	0.81	15.62	1.12	-90.02	90.02	-12.57	12.57
Lamoille River (1758 km^2)	-1.24	0.72	34.20	1.17	-92.13	92.13	-26.88	26.88
Missisquoi River(326 km^2)	-0.16	0.51	15.61	1.19	-76.41	76.41	-10.00	10.00
Missisquoi River (1152 km^2)	0.17	0.79	47.19	0.84	-62.04	62.04	-34.80	34.80
Missisquoi River (2249 km^2)	0.02	0.83	73.79	0.92	-68.05	68.05	-54.52	54.52
	C2 RADAR							
Great Chazy River	-0.18	0.76	28.52	1.14	-78.63	78.63	-19.74	19.74
Saranac River	-1.96	0.72	50.76	1.08	-92.74	92.74	-43.54	43.54
Ausable	-1.13	0.52	80.95	1.36	-99.57	99.57	-59.12	59.12
Putnam Creek	0.13	0.63	17.19	1.02	-55.72	56.50	-9.36	9.49
Lake George	-	-	-	-	-	-	-	-
Poultney River	0.02	0.55	12.42	0.95	-62.20	64.72	-8.16	8.49
Mettawee River	-1.40	0.02	17.30	1.30	-99.54	99.54	-13.23	13.23
Otter Creek (789 km^2)	-3.00	0.45	25.80	0.99	-89.53	89.53	-23.40	23.40
Otter Creek (1573 km^2)	-1.79	0.31	35.82	0.76	-64.89	65.63	-30.50	30.85
New Haven River	0.38	0.78	14.15	1.06	-59.63	59.73	-7.96	7.97

Little Otter Creek	0.07	0.30	4.72	1.23	-61.39	70.34	-2.35	2.69
Laplatte River	0.00	0.67	2.36	1.52	-83.41	83.41	-1.29	1.29
Winooski River	-0.66	0.53	30.63	0.90	-70.10	70.50	-23.81	23.94
Dog River	0.00	0.43	5.89	1.00	-65.05	65.05	-3.85	3.85
Mad River	0.26	0.66	11.97	0.98	-65.25	65.25	-7.94	7.94
Little River	-	-	-	-	-	-	-	-
Winooski River	-0.28	0.71	83.47	1.03	-76.20	76.23	-61.55	61.58
Lamoille River(770 km^2)	-1.30	0.80	16.22	1.16	-92.95	92.95	-12.98	12.98
Lamoille River (1758 km^2)	-1.41	0.57	35.45	1.22	-95.26	95.26	-27.79	27.79
Missisquoi River(326 km^2)	-0.38	0.53	17.01	1.30	-85.46	85.46	-11.18	11.18
Missisquoi River (1152 km^2)	0.00	0.83	51.78	0.92	-68.70	68.70	-38.54	38.54
Missisquoi River (2249 km^2)	-0.14	0.88	79.52	0.99	-73.37	73.37	-58.77	58.77
	C3 RADAR							
Great Chazy River	-0.24	0.74	29.20	1.16	-80.31	80.31	-20.16	20.16
Saranac River	-2.06	0.71	51.67	1.10	-94.02	94.02	-44.15	44.15
Ausable	-1.14	0.21	81.04	1.37	-99.61	99.61	-59.14	59.14
Putnam Creek	0.00	0.74	18.47	1.10	-68.02	68.02	-11.42	11.42
Lake George	-	-	-	-	-	-	-	-
Poultney River	-0.38	0.67	14.73	1.12	-80.03	80.03	-10.50	10.50
Mettawee River	-1.40	0.01	17.30	1.30	-99.51	99.51	-13.22	13.22
Otter Creek (789 km^2)	-3.58	0.33	27.60	1.06	-95.13	95.13	-24.86	24.86
Otter Creek (1573 km^2)	-2.14	0.36	37.96	0.81	-71.76	71.76	-33.73	33.73
New Haven River	0.40	0.81	13.93	1.04	-60.47	60.47	-8.07	8.07
Little Otter Creek	0.10	0.30	4.64	1.21	-55.43	70.46	-2.12	2.70
Laplatte River	0.01	0.67	2.35	1.51	-83.05	83.05	-1.29	1.29
Winooski River	-1.17	0.49	35.10	1.03	-82.30	82.30	-27.95	27.95
Dog River	-0.63	0.53	7.50	1.27	-90.73	90.73	-5.38	5.38
Mad River	-0.13	0.73	14.75	1.21	-82.81	82.81	-10.08	10.08
Little River	-	-	-	-	-	-	-	-
Winooski River	-0.69	0.70	96.02	1.19	-87.43	87.43	-70.63	70.63
Lamoille River(770 km^2)	-1.47	0.71	16.79	1.20	-95.50	95.50	-13.34	13.34
Lamoille River (1758 km^2)	-1.49	0.44	36.01	1.23	-96.51	96.51	-28.16	28.16
Missisquoi River(326 km^2)	-0.43	0.55	17.31	1.32	-87.02	87.02	-11.38	11.38
Missisquoi River (1152 km^2)	-0.22	0.73	57.13	1.02	-75.15	75.15	-42.16	42.16
Missisquoi River (2249 km^2)	-0.35	0.80	86.40	1.08	-79.39	79.39	-63.60	63.60

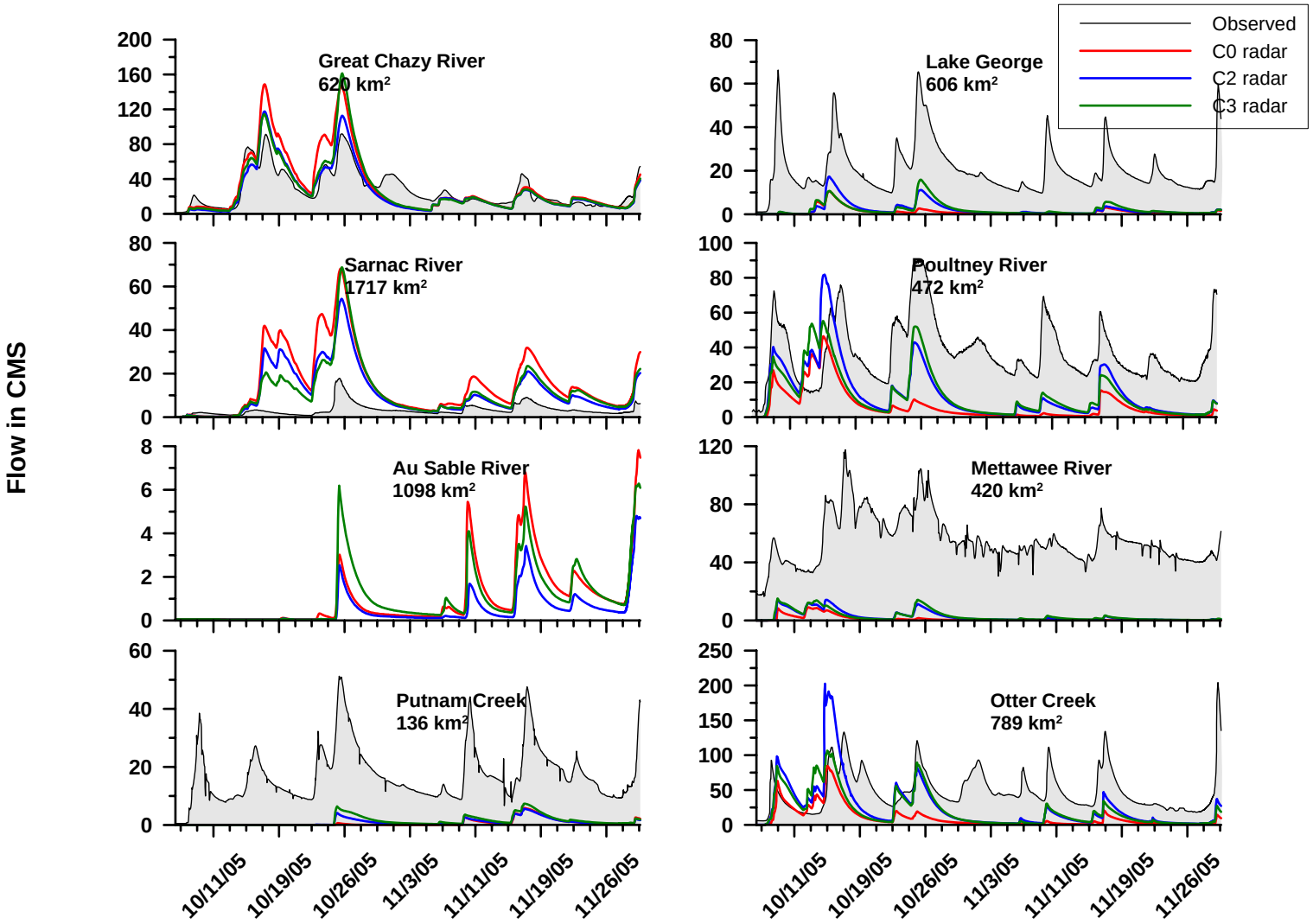

Figure D.52- Lake Champlain Basin, October 7th to November 30th 2005

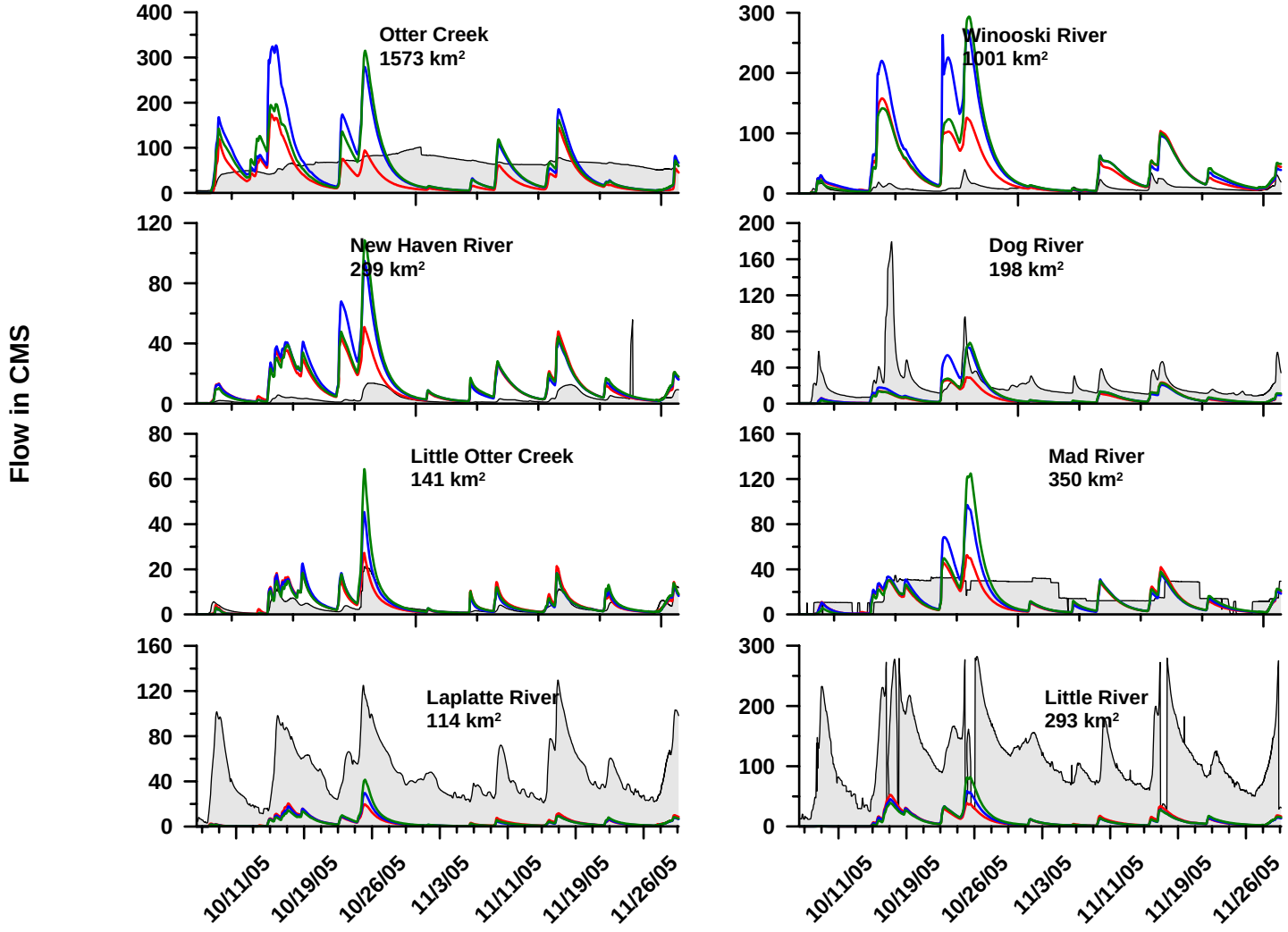

Figure D.53- Lake Champlain Basin, October 7th to November 30th 2005 (continued)

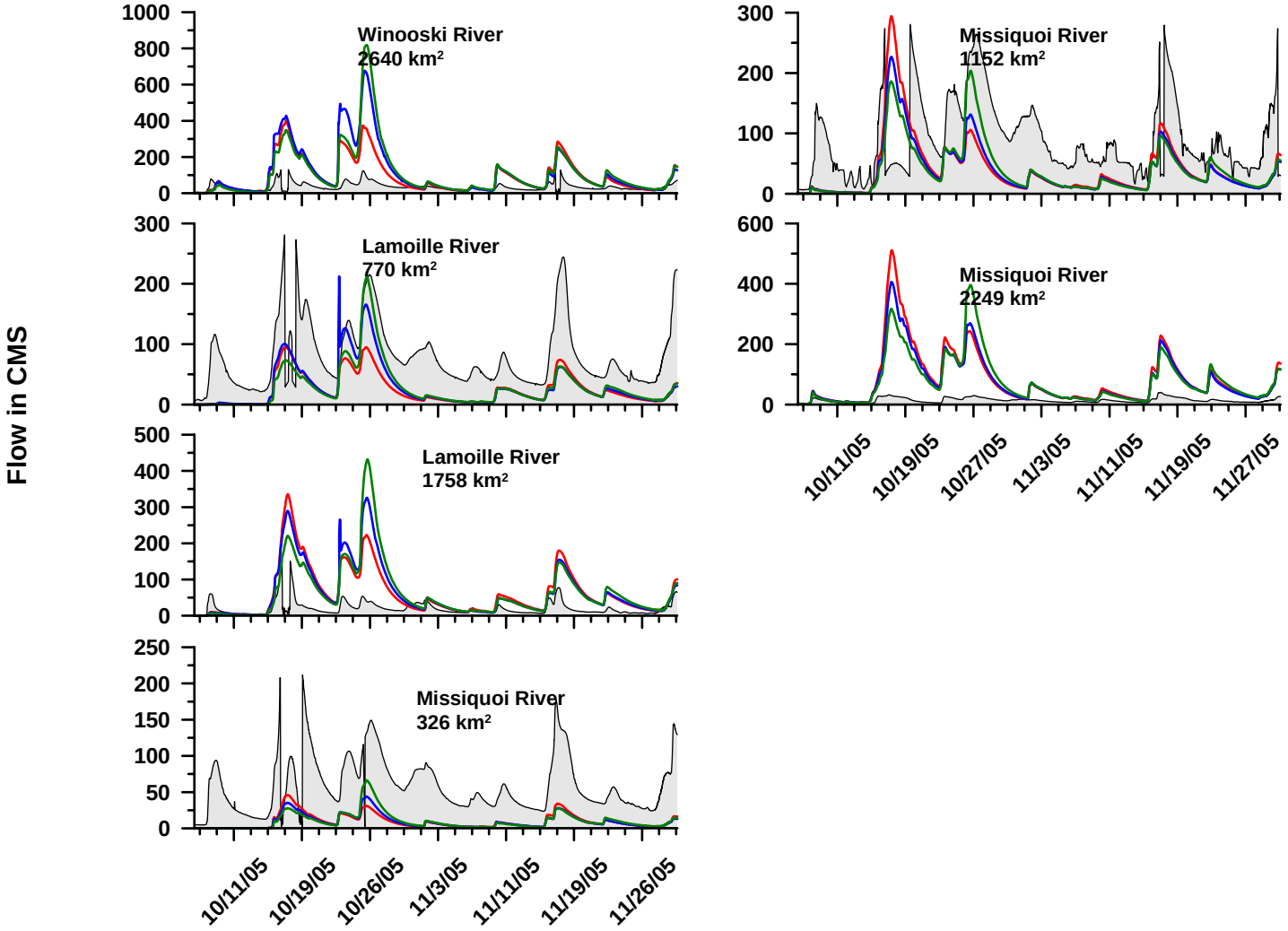

Figure D.54- Lake Champlain Basin, October 7th to November 30th 2005 (continued)

Table D.42- Statistical criteria for Lake Champlain Basin, October 7th to November 30th 2005

	Statistical Criteria							
	Nash	R^2	RMSE	RMSE/qbar	%Dv	APB	Bias	MAE
	C0 RADAR							
Great Chazy River	0.14	0.77	19.55	0.72	15.40	46.32	4.19	12.60
Saranac River	-40.39	0.44	17.59	5.37	364.12	370.95	11.93	12.15
Ausable	-	-	-	-	-	-	-	-
Putnam Creek	-3.00	0.22	18.73	1.09	-96.04	96.04	-16.50	16.50
Lake George	-2.75	0.17	22.15	1.08	-94.32	94.32	-19.32	19.32
Poultney River	-2.99	0.03	35.25	0.96	-81.82	85.83	-30.09	31.57
Mettawee River	-10.26	0.00	56.48	1.03	-98.04	98.04	-53.90	53.90
Otter Creek (789 km^2)	-1.65	0.08	48.01	0.99	-78.58	82.51	-38.02	39.92
Otter Creek (1573 km^2)	-7.50	0.01	50.75	0.79	-46.28	68.68	-29.60	43.92
New Haven River	-7.83	0.16	13.40	3.70	229.84	242.28	8.33	8.78
Little Otter Creek	0.12	0.56	3.51	0.98	32.60	63.53	1.17	2.27
Laplatte River	-2.78	0.57	49.18	1.03	-91.86	91.86	-43.84	43.84
Winooski River	-48.23	0.36	40.90	4.64	279.08	284.21	24.61	25.06
Dog River	-0.35	0.18	24.03	1.13	-70.26	71.82	-14.91	15.23
Mad River	-	-	-	-	-	-	-	-
Little River	-	-	-	-	-	-	-	-
Winooski River	-18.80	0.47	97.90	2.80	161.70	170.47	56.45	59.51
Lamoille River(770 km^2)	-0.56	0.57	65.87	0.84	-69.22	71.18	-54.02	55.55
Lamoille River (1758 km^2)	-13.01	0.34	71.48	3.57	206.30	221.70	41.35	44.44
Missisquoi River(326 km^2)	-1.41	0.40	58.46	1.01	-83.80	84.82	-48.73	49.32
Missisquoi River (1152 km^2)	-0.83	0.08	82.59	0.93	-54.63	76.15	-48.39	67.45
Missisquoi River (2249 km^2)	-191.66	0.55	110.77	8.00	493.51	493.51	68.30	68.30
	C2 RADAR							
Great Chazy River	0.65	0.79	12.44	0.46	-7.25	32.52	-1.97	8.85
Saranac River	-19.27	0.45	12.31	3.76	240.64	248.16	7.88	8.13
Ausable	-	-	-	-	-	-	-	-
Putnam Creek	-2.86	0.47	18.39	1.07	-94.63	94.63	-16.26	16.26
Lake George	-2.30	0.40	20.78	1.02	-89.46	89.46	-18.32	18.32
Poultney River	-1.71	0.22	29.04	0.79	-63.41	71.85	-23.32	26.43
Mettawee River	-9.55	0.09	54.67	0.99	-95.02	95.02	-52.24	52.24
Otter Creek (789 km^2)	-1.10	0.15	42.76	0.88	-49.62	73.92	-24.01	35.77
Otter Creek (1573 km^2)	-15.93	0.00	71.63	1.12	-4.40	84.35	-2.82	53.94
New Haven River	-16.76	0.15	19.01	5.24	303.77	316.02	11.01	11.45

Little Otter Creek	-0.28	0.65	4.23	1.18	41.74	64.03	1.49	2.29
Laplatte River	-2.78	0.52	49.17	1.03	-92.03	92.03	-43.92	43.92
Winooski River	-142.07	0.26	69.73	7.91	438.82	442.02	38.69	38.98
Dog River	-0.29	0.12	23.51	1.11	-58.07	70.89	-12.32	15.04
Mad River	-	-	-	-	-	-	-	-
Little River	-	-	-	-	-	-	-	-
Winooski River	-41.66	0.48	143.70	4.12	221.62	229.79	77.37	80.22
Lamoille River(770 km^2)	-0.41	0.46	62.67	0.80	-63.02	66.49	-49.18	51.89
Lamoille River (1758 km^2)	-15.40	0.31	77.34	3.86	217.05	232.30	43.51	46.57
Missisquoi River(326 km^2)	-1.42	0.44	58.53	1.01	-84.22	84.94	-48.97	49.39
Missisquoi River (1152 km^2)	-0.65	0.15	78.29	0.88	-58.00	74.29	-51.37	65.80
Missisquoi River (2249 km^2)	-146.32	0.60	96.86	7.00	446.93	446.93	61.85	61.85
	C3 RADAR							
Great Chazy River	0.43	0.79	15.87	0.58	3.49	37.69	0.95	10.25
Saranac River	-20.43	0.68	12.66	3.86	247.27	254.88	8.10	8.35
Ausable	-	-	-	-	-	-	-	-
Putnam Creek	-2.64	0.52	17.87	1.04	-92.32	92.32	-15.86	15.86
Lake George	-2.25	0.49	20.63	1.01	-89.02	89.02	-18.23	18.23
Poultney River	-1.70	0.25	29.02	0.79	-65.88	73.53	-24.23	27.05
Mettawee River	-9.49	0.06	54.52	0.99	-94.60	94.60	-52.01	52.01
Otter Creek (789 km^2)	-1.07	0.09	42.42	0.88	-57.38	72.43	-27.77	35.05
Otter Creek (1573 km^2)	-10.87	0.00	59.97	0.94	-13.83	75.80	-8.84	48.48
New Haven River	-16.11	0.22	18.65	5.15	296.10	307.98	10.73	11.16
Little Otter Creek	-1.22	0.69	5.56	1.56	55.48	71.56	1.98	2.56
Laplatte River	-2.71	0.47	48.72	1.02	-91.33	91.33	-43.59	43.59
Winooski River	-103.34	0.36	59.55	6.75	381.31	384.24	33.62	33.88
Dog River	-0.30	0.13	23.53	1.11	-61.48	68.95	-13.04	14.63
Mad River	-	-	-	-	-	-	-	-
Little River	-	-	-	-	-	-	-	-
Winooski River	-42.61	0.47	145.29	4.16	213.53	222.78	74.55	77.78
Lamoille River(770 km^2)	-0.41	0.48	62.72	0.80	-63.81	65.41	-49.79	51.05
Lamoille River (1758 km^2)	-17.53	0.23	82.20	4.10	218.28	233.91	43.76	46.89
Missisquoi River(326 km^2)	-1.34	0.41	57.55	0.99	-82.91	83.53	-48.21	48.57
Missisquoi River (1152 km^2)	-0.43	0.27	72.95	0.82	-56.32	69.34	-49.88	61.42
Missisquoi River (2249 km^2)	-147.12	0.59	97.13	7.02	452.22	452.23	62.58	62.58

Table D.43- Lake Champlain Basin event summary, best-performing radar precipitation product

	Apr 14 to May 5/04			Mar 23 to Apr 30/04			May 31 to Jun 10/04			July 1 to Aug 8/04			Sept 8 to Sept 17/04			Nov 20 to Dec 11/04		
	C0	C2	C3	C0	C2	C3	C0	C2	C3	C0	C2	C3	C0	C2	C3	C0	C2	C3
Great Chazy River			X	-	-	-	X				X		X				X	
Saranac River			X	-	-	-	X			X			X			-	-	-
Ausable	X			X			X			X			X			X		
Putnam Creek	X					X	X				X			X				X
Lake George	-	-	-	-	-	-	-	-	-	-	-	-	-	-	-	-	-	-
Poultney River		X				X		X				X	-	-	-			X
Mettawee River	X					X		X			X			X				X
Otter Creek (789 km^2)	X					X		X			X			X				X
Otter Creek (1573 km^2)			X			X		X				X		X				X
New Haven River	X			X				X				X	X			X		
Little Otter Creek			X		X				X			X	X				X	
Laplatte River	X				X				X			X	X				X	
Winooski River		X				X			X			X	X					X
Dog River		X				X			X			X	X				X	
Mad River	X					X			X			X	X				X	
Little River	-	-	-	-	-	-	-	-	-	-	-	-	-	-	-	-	-	-
Winooski River			X			X			X			X	X				X	
Lamoille River(770 km^2)			X			X		X			X		X					X
Lamoille River (1758 km^2)	X			-	-	-		X			X		X					X
Missisquoi River(326 km^2)	X					X		X			X		X			X		
Missisquoi River (1152 km^2)	X			-	-	-		X				X	X			X		
Missisquoi River (2249 km^2)			X			X		X					X					

Table D.44- Lake Champlain Basin event summary, best-performing radar precipitation product (continued)

	Mar 29 to May 5/05			Jun 9 to Jun 23/05			Oct 7 to Nov 30/05			SUM		
	C0	C2	C3	C0	C2	C3	C0	C2	C3	C0	C2	C3
Great Chazy River		X		X				X		2	4	1
Saranac River	X			X				X		4	1	1
Ausable	X			X			-	-	-	7	0	1
Putnam Creek			X	X					X	4	1	4
Lake George	-	-	-	-	-	-			X	0	0	1
Poultney River			X		X			X		0	4	4
Mettawee River			X			X			X	2	2	5
Otter Creek (789 km^2)			X		X				X	2	3	4
Otter Creek (1573 km^2)			X	X			X			3	1	5
New Haven River	X			X			X			6	1	2
Little Otter Creek		X				X	X			1	3	4
Laplatte River		X		X					X	2	3	3
Winooski River		X			X		X			1	3	4
Dog River			X		X			X		0	4	4
Mad River	X			X			-	-	-	3	1	3
Little River	-	-	-	-	-	-	-	-	-	0	0	0
Winooski River	X			X			X			3	1	4
Lamoille River(770 km^2)	X			X				X		2	3	3
Lamoille River (1758 km^2)		X		X			X			3	3	1
Missisquoi River(326 km^2)	X			X					X	4	2	3
Missisquoi River (1152 km^2)		X		X					X	3	2	3
Missisquoi River (2249 km^2)		X		X				X		1	3	2
										53	**45**	**62**